THE EFFECT OF LIGHT ON THE THERMOLUMINESCENCE OF QUARTZ

BY

NIGEL ANTONY SPOONER , B.Sc.(HONS.)

A THESIS

presented for the degree of

MASTER OF SCIENCE

in the

Department of Physics

UNIVERSITY OF ADELAIDE

February 1987

CONTENTS

SUMMARY

The thesis examines the effect of light on the thermoluminescence (TL) of natural quartz extracted from sedimentary deposits. Emphasis is on the investigation of factors affecting the TL level remaining after deposition ("residual"), and determining the relative efficiencies with which wavelengths present in the solar spectrum reduce ("bleach") the natural TL (NTL).

The light source for bleaching was an Oriel 1000 W solar simulator, producing controllable illumination of intensity and spectrum comparable to that of clear-day natural sunlight. TL measurements were taken by a Risφ automated TL reader unit.

Coarse grain (90-125 μm) quartz from Lake Woods, Northern Territory, was used throughout. The requirements of the work gave rise to a sample preparation technique that minimized sampling reproducibility problems. A supplementary investigation looked for sources of the remaining variability and concluded it was intrinsic to the quartz, originating from mineral inclusions and a small proportion of high TL sensitivity quartz grains.

Principal findings from bleaching by simulated sunlight are that the residual is not an inherently unbleachable TL component, but should instead be considered a zone (rather than a defined level) to which bleaching proceeds relatively rapidly, the precise rate being dependent on bleaching conditions (spectrum, luminous flux, ambient temperature), and in which further TL reduction occurs monotonically at a slower and decreasing rate. This residual zone relates to some characteristic

concentration of trapped charge within the crystal, and not to a proportion of the initial TL. Generally, the TL at all glow curve temperatures can be bleached, but at different rates and to differing extents, with susceptibility to bleaching declining with increasing glow curve temperature. The glow peak at 325°C was found to be a significant exception to the general behaviour, bleaching approximately two orders of magnitude more rapidly than other NTL glow peaks.

Marked dependence of bleaching efficiency on wavelength was found. Wavelengths less than 400 nm (UV) actively bleached all NTL glow peaks, and are the only components of natural sunlight capable of reducing the glow peaks at 370°C and 480°C. Visible light bleached only the 325°C glow peak, while infra-red wavelengths had no effect on any NTL peak. In general, bleaching efficiency increases approximately exponentially with decreasing wavelength.

Subsidiary work suggested preferential bleaching of the 220°C glow peak by wavelengths of ~ 500 nm.

A precautionary search for effects attributable to the laboratory safelight illumination (see Appendix 4) found significant disruption of the quartz TL by exposures exceeding several hours. A report of this work is to appear in "Ancient TL".

A general conclusion is that a productive line of development for dating applications would involve "reading" the readily bleachable NTL component - the 325°C glow peak - by an optical rather than thermal stimulation technique.

STATEMENT

This thesis contains no material which has been accepted for the award of any other degree or diploma in any University, and to the best of the author's knowledge and belief, contains no material previously published or written by another person, except where due reference is made in the text.

The author consents to the thesis being available for photocopying and loan.

Nigel A. Spooner

Adelaide

February, 1987

ACKNOWLEDGEMENTS

I firstly thank my supervisor Professor John Prescott for his enthusiasm, advice and some interesting discussions in the course of this work. Thanks also are due to John Hutton for his encouragement and advice, particularly in the mineralogical studies of quartz samples, and not least for his interpretation of the X-ray emission spectra.

Some useful discussions with Riaz Akber were very much appreciated, as was the enthusiasm of the other group members, Gillian Robertson, Philip Fox and Honours students Steven Lee and John Keller.

Much of the work on quartz TL reproducibility would not have been possible without the assistance of others, particularly Dr. Brendon Griffin of the University of Adelaide Electron Optical Centre. Time given by Dr. Karl Bartusek and Sally Phillips, also of the E.O.C., and Mr. E.J. Bleys, Department of Geology, was also appreciated. I am indebted to Dr. Keith Norrish for his kind permission to prepare the thin sections at the CSIRO Division of Soils, Mineralogy Section, and to Mr. Heinz Konczalla for his keen guidance of that work.

Thanks also go to Peter Schebella and Graham Eames of the Physics Department Mechanical Workshop, and particularly to Bill Old for his construction of the solar simulator exposure chamber.

Assistance given by members of the technical staff, especially Leon Thomas, was also appreciated.

The preparation of this thesis owes much to the efficiency and patience of Argyro Magoulianos, whose typing of all figure labels and captions, and the majority of the text, is deeply appreciated. Thanks are also due to Jill Allen for completing the typing of the text.

More personally, the period of my candidature was much enhanced by the friendship of the other Postgraduate students.

It would also be remiss of me not to thank Mary-Anne for her constancy and ability to keep things in perspective.

Finally, I must thank my parents for their support in making this period of study possible.

CHAPTER 1 INTRODUCTION AND REVIEW

1.1 Introduction

TL dating is a technique based on the measurement of accumulated trapped charge in crystals, and was originally applied to heated objects such as pottery, where the event dated was the erasure of previously acquired TL by the act of firing. Since the discovery in the mid 1960's that older sediments of a profile possess more TL than younger, the technique has also been applied to sedimentary materials, with increasing intensity of effort. TL dating of sediments depends on there being some mechanism that reduces the TL content of minerals during the sedimentation process. Although early uncertainty over this mechanism was resolved in favour of exposure to sunlight - "bleaching" - as the agent responsible, assessing the TL remaining after deposition, the "residual", has remained the central problem in TL sediment dating. This complication has given rise to a number of interrelated questions concerning the bleaching process, some of the more prominent of which are listed in section 1.11 and give motivation for this work.

The thesis investigates the bleaching behaviour of the NTL of selected sedimentary quartz samples. Emphasis is on examining the factors affecting the residual achieved, and on determining the response of the quartz NTL glow peaks to the various wavelengths present in natural sunlight. Some of the other questions on bleaching are examined in supplementary experiments.

Chapter 1 introduces the phenomenon of TL, then outlines the development of TL dating for heated materials and its subsequent extension to optically bleached sediments. Current TL sediment dating techniques and some applications are then described. The chapter concludes with a review of the bleaching of quartz TL and poses a series of questions addressing current topics in bleaching.

Chapter 2 presents the procedures for extracting coarse grain (90-125 μm) quartz from the bulk sediment, and describes and justifies a sample spreading technique developed to minimize sample reproducibility problems. While this markedly improved sample reproducibility, a component of variability still remained. Further work, based on electron microscopy, and which concluded that this remaining variability was intrinsic to the quartz samples, is presented in Chapter 6.

Instrumentation is described where appropriate in the text:- the laboratory illumination source (Oriel 1000W solar simulator) in section 4.2., the TL measurement and irradiation unit (Risφ automated TL Reader) in section 2.5 and Appendix 3, and laboratory irradiation source calibrations in Appendix 1.

The work program was based on a standardised natural quartz - the selection and characterisation of this material is described in Chapter 3, along with additional work to determine the optimum pre-treatment and glow conditions.

Chapter 4 presents investigations into the bleaching of quartz TL by a simulated sunlight beam closely matching natural sunlight in both spectrum and intensity, while the bleaching efficiencies of the component wavelengths of sunlight are examined in Chapter 5.

Chapter 7 gives some suggestions for future directions of study.

1.2 Thermoluminescence

Thermoluminescence (TL) is the light emitted by some solids when heated.

Distinct from incandescence, this light is energy stored in the crystal from previous excitation events, usually exposure to ionizing radiation, and released on heating.

A simplified explanation of TL can be given from the energy band theory of solids (see Fig. 1.2.1). Though crystals consist of regular periodic arrays of atomic or molecular structural units, invariably lattice defects are present. Ionizing radiation (from cosmic rays and natural radioisotopes ^{40}K, ^{87}Rb and the U and Th series) incident on the crystal produces charge pairs - free electrons and positive holes. The majority recombine immediately, dissipating the excitation energy in heat or prompt luminescence processes. However, for a small proportion, the electron diffuses via the conduction band until it reaches a suitable lattice defect and is trapped. Likewise the positive hole diffuses in the valence band until similarly captured. Heating then provides the activation energy to untrap a charge carrier, usually the electron, which again diffuses in the conduction band until it recombines at the hole site. The stored energy is emitted as a photon having an energy characteristic of the hole trap.

Although this energy band model gives a good illustrative picture of the process, the actual mechanism of quartz TL on the atomic level is little known. The most generally accepted model involves the Al/alkali centre, first described by O'Brien (1955). This centre is created when

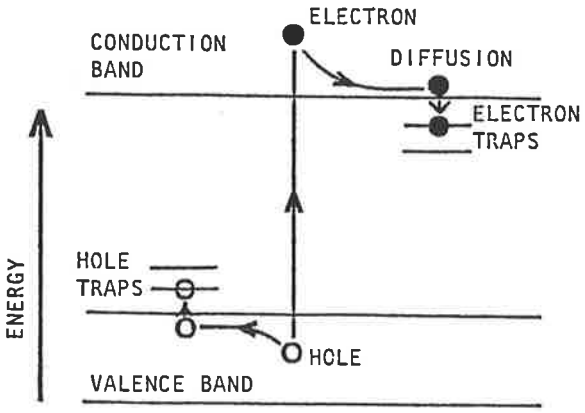

a) Excitation by ionizing radiation, followed by charge diffusion and trapping.

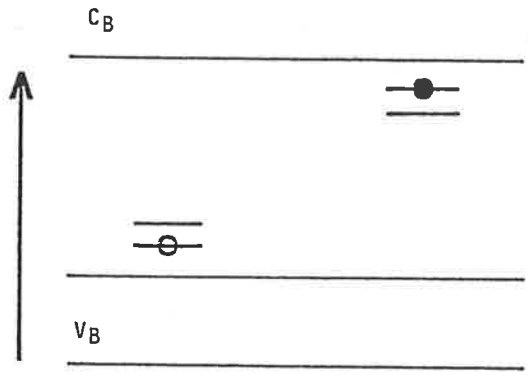

b) Crystal with metastably trapped charge. Further charge accumulates with time.

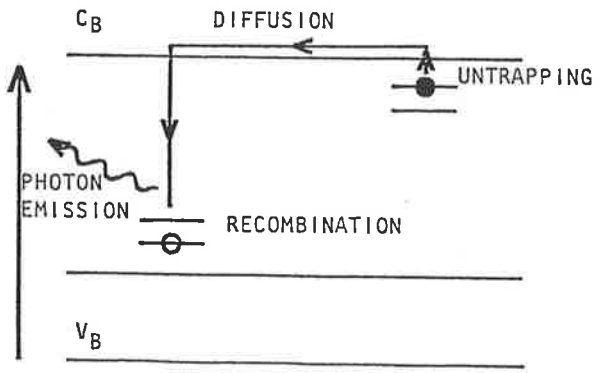

c) Heating provides the activation energy to untrap the electrons, which diffuse until recombination and photon emission occur at the hole site.
The photon energy is characteristic of the recombination centre.

FIG. 1.2.1 Shows a simple energy band model for the TL process (After : Halperin and Braner (1960), and Aitken (1985)).

trivalent Al^{3+} substitutes for tetravalent Si^{4+} in the SiO_2 lattice - one adjacent oxygen is therefore left unbonded. The resultant charge imbalance attracts a charge compensating monovalent ion which becomes localized in the adjacent c-axis channel. Suitable compensating species are protons (H^+) and the lighter alkali metals (Li^+, Na^+, and possibly K^+).

The range of available charge compensators and physical configurations gives rise to several types of Al/alkali centres.

On irradiation, a hole is trapped by the non-bonding oxygen, and the now superfluous alkali ion is free to diffuse away down the c-axis channel.

The Al/alkali centre has thus become an Al/hole centre - $(Al^{3+})^o$ - believed to be the dominant luminescence centre in most forms of quartz.

The free electron can become trapped at a variety of electron traps, giving rise to the complex structure of quartz glow curves. Substitutional Ge^{4+}, because of a high electron affinity, is a likely candidate as an important electron trap. Other possibilities are protons, alkali ion clusters, substitutional Ti^{4+} and self-trapping at Si^{4+}. The destination of the diffusing alkali ion is unknown, though it may become localized at the electron trap.

Subsequent heating untraps the electron which then recombines at the $(Al^{3+})^o$ centre, emitting a photon. Some time later the alkali ion returns, so restoring the original Al/ alkali centre.

The roles played, if any, by other ionic species are virtually unknown. An exception is Fe^{3+}, which is believed to act as a non-luminescent recombination centre (see Medlin, 1968).

It must be noted that the emission spectra - while typically broad band emissions centred on ~470nm - vary considerably for samples of

different origins, and for any one sample contain several closely spaced, overlapping bands. (McKeever, 1984).

This uncertainty regarding the recombination centres, and the even less well known electron traps, makes interpretation of observed TL effects in terms of specific defects and their behaviour a speculative exercise at present.

1.3 TL Dating

As charge accumulates at defect sites with exposure to ionizing radiation, some dose will eventually be reached at which the available traps are filled. Consequently, further irradiation produces no further TL - the crystal is said to be saturated. This is found to be the case for the majority of geological specimens, which, along with other saturated materials, are not datable by present TL techniques.

Given that a sample can produce detectable TL, the prime requirement for dating to be feasible is an increase in TL signal with dose. This implies the sample has not yet reached saturation, being either too recently formed or subjected to some other event capable of removing or reducing the geological TL. Such an event - "zeroing" - is the act dated. Datable zeroing events fall into the broad categories of heating, crystal formation and exposure to sunlight - "bleaching". The latter is a reduction rather than zeroing mechanism as some low level of TL signal - the "residual" - always remains.

Nonetheless, assuming TL increases with dose following the zeroing event, the age can be found from the age equation:

$$\text{age(years before present)} = \frac{\text{acquired dose}}{\text{annual dose}}$$

$$= \frac{\text{Natural TL}}{\text{(TL/unit dose) x (annual dose)}}$$

$$= \frac{\text{ED}}{\text{(annual dose)}}$$

where: Natural TL (NTL) is that acquired since the previous zeroing event.

TL/unit dose is the sensitivity to radiation measured in the laboratory.

Annual dose is the dose delivered yearly from environmental and self-irradiation, and can be estimated from the radioisotope content of the sample and the immediate surrounds, plus a cosmic ray component.

ED is the "equivalent dose" - the laboratory administered dose necessary to replicate the natural TL.

1.4 Applications

Historically, the earliest known report of TL was that of the luminescence from a diamond, by Robert Boyle (1664). In following years the phenomenon was observed in numerous other minerals and, until the development of sensitive detection systems in the 1940's, found chief application in mineral identification.

In the early 1950's, the relationship of total TL to total dose and hence to dose rate x time was recognized as providing new dating possibilities for geology and archaeology (F. Daniels et al, 1953). Simultaneously the use of TL phosphors was developing in radiation dosimetry for such diverse purposes as monitoring nuclear explosions or

radiation dosage to patients undergoing radiotherapy. Medical and environmental dosimetry have remained the largest fields of application.

Other areas include solid state physics (probing defects in semiconductors and insulators) and a range of minor uses.
These will not be considered further - of interest here are the applications to geology and archaeology.

1.5 TL in Geology

Dating comprises the greater part of the geological uses of TL, although the onset of saturation limits the datable range to the Quaternary ($<10^6$ years). Pre-1968 applications are summarized in McDougall (1968).

A variety of applications in addition to dating has been attempted, generally relying on linking glow curve characteristics to particular phenomena, for example chemical impurities, past radiation or thermal conditions, pressure or shock induced glow curve changes, or chemical changes. Some examples are: the weathering of rocks,(Göksu Ögelman and Kapur, 1982); mineral prospecting - changes in TL properties can enable the location and mapping of ore bodies (Levy, 1979; Nambi, Bapat and David 1978); studies of meteoritic material to determine time elapsed since fall, ablation during fall, orbital parameters (reviewed by McKeever and Sears, 1979, and McKeever, 1985); earthquake prediction from pressure induced glow curve changes (Nambi, 1981); shock detection relating to meteorite impacts (reviewed by Stöffler, 1974); and temperatures of formation (Levy, 1979).

Unfortunately the difficulties of unambiguously attributing glow curve properties to the effect under investigation have meant these applications are not all on a sound footing at present.

Somewhat more established are dating applications, examples of which are: mineral formation - notably speleothems (Aitken and Bussell, 1982) and recrystallizations, and products of vulcanism such as lavas (Wintle, 1973), baked sediments (Huxtable et al 1978, Smith 1983) and volcanic glasses (Berger and Huntley, 1983).

Finally, the dating of Quaternary sediments zeroed by sunlight holds promise of becoming a most important application of TL in Geology.

1.6 TL in Archaeology - Pottery dating

The dominant archaeological role for TL is dating fired materials, particularly pottery - the material for which the technique was originally developed.

Pottery is a most desirable class of artifact for absolute dating, being almost universal in occurrence, resistant to weathering and already a long established tool in defining chronologies. The event dated is the act of firing. After firing, TL accumulation immediately recommenced due to radiation from the environment and radioisotopes in the pottery fabric. Knowledge of the resulting radiation dose-rate, combined with measurements of the accumulated TL and TL sensitivity of the pottery minerals, yields the time since firing.

Extensions of the technique to other materials such as oven stones (Huxtable et al, 1972; Prescott et al, 1982; Mejdahl, 1983) and burnt flints (Göksu et al, 1974) are generally based on the methods developed for dating pottery, and will not be discussed further.

TL from pottery was first observed by Grögler et al (1960) and Kennedy and Knopff (1960).

Fremlin and Srirath (1964) showed most of the luminescence originated in crystalline inclusions embedded in the clay matrix, although the matrix contained the majority of the radioactivity.

Absolute dates were not possible until this inhomogeneity was accounted for. This was largely done in the 1960's by the Oxford laboratory under M. Aitken. Key developments in technique are described by Aitken, Tite and Reid, (1964) and Aitken, Zimmerman and Fleming, (1968). The introductions of the coarse grain quartz inclusion method by Fleming (1966) and the fine grain method by Zimmerman (1967), along with later refinements, established TL as a reliable pottery dating technique. Both methods evolved from dosimetric considerations - α, β and γ rays have approximate ranges in pottery minerals of 20μm, 2 mm and ~25 cm respectively, hence the methods were designed to exclude the α contribution (coarse grain inclusion dating) or fully include it (fine grain method).

To these were added the pre-dose technique (Fleming, 1973), and subtraction method (Fleming and Stoneham, 1973).

Because of their ancestry to sediment techniques, the quartz inclusion and fine grain methods are briefly outlined below.

The fine grain technique utilizes 2-8μm or 4-11μm polymineral grains extracted from the pottery sample by gentle crushing followed by sedimentation particle sizing. The age equation includes the full contribution from β, γ and cosmic rays. The α component is qualified by an efficiency factor "k" because of the lower TL/unit dose induced by α irradiation.

Define $k = \frac{(TL/\text{unit dose})\ \alpha}{(TL/\text{unit dose})\ \beta}$, typically $k \sim 0.1$

The age equation is then

$$\text{age} = \frac{NTL/\ (TL/\text{unit dose})}{k\ R_\alpha + R_\beta + R_\gamma + R_c}$$

where R_α, R_β, R_γ, R_c are the α, β, γ and cosmic ray dose rates respectively.

The coarse grain technique selects quartz inclusions of ~100μm which are then etched in HF acid to remove the outer, α irradiated layer. Consequently the α contribution is ignored and the age equation becomes

$$\text{age} = \frac{NTL/\ (TL/\text{unit dose})}{R_\beta + R_\gamma + R_c}$$

A notable spin-off from pottery dating that has assumed great importance for archaeology and antiquities in general is TL authenticity testing (see Fleming, 1979).

1.7 TL dating of sediments - historical

The earliest application of TL to sediment dating is attributed to Shelkoplyas and Morozov (1966), who noted "an increase in intensity of thermoluminescence from young to more ancient deposits,...., allowing the determination of their relative age". This inspired an active dating program based in Kiev and working on Central Russian deposits, although

faulty methodology has invalidated most of the resultant dates (Dreimanis et al, 1978, Wintle and Huntley, 1982, Hütt and Smirnov, 1982).

In the west, Bothner and Johnson (1969) found an increase in TL signal with depth in high carbonate marine cores, but the significance of this was apparently missed until Huntley and Johnson (1976) observed a similar effect in deep sea sediment cores. Follow up papers by Wintle and Huntley (1979 a,b) recognized detrital grains as the source of the TL signal, not foraminiferal materials as previously supposed, and produced the first correct series of dates for deep sea sediment. They then described the application of the fine-grain method to marine sediment cores. A key paper, Wintle and Huntley (1980), showed exposure to sunlight was the dominant zeroing mechanism for the fine-grain sediments, finding a fivefold TL reduction from 20 minutes of natural sunlight exposure, and also proposed three methods for estimating the equivalent dose, based on bleaching by sun or sunlamp. Of these, method (c) - "partial bleaching" - was recommended for simplicity.

Highly bleached terrestrial sediments motivated the introduction of the total bleach (additive) method by Singhvi et al (1982), and the logical extension by Prószyńska (1983) and Debenham and Walton (1983) to produce the total bleach - regeneration method.

The availability of suitable Scandinavian quartz and feldspar sediments has led to the recent proposal by Mejdahl (1985) of the quartz-feldspar method.

Currently, a most promising new technique - optical dating - is developing from partial bleaching. This method extracts the easily bleached TL component by optical rather than thermal stimulation (Huntley et al, 1985).

1.8 Techniques for estimating sediment equivalent doses

In many situations the extent to which natural bleaching proceeded can only be guessed at. For example, while loess particles and desert dune sands can reasonably be expected to have bleached to their practical limit, other sediments such as marine and glacial deposits may have received minimal light exposure. Consequently, techniques capable of finding the ED for a variety of zeroing conditions have been developed. These can be broadly classed as either total bleach or partial bleach methods.

Total bleaching is preferable where an exposure sufficient to reduce the TL to the residual level can be assumed (typically $\tilde{>}$ 1 day). In all other cases, partial bleaching is probably more suitable, as it relies on only removing that fraction of TL readily bleachable by limited light exposure.

The currently favoured methods for estimating ED are described below.

Partial Bleach Method.

Also known as the R-T or R-β method, partial bleaching was introduced as "method (c)" by Wintle and Huntley (1980). Previously, Wintle and Huntley (1979a) had proposed that the NTL (at a given temperature) of a sediment sample could be resolved into two components:

$$I_{nat} = I_o + I_d$$

where I_{nat} = NTL

I_o = an unbleachable residual

I_d = TL acquired since deposition.

The corresponding dose expression is $D = D_o + ED$.

Three methods for determining ED were then proposed. Method(a) equated ED to G/(1-f), where G was the γ dose needed to restore the NTL level following a standard sunlamp exposure of 40 minutes, and f was the fraction of I_d remaining after the standard exposure. Problems of sensitivity changes and difficulties in determining f led to method (b). This technique finds G for a range of NTL and NTL + Γ samples; an extrapolation to G = 0 on a G Vs Γ plot then gives ED as the Γ intercept. However, the excessive laboratory work required gave rise to the simplified version introduced as method (c). The reduction in the TL (R) from a standard sunlamp exposure is plotted against added laboratory gamma (or beta) dose, and ED is found as the intercept on the dose axis. Experimentally, two sets of NTL samples are irradiated, one providing the growth curve, the second receiving a short sunlamp bleach before measurement. The difference between corresponding samples, R, is then determined and plotted as a function of dose. In practice it was preferable to plot the growth and bleached curves independently, ED being found from their intersection. (see Fig. 1.8.1.)

While this method is in principle the only established technique applicable to poorly bleached sediments, in practice the unknown duration and spectrum of the depositional exposure makes selection of the correct laboratory bleaching conditions an educated guess at best. Problems of overbleaching (or underbleaching) are then possible. Consequently it is probably prudent to restrict use of the R-Γ method to sediments for which a reasonable estimate of depositional exposure can be made.

A further class of sediments for which this method may not perform to expectations is young, well bleached sediments, where the errors in extrapolating the N+γ and N+γ+SUN curves can dominate the ED. At the other end of the time-span measured by the quartz TL "clock", old sediments exhibiting non-linear TL growth are ruled out by the method's reliance on linear extrapolations. However, the volume of apparently successful dating work published based on this method indicates an otherwise general applicability.

Total Bleach Method

Introduced by Singhvi et al, (1982), the total bleach method assumes that predepositional bleaching reduced the geological TL to the residual level I_o, beyond which bleaching does not proceed. At least one full day of sunlight exposure is assumed. I_o can then be approximated in the laboratory by a long sunlamp bleach, typically 1000 minutes, and expressed as a fraction R of I_{NAT}:

$$R = \frac{I_o}{I_{nat}}$$

Previously I_{nat} was resolved into a bleachable component I_d and the unbleachable residual I_o, hence I_d in terms of R gives $I_d = I_{nat}\ (1-R)$. Graphically, the growth curve extrapolated to the dose axis yields ED as the intercept with $TL = I_o$, (see Fig.1.8.2.). Advantages of the total bleach method are simplicity, non-reliance on a linear growth curve and no bleach-induced sensitivity changes (as no post-bleach data are required). A disadvantage is the possibility of incorrectly

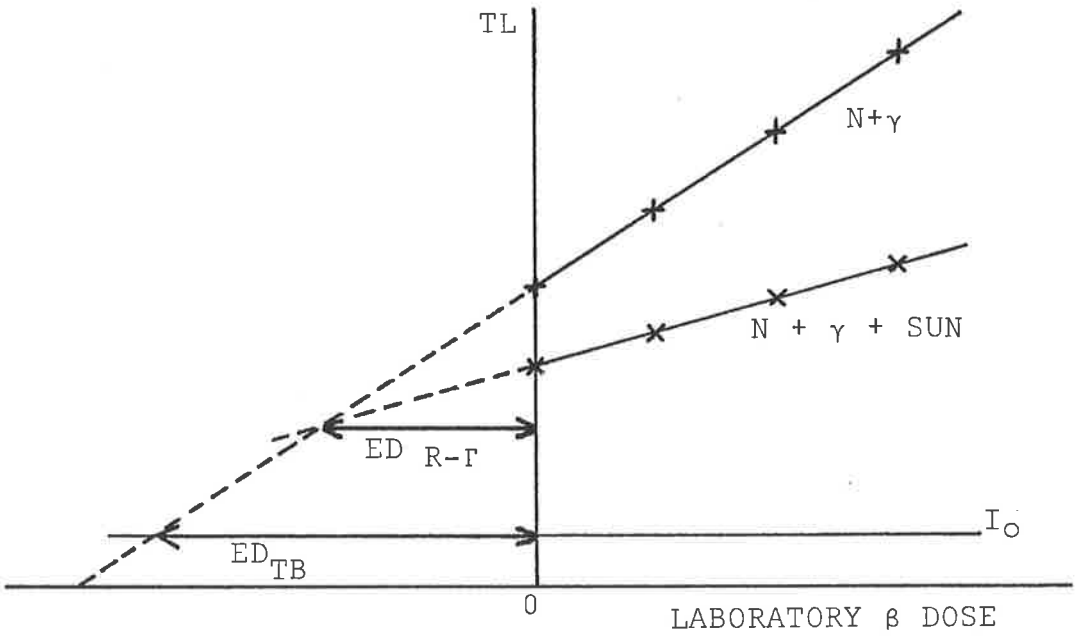

FIG 1.8.1. The R-Γ method - "Partial Bleaching". Two similar sets of samples are γ (or β) irradiated, one then also receives a short sunlamp exposure. The intersection of the bleached and unbleached growth curves yields the correct ED.

In comparison, the total bleach method (shown) would overestimate ED. (After Huntley, 1985).

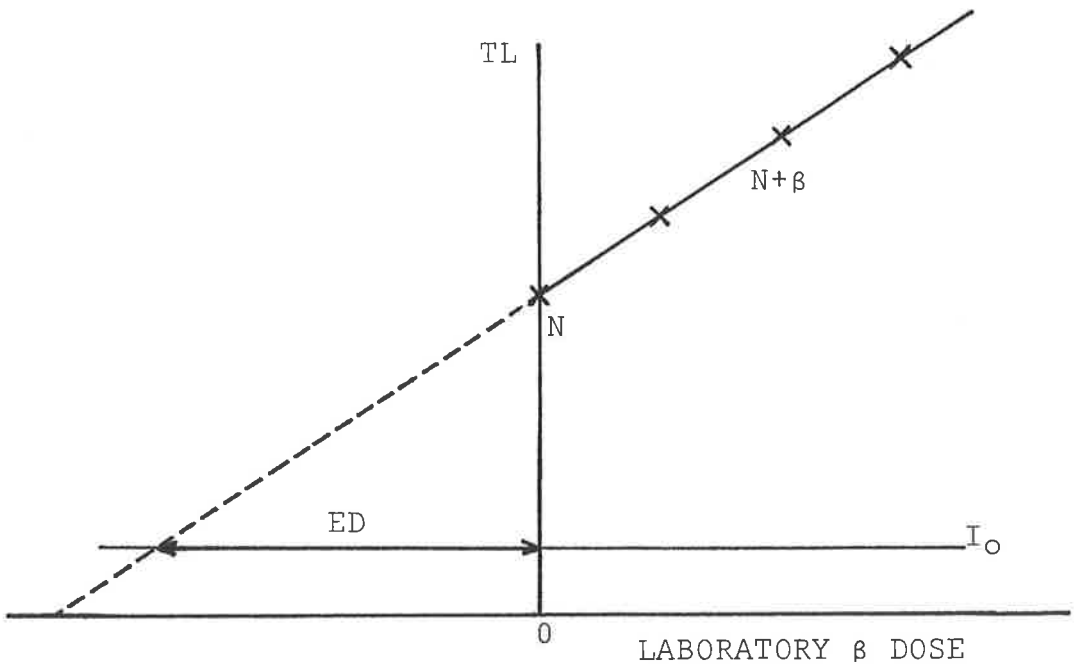

FIG 1.8.2. The Total Bleach Method.
The additive dose growth curve is extrapolated back to the dose axis; ED is found from the intersection with $TL=I_o$.

reproducing I_o, usually by overbleaching, and so incorrectly determining I_d. This technique is generally inapplicable to waterlaid and other poorly-bleached sediments.

Total Bleach-Regeneration Method

Introduced independently by Prószyńska (1983) and Debenham and Walton (1983), this method makes the same assumption as total bleaching in that predepositional exposure was sufficient to reduce the TL level to the unbleachable residual I_o. Here however, a set of samples totally bleached in the laboratory are administered radiation doses to produce a regenerated growth curve. ED is that dose required to match the NTL level (see Fig.1.8.3.). A significant advantage shared with the TB method is the possibility of estimating ED for samples showing non-linear growth.

Key stipulations by Debenham and Walton are that the laboratory bleaching has (a) accurately reproduced the depositional TL level and (b) not altered the TL sensitivity (the 1st growth and regenerated growth curves have the same slope). Although Prószyńska states "common minerals exposed to sunlight or mercury sunlamp do not change their TL properties in the 250-350°C region", this must be considered a questionable assertion (Wintle, 1985) and bleaching induced sensitivity changes pose unresolved problems for this method.

The above three methods currently form the basis of TL sediment dating, and though there is much promise in the new quartz-feldspar and optical methods, these are outlined below largely for the sake of completeness, as they have not yet received widespread application.

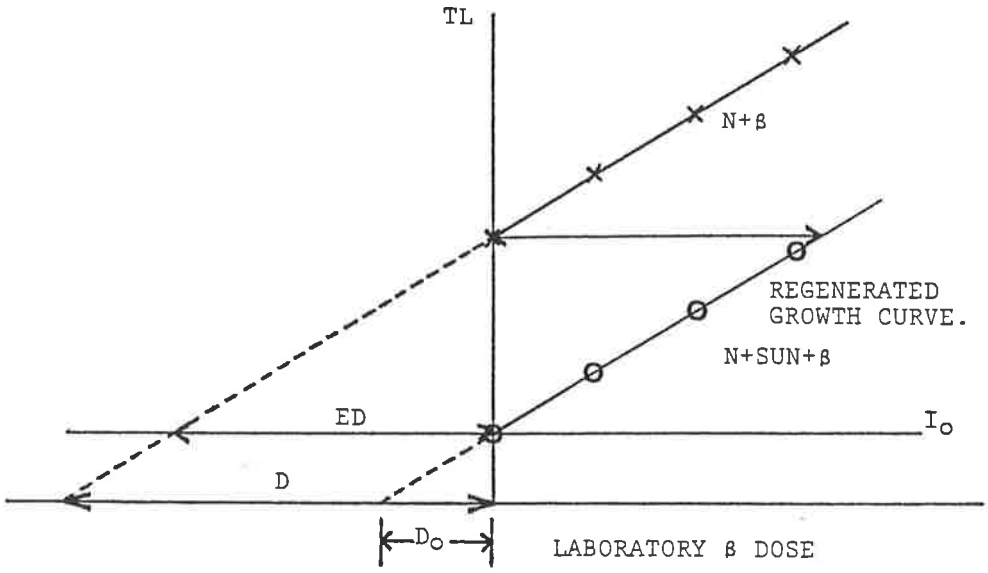

FIG 1.8.3. The Total Bleach-Regeneration Method. Key assumptions are that predepositional bleaching proceeded to the residual level I_o, and that no sensitivity changes occurred on bleaching in the laboratory.

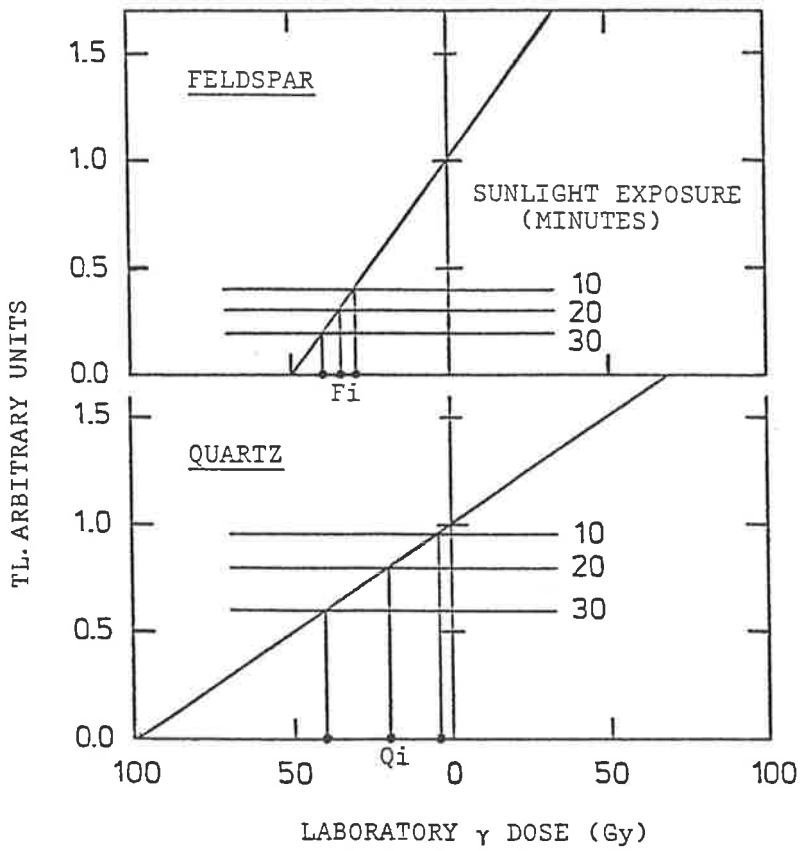

FIG 1.8.4. The Quartz-Feldspar Method.

The intersections of the residuals resulting from various sunlight exposures with the growth curves give sets of ED -the Fi and Qi. The correct bleach time, t, gives an ED ratio F_t/Q_t equal to the F/Q dose-rate ratio. (After Mejdahl, 1985).

Quartz-Feldspar Method

Mejdahl (1985) proposed this method to utilize the different bleaching rates and dose rates of quartz and feldspars. The assumption is that only one bleach time exists that will bleach to precisely the depositional TL level. Given that suitable coarse grain quartz and feldspars can be separated from the same sample, the correct bleach time is found as follows:

(1) Construct the quartz and feldspar growth curves.

(2) Simultaneously bleach aliquots of quartz and feldspar for various times. The intersections of the resultant TL levels with the growth curves allows the ED ratio Fi/Qi to be evaluated for each bleach time, (Fi and Qi are the feldspar and quartz ED's for the i^{th} bleach time).

(3) The correct bleach time is that which produces an ED ratio equal to the feldspar/quartz dose rate ratio. (See Fig.1.8.4.).

This method has not yet been widely applied, although preliminary work by Mejdahl (1985) on some young aeolian deposits seems promising.

Drawbacks are the need for suitable quartz and feldspars in the same sample, and limitations imposed by the relatively early saturation of quartz. The volume of laboratory work required is also a disadvantage, though a short-cut is possible if a relation exists between the quartz and feldspar residuals. Mejdahl empirically determined the approximation Res. (Feldspar) = 0.5 x Res. (Quartz) for a glacial sand deposit examined and showed this permitted a reasonable ED ratio to be found.

This technique is still under development.

Optical Stimulation Method

Introduced by Huntley et al (1985), the optical stimulation method relies on there being a component of trapped charge readily bleachable by visible light. It is found that any predepositional bleaching exceeding the equivalent of about 10 seconds of sunlight will completely erase this TL. A novel departure from previous TL reading techniques is that optical rather than thermal activation is used to untrap this light sensitive component. The 514.5 nm (green) light from an argon-ion laser was chosen as the stimulating wavelength, only untrapping the readily bleachable TL acquired since deposition. A great advantage of probing only these bleachable traps is the elimination of the need to estimate a residual TL level. Preliminary work has found this method satisfactorally resolved discrete depositional events in two sequences (stranded South Australian beach dunes, aged from 0 - >700 ka, and quartz extracts from soils formed on aeolian parent material, aged 0-6 ka), and determined the ED of three samples of known age (Huntley et al, 1985).

1.9 Some applications of sediment dating

Given the criterion of predepositional exposure to sunlight any bleachable sedimentary material is in principle datable by TL - this has motivated applications of the technique to a wide range of sediments. These are perhaps best grouped according to the landform dated.

The major categories are then dune sands, loess, marine sediments and various fluvial deposits. Less well established are applications such as the dating of glaciers or polar ice sheets by the TL of their aeolian dust load (Bhandari et al, 1983), and discussion here will exclude these.

Dune Sands

Lengthy bleaching can frequently be assumed for dune sands, and has permitted successful dating, usually by the total-bleach (TB) or total bleach-regeneration (TB-R) methods. The TB method was proposed, and first used, by Singhvi (1982) to date the Thar desert, Rajasthan, India. Both polymineral fine-grains (1-8μm) and coarse grain quartz (100μm) were eventually used, and in general the dates agreed.

More recent are some European studies. Bluszcz and Pazdur (1985) used 150μ quartz and the R-Γ method on samples from aeolian dune profiles in Poland. Six of the fourteen dates appeared correct, the remainder gave varying overestimates due to overbleaching in the laboratory (24 hours sunlamp).

Jungner (1985) in Finland compared the R-Γ (30 minutes bleach) and TB (20 hours bleach) methods as applied to 100-300μm quartz and feldspar fractions from post-glacial dunes of known age. Results agreed with accepted ages, except for the quartz based value found for the only glaciofluvial deposit examined; this was 300% high, the discrepancy being attributed to insufficient zeroing at deposition.

Australia. The Adelaide group has determined a chronology for aeolian dune sands at Roonka, South Australia. This site shows evidence of human habitation for back to 20ka BP, and is of major archaeological significance. The dates determined by applying the total bleach method

(60 hours sunlight) to 90-125μm quartz generally concurred with ^{14}C dates, where these were available (Prescott, 1983, Prescott et al, 1982).

The Lake Woods (Northern Territory) site was a case requiring only that the antiquity of a landform was verified. 90-125μm quartz gave an age of about 20ka, compatible with geomorphological evidence (Hutton et al, 1984). Current investigations concern a sequence of stranded beach dunes in the South-East of South Australia representing a series of discrete depositional events over the last ~600ka. 90-125μm quartz grains reveal increasing TL with age for the whole time-span; these dunes therefore constitute an ideal test sequence for TL techniques over this time range (Huntley et al, 1985).

Readhead (1982) has reported dates from two sites at Lake Mungo (N.S.W., Australia). The TB-R method with 90-125μm quartz gave ages similar to ^{14}C findings.

Marine sediments

As mentioned previously, TL sediment dating originated with the discovery of a TL/core depth relationship in deep ocean cores. The earliest marine TL dating program, by Wintle and Huntley (1979a,b, 1980), used 4-11μm detrital grains from North Pacific and Antarctic Ocean cores. Deep ocean cores are significant in that they preserve an unbroken record of sedimentation, and so contain palaeoclimatic information unavailable from terrestrial deposits.

Continental Margins. Spencer Gulf (Australia) cores have been dated using polymineral fine-grains (4-11μm) and 90-125μm quartz grains (Smith et al, 1982; Smith, 1983; Belperio et al, 1984). Comparisons between ^{14}C, geological predictions and TL dates generally gave good agreement,

with some instructive exceptions. Polymineral fine-grain samples gave low ages due to anomalous fading; when the fading component was removed by hydrofluorsilicic acid (H_2SiF_6) treatment, the remaining grains, quartz, gave correct ages. Also, some coarse grain quartz samples gave unacceptably large ages for geologically young deposits. The suggested explanation was preferential bleaching of the lower temperature NTL by the reddened sunlight transmitted through the Gulf waters, given the entire sedimentation process occurred underwater.

Castagnoli et al (1982) studied sediment cores from the Tyrrhenian sea, and found an apparent correlation of TL intensity peaks with historical supernovae events. However, there are major queries concerning this interpretation. Chief of these is how grains, which of necessity were irradiated in the upper atmosphere, could, in spite of solar bleaching, retain their enhanced TL signal through prolonged periods of settling in atmosphere and water. Furthermore, enough extra signal must be retained to produce the clearly defined peaks distinct from the background signal from unirradiated material.

Loess

Loess deposits have received much attention, particularly in Europe, and more recently China. The Chinese deposits are potentially a valuable test sequence for TL, analogous to the previously mentioned stranded Australian beach dunes. Most reported work has used separated quartz of various grain sizes up to 100μm, but details are not readily available.

Studies of N.W. Pakistan deposits by Rendell et al (1983) using the TB-R method and 2-10μm fine-grains revealed complex sensitivity changes induced by laboratory bleaching, and more recently (Rendell, 1985), difficulties regarding water content estimation.

Europe. Dating programs have been undertaken for a number of European sites. The most significant finding is the possibility that fading may put severe age limitations on the applicability of polymineral fine-grain techniques. Studies by Debenham (1985), Northern France, Wintle (1985), St. Romain, France and Wintle (1985), Karlich, Germany, all yielded an apparent TL age limit of ~120ka. Debenham proposed time dependent loss of luminescence centres as the cause, whereas Wintle proposed dose-dependent sensitivity changes occurring when the sample was exposed to light. A consequence of these findings may be a move to "reliable" minerals, particularly quartz and K-feldspar, and away from polymineral-mix sampling. Numerous other loess studies are now in the literature, examples being: Wintle, (1981), late Devensian deposits, Southern England, Prószyńska (1983), Wintle and Prószyńska (1983), Prószyńska - Bordas (1985), various Polish loess and fossil soil deposits, Balescu et al (1986) N.W. Europe, particularly Belgium, Borsy et al (1979), Hungary, Singhvi et al (1986), Wintle and Brunnacker (1982), Germany.

Fluvial Deposits

Waterlaid sediments are not ideal for TL dating, though judicious selection of TL method and mineral fraction can permit good results. Quartz has been widely reported as resistant to bleaching under fluvial transportation (e.g., Mejdahl, 1985, Berger, 1985, Hütt et al, 1982), and consequently most studies have used K-feldspars or fine-grains. Notable work has been performed in Denmark (Kronborg, 1983, Mejdahl, 1985,) Canada (Berger and Huntley, 1982, Lamothe, 1984, Berger, 1984, 1985a,b, Huntley, 1985), Scotland (Murray et al, 1983), Finland (Jungner, 1983) and Eastern Europe (review by Hütt et al, 1982).

1.10 The bleaching of quartz

Following the discovery that exposure to sunlight was the dominant mechanism for zeroing sediment TL, and the ensuing development of bleach-based techniques to evaluate ED, it has become clear that a necessary element to remove much of the empiricism from sediment dating is an understanding of the behaviour of sediment TL when exposed to sunlight.

Although estimating the TL level at deposition has remained a central problem in sediment dating, little systematic work examining bleaching properties of common minerals has been carried out. With reference to quartz, most published work originates from studies ancillary to dating programs - the bleaching of quartz NTL by natural sunlight has received very little attention per se. Furthermore, the few studies existing have used either excessive radiation doses, or "unnatural" photons in the illuminating spectrum, or both. Extrapolating from such experiments to the natural sunlight bleaching of sedimentary quartz NTL seems an uncertain proposition at best.

The aspects of the bleaching mechanism of direct relevance to dating applications are briefly discussed below. Though interrelated in effect, they may be broadly classed as (1) the effect of exposure duration, (2) the relative efficiencies of various wavelengths, (3) sensitivity changes induced by bleaching, (4) dependence of the rate and ultimate extent of bleaching on temperature. Fig. 1.10.1 shows a selection of bleach curves for quartz samples exposed to broad spectrum light sources or natural sunlight.

Detailed comparisons are precluded by the dissimilarities of both quartz and bleaching conditions, though some generally valid observations may be made. The curves are characterised by an approach to a "residual" level, typically within 2-3 hours, followed by a slowing and apparently

monotonic reduction thereafter. Similar behaviour, observed in deep ocean sediments (Fig. 1.10.2, no.(1), and Fig. 1.10.3, no.(1)) by Wintle and Huntley (1979a,b) led to the representation of I_{nat} as $I_o + I_d$, and forms the physical basis of the long bleach methods. The same authors noted and utilized the similar fractional reductions given by similar bleach times.

Huntley (1985) concluded from the non-exponential form of the bleach curves that there is a variety of traps, each having a specific sensitivity to optical bleaching. The R-Γ method was based on this observation, being designed to separate the readily bleachable component on the assumption that it at least was removed during deposition.

Bleach curves, while mainly due to untrapping, also involve contributions from retrapping, and possibly from changes in luminescence efficiency. However, useful conclusions can be drawn from a model in which only untrapping, retrapping and recombination processes occur. Levy (1982), considering the case of a material with one glow-peak, a bleaching rate proportional to trapped e^- concentration and in which only e^-'s are thermally untrapped, derived the equation for trapped charge concentration as a function of bleach time:

$$\frac{dn_1}{dt} = (-1)\left(\Phi n_1 \sigma_{u1}\right)\left[1 - \frac{\sigma_{t1}\,(N_1 - n_1)}{\sigma_{t1}\,(N_1 - n_1) + \sigma_r\, n_r}\right]$$

where Φ = photon flux

n_1 = trapped e^- concentration at time t.

σ_{u1} = cross section for photon induced untrapping.

σ_{t1} = cross section for retrapping from the conduction band.

N_1 = total number of e^- traps, containing n_{o1} electrons at t = 0, hence $(N_1 - n_1)$ = concentration of empty e^- traps.

n_r = trapped hole concentration.

σ_r = cross section for recombination at hole site.

Solving yields $$t = \frac{1}{(\Phi\sigma_{ul})} \left[\frac{\sigma_{tl}}{\sigma_r} N_1 \left(\frac{1}{n_1} - \frac{1}{n_{ol}}\right) + \left(\frac{\sigma_{tl}}{\sigma_r} - 1\right) \ell n \frac{n_1}{n_{ol}}\right]$$

if $n_1 = n_{ol}$ at $t = 0$ and $n_1 = n_r$.

Two important conclusions are drawn from the solution. Firstly, we find that $n_1 \to 0$ only as $t \to \infty$, showing trapped charge requires an infinite bleach time to be completely removed. The practical consequence is that while some very long bleach time will reduce the TL to some given low level, optical bleaching alone cannot truly "zero". The residual is therefore not a fixed definite level but depends on the bleaching conditions - specifically, duration of exposure for a given temperature and illumination.

Secondly, the trapped charge vs bleach time curve is non-exponential in form, in agreement with experimental data (see, for example, Fig. 1.10.1, no. (5) and Figs. 1.10.2, nos. (1),(2)), and lending justification to the rationale behind total and partial bleaching methods.

These conclusions hold when the model is generalized to material having two or more glow peaks, and additionally predict that peaks whose traps are empty at the commencement of bleaching will first grow by retrapping, then themselves be reduced as bleach time increases. This behaviour is also experimentally observed (Fig. 1.10.3, nos. (1),(2),(5)). While these findings form a useful predictive and interpretative base for general bleaching studies, they provide no information on the practically important questions of spectral or temperature dependence, or sensitivity changes. Observational deductions relevant to these problems are outlined below.

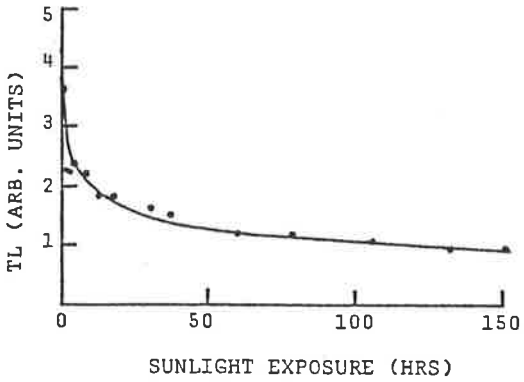

1) Natural Pink Quartz.
Sunlight bleaching
(After David and Sunta, 1981)

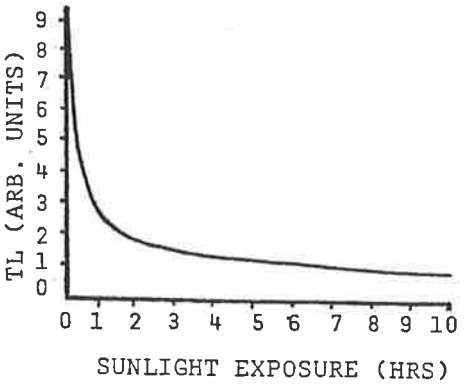

2) Lake Mungo (Australia)
Quartz, 90-125μ grains.
TL at 375°C.
(After Readhead, 1982)

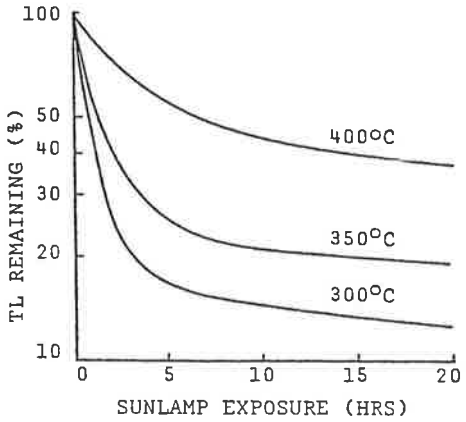

3) Post-Glacial Sand Dunes,
Finland.
100-300μ Quartz Grains.
Bleaching Source - Philips
Black Light Fluorescent Lamp.
TL at temperatures as shown.
(After Jungner, 1985)

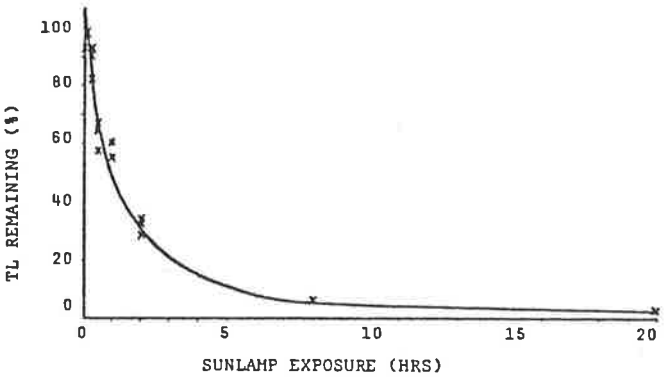

4) Wind-Blown Sand, Holland.
125-150μ Quartz Grains
Mercury Sunlamp.
TL at 360°C.
(After Dijkmans and Wintle, 1985).

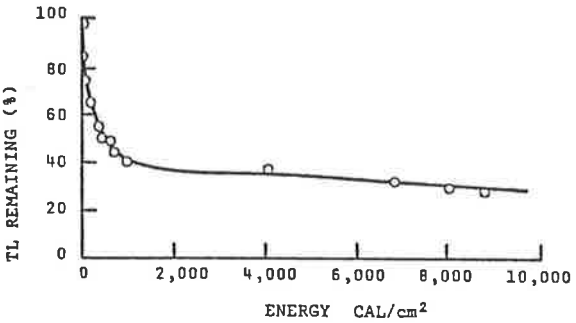

5) Quartz.
Solar radiation, 300-3000 nm.
(From Wintle and Huntley, 1982, after
Vlasov et al, 1979).

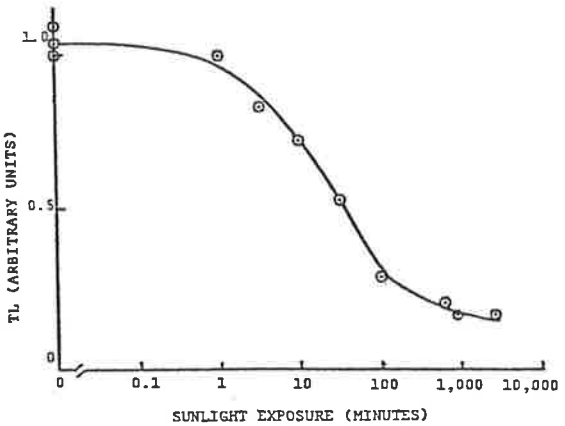

6) South Australian Beach Sand.
100μ Quartz Grains.
TL at 400°C.
(After Huntley, 1985).

FIG. 1.10.1 Bleach curves for a selection of Quartz samples.

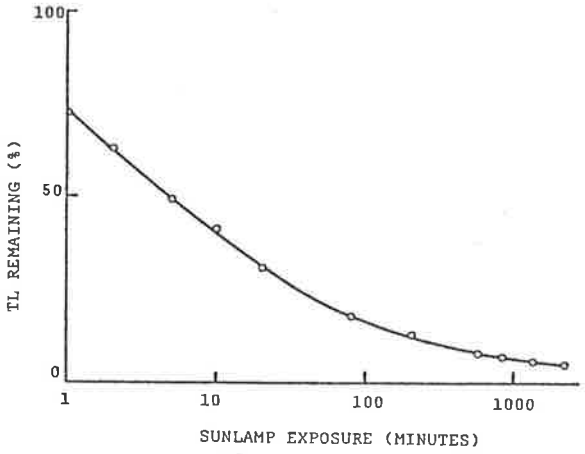

1) Deep Ocean Sediment, Antarctic Ocean.
4-11μ Fine Grains. TL at 300°C.
Sylvania Sunlamp.
Samples received 4 kGy γ dose before exposure.
(After Wintle and Huntley, 1979a).

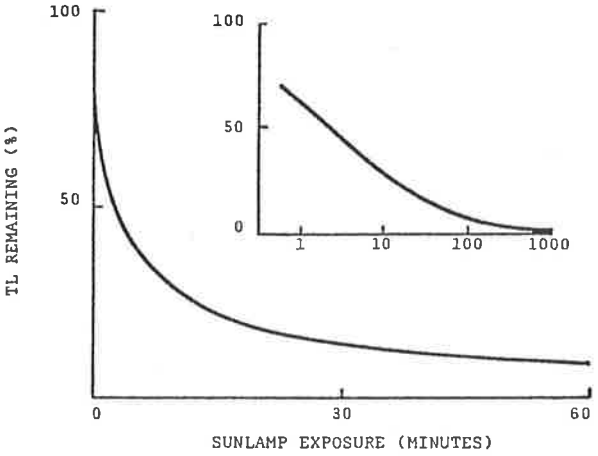

2) River Sediment, Canada.
4-11μ Grains.
TL at 275°C.
(After Huntley, 1983)

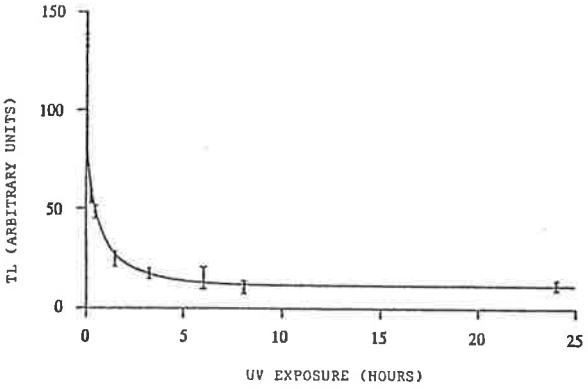

3) Soliflucted material of glaciofluvial origin, Scotland.
Fine Grains. TL at 350-375°C.
Bleaching conditions: 125W mercury discharge bulb, peaking at 365nm, positioned 30cm from samples.
(After Murray et al, 1983)

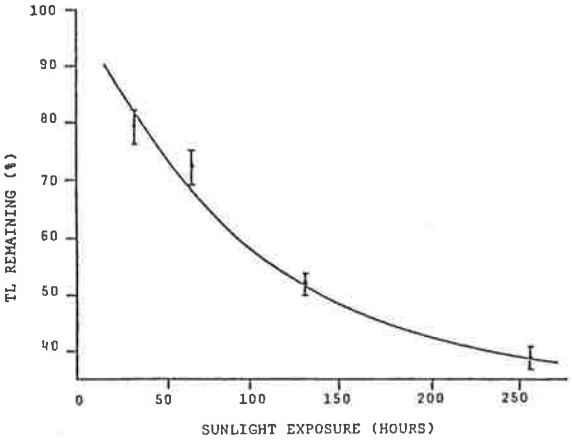

4) Soliflucted material of glaciofluvial origin, Scotland.
Fine Grains. TL at 350-375°C.
Bleaching Conditions: exposed in agitated aqueous suspension to natural sunlight.
(After Murray et al, 1983).

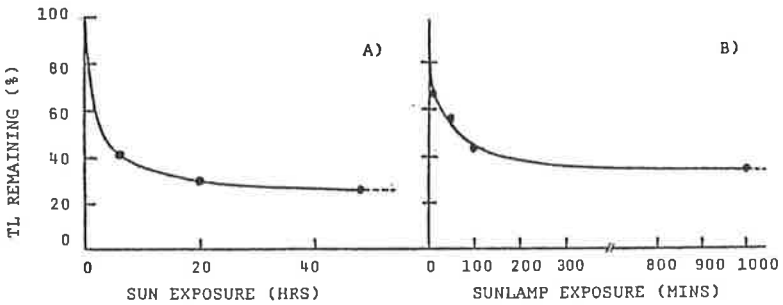

5) Dune Sand, Rajasthan, India.
1-8μ fine grains. TL at 320°C.
Illumination source A) Natural Sunlight, B) 300W "Wotan" Sunlamp, 30cm from samples.
(After Singhvi et al, 1982).

FIG. 1.10.2 Shows Bleach Curves for a selection of Polymineral samples.

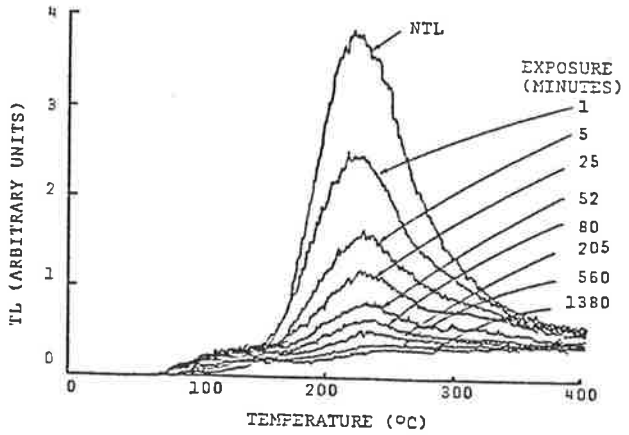

1) Deep Ocean Sediment, North Pacific.
4-11μ Detrital Grains.
UV sunlamp, exposure times as shown.
(After Wintle and Huntley, 1979b).

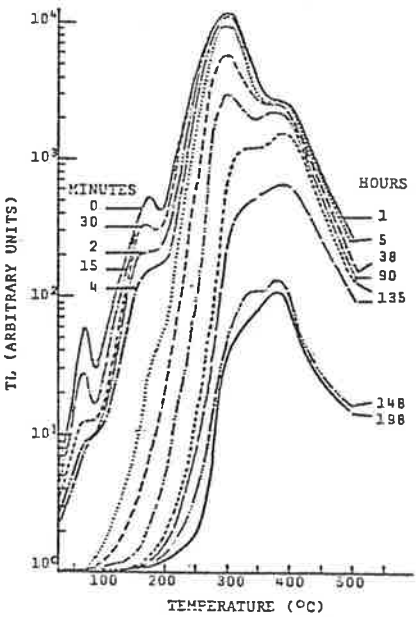

2) Pink Quartz.
10^6 Gy γ dose prior to bleaching.
Illumination source: 40W Philips Mercury Lamp, peaking at 253.6 nm, positioned 10cm from sample.
Exposure times shown.
(After David and Sunta, 1981).

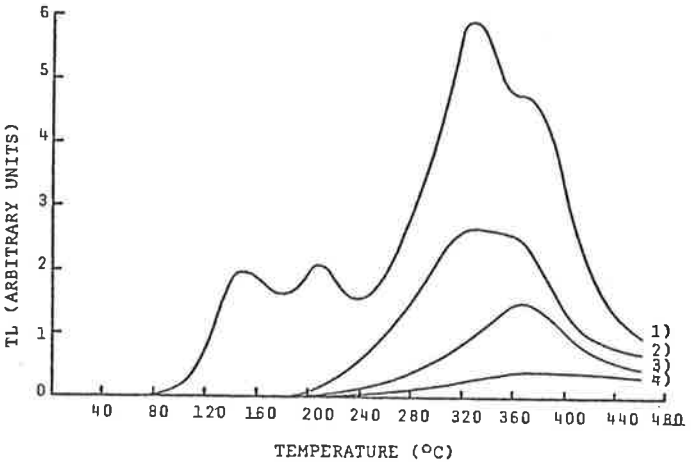

3) Marine Sediment, Spencer Gulf, Australia.
90-125μ Quartz. 1) NTL+40 Gy β, 2) NTL
3) NTL+20 minutes mercury sunlamp. 4) NTL + prolonged (up to 200 hrs) sunlight. (After Belperio et al, 1984).

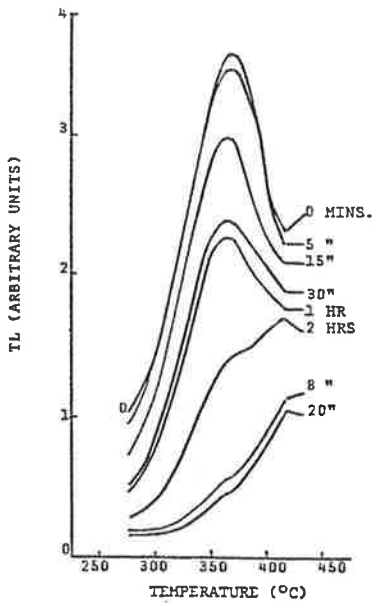

4) Wind-Blown Sand, Holland.
125-150μ Quartz.
Mercury Sunlamp, exposure times as shown.
(After Dijkmans and Wintle, 1985).

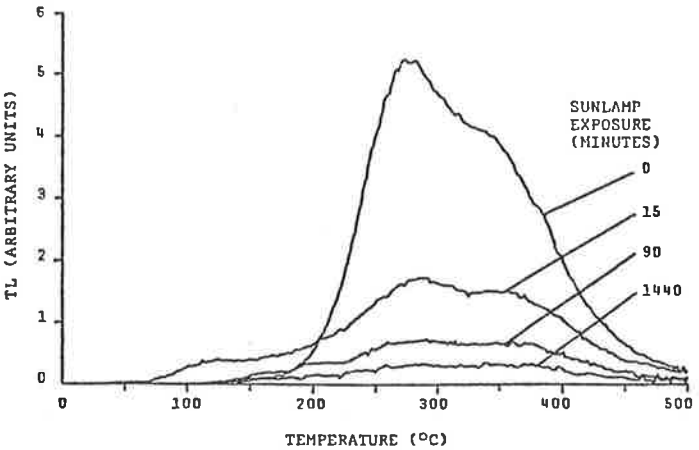

5) Soliflucted material of glaciofluvial origin, N.E. Scotland.
Fine Grains, Natural TL.
Bleaching source - UV sunlamp, exposures as shown.
(After Murray et al, 1983).

FIG. 1.10.3 Shows families of glow curves after various bleach times for a representative selection of Quartz and Polymineral samples.

Wavelength dependence

No systematic study of the efficiencies of various wavelengths for bleaching quartz TL has been performed. Indeed, the work by Kronborg (1983) on feldspars is notable as the only detailed published data on the relative efficiencies of UV and visible wavelengths in bleaching any mineral. Unfortunately, the great differences in the relative bleachability of quartz and feldspars, as shown by Berger (1985a), prevents transfer of Kronborg's findings to quartz. Some conclusions, apparently confirming the consensus that UV is the active bleaching component of the spectrum, are given in a series of papers by Berger and Huntley (Berger and Huntley, 1982; Berger et al, 1984; Berger, 1984; Berger, 1985a,b) in which the applicability of the R-T method to rapidly deposited glaciolacustrine silts was examined. Jerlov (1976) has determined that the solar spectrum, when transmitted through water, is attenuated and shifted towards longer wavelengths by scattering and absorption. From this, Berger and Huntley (1982) then found that restricting the sunlamp spectrum gave better results by removing overbleaching. This procedure was continued in later work and Berger (1985a), concluded that quartz was very resistant to bleaching by wavelengths $\gtrsim$ 400nm, with wavelengths $\gtrsim$ 550nm not bleaching at all.

Phototransfer studies provide additional, though indirect, information. Bailiff et al (1977) found a monotonic increase of approximately 2 orders of magnitude in relative quantum efficiency for phototransfer as wavelength decreased from 360nm to 260nm (sample material Norwegian α- quartz). Assuming phototransfer efficiency reflects the efficiency with which electrons are released from deeper traps, this indicates a correspondingly strong monotonic wavelength

dependence for bleaching efficiency. Supporting evidence is provided by Mobbs (1979) who concluded, from an examination of low temperature phototransfer properties in deep ocean sediment fine-grains, that 320nm, 400nm and 500nm wavelengths probed successively different, shallower traps.

Bleaching underwater - turbidity and attenuation influences

Murray et al (1983) examined the effect of attenuated sunlight on a turbid aqueous suspension, and concluded bleaching still proceeded but at a much reduced rate (see Figs. 1.10.2, nos. (3),(4)). Similar findings came from a systematic study by Gemmell (1985) who exposed a polymineral fine-grain suspension in a flow tank to a UV source. Bleaching rate was found to depend on (1) sediment concentration, (2) flow rate and (3) turbulence.

The reduced bleaching rates found in these laboratory simulations agree with those found in natural situations, and consequently the resistance of quartz to bleaching has so far limited its usefulness for dating in such cases. An example: Smith (1983) deduced from the findings of Jerlov (1976) that preferential scattering and absorption of shorter wavelengths, by modifying the incident sunlight spectrum, resulted in poor depositional bleaching of Spencer Gulf sedimentary quartz, and rendered it undatable by the techniques used. Similarly, Mejdahl (1985) noted that in waterlaid sediments the feldspar fraction gave an acceptable age but quartz was poorly bleached, a conclusion also reached by Berger (1985a).

In summary, it appears that dating waterlaid sediments requires techniques sampling only those traps bleachable by a spectrum low in UV,

similar to that to which they were exposed at deposition. Such techniques are the R-Γ method with a suitably filtered source, and the newer optical dating method.

Temperature effects

The varied environments in which sedimentation occurs permit a range of ambient temperatures - extremes being encountered by dust embedded in Antarctic ice or surface grains in hot deserts. The temperature at which natural bleaching took place may be of significance, particularly to long bleach methods relying on approximating an I_0 level originally reached under conditions that may differ greatly from laboratory conditions. Recognition that laboratory bleaching should replicate the natural situation as closely as possible has led to the practice of cooling samples during laboratory exposures. Nevertheless, there is an absence of formal study on the dependence of bleaching rate and extent on temperature.

Optically-induced sensitivity changes

An effect occasionally reported is a change in sample sensitivity to radiation, activated by optical bleaching. Such changes pose major problems to techniques where the TL measurements are made when irradiation has followed bleaching - the total bleach-regeneration method being most affected.

No model currently exists to provide either an "energy band diagram" or atomic-scale description of the processes involved, or even whether

electron traps, recombination centres or both are being affected. Also unknown are the efficiencies with which various wavelengths induce these changes.

The existence of complex sensitivity changes is well established in loess samples (Rendell et al 1983; Wintle 1985; Debenham 1985). However, the situation for quartz is less clear, with reports varying from "gross changes in sensitivity to γ doses added after light exposure" in fine grain quartz separated from river silt (Berger, 1984) to no changes, for Lake Mungo quartz, 90-125μm fraction (Readhead, 1982). Differences in material and illumination conditions again prevent detailed comparisons.

Huntley (1985) states sensitivity changes are typically small (<10%) and can be found and possibly corrected for by measuring a regenerated growth curve. Two types are postulated: (1) changes in charge trapping efficiency and (2) changes in luminescence efficiency.

Incomplete bleaching

A problem addressed by Jungner (1983) is that found when depositional conditions permit a sediment to contain a mixture of bleached and unbleached grains. Jungner found the apparent sensitivities of additive growth curves from a set of samples to vary almost twofold, although post-bleach sensitivities were within 10%, and attributed this to a fraction of unbleached grains present in the samples. An equation was proposed to correct for this effect:

$$D_o = (1-f)D_1 - f\ D_s,$$

where D_o = corrected ED

f = proportion of unbleached grains

D_1 = apparent ED as determined by the R-Γ method

D_s = additional dose required to reach saturation (hard to accurately define).

The general applicability of this approach is yet to be tested.

1.11 The Aims of this Project

The greatest problems remaining to TL sediment dating are uncertainties regarding water content and radioactive equilibrium, and the extent to which "zeroing" of geological TL progressed during the depositional processes.

The combination of these, and lesser uncertainties, realistically restricts sediment dating to a precision of ~±20%.

Perhaps the dominant source of error is assessing the TL component remaining after zeroing - the "residual". Natural sunlight bleaching has been shown to be the principal zeroing mechanism, and so has become the basis on which current TL sediment dating techniques are founded.

A number of questions have arisen concerning the bleaching mechanism, and its behaviour under varied natural conditions and laboratory simulations. Some of these relate to the rate and extent of bleaching:

1) Is there a monotonic TL decrease with increasing bleach time?

2) Does bleaching proceed uniformly across the entire glow curve?

3) Is the residual an inherently unbleachable component, or is I_o dependent on bleach conditions?

4) Is there a dependence on initial TL level?

5) Is there some recovery of TL following a long exposure?

Further questions are posed by the environmental framework in which bleaching took place:

6) What is the effect of temperature during exposure?

7) Does bleaching under water have any effect?

8) Do natural coatings on grains have any effect?

Finally come the physical and practical questions of

9) What range of wavelengths bleach, and with what efficiencies?

10) Does bleaching alter the TL sensitivity to radiation, and if so, is there a wavelength dependence?

11) Can laboratory simulation effectively reproduce depositional bleaching conditions?

Given the complexities and interrelations of the phenomenon, the aims of this project were to generally examine the effect of light on the TL of natural sedimentary quartz, and so hopefully remove or justify some of the empiricism of current TL sediment dating techniques. More specific goals were: investigation of some factors affecting the residual, particularly duration of exposure, and to determine the bleaching efficiencies of wavelengths present in the solar spectrum.

CHAPTER 2 TECHNIQUES AND INSTRUMENTATION

2.1 Introduction

This chapter describes the procedures used to prepare quartz samples, and introduces the apparatus used for TL measurements and irradiations.

As most of the equipment is commercially available, descriptions are restricted to developmental changes made to the TL reader software (see Appendix 3), and the major features of an accessory purpose-built to facilitate controlled bleaching experiments using an Oriel solar simulator (see section 4.2).

The procedure by which the desired quartz fraction was separated from the parent sediment is outlined, and the technique for spreading the prepared grains onto sample discs for TL work is described and justified in some detail. This technique was developed contemporaneously with a study revealing that not only did considerable intrinsic sample variability exist in "pure" separated quartz (see chapter 6), but that a further component of variability is introduced by uneven sample spreading. The technique was designed to minimize such disc-to-disc TL variations, and also by its simplicity to permit the rapid and reproducible preparation of the large numbers of sample discs required by the planned work program.

2.2 Sample Preparation

This study used only coarse grain quartz (90-125μm) separated from dune sands. The standard coarse grain preparation procedure of the Adelaide TL laboratory was followed throughout. This is closely based on the Oxford method, adapted from the quartz inclusion technique for pottery.

All samples were prepared under subdued yellow light, unless otherwise stated.

The procedure is outlined below.

1. Soak ~50gms sediment for ~ ½ hour in warm ~2.0 molar HCl.
   (mainly to remove carbonates and sulphides).

2. Wash in demineralized water, then 5 minute soak with stirring in 1.25 molar NaOH, in ultrasonic bath (breaks up clay aggregates).

3. Drain, wash to neutrality in demineralized water, dry with methanol then acetone.

4. Dry sieve for 90-125μm fraction.

5. Magnetic separation (Franz magnetic separator, set at 20° slope, 2A current).
   Two passes at each of the three tilt settings:
   +10° (ferromagnetics), -2° (diamagnetics), +2° ("higher" magnetics").

6. Etch in 40% HF acid for 40 minutes, at ~20°C.
   (removes outer discoloured and α irradiated layer, and contaminant mineral grains such as feldspars).

7. Wash in 2.0 molar HCl for ~10 minutes (removes fluorides).

8. Drain, wash to neutrality in demineralized water, dry with methanol then acetone.

9. Store separated etched quartz in stoppered glass vials under light proof conditions.

2.3 Sample spreading

For all TL operations in this study the prepared quartz grains were spread onto stainless steel sample discs, 9.7mm in diameter and 0.5mm thick, and "glued" to the disc surface by a thin layer of silicone oil applied by aerosol spray prior to loading.

The procedure for spreading coarse grains on TL sample discs by disc inversion is presented below, with discussion following.

1. Position TL sample disc in an aperture of the spraying mask (see Fig. 2.3.1).

2. Spray with silicone oil (3% silicone mold release, Crown Corning aerosol pack). It is crucial that the layer of silicone wetting the disc is thin and smooth. A layer thick or uneven

(due to spray "spattering") will produce grain "clumps" and multilayers. The optimum layer mass was found to be ~0.1 mg.

3. Dry at ~80°C for ~3 minutes (hotplate) to remove solvent.

4. Weigh for "Disc + Silicone" weight.

5. Spread quartz as thick levelled heap on clean card.

6. Place disc, wetted side down, onto grains.

7. Apply light pressure to back of disc.

8. Lift disc with tweezers, hold inverted and flick tweezers hard several times to dislodge loose grains.

9. Weigh to find quartz mass.

The maximum possible mass of an ideal monolayer on a 9.7 mm diameter disc, assuming 100μm spherical quartz grains packed in a square lattice, is ~11mg. Given there are ~720 such grains/mg, this corresponds to a maximum of about 8,000 grains/disc.

In this study aliquot masses were held between 6 and 8 mg (about 4,300 to 5,800 grains/disc).

It is important the grains are distributed as a homogeneous monolayer across the full disc surface, as uneven distribution, with multilayers and bare areas, introduces disc-to-disc reproducibility

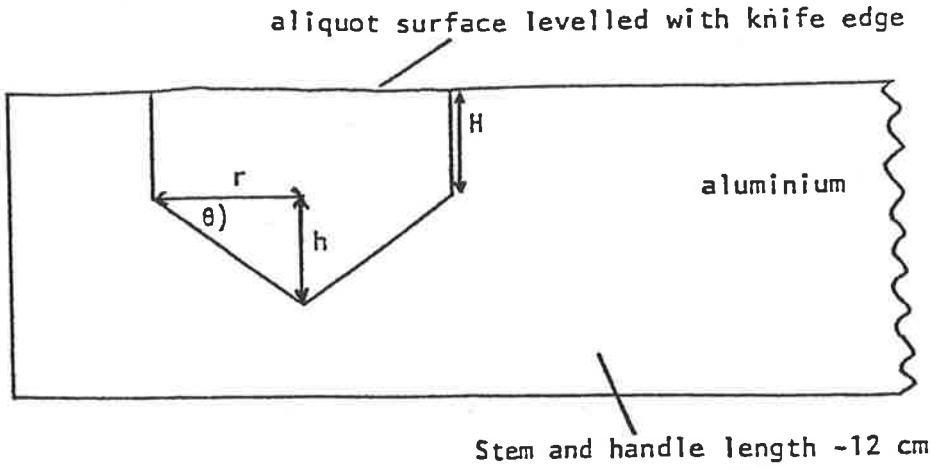

FIG. 2.3.2 Shows a scale cross-section of a phosphor "scoop" fashioned to deliver 5mg aliquots of etched quartz. Dimensions were determined as follows:

Volume required for 5mg aliquot, assuming grains occupy ~2/3 volume, is $2/3\ m/\rho \approx 2.9mm^3$.
Selected design has total volume $V = \pi r^2 (H + \frac{r \tan\theta}{3})$.

For r = 1mm, $\theta = 35^\circ$ (gives a broad shallow scoop enabling easy cleaning) find H ≈ 0.7mm.

Typical aliquot mass reproducibility is ~2%. eg, the above scoop delivers 5.28 ± 0.09 mg (1σ).

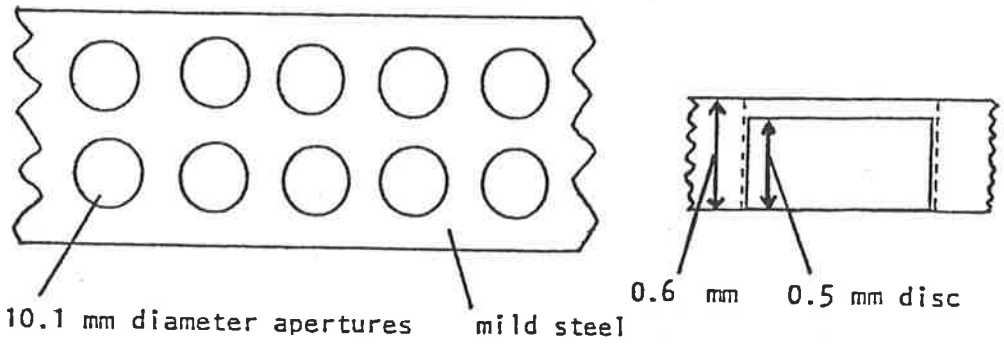

FIG. 2.3.1 Shows plan and cross-section views of the spraying mask used in step (1), (section 2.3) to shield disc rims from silicone spray. Discs should be loaded within ~ 10 minutes of spraying:- longer delays permit the silicone to "creep" onto the rims.

problems for both NTL and ATL, among which are grain transparency and periphery-centre effects. Transparency influences may be either optical (grain coloration) or surface roughness ("frosty" and "shiny") in nature. Periphery-centre effects result from the sample/detector geometry permitting the collection of a greater fraction of emitted TL from centrally located grains. ATL (β induced) is additionally affected by dose build-up and backscattering.

Dose build-up in quartz has been shown by Wintle and Murray (1977) to reach a maximum ≈ 20% above the surface value at ~40mg/cm^2 (for a sample to ^{90}Sr-^{90}Y β source distance of 16mm). A 100μm quartz layer is about 26.5mg/cm^2, so the lower grains of a multilayer configuration receive a greater dose.

Backscattering of β particles by the disc material likewise preferentially doses the lower grains. β irradiation also exacerbates the periphery-centre effect. Zimmerman (1970) found the outermost 10% of grains received ~10% less dose than the innermost 10%, for a 16mm sample to ^{90}Sr-^{90}Y β source distance - a finding confirmed by the author for Lake Woods quartz under similar irradiation conditions. The effect can be minimized by restricting grains to the central region of the disc using an annular mask, though with the greater disadvantage of small sample size - the unavoidable presence of some bright grains in each sample makes the largest possible monolayer mass desirable (see Section 6.8).

These problems are eliminated or controlled if the grains form a homogeneous monolayer over the full disc surface (see Plate 2.3.1). Such a grain distribution on all discs will minimize periphery-centre variations, and also account for dose build-up, backscattering and optical colouration if the β source is calibrated for that particular sample/substrate/irradiation combination. Additionally, Benkö (1983)

found no calibration differences related to the frosty/shiny ratio if a monolayer was used. This is a significant result given the ubiquity of these grain types (see Plate 2.3.2).

When the desirability of large aliquot masses is also considered, the optimum sample distribution is seen to be a full disc surface monolayer. Most techniques for sample spreading are based on the sprinkling of grains onto silicone oil wetted discs, which are then inverted and tapped to remove loose grains. A refinement is to deliver aliquots of known constant mass using various types of phosphor dispenser. To this end, a volumetric phosphor scoop was designed (see Fig. 2.3.2).

The sample spreading procedure then becomes:

1. Place disc in spraying mask aperture.
2. Spray with silicone oil.
3. Dry to remove solvent.
4. Decant measured aliquot onto disc.
5. Hold disc with tweezers above clean card, invert and tap to remove loose grains.
6. "Mop" loose grains off card using wetted disc face.

Although this gives satisfactory known mass monolayers, it does not uniformly cover the full disc surface, hence periphery-centre effects can be significant. It can also be tedious.

Previous tests had shown the silicone mold release to be a sufficiently good "glue" to hold any grains it contacted, and established that its tack was unaffected by drying time or temperature. Utilizing these properties led to the disc inversion procedure given previously,

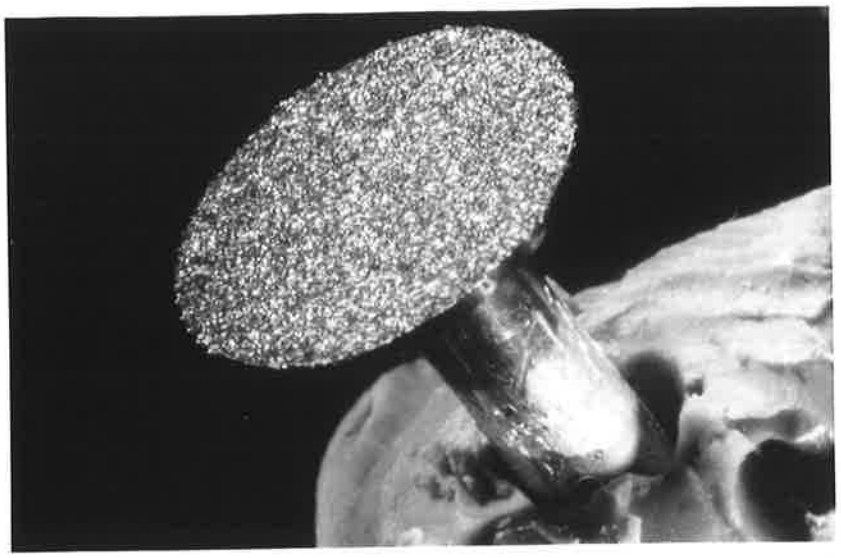

PLATE 2.3.1 Shows a typical disc loaded by the disc inversion technique. The clean rim and homogeneous coverage of the surface are apparent. Sample mass 6.6mg, X7 magnification. (LW(S3,TD,1m) quartz, 90-125μ, HF etched). (The "sparkly" appearance is a consequence of carbon coating for electron microscopy).

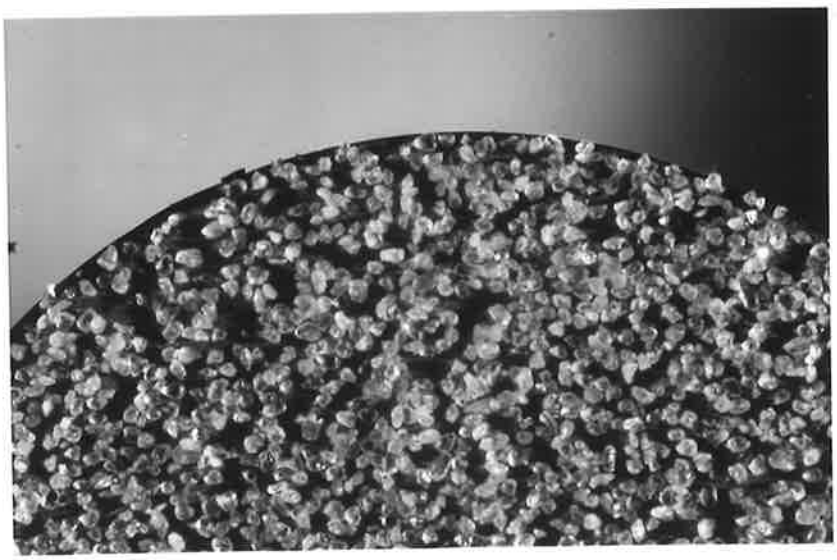

PLATE 2.3.2 Shows a disc similar to the above without the carbon coating. Sample mass 6.8mg, X20 magnification. The monolayer arrangement and clean disc rim are distinct. Also of note is the presence of grains having distinctly different optical appearances - "frosty" and "shiny", along with a range of intermediate types.

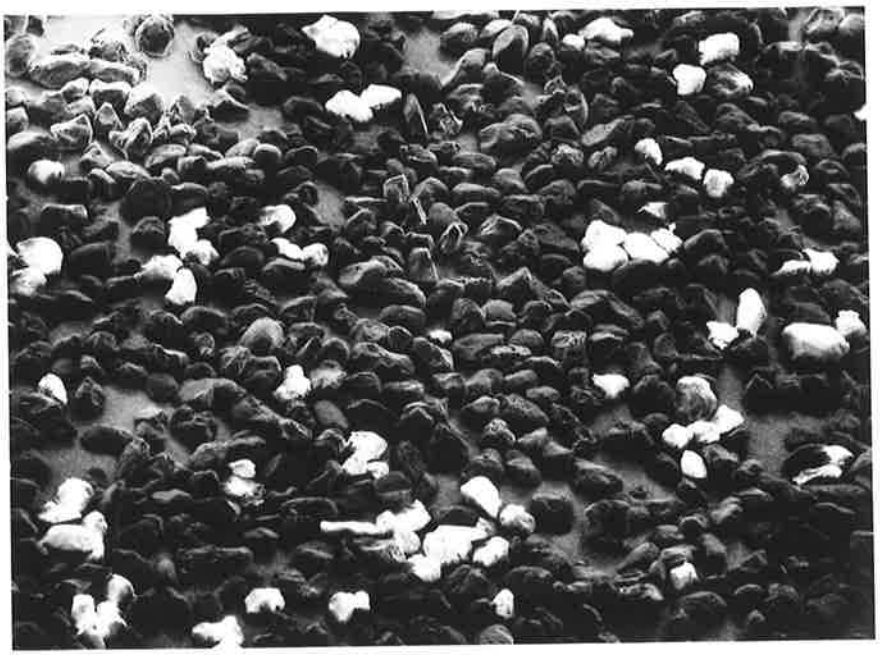

PLATE 2.3.3 Shows a typical area of the disc from PLATE 2.3.1. Minimal grain overlap is seen. The small bare areas are expected for these aliquot masses (ideal square packing could permit a ~11mg monolayer). Charging effects are responsible for the "bright" grains apparent in this X41 electron micrograph.

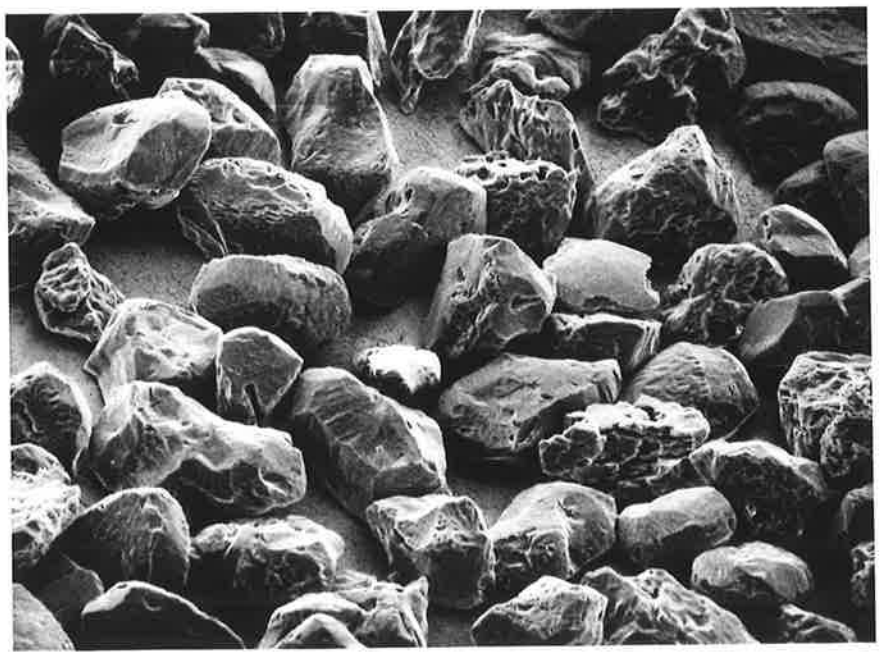

PLATE 2.3.4 Shows a field selected from PLATE 2.3.3 to illustrate the absence of significant grain overlap in even the most densely packed areas.
X137 electron micrograph.

the principle now being to apply the silicone wetted disc to the grains rather than vice-versa.

Problems noted were grains attached to the wetted disc rims, and multilayer and clump formations caused by thick or uneven silicone coatings.

The former was countered by masking the rims during the spraying step (see Fig. 2.3.1), the latter when practice enabled a smooth, thin silicone coating to be routinely applied. There appear to be no other disadvantages. The advantages are those given by a full surface monolayer, and discussed above, as well as the practical benefits of simplicity and reduced risk of inter-sample contamination.

The quality of monolayers produced is consistently high, as the typical examples in Plates 2.3.1 - 2.3.4 show.

2.4 Laboratory Irradiation Sources

Details of the irradiation sources used and some calibration values for coarse grain quartz are given in Appendix 1.

2.5 The TL reader apparatus

This study was greatly assisted by the availability of an automated microprocessor-controlled TL reader system (type TL SYSTEM TL-DA-84) made at the Risφ National Laboratory, Denmark.

The central component is a 24 position sample changer incorporating a nominal 40mCi ^{90}Sr-^{90}Y β source in a timer controlled irradiation unit.

An HP86B computer controlled the hardware, provided data manipulation and high resolution graphics capabilities, and was interfaced to a dual disc drive unit (HP9121) and a printer unit (HP82905B) to provide data storage and hardcopy facilities.

The PMT was an EMI 9635 QA (installed at Adelaide).
The unit was temperature calibrated during construction.
A calibration of the β source for coarse grain quartz on stainless steel is given in Appendix 1.
Appendix 3 contains a brief description of the software, and includes listings of the analysis programs.

Further details of the development of the automated unit can be found in Bøtter-Jensen and Bundgaard (1978), Bøtter -Jensen and Mejdahl (1980), Bell et al (1980) and Bøtter -Jensen et al (1983). The software was completely reviewed by the author and corrected and rewritten where necessary.

CHAPTER 3 SELECTION OF STANDARD MATERIAL AND CONDITIONS

3.1 Introduction

The aims of this project, as outlined previously, are primarily twofold. Firstly, to study the bleaching of quartz by simulated sunlight, with emphasis on the "residual", and particularly the extent to which the division of I_{nat} into I_o and I_d is valid. Secondly, to determine the relative bleaching efficiencies of the various wavelengths present in the solar spectrum. The complexity of the bleaching phenomenon, as apparent from the questions posed in section 1.11, make it a helpful simplification to treat the effects of bleaching as an interdependence on a number of dominant parameters: Φ, λ, t, T and Q. Φ represents the illumination flux, λ the illumination spectrum, t the duration of exposure and T the crystal temperature. Q is a crystal-dependent term accounting for all factors contributing to crystal bleaching susceptibility, such as previous thermal and irradiation histories, impurity content and sensitivity changes.

Such a description provides a framework within which a systematic phenomenological study of bleaching may be constructed. Given this approach, the project aims dictate use of a "standard" quartz, with standard reproducible bleaching and TL measurement conditions, so permitting isolation of the parameters of interest for a given sample.

Control over bleaching conditions was achieved through the use of a calibrated Oriel 1000W solar simulator (see section 4.2). The selection

of the standard quartz and the optimization of glow conditions - heating rate and maximum temperature - are described in this chapter. Also presented are typical TL glow curves and growth curves of the standard quartz, along with some investigations of the effects of specific thermal treatments. Given the variety of published quartz glow curves, this rather detailed characterization is necessary to assist extrapolation of the observed bleaching behaviours to quartz from different origins.

A note on errors. Throughout this report errors are incorporated in the data points unless otherwise indicated. The dominant source of error is found to be intrinsic sample variability (see Chapter 6).
All work was performed on pairs of similar discs, and all glow curves shown are averages of the given pairs. No allowances have been made for intrinsic sample variability, other than discarding the occasional, obviously misfitting, sample disc (typically $\lesssim$ 1 disc in 20).
The uncertainty on glow curves is estimated at $\lesssim \pm$ 5% at all glow curve temperatures.

3.2 Selection of quartz standards

From the range of quartz bearing sediments available, samples were selected from terrestrial sites representing three geological regimes. Comparisons with quartz available from other Australian sources, including commercial building sand and Spencer Gulf marine sediments (see Fig. 1.10.3, no.(3)), revealed a similarity of glow curve forms.

As the extent of pre-depositional bleaching and subsequent NTL regrowth were only well known for the terrestrial samples, further work was restricted to them. The sites are Lake Woods (Northern Territory),

Roonka (Murray Valley) and Robe and Woakwine (South East of South Australia).

Typical ATL glow curves for the 90-125μm, HF etched quartz fractions are shown in Fig. 3.2.1, the NTL being previously erased by twice preheating at 5 Ks^{-1} to 550°C.

The Lake Woods samples were collected from a relic lake-shore dune; laboratory reference Lake Woods, site 3, toe of dune, 1m,(LW (S3,TD,1m)). Further details may be found in Hutton et al, (1984).

The Roonka samples came from the near top and bottom levels revealed during excavation of an aeolian dune at the East bank archaeological site. Sample EB 1/S/0.10 was collected from 10cm below the present-day dune surface, and EB 1/S/2.1 from a depth of 2.1m. For further details: Prescott et al, (1982), Prescott, (1983).

The Robe and Woakwine samples are from the two youngest members of a series of stranded beach dunes, parallel to the South East coast of South Australia (SESA), (Huntley et al, 1985).

As each site provided quartz possessing glow curves of similar form, and high but pre-saturation NTL levels, the criteria for selection of a standard became the practicalities of supply and separation.

Lake Woods (S3,TD,1m) quartz was chosen mainly because freedom from contaminants, notably zircons, gave "clean" glow curves. Further advantages were high yield of the magnetically separated, HF etched, 90-125μm fraction (~ 7% of the bulk sample), and an ample supply on hand.

For experiments planned to compare the bleaching of quartz samples from various origins under similar conditions, the SESA WK 1S/2 and Roonka EB 1/S/2.1 (or the near-equivalent EB 1/S/1.9) samples were chosen.

All work used the 90-125μm quartz fraction, magnetically separated and HF etched as described in section 2.2, unless otherwise indicated.

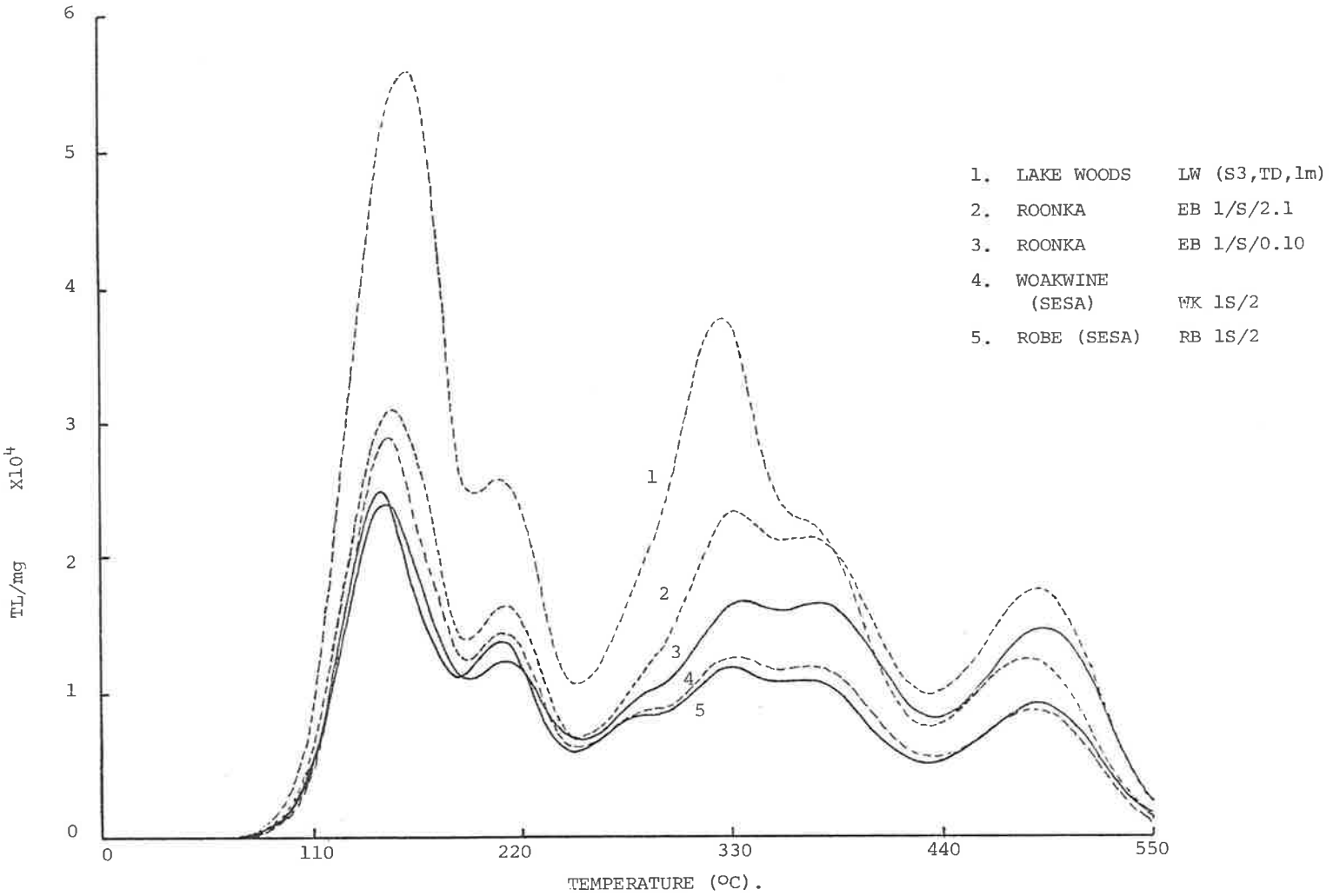

FIG. 3.2.1 Shows mass normalized second glow curves from a range of quartz samples representing the three geological regimes considered in this study.
The 90-125μm fraction, magnetically separated and HF etched, was used in each case.
Conditions: NTL erased by preheating to 550°C; 42 Gy β irradiation; 24 hour delay; heated at 5K/second to 550°C maximum; background subtracted.

3.3 Glow curves and growth curves of Lake Woods quartz

Probably the most important properties for the characterizing of a quartz sample are typical glow curves and the growth curves of the peaks. These are presented and briefly discussed for Lake Woods (S3,TD,1m) quartz, for cases of (a) NTL + various β doses (Figs. 3.3.1, 3.3.2); (b) "low β doses", (2nd glow curves, Figs. 3.3.3, 3.3.4); (c) "high γ doses", (2nd glow curves, Fig. 3.3.5).

Considering each in turn:

Fig. 3.3.1 shows a family of additive β-dose glow curves. Prominent NTL peaks are seen at ~325°C, 375°C and 480°C, and ATL peaks at ~160°C and 220°C. Another, barely discernible, peak appears at ~280°C; this peak is revealed more clearly by an optical bleach just sufficient to remove the 325°C peak (e.g., App. 4, Fig. 1(a)).

No evidence of further peaks was found when heating continued from 480°C to 650°C, the practical limit of the apparatus. The 480°C peak is common to all natural quartz samples so far examined here, regardless of origin. Generally, the observed glow curve peaks coincide with peaks of published glow curves in temperature, if not in relative intensities. For examples, see Fig. 1.10.3., Boden et al (1985), David et al (1977). Fig 3.3.2 shows the growth curves of the prominent NTL and ATL peaks (the 110°C peak has not been considered as it is not used in current sediment dating techniques).

The NTL level corresponds to an ED of ~50Gy. Non-linearity commences simultaneously for all peaks at added β doses of ~30Gy, the total linear region being ~80Gy under these conditions. Assuming that the traps giving rise to different peaks represent different classes of e^- trapping site, it is then most unlikely that simultaneous peak saturation reflects

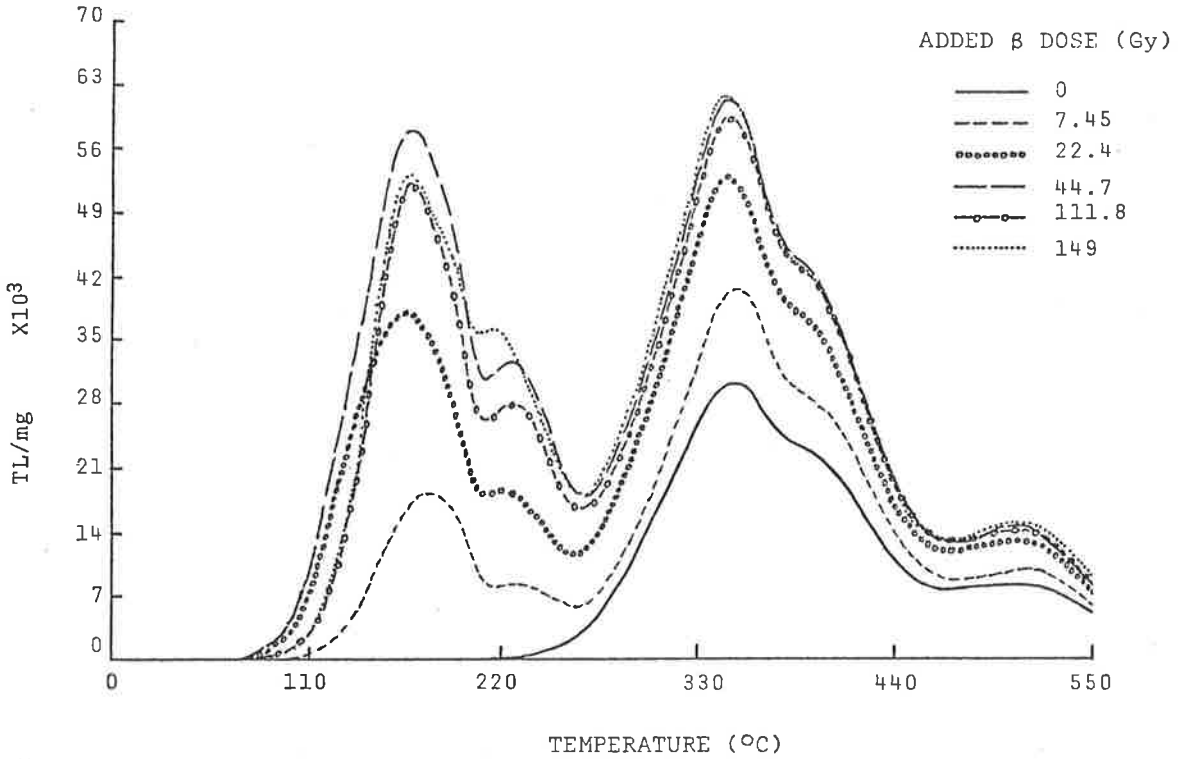

FIG 3.3.1 Shows the growth of TL in natural LW (S3,TD,1m) Quartz for added ^{90}Sr-^{90}Y β doses of 7.45 - 149 Gy.

24 hours delay between irradiation and heating.

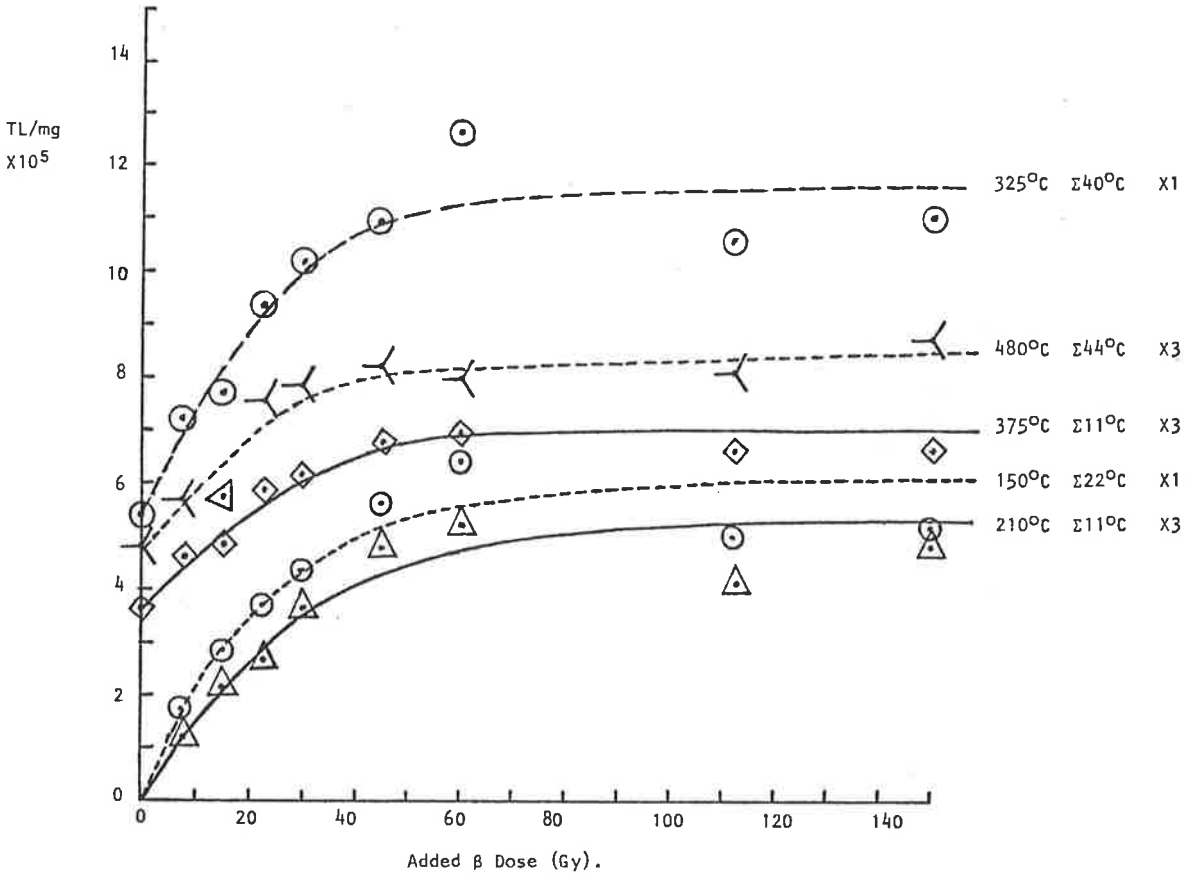

FIG 3.3.2 Growth curves for the prominent higher temperature peaks of Lake Woods (S3,TD,1m) quartz. Added β doses as shown. NTL indicates an ED of ~50Gy. Conditions as shown in Fig 3.3.1.

saturation of the traps, but is due to saturation of the recombination centres. This appears a plausible explanation if only one class of recombination (R) centre is present. TL emission spectra provide evidence that this is the case - these peaks do appear to share a common R centre, giving a broad band emission centred on ~450-470nm and identified with recombination at $(Al^{3+})^{o}$ sites. The equivalence of total glow curve count sums after "saturation" (see Fig. 3.3.1.) can be then interpreted as a consequence of the sample possessing only a limited supply of such intrinsic R centres. This raises a possible consequence for the generation of additive dose growth curves: the onset of non-linearity in laboratory irradiated samples may occur at lower doses than would be the case in nature, due to competition for R centres.

Low β dose growth: thermal drainage of NTL by preheating to 550°C at $5Ks^{-1}$ permitted examination of the regrowth of TL for small added β doses. Although this method of draining TL is not desirable for optically bleached sediments as distorted growth patterns may result from thermally induced changes (for example pre-dosing, sensitivity changes or transparency changes), there is no practical alternative.

Fig. 3.3.3 shows a family of second glow curves for additive β doses up to 7.25Gy; the corresponding growth curves are given in Fig. 3.3.4. Uniform growth is observed across the entire glow curve, in contrast to the report by David and Sunta (1981) that growth of peaks only commenced when the immediate lower temperature peaks approached saturation. Also noteworthy is the significant pre-dosing of the 325°C peak, showing ~50% enhancement of sensitivity, along with linear growth. This agrees with the generally accepted behaviour of the 325°C peak - unwanted pre-dosing has given it the label "malign" in the dating context. In contrast, the "benign" 375°C peak shows no detectable pre-dosing, but does display supralinear growth for up to ~5Gy added β dose.

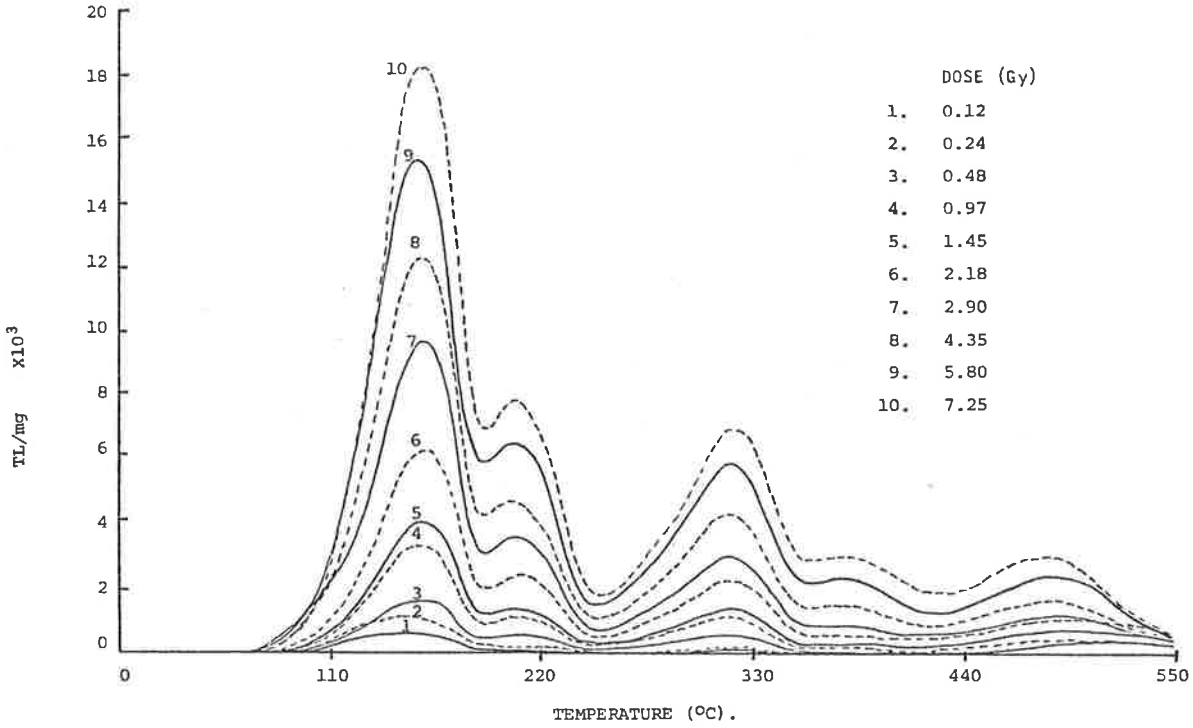

FIG 3.3.3. Shows the growth of TL in Lake Woods Quartz (S3,TD,1m) for ^{90}Sr-^{90}Y β doses of 0.12 - 7.25 Gy. Heating at 5K/second to 550°C followed a 24 hour delay after irradiation. The material had undergone the standard preparation procedure, and the NTL had been erased by preheating to 550°C at 5K/s.

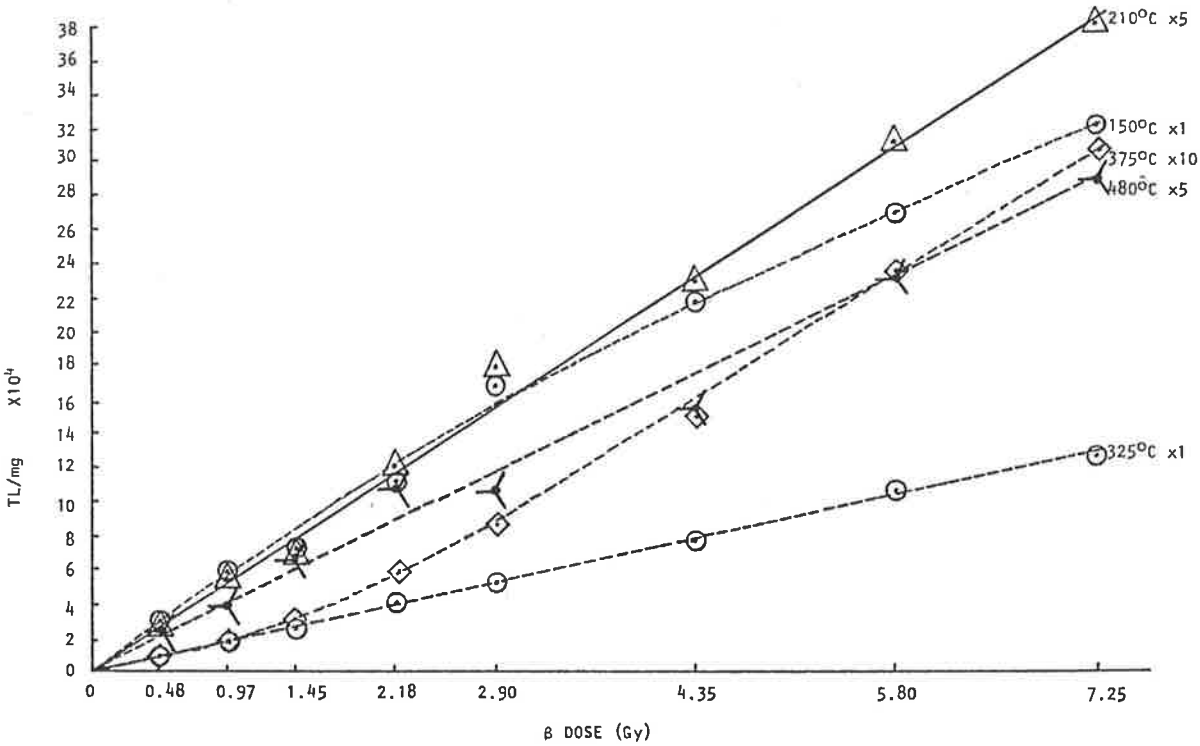

FIG 3.3.4 Shows the growth of the most prominent higher temperature peaks of Lake Woods (S3,TD,1m) Quartz. (Fig 3.3.3).

The growth of ATL at 350°C for ^{60}Co γ doses of 0-3800Gy administered to thermally drained quartz is shown in Fig. 3.3.5. The growth curve consists of a short linear region from 0 to ~100Gy, followed by a non-linear section from ~100 to ~1000Gy, where a second linear region commences. An explanation: the first linear and non-linear regions result from the exponential filling of existing intrinsic traps which use $(Al^{3+})^{o}$ centres for recombination, while the second linear region reflects linear growth of the population of damage created defects (possibly broken Si - O bonds). Similar growth curve behaviour in quartz was described by Hütt and Smirnov (1982), who fitted an equation of the form

$$I = I_o \left[1 - e^{-a\ (D_n + D_a)}\right] + b\ (D_n + D_a).$$

where I_o, a are coefficients related to the trap concentrations and trapping cross-sections.

b relates to the formation of new defects by radiation damage.

D_n is the ED.

D_a is added laboratory dose.

In this model, saturation of the second linear region would only occur when the rate of radiational destruction of traps equals the rate of trap creation. Although this opens the enticing possibility that the second linear region may permit the dating of quartz for ages exceeding 10^6 years, there is also a likelihood of loss of R centres and traps by long time-scale annealing processes at ambient temperatures. Absolute dating based on this section of the growth curve must therefore be regarded as an uncertain proposition at present.

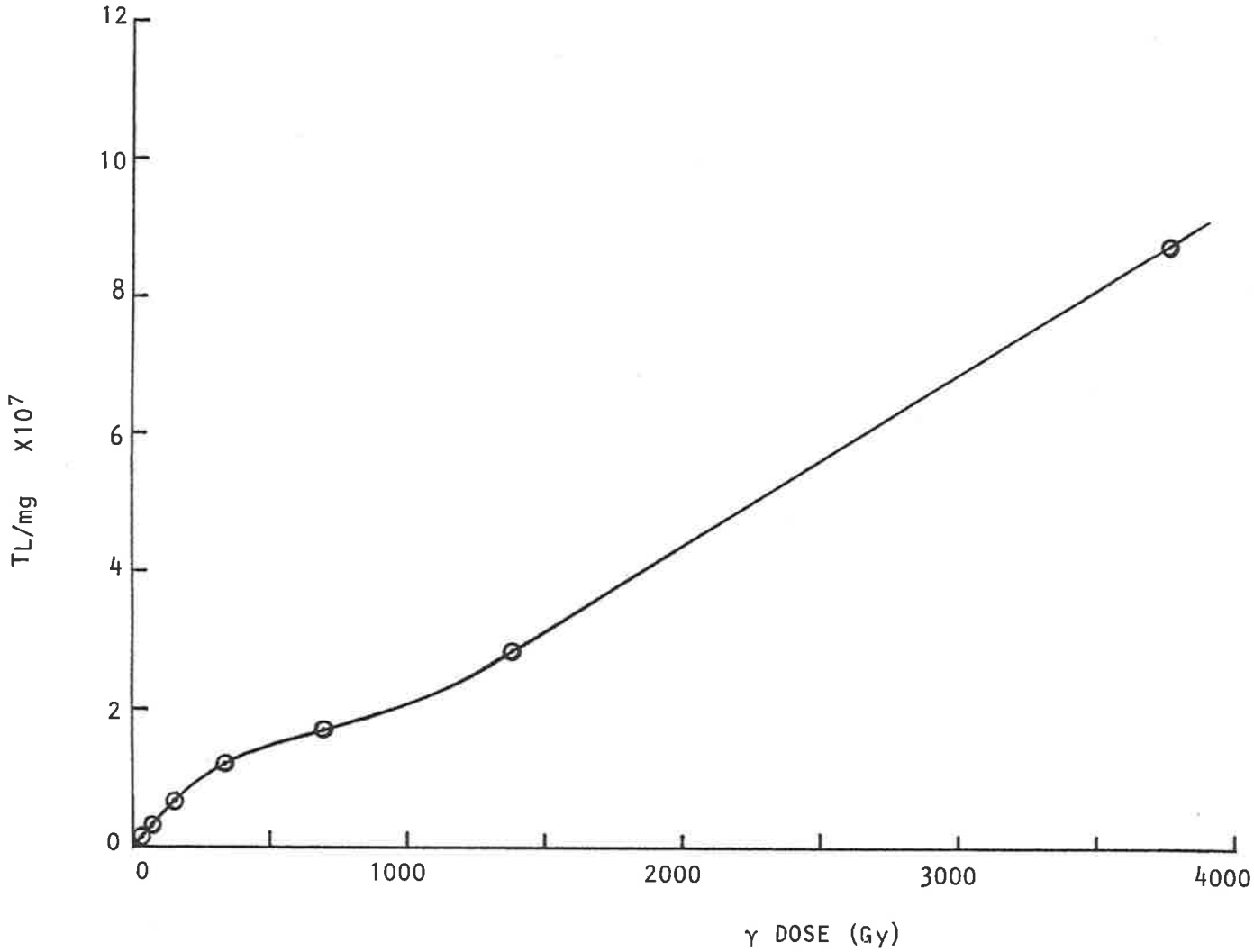

FIG. 3.3.5 Shows the ^{60}Co γ induced growth of TL at 350°C in Lake Woods (S3,TD,1m) Quartz.
Heating: 10K/second to 480°C maximum.

3.4 TL growth and bleaching in annealed Lake Woods quartz

Following the selection of Lake Woods (S3,TD,1m) quartz, it remained to determine what, if any, thermal pre-treatments should be given.

Previously, (Smith, 1983) annealed quartz had been used successfully in preference to natural quartz for laboratory radiation source calibration, largely because of superior disc-to-disc reproducibility. The possibility of similar advantages for bleaching studies motivated inspection of the TL growth and bleaching behaviour of annealed quartz.

Several grams of HF etched, 90-125μm Lake Woods (S3,TD,1m) quartz were annealed at 800°C for 24 hours in an electric furnace then slowly cooled to room temperature overnight. The sample was exposed to air in an open platinum crucible throughout.

Fig. 3.4.1 compares the TL growth at 350°C for annealed and natural LW (S3,TD,1m) quartz.

Annealing enhanced the sensitivity by almost fourfold in the linear region, but non-linear growth commenced at a lower total dose - about 50Gy compared to $\gtrsim$ 80Gy for the natural sample. This behaviour was unexpected: repetition using a well bleached surface sample of Roonka quartz (EB 1/S/0.10) gave similar results, with ~ sixfold enhancement of sensitivity and the onset of non-linearity at a lower dose than for non-annealed samples.

The growth of TL in annealed LW (S3,TD,1m) quartz is shown in Fig. 3.4.2 by a family of glow curves induced by various added ^{90}Sr-^{90}Y β doses. Comparison with Fig. 3.3.1, over the same dose range, reveals major dissimilarities of glow curve form. Although the peaks at ~160°C and 220°C largely retain their relative positions and intensities, those formerly at 370°C and 480°C are no longer detectable. As dose increased to >300Gy, relative peak increases are seen at ~220°C and ~370°C.

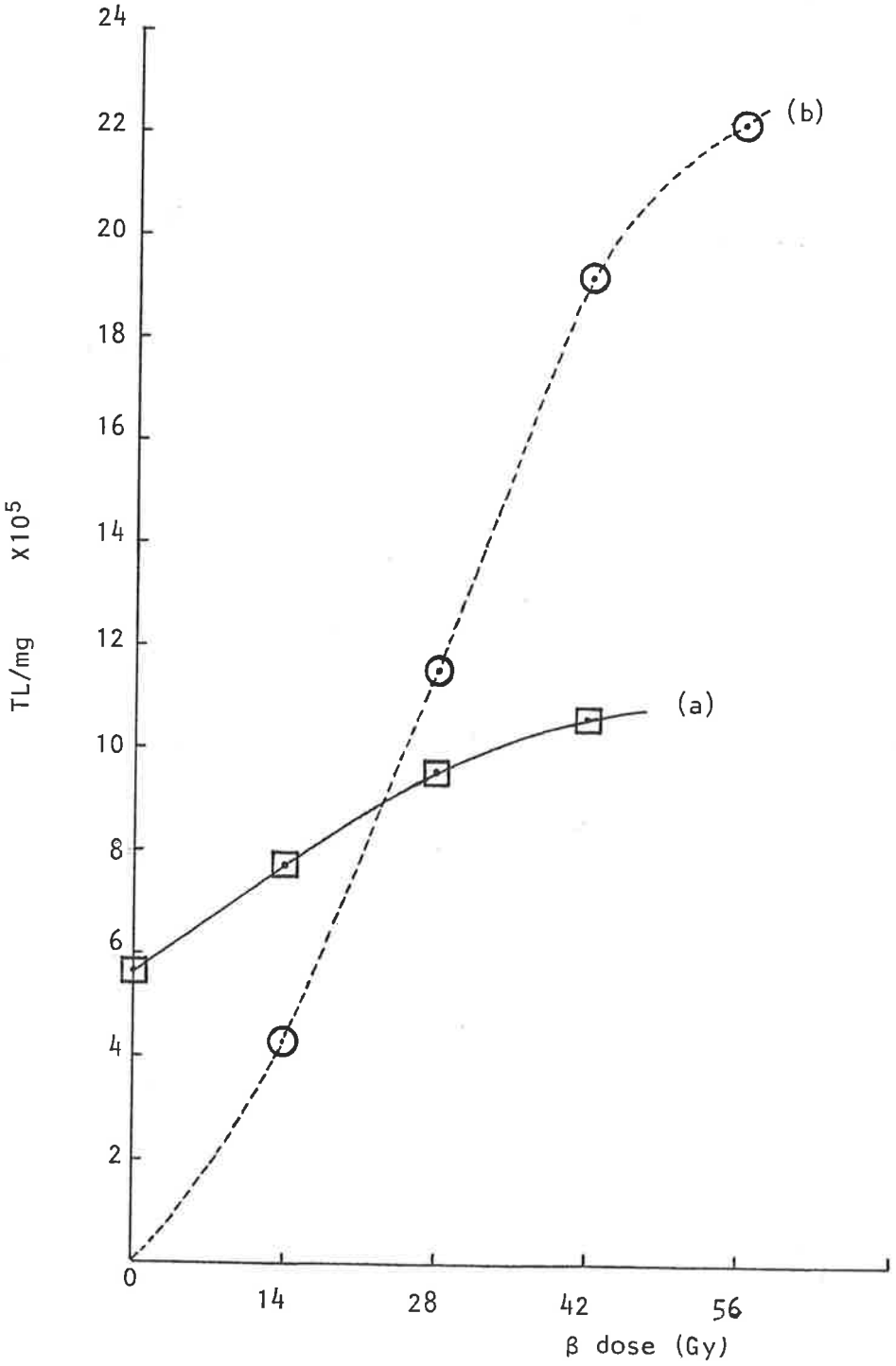

FIG 3.4.1. Compares the responses of (a) natural and (b) annealed Lake Woods (S3,TD,1m) Quartz to ^{90}Sr-^{90}Y β irradiations. The sensitivity of the annealed material is ~3.6 times that of the natural quartz for the linear regions of the growth curves. Summations were of 44°C centred on 350°C in both cases.

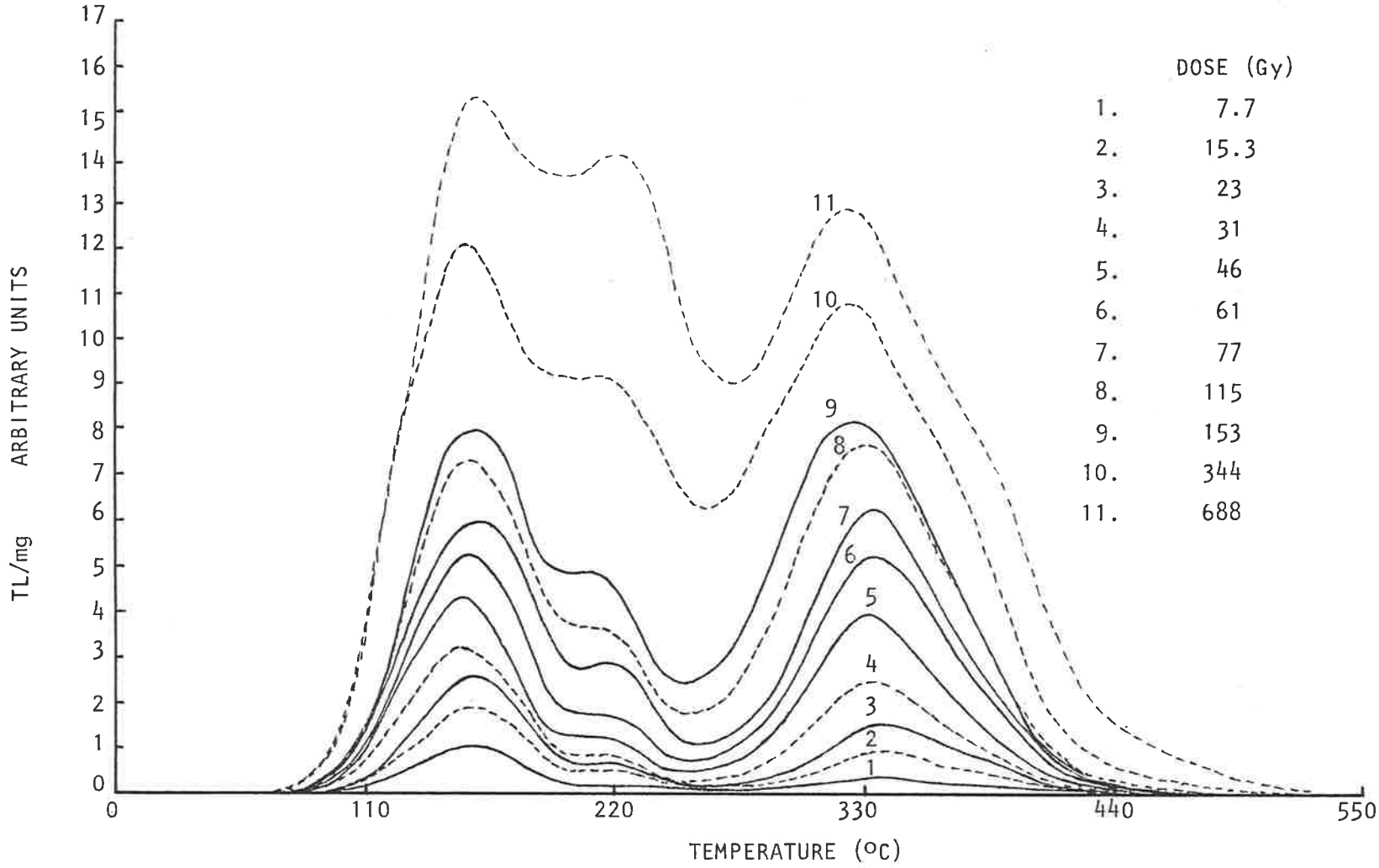

FIG 3.4.2. The growth of TL in annealed Lake Woods (S3,TD,1m) Quartz is shown for ^{90}Sr- ^{90}Y β doses of 0 - 688 Gy.
Annealing conditions: 800°C for 24 hours in air, slow cooling.
24 hour delay between irradiation and TL measurement.

The final test of the suitability of an annealing pretreatment for the stock quartz was an examination of the bleaching behaviour of annealed quartz ATL.

A set of similar samples was given 46Gy ^{90}Sr-^{90}Y β irradiations then stored for one day to permit the decay of the 110°C peak before receiving various simulated sunlight exposures. The results are shown in Figs. 3.4.3 and 3.4.4. A general and rapid early reduction of ATL is seen, followed after ~10 minutes by a slower monotonic decrease. Unexpectedly the resistance to bleaching of the 160°C peak appears comparable to that of the 330°C peak over intermediate bleach times, but the indications are that for exposures exceeding ~1000 minutes a continued exponential decline occurs at 160°C, and a slowing decline at 330°C.

Lack of knowledge of the defects involved in the TL processes (see section 1.2) prevents confident discussion of the thermally induced changes and the subsequent TL behaviour, but some deductions may be made. Defect modification by thermal treatment is known to be capable of increasing or decreasing the sensitivity of various peaks. If the assumption that different peaks correspond to different types of e^- trap is extended by considering several trap types, and hence several peaks, to occur as differing configurations of the same trapping centre, then heating may provide the activation energy to permit relaxation of the centre to some most stable configuration.

The apparent loss of the 370°C and 480°C peaks may be examples of such configurational changes. An alternative possibility is that the traps responsible for these peaks involve broken Si-O bonds, and not "permanent" elemental impurities such as Ge or Ti, and are being annealed out. This proposition may be tested: damage by large doses of ionizing radiation should permit some peak structure related to broken Si-O bonds to be regenerated. Fig. 3.4.2 shows there is no apparent peak

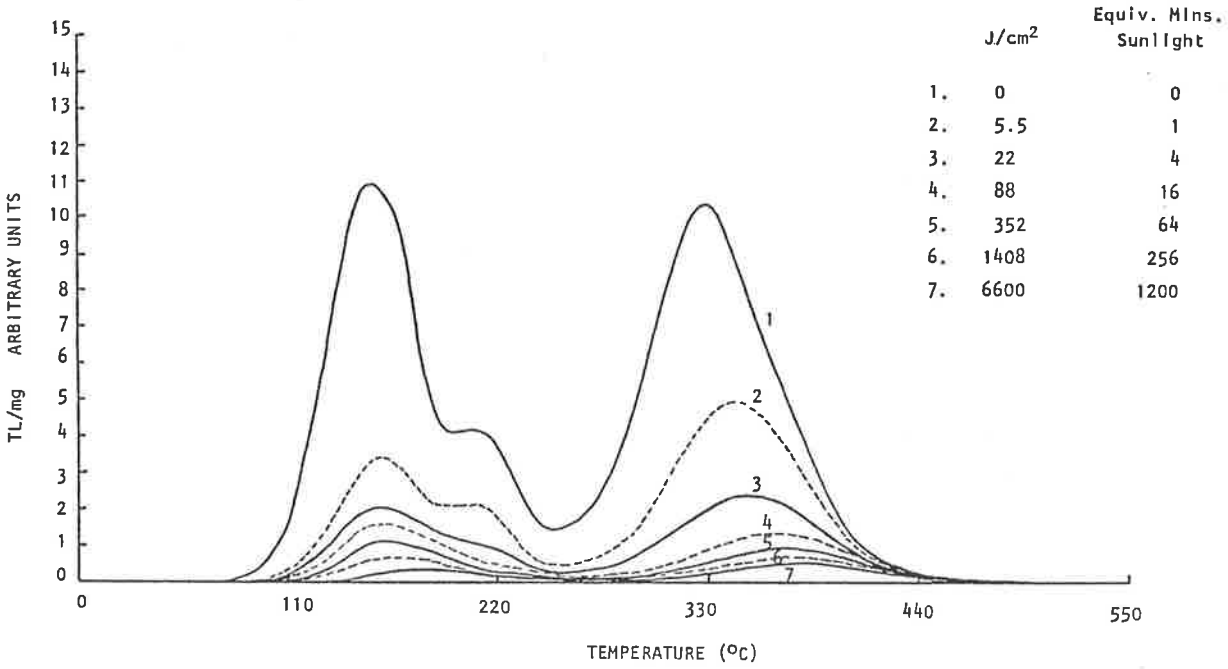

FIG 3.4.3 Shows the simulated sunlight bleaching of annealed Lake Woods (S3,TD,1m) quartz. Annealing conditions: 800°C for 24 hours in air, slow cooling. Irradiations: 46 Gy ^{90}Sr-^{90}Y β, with one day delay before bleaching, and a similar delay before TL measurement.

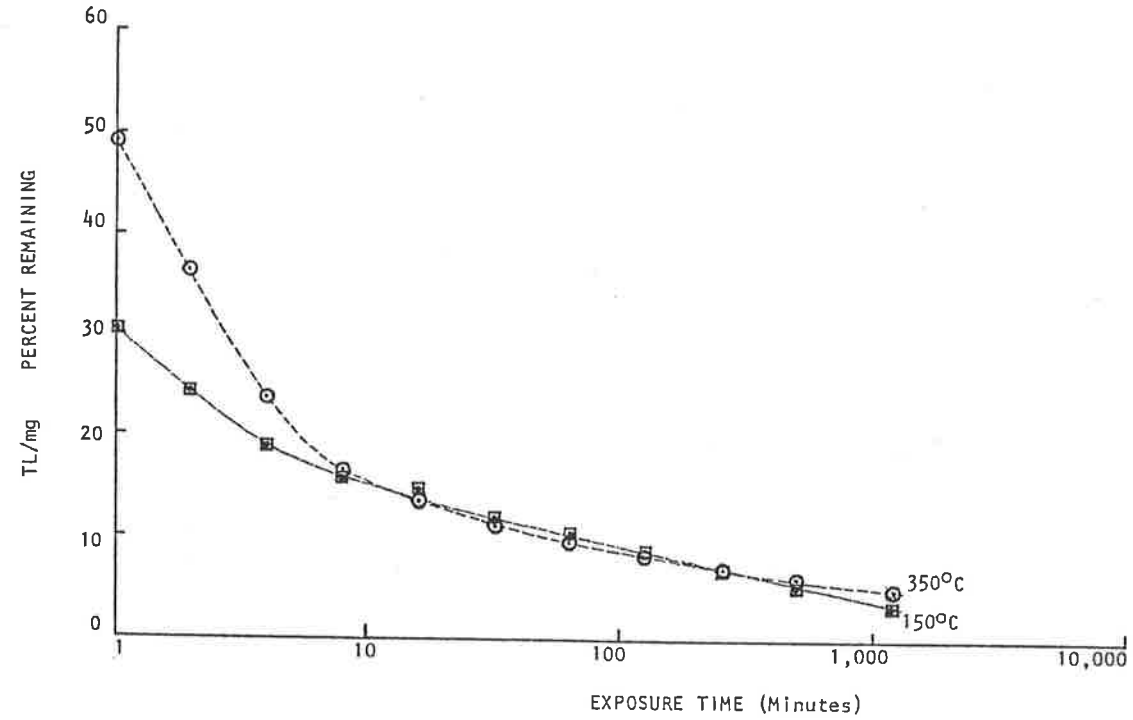

FIG 3.4.4. Shows the bleaching of the 150°C and 350°C peaks in annealed Lake Woods (S3,TD,1m) Quartz. (From Fig. 3.4.3.). The simulated sunlight illumination delivered 5.5 J/cm²/minute.

regrowth at 480°C for β doses up to 688Gy, supporting configurational changes to impurity related traps as causing the desensitization of this trap. The 370°C peak does seem to reappear somewhat, indicating a possible origin in radiation damage, but these doses are probably too low to clearly regenerate a significant population of damage sites.

Changes in the number of luminescence centres may also be taking place. However, Fox (Pers. Comm., 1986) reports the TL emission spectra of annealed quartz to be indistinguishable from that of natural quartz for glow curve temperatures > 130°C, with the peak wavelength consistent with recombination at $(Al^{3+})^{o}$ sites in both cases, showing that the type, if not the density, of R centres is unchanged.

The greater TL efficiency of annealed quartz may be attributable to the activation of additional R centres, given the earlier finding (section 3.3) that saturation of these centres sets the limit on TL growth in untreated quartz. Conversely, there is the possibility that annealing is reducing an unidentified population of competing, non-luminescent R centres.

Considering bleaching: the 330°C peak reveals an absence of structure suggestive of there being only one class of trap contributing. Noteworthy effects seen in Fig. 3.4.3 are (a) the rapid TL reduction to a slowly declining "residual" and (b) the shifting to higher temperatures of T_{max} as bleach time increases. Both effects have two plausible, though untested, explanations.

The bleaching rate may reflect a greater inherent sensitivity to UV/visible photons of the modified trap structure. Alternatively, the absence of deeper traps may remove the resupply reservoir of trapped charge as well as increasing the probability of recombination for a released charge, as there are now reduced options for retrapping.

Retrapping also provides an explanation for the shift of T_{max}: the glow curves are consistent with government of the bleaching process by 2nd order kinetics (Levy, 1982), applicable where significant retrapping occurs.

Alternatively, the traps contributing to each peak may together comprise a band of energy levels, and so bleaching is seen to proceed from the low temperature side of the glow peak as the shallower traps are preferentially emptied.

Summarizing, the ATL growth, glow curve structure and bleaching behaviour of annealed Lake Woods quartz differs significantly from that of the NTL of natural quartz under similar conditions, possibly due to thermally activated changes to defect configurations. The difficulty of then generalizing results to natural untreated quartz outweighed any benefits of annealing, hence thermal pretreatment was discontinued, and all further bleaching work performed on "natural" quartz.

3.5 Optimisation of glow conditions

The optimum combination of TL measurement conditions - heating rate and maximum temperature - was found to be heating at $5Ks^{-1}$ to 550°C maximum. Greater heating rates produced poorer glow peak resolution, whereas slower rates gave no improvement and were time consuming. The maximum temperature of 550°C was chosen as being the lowest temperature permitting the complete glow curve to be read. Routine maximum temperatures exceeding 550°C were not used due to rapidly increasing blackbody signal at these temperatures, absence of any detectable quartz TL beyond ~550°C, and the possibility of thermally inducing changes in the quartz TL characteristics.

A series of heat/irradiation cycles was performed to determine the extent of any such changes from heating to 550°C. The results and a description of the procedure are given in Figs. 3.5.1, 3.5.2 and 3.5.3.

Significant changes in peak sensitivities are seen, the continuation of which would appear to produce a glow curve similar to that found previously for annealed quartz (see Fig. 3.4.2). These observations are similarly explicable as thermally activated modifications to the e^- trapping centres producing the peaks.

It is also seen that the total glow curve TL sum increased by ~25% between the 1st and 16th cycles, agreeing with the greater TL efficiency found for annealed (800°C for 24 hrs) quartz. Given the earlier finding that saturation of R centres limited the TL growth in unheated LW quartz, this enhanced TL efficiency may result from activation of additional R centres or elimination of competing non-luminescent R centres. Conversely, the apparent pre-dosing of the 325°C peak may be the consequence of there being an energetically preferred configuration possessed by the corresponding class of e^- traps, and to which the trapping centres responsible for several peaks "relax" on suitable thermal activation. If so, this "pre-dose" behaviour is not the "true" pre-dose effect, attributed by J. Zimmerman (1971) to the thermal transfer of holes from "reservoir" non-luminescent R centres to luminescent R centres, and reversible by exposure to UV light.
This hypothesis may be tested: the pre-dosing of the 325°C peak should not be reversible by UV irradiation if it is a consequence of modifications to e^- trapping centre configurations.

From a practical standpoint, while the mechanism responsible for these glow curve changes remains unclear, its effects must be accounted for in experimental design, and strongly support the practice of using first glow data wherever possible.

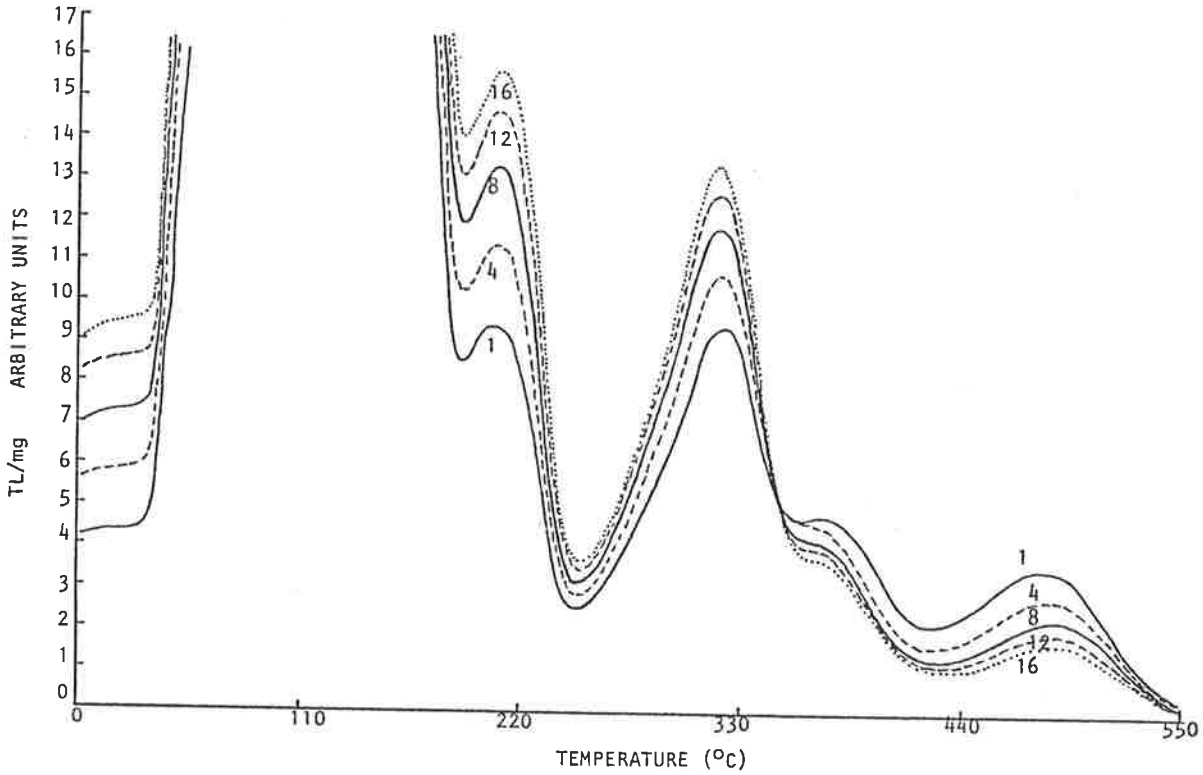

FIG. 3.5.1. Shows the sensitization of natural Lake Woods (S3,TD,1m) Quartz induced by heat-irradiation cycling.
Pretreatment: Standard preparation, followed by erasure of NTL by preheating to 550°C. Each cycle consisted of a dose of 11.8 Gy ^{90}Sr-^{90}Y β, followed by immediate heating at 5K/second to 550°C maximum, and background subtraction. The cycle numbers are shown.

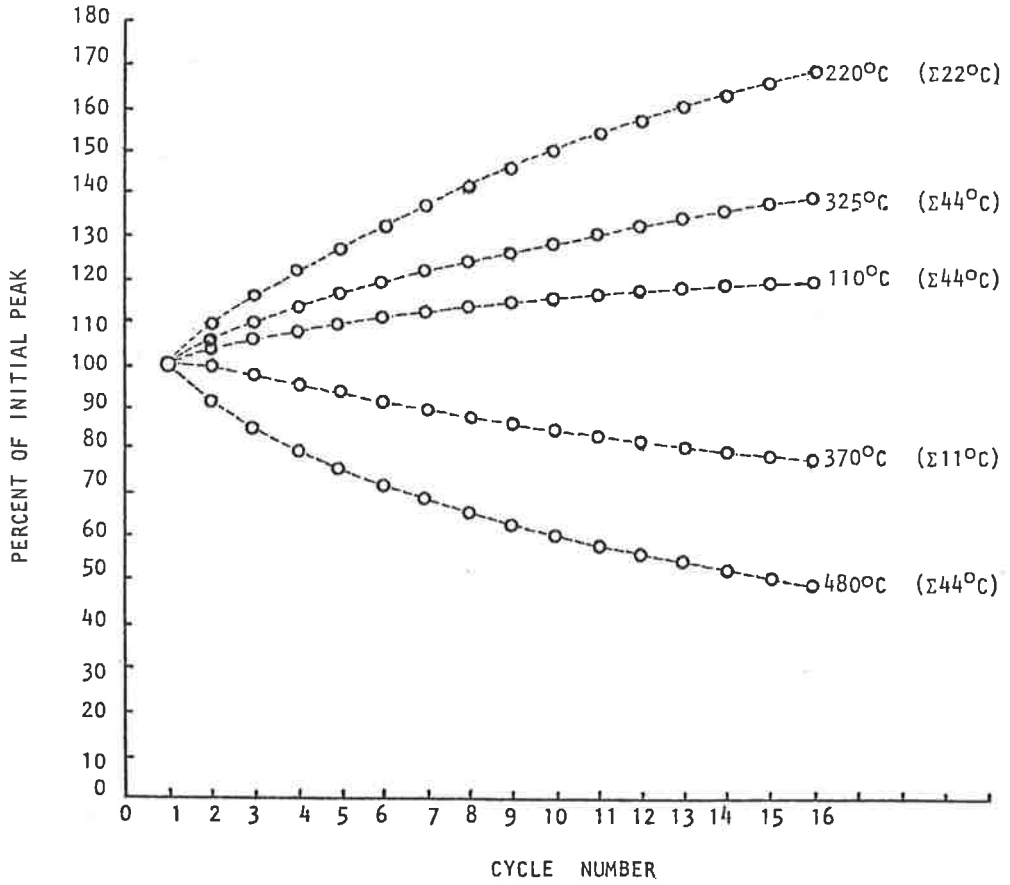

FIG. 3.5.2. Is a representation of the peak sensitization shown in Fig 3.5.1. The "Initial Peak" value is that measured following the first irradiation. The temperature ranges summed for each peak are shown.

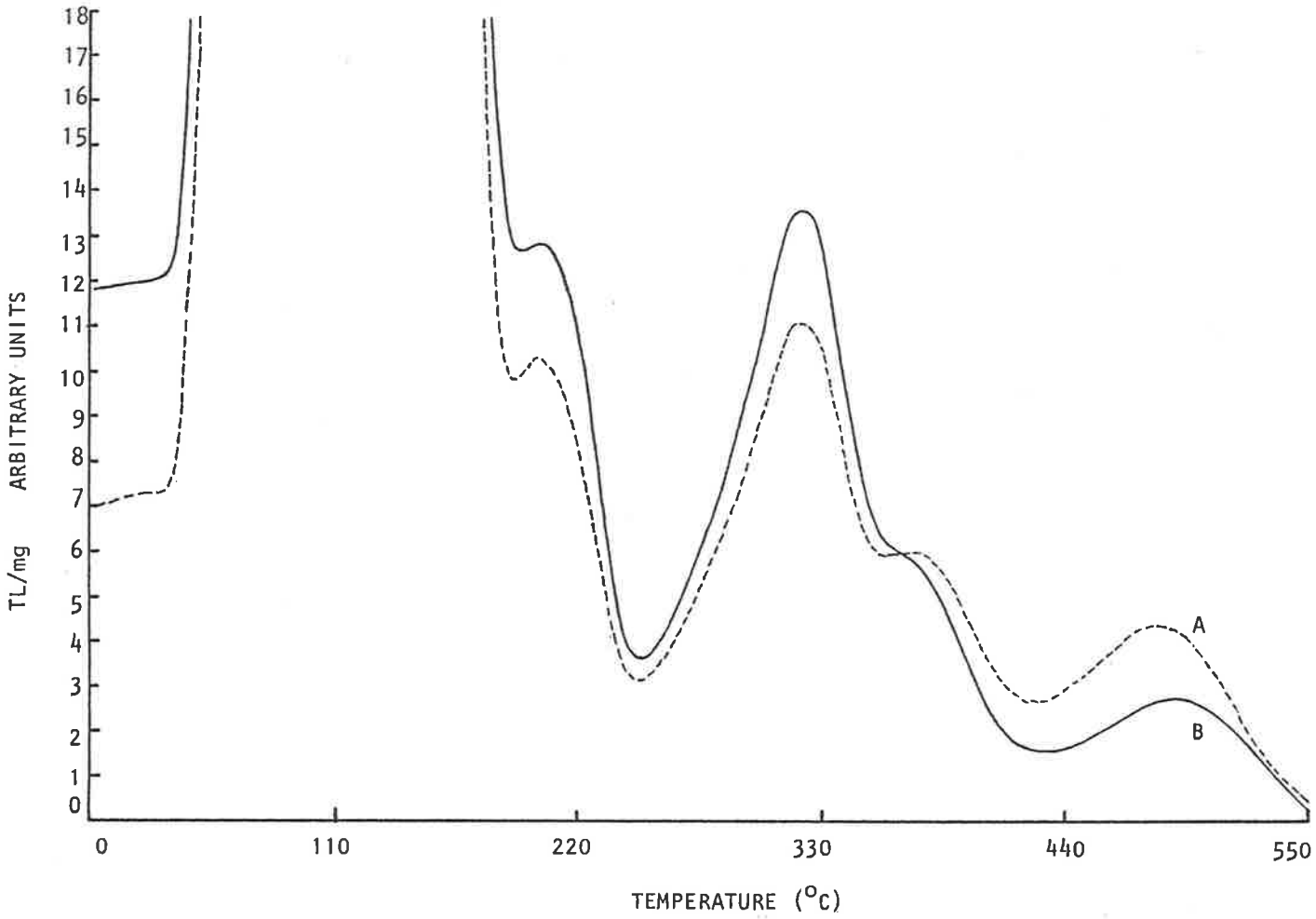

FIG 3.5.3. Shows the effect of thermal cycling only on the sensitivity of Lake Woods (S3,TD,1m) Quartz.

Procedure:
1) Standard preparation, then erasure of NTL by preheating to 550°C.
2) 11.8 Gy ^{90}Sr-^{90}Y β test dose with immediate TL measurement and background subtraction (Curve A)
3) 14 Cycles of twice heating to 550°C at 5K/second.
4) Second test dose (as for Curve A) to measure final sensitivity (Curve B).

Applying these findings to the design of the bleaching experiments led to routine measurement of TL to a maximum temperature of 550°C at $5Ks^{-1}$, followed by the subtraction of a similarly acquired reheat curve. Additionally, there were no pretreatments, either thermal or radiational, given to the quartz prior to bleaching other than the separation steps outlined in section 2.2.

CHAPTER 4 THE BLEACHING OF QUARTZ BY SIMULATED SUNLIGHT

4.1 Introduction

This chapter considers the bleaching of natural quartz TL by laboratory simulated sunlight. The "full solar spectrum" illumination was used in experiments designed to investigate some of the questions concerning the bleaching rate and residual posed in section 1.11. These questions (1-4) are framed in the TL dating context, and to assist the experimental findings to be of direct applicability to sediment dating problems, the laboratory bleaching conditions were set up to replicate nature as closely as possible. This follows from the uncertain validity of extrapolations from studies using "unnaturally" short WAVELENGTH UV photons or artificially treated (radiation or heat) quartz to the "real" case of the natural sunlight bleaching of quartz NTL.

The illumination source was an Oriel 1000W solar simulator, chosen to closely match natural sunlight both in spectrum and intensity (see section 4.2). The questions addressed relate to exposure-time-dependent glow curve changes, and the approach taken was to observe the progress of these changes by bleaching sets of similar quartz samples for various times. The effects seen were found to be explicable in terms of a balance between photo-excitation of trapped electrons (optical untrapping) and the retrapping of released electrons at any available vacant trap sites. A model for optical untrapping, by Levy (1982) was found to agree with the experimental findings in all important details.

The bleaching of LW (S3,TD,1m) quartz for the case of NTL + added ^{90}Sr-^{90}Y β doses is also considered. Finally, the influence of on-site physical conditions is briefly discussed, specifically, ambient temperature during bleaching, attenuation of incident sunlight by the grain's oxide coatings, and the thickness of overburden with which grains must be covered for bleaching to cease.

4.2 Light sources for bleaching

Most laboratory bleaching used an Oriel Corporation 1000W solar simulator - although some early work used natural sunlight.

Essential requirements of an artificial light source were held to be:

1. Representation of all wavelengths present in the solar spectrum, with no significant UV overabundance.

2. No shorter wavelengths present in the artificial spectrum than in natural sunlight.

3. Long term spectral output stability.

Fig. 4.2.1 compares the natural sunlight and simulated sunlight spectra. The simulation is generally very good, with the greatest mismatches in relative power occurring at IR wavelengths, and so being inconsequential. The "spike" at ~450 nm can be accounted for in calibration, and is anyway at wavelengths too long to be significant in high temperature TL bleaching (325°C peak excepted - see section 5.2).

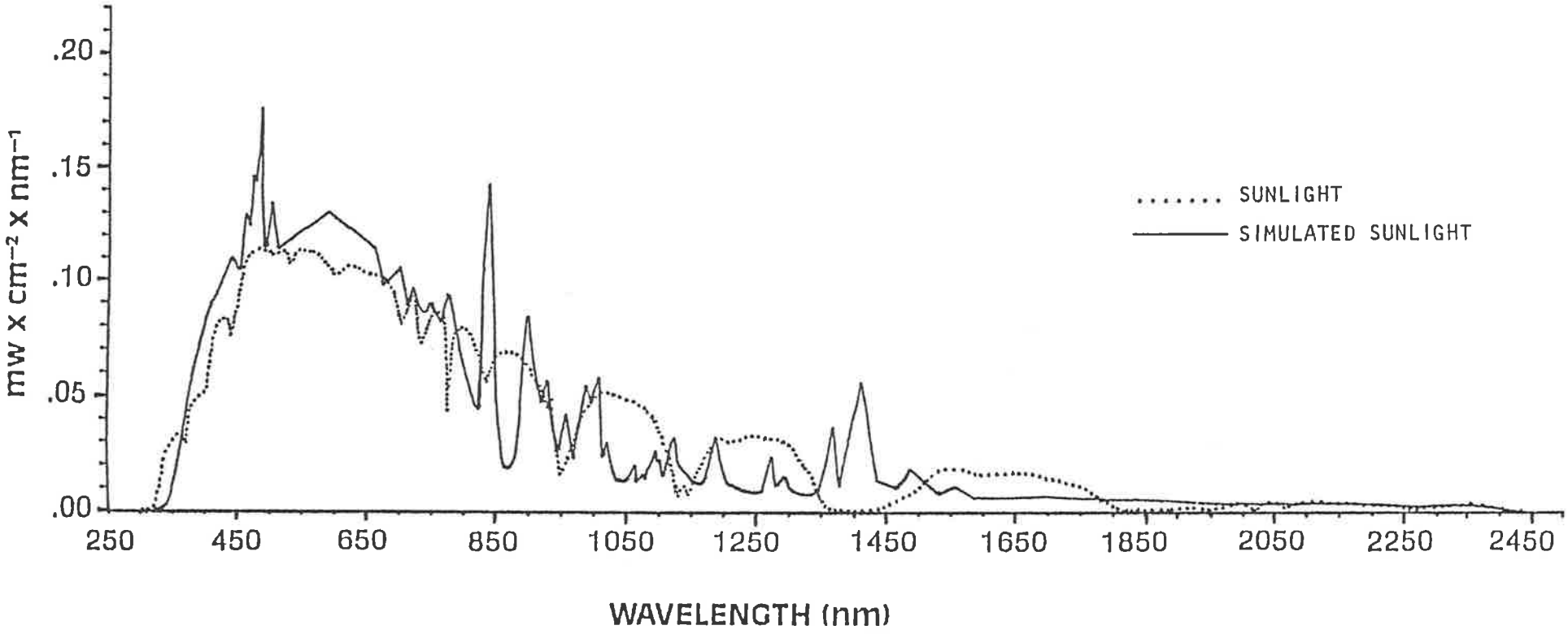

FIG 4.2.1. Spectral irradiance of sunlight and simulated sunlight for air mass 1.5 global filtering (solar zenith angle = 48.2°).
The Solar Simulator Data was from a lamp with 50 hours running time, and normalized to 1 sun. Total irradiance from 250-2500 nm is 95 mW/cm^2.

The Solar Spectrum, also from the Oriel Corporation Solar Simulation Catalogue, is the Seri (Solar Energy Research Institute) proposed air mass 1.5 global standard:
from work by M.P. Thekaekara.

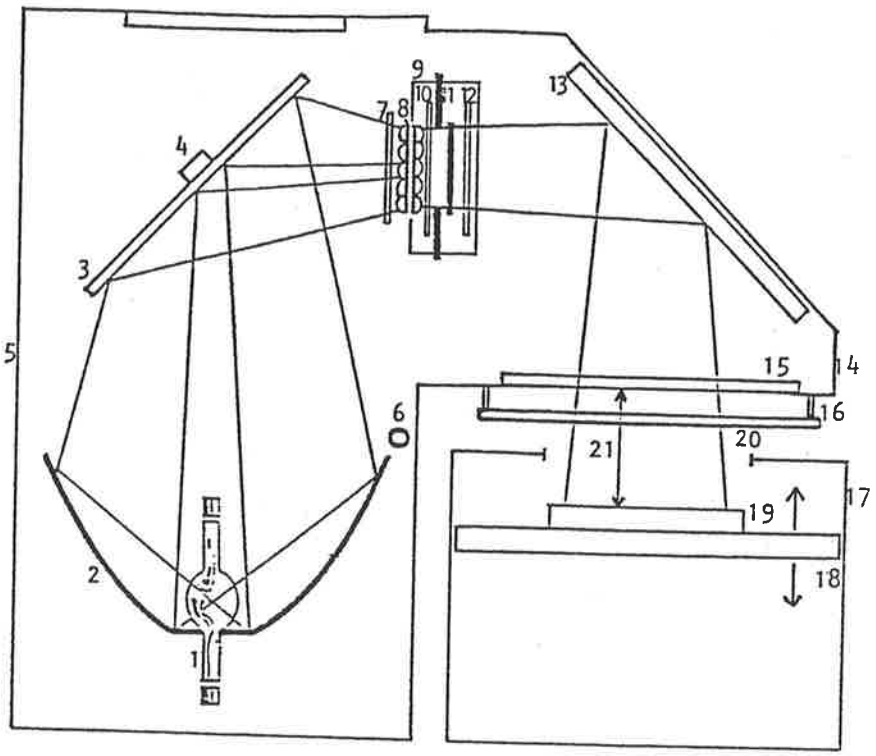

1. 1000W Xenon Lamp
2. Ellipsoidal Reflector
3. 45° Aluminised Mirror
4. Thermostat
5. Lamp Housing
6. Photodiode (Records Lamp Use)
7. Slide-in aperture (Intensity Control)
8. Optical integrator
9. Filter fan
10. Spectral correction filter A, for air mass 1.5 global (coated side toward lamp)
11. Shutter
12. Spectral correction filter B, for air mass 1.5 global (coated side toward lamp)
13. 45° aluminised mirror
14. Mirror housing
15. Plane exit window
16. Spectral correction filter C, for air mass 1.5 global (tempered IR absorbing glass)
17. Exposure chamber (sealed against extraneous light)
18. Adjustable base plate (30x30x1cm Aluminium)
19. Workplane (Disc holder having 53 concentrically arranged disc sites)
20. Beam entrance port (Interchangeable masks giving either 15x15cm or 5x5cm aperture)
21. Window - Disc distance.

FIG.4.2.2. SCHEMATIC OF THE ORIEL 1000 W SOLAR SIMULATOR. (BASED ON ILLUSTRATIONS IN THE ORIEL SOLAR SIMULATOR MANUAL).

More serious is the under-representation of UV at wavelengths less than ~320 nm in the simulated sunlight spectrum, compounded by the decline of UV output with lamp age. The latter is not well documented - enquiries to manufacturers and users of high pressure short arc Xe lamps show agreement that the UV output drops rapidly at first but by 50 hrs lamp age it is considered stable for normal use, though details on further spectral changes are lacking.

As a guide to the acceptibility of the Oriel simulator as a sun substitute, the bleaching of similar sets of Lake Woods quartz samples was compared for natural and simulated sunlight. Good agreement was generally found, indicating that the calibrated simulator effectively simulated the intensity and spectrum of natural sunlight for "full spectrum" exposures.

The Oriel 1000W solar simulator is shown schematically in Fig. 4.2.2. The lamp and mirror housings and their components are proprietary, the exposure chamber (17) was designed by the author and built in the University of Adelaide Physics Department workshops.

The chamber is a light-proof mild steel box, the lids of which are interchangeable masks whose apertures permit the use of either 5 x 5cm square filters, or an unobstructed "full spectrum" 15 x 15cm beam. The workplane is the top surface of an aluminium plate whose distance from the output window can be varied by a geared support mechanism. This facility along with the use of an Oriel Solar Simulator Radiometer (model 81020) to monitor beam strength, allowed an effectively constant power output beam (mW/cm^2) to be maintained as the lamp aged, by changing the window - disc distance to compensate.

Reproducible positioning of samples was aided by an XY grid painted on the workplane and a vertical scale on the chamber wall. The chamber itself was bolted to the benchtop.

Calibration was carried out using the Oriel radiometer at the recommended beam reference points and intermediate sites, and was checked before each experimental run.

The sample holder is unpainted aluminium, and accommodates up to 53 discs in sites arranged concentrically. Access is by a hinged front panel of the chamber. All surfaces of the workplane and chamber are painted matt black. Cooling is available by a copper water tube attached to the underside of the workplate, but was found unnecessary.

4.3 Effects of exposure duration

An investigation of the effects of exposure duration on bleaching was conducted using the calibrated Oriel Solar Simulator as a controllable laboratory light source. This permitted the illumination spectrum and intensity, and crystal temperature, to be reproducibly maintained, and the variable of interest - exposure time - to be accurately controlled.

Forty similar sample discs were prepared from Lake Woods (S3,TD,1m) quartz (90-125μm fraction, magnetically separated and HF etched but otherwise untreated) then exposed in pairs to simulated sunlight for periods of 0,1,2,4,8,16,32,64,128,256,512, 1200 minutes and 32,44,56,68, 80,92,104,124 hours.

To broaden somewhat the applicability of the findings, the experiment was expanded to include quartz samples from two sites other than Lake Woods, chosen so that in all quartz from three geological regimes was represented. The additional sediments were from the Roonka site (EB 1/S/2.1) and the Woakwine Range (WK 1S/2), (see section 3.2), with sets of forty similar sample discs prepared for each. Quartz separation was as for the Lake Woods sample.

Because the holder used to position sample discs during exposures had a capacity of 53 discs (see Fig. 4.2.2, #19), several same-exposure-time pairs for each quartz were bleached simultaneously to minimize effects of exposure timing errors and lamp output fluctuations.

Families of bleached glow curves for the three samples after various exposure times are shown in Figs. 4.3.1, 4.3.2 and 4.3.3. The most notable feature is perhaps the overall similarity of bleaching behaviour, which permits some general observations to be made.

Most striking is the apparent removal of the 325°C peak within the first minute, and the consequent generation by retrapping of peaks at 160°C and 220°C. Further discussion of the susceptibility to bleaching of the 325°C peak is given in Chapter 5.

As bleach time increases, TL reduction occurs across the glow curve, but at differing rates at different temperatures, with higher temperature features generally resisting bleaching to a greater extent. This disagrees with the findings of David and Sunta (1981), who observed in the UV bleaching of a non-saturated sample of natural pink quartz (irradiation 100Gy ^{60}Co γ), "that the glow-curve peaks at the lower-most and the upper-most temperatures decay faster than those at the middle temperature regions". These contrary findings may be due to dissimilarities of the quartz samples, compounded by an illumination spectrum dominated by energetic photons not present in the sea level solar spectrum (the UV sources were mercury lamps, emitting mostly at 253.6nm). Nevertheless, such significant disagreement highlights the need for caution when generalizing findings to samples with different origins and histories.

As bleaching proceeds, most TL reduction occurs within the first 20 hours, along with a pronounced shift to higher temperatures of T_{max} of the 480°C peak. Over the next 100 hours a continuing slight reduction is seen at most glow curve temperatures, but there is some evidence for TL

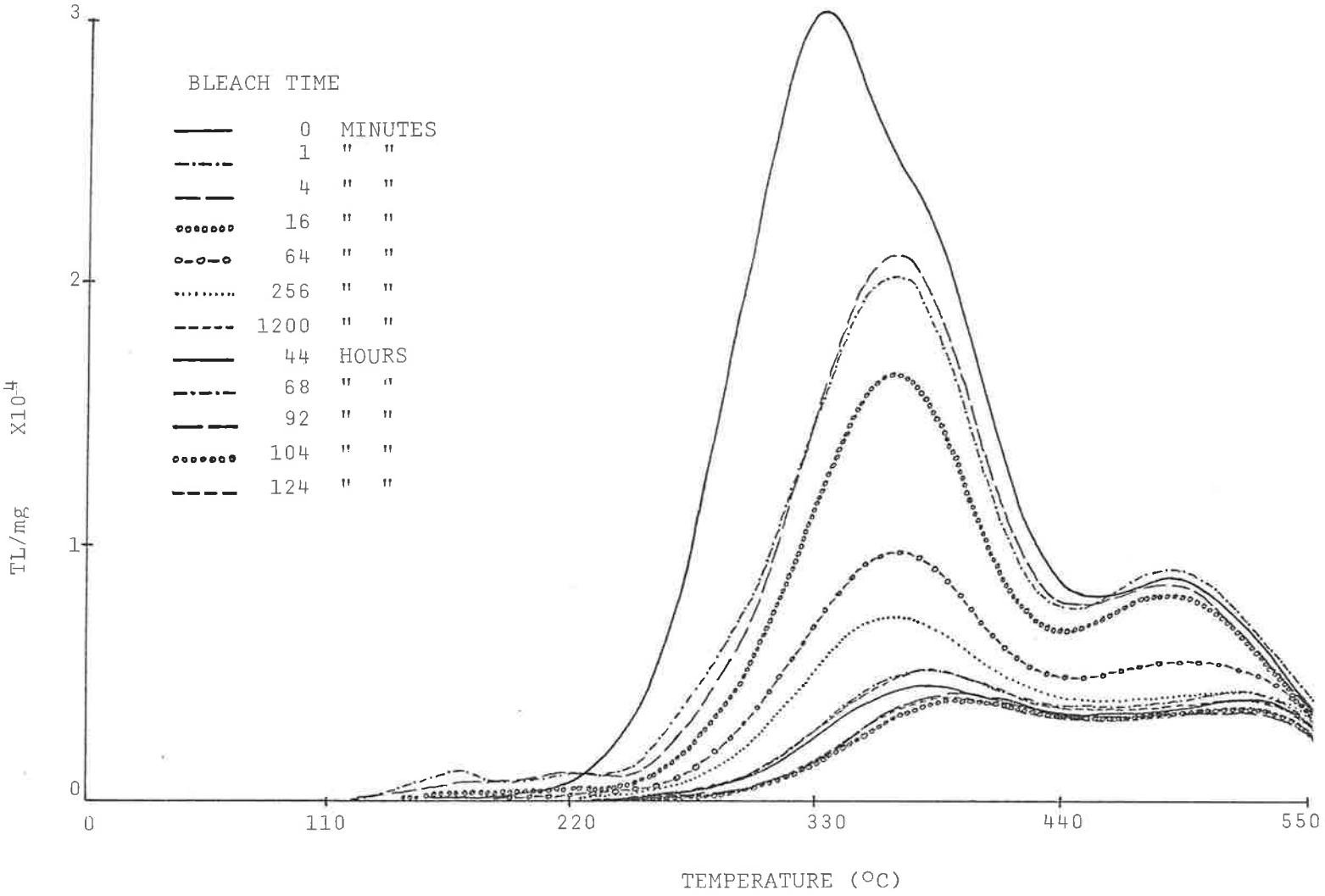

FIG. 4.3.1. Shows the bleaching of LW (S3,TD,1m) Quartz by simulated sunlight for various exposure times up to 124 hours.
Conditions: 90-125μm, magnetically separated and HF etched fraction; two sample discs per bleach time; NTL only; Heating at 5K sec^{-1} to 550°C, reheat subtracted; illumination source delivered 5.5 J/cm^2/Minute.

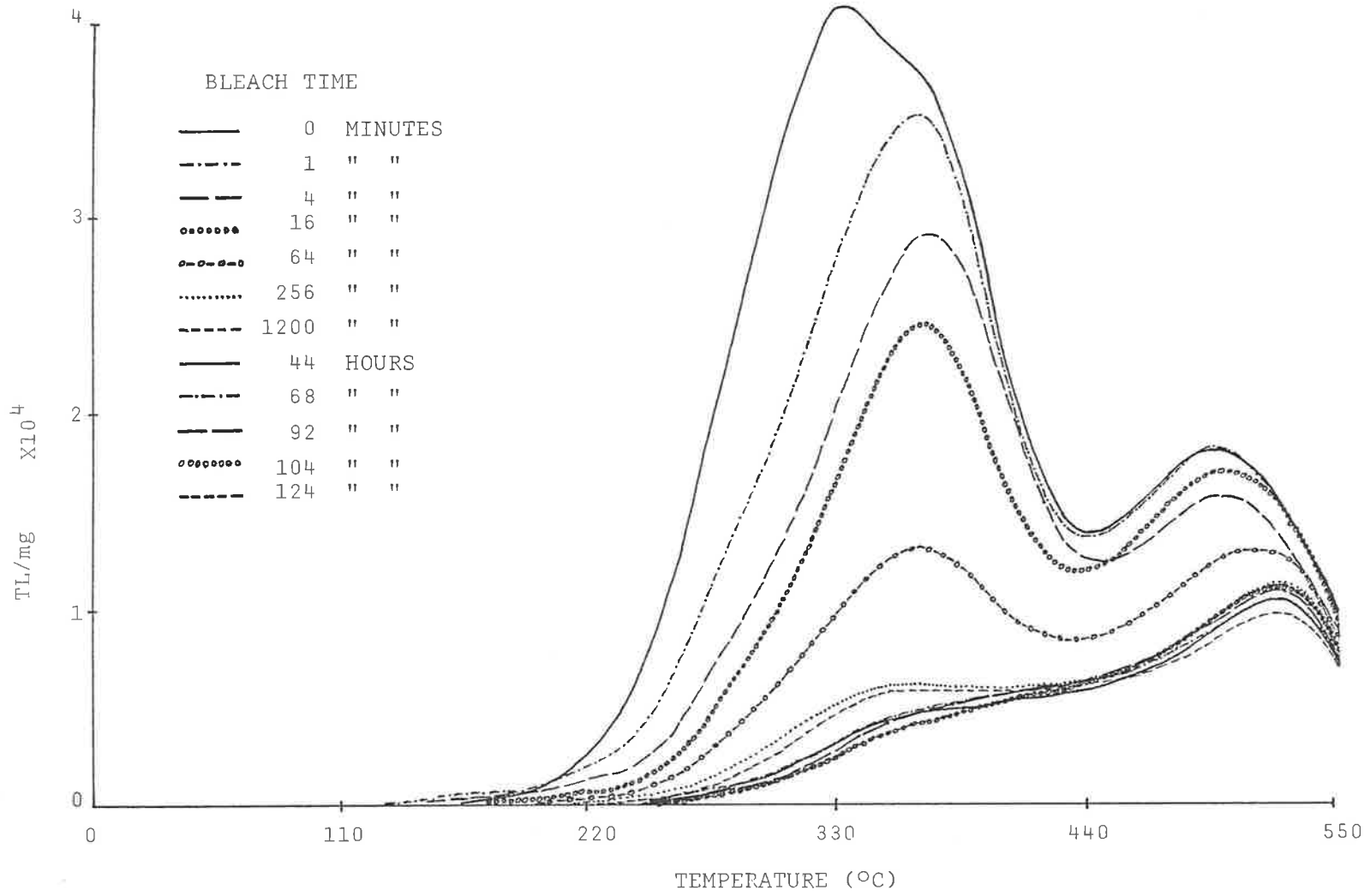

FIG. 4.3.2. Shows the bleaching of EB 1/S/1.9 Quartz by simulated sunlight for various exposure times up to 124 hours.
Conditions: 90-125μm, magnetically separated and HF etched fraction; two sample discs per bleach time; NTL only; heating at 5K sec^{-1} to 550°C, reheat subtracted; illumination source delivered 5.5 J/cm^2/minute.

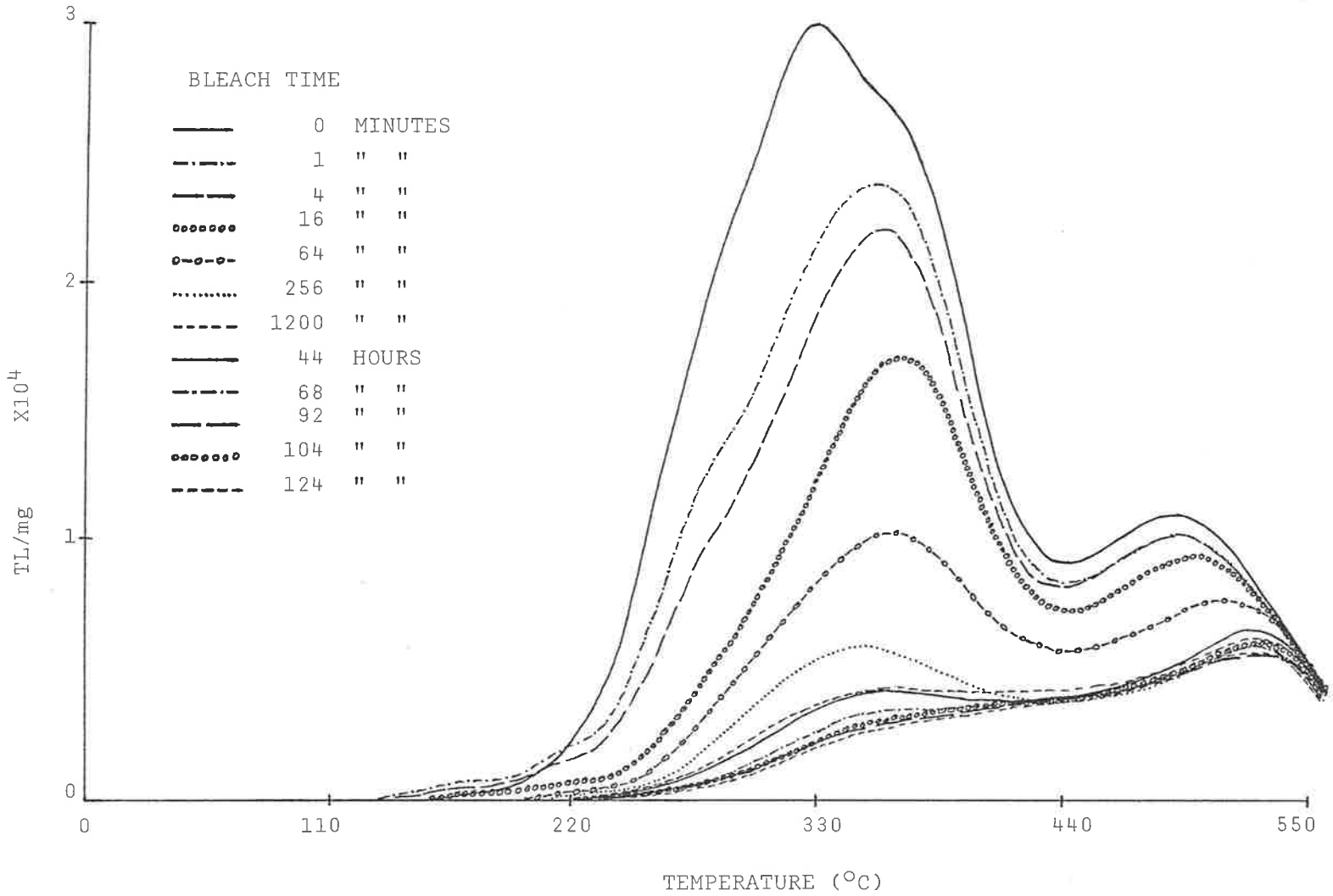

FIG. 4.3.3. Shows the bleaching of WK 1S/2 Quartz by simulated sunlight for various exposure times up to 124 hours.
Conditions: 90-125μm, magnetically separated and HF etched fraction; two sample discs per bleach time; NTL only; heating at 5K sec^{-1} to 550°C, reheat subtracted; illumination source delivered 5.5 J/cm^2/Minute.

growth at temperatures >500°C in certain samples when exposure times exceed ~100 hours.

A likely explanation is that the balance between retrapping and untrapping becomes favourable to nett trapping as the concentration of R centres, and hence the probability of loss of an untrapped e^- by recombination, declines with increasing bleach time.

Fig. 4.3.4 shows the bleaching curves for the 370°C peaks of the three quartz samples. The curves are of similar form and comprise three distinct sections. Initially (0 to ~10 minutes) the rate of untrapping is ~ equalled by the rate of retrapping of charge released from the 325°C peak and, after the first minute, from the lower temperature peaks - themselves generated by retrapping. Then follows a period (from ~10-100 minutes) in which this supply of e^-'s for retrapping is largely exhausted, and the 370°C traps are emptying at an approximately exponential rate. After ~100 minutes, the concentration of filled traps has been reduced to a level where the probability of self retrapping (retrapping at 370°C trap sites) has increased, due to the increasing ratio of empty traps to activated R centres. As bleaching continues and the self-retrapping probability continues to rise, retrapping becomes increasingly dominant, with the consequence that the rate of TL reduction continues to slow. This third region of the bleach curve is the "residual". Linear extrapolation from the residual sections of the bleach curves in Fig. 4.3.4 indicates a total energy of $\gtrsim 10^7$ J/cm^2 is required to fully remove the TL at 370°C. This is equivalent to $\gtrsim$3-4 years continuous exposure to natural sunlight, in agreement with theoretical predictions (Levy, 1982) that extremely long bleach times are required for ~ total TL removal.

These excessive bleach times result from the dominance of retrapping at low trapped e^- concentrations; the effects are best illustrated by example. The time constant estimated for the 370°C peak under the same

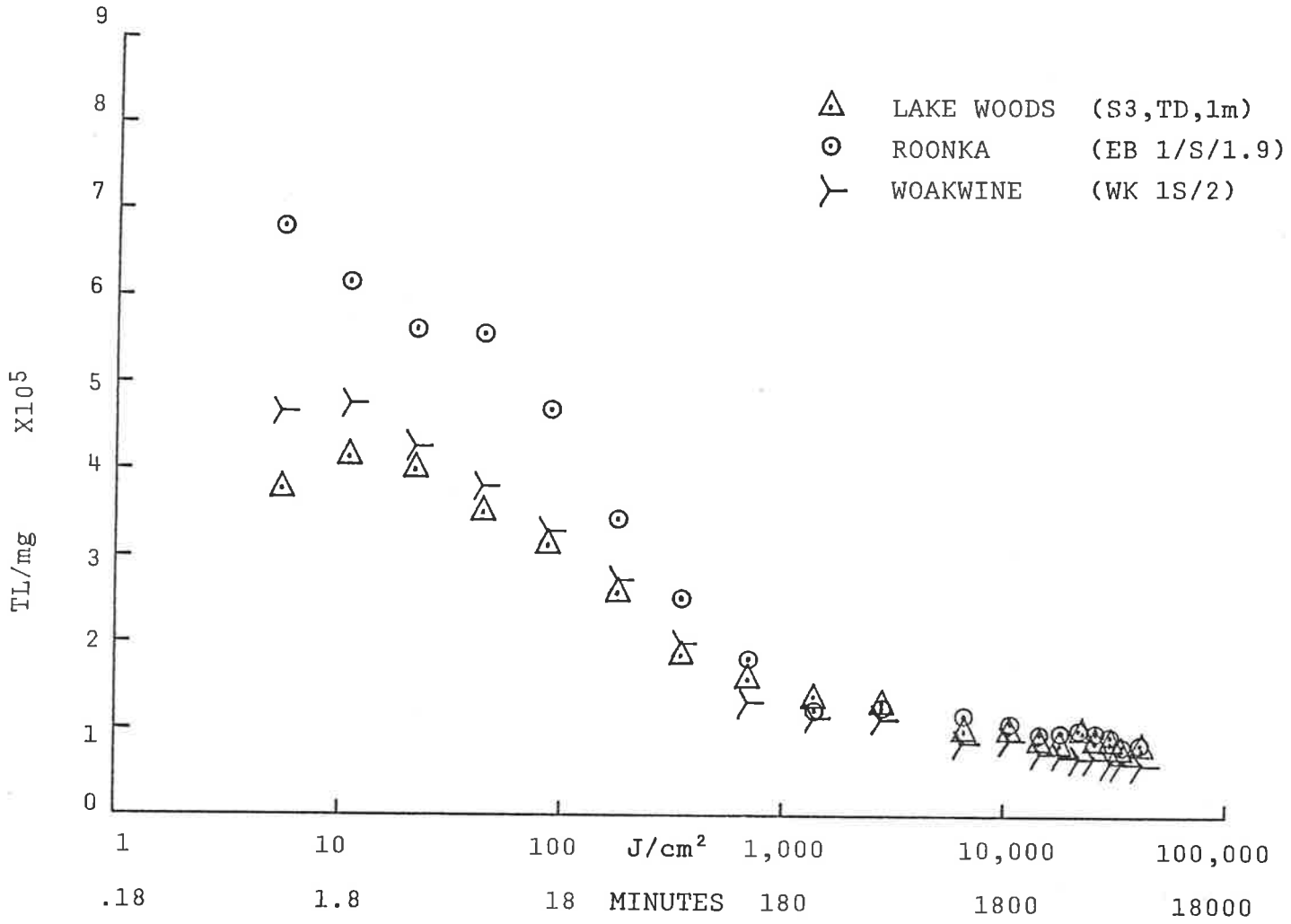

FIG 4.3.4 Shows the simulated sunlight bleaching of the NTL of selected quartz samples, for exposures up to the equivalent of ≈ 124 hours of natural sunlight. (simulated sunlight flux 5.5 J/cm²/minute).

TL integration is over 44°C centred on 370°C.

illumination conditions was 50±5 minutes (the error relates only to curve-fitting uncertainties, no allowance was made for retrapping). This value was determined in the 10-200 minute time range, as it was assumed that retrapping effects are of least significance in this period (as retrapping of e^-'s originating from 325°C peak traps has largely ceased, and the trapped e^- concentration has not yet been reduced to levels at which self-retrapping dominates). A 50 minute time constant, interpreted as the time required for untrapping to reduce the trapped electron concentration by a factor of e, implies a reduction to 10% of the initial TL within 2 hours. That such a reduction is not approached by 124 hours exposure (residual ~17%) emphasises the importance of retrapping processes during extended bleaching periods.

Similar interpretations based on a balance between retrapping and optical untrapping may be given for the bleach curves at any glow curve temperature. Selected examples of bleach curves for the LW (S3,TD,1m) quartz are shown in Fig. 4.3.5. Generally, the resistance to bleaching is seen to rise with increasing glow curve temperature (the notable exception being the 325°C peak) until at ~540^{0}C, even 124 hours of simulated sunlight has produced a reduction of only ~30%.

The slowing rate of TL reduction with increasing bleach time, attributed to the declining concentrations of activated R centres and trapped e^-'s, permits the deduction that if empty traps deeper than those producing the 480°C peak exist, they must be either few in number or possess a very low trapping cross-section, or both, and play no detectable role in the bleaching behaviour of these quartz samples. This may be demonstrated by assuming that such traps exist: a class of deep e^- traps requiring temperatures >700°C (no glow peaks were observed in heating to ~650^{0}C - the glow apparatus limit) for untrapping would almost certainly possess an optical activation energy greater than the photon energies available in natural sunlight and so would not donate

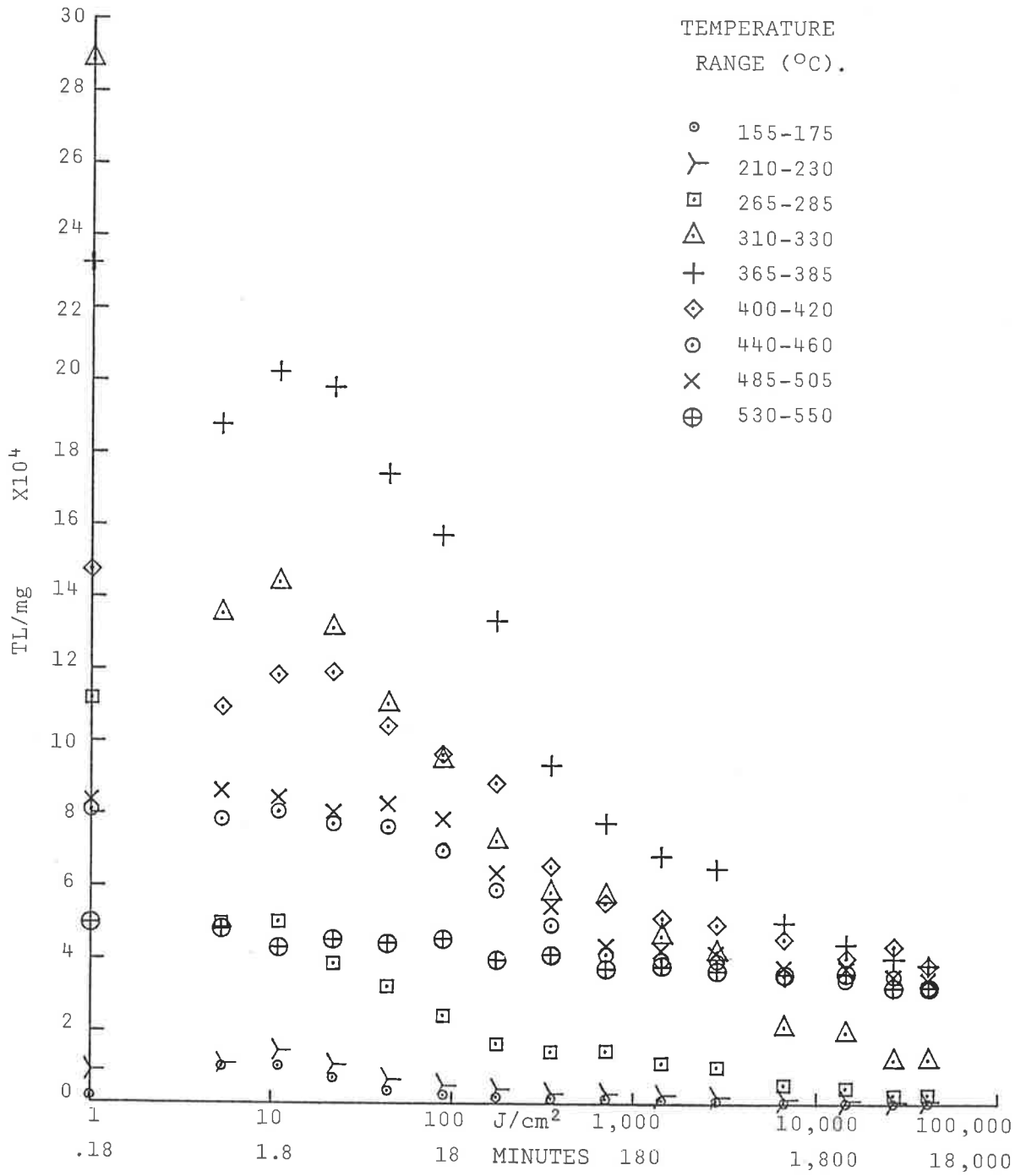

FIG. 4.3.5. Shows the progress of bleaching of LW (S3,TD,1m) Quartz by simulated sunlight, in temperature ranges mostly selected to include the prominent TL peaks. (From the same data set as Fig. 4.3.1). Data from unbleached discs has been plotted at 1J/cm^2 or .18 minutes exposure to permit the TL changes within the first minute to be seen.

any e^-'s into the conduction band during natural or simulated sunlight exposure. Furthermore, both the corresponding R centres (which may or may not be of the type producing lower temperature TL emission) and empty deep e^- traps would accept optically untrapped charges, and so provide the conditions whereby observable TL can be fully removed in a finite time, ie. the combined concentration of effective electron "sinks" ("normal" R centres + empty deep e^- traps + activated R centres corresponding to the filled deep e^- traps) would exceed the concentration of available electrons - those e^-'s trapped at sites producing the observable bleachable peaks.

These conditions favour a relatively rapid reduction of the observed shallow trap e^- populations to very low levels: as such behaviour is not seen it is concluded that no significant glow curve structure exists at temperatures >550°C.

A comment on a model for optical untrapping: the previously outlined model by Levy (1982), (see section 1.10), which assumes 3 types of e^- traps, 1 type of hole trap and a rate of untrapping proportional to the trapped e^- concentration, appears to correctly predict all major features seen on bleaching. This model is based on competing untrapping, retrapping and recombination processes, and its success gives some justification for similarly based explanations of the bleaching behaviour exhibited by quartz.

Fig. 4.3.6 shows a numerical solution of the equations from the above model describing the trapped charge concentration as a function of bleach time. Comparison with similarly plotted bleach data from LW (S3,TD,1m) quartz (Fig. 4.3.7) reveals the differences are of detail rather than quality. Those most prominent are the relatively minor degree of retrapping at the initially empty 160°C peak traps, followed by rapid untrapping, and the near equilibrium between retrapping and untrapping for short bleach times at ~500°C.

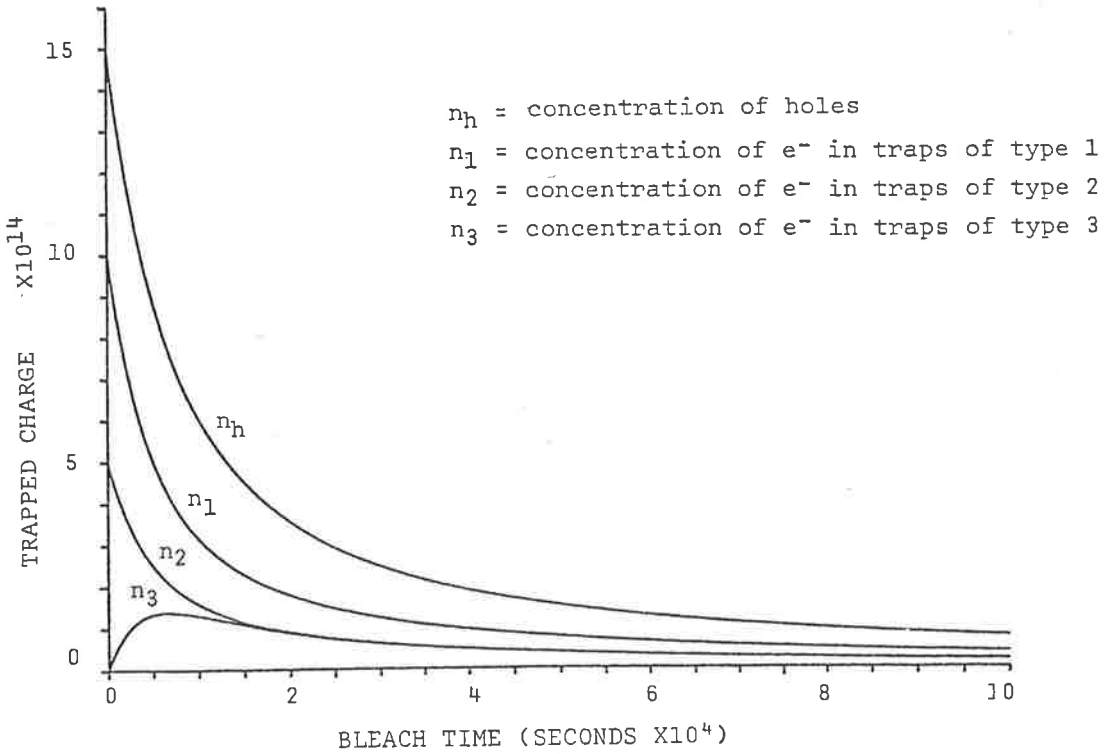

FIG. 4.3.6. Shows numerical solutions of a model for the reduction of trapped charge with bleaching time. The case shown is for a material possessing three types of e⁻ trap and one type of hole trap, and a bleaching rate proportional to the trapped e⁻ concentration. The type 3 e⁻ traps are initially empty.
(After Levy, 1982).

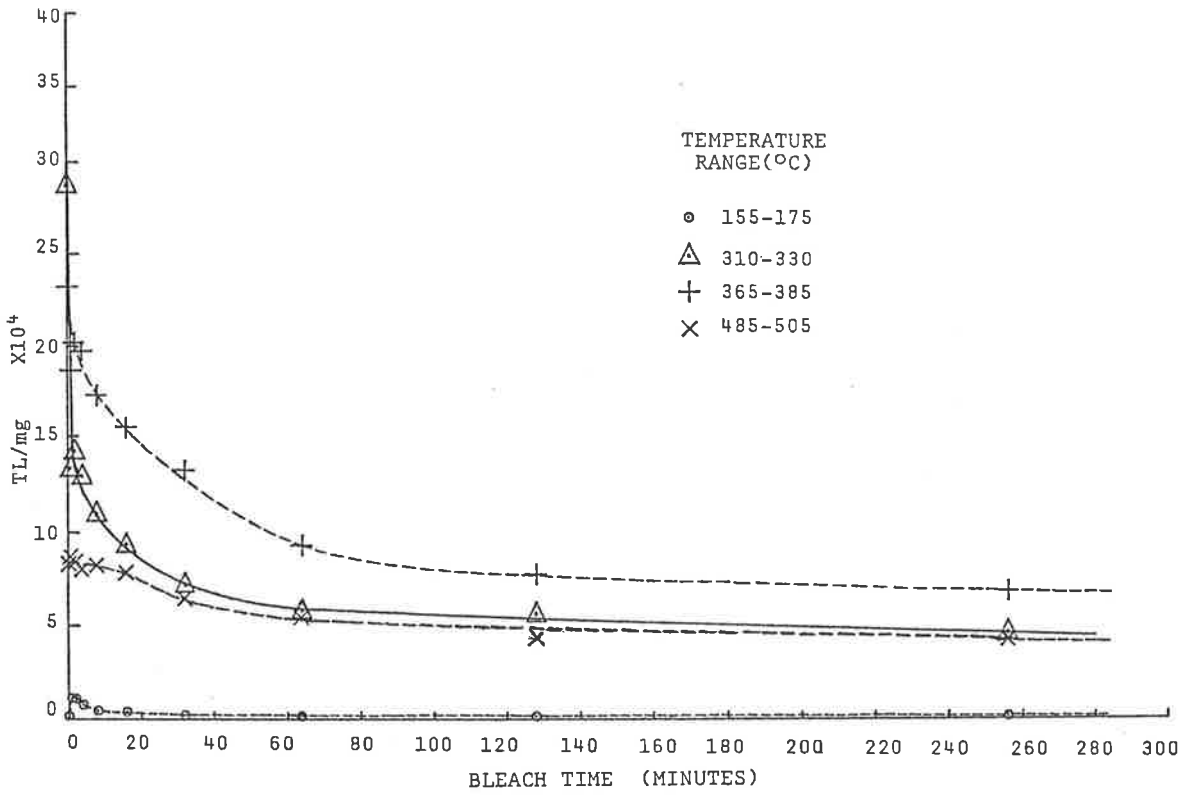

FIG 4.3.7. Shows the TL of LW (S3,TD,1m) quartz in selected temperature ranges for various exposures to simulated sunlight. (From the same data set as Fig. 4.3.1.).

More importantly, the model lends support to the experimental findings showing the residual level to depend on duration of exposure and to continue to decline as bleach time increases. The model also predicts that complete TL removal will not occur within a finite bleach time - a prediction supported by inspection of Fig. 4.3.4.

A possible application suggested by the existence of the 480°C peak and the general increase in resistance to bleaching with glow curve temperature, was the use of the 480:370°C TL ratio from a contemporary surface sample as a convenient means of estimating the effective exposure time undergone by previously deposited layers, assuming current site conditions to be comparable with those of earlier times. Unfortunately the difference in TL reduction after bleach times of several hours or more is too small for meaningful ratios to be obtained, given the complications of intrinsic sample variability and low light levels. This result does, however, largely validate the zeroing assumptions of the total bleach-based methods where long exposures can be assumed.

Summarizing, answers may now be proposed for the first three questions posed in section 1.11.

The residual is <u>not</u> an inherently unbleachable component, but should instead be considered to be a zone (rather than a defined level) to which bleaching proceeds relatively rapidly, the precise rate being dependent on bleaching conditions (spectrum, luminous flux, ambient temperature), and in which further TL reduction occurs monotonically at a slower and decreasing rate. This residual zone relates to a given characteristic concentration of trapped charges in the crystal, and not to some proportion of the initial TL.

All parts of the glow curve bleach, but at different rates and to differing extents. Generally, bleaching rate declines with increasing glow curve temperature, the only significant exception being the 325°C peak.

4.4 The bleaching of artificially irradiated Lake Woods quartz

The bleaching of quartz TL was earlier investigated (section 4.3) only for the case where traps having mean trapping lifetimes $>10^3$a were occupied, so effects dependent on the presence of lower temperature ATL peaks prior to bleaching were not seen. In practice, such effects may be of significance to applications of the partial bleach method - the only established technique of ED estimation relying on data from samples bleached after laboratory irradiation. In addition, the bleaching behaviour when many of the lower temperature, shallower, trap sites are occupied may provide further insight into the bleaching process.

A situation analogous to that encountered in the partial bleaching procedure was produced by giving each of a set of LW (S3,TD,1m) quartz samples a 47 Gy ^{90}Sr-^{90}Y β irradiation (the dose being selected so as to raise the TL to the near-saturation end of the linear growth region) followed by a one day delay before bleaching for various times by simulated sunlight. Fig. 4.4.1 shows the resulting family of glow curves, with the bleach curves of the prominent peaks given in Figs. 4.4.2 (a), (b).

An obvious difference between the irradiated and NTL cases is the greater quantity of charge released in the irradiated samples by the first minute of exposure (cf. Fig. 4.3.1). Much of this charge originates from the 160°C and 220°C peak traps, which are now acting as nett e^- sources rather than nett retrapping sites, as they do if vacant at the commencement of bleaching. A consequence is increased retrapping at the 370°C and 480°C peak trap sites during the first 10 minutes of exposure. The 370°C peak is seen in Fig. 4.4.2 to be apparently untouched by bleaching until exposure times exceed 5 minutes:

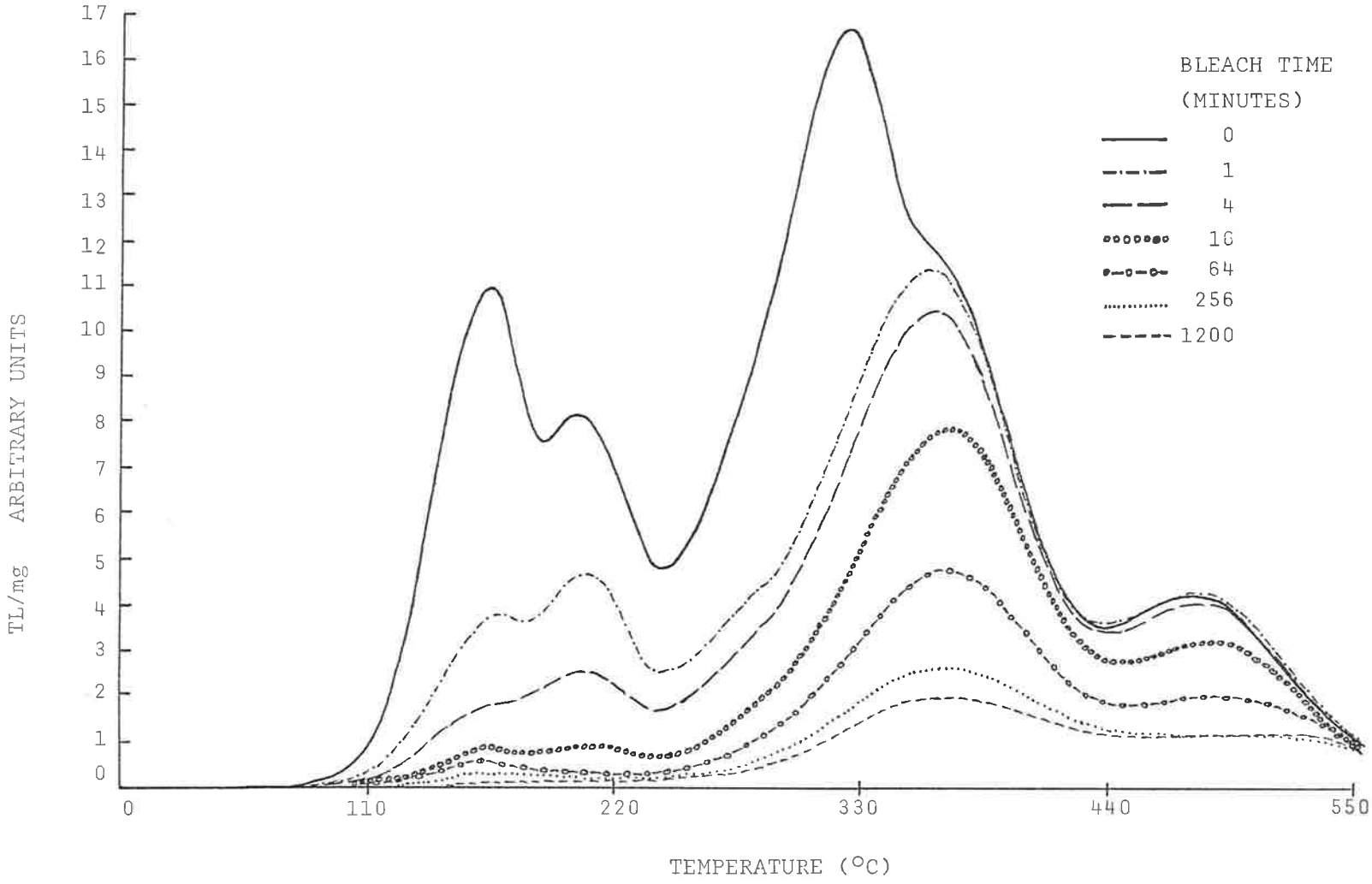

FIG. 4 .4.1. The bleaching of LW (S3,TD,1m) quartz TL by various exposures to simulated sunlight.
Conditions: 90-125μm, magnetically separated and HF etched fraction; NTL + 47 Gy ^{90}Sr-^{90}Y β irradiation; one day delay before bleaching, similar delay before TL measurement; heating at $5Ksec^{-1}$ to 550°C maximum, reheat subtracted.

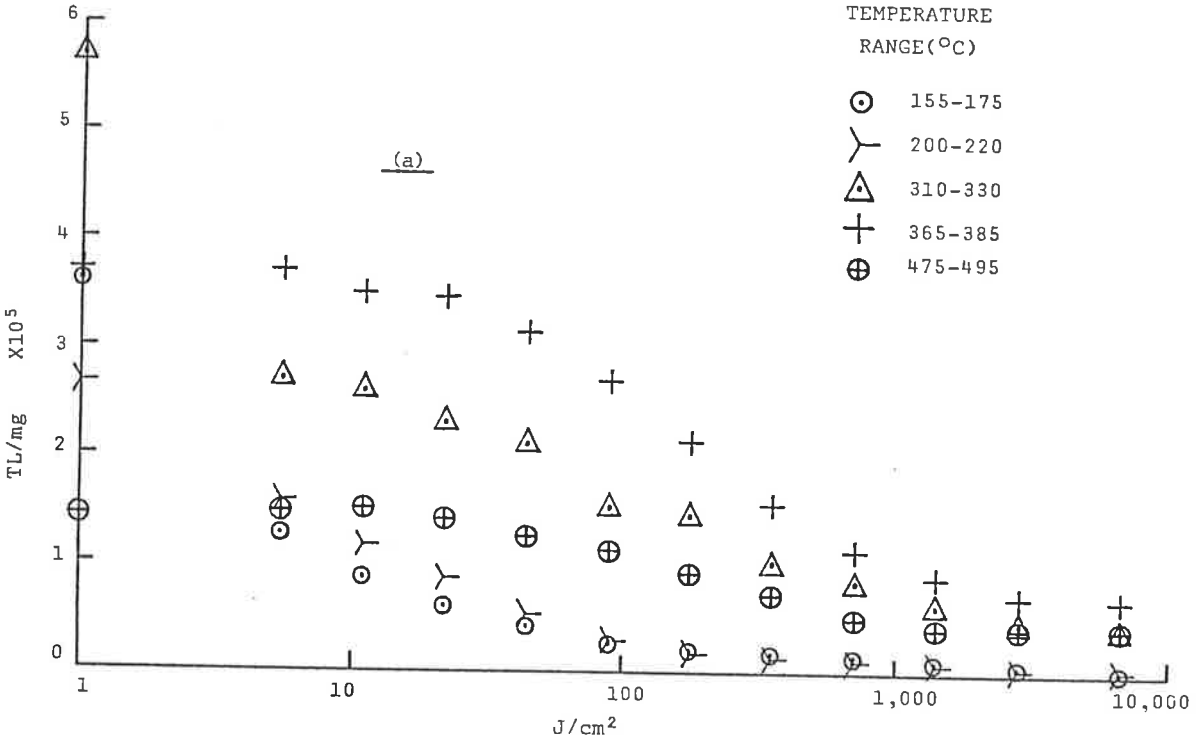

FIG. 4 .4. 2.(a) Shows the simulated sunlight bleaching of LW (S3,TD,1m) quartz in selected temperature ranges, after exposures up to 20 hours (5.5 J/cm²/Minute). From the same data set as Fig. 4 .4.1. TL from unbleached discs has been plotted at one J/cm² to permit changes within the first minute to be seen.

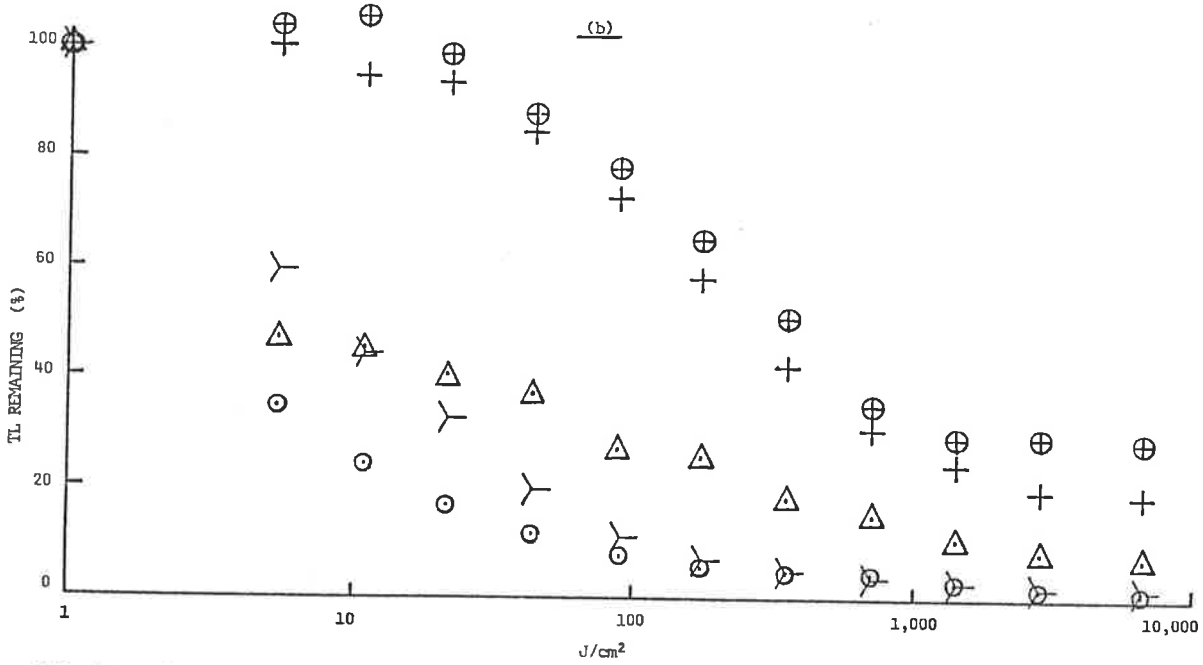

FIG. 4.4.2 (b) Shows the above data as relative TL reductions and is included to emphasise the deviation of the 325°C peak from the progression of increasing resistance to bleaching with increasing glow curve temperature. The 325°C peak is apparently fully removed by <1 minute of sunlight - the TL remaining in this temperature range after the first minute of exposure is interpreted as being the sum of contributions from adjacent glow peaks.

this is interpreted as evidence of an early equilibrium existing between retrapping and untrapping, which shifts in favour of untrapping as the available electron supply for retrapping diminishes with the emptying of the lower temperature peak traps.

A point to note if TL measurements are taken after short bleach times (as often required by the partial bleach method) is the possibility that the "unbleachable" residual remaining after the short bleach may exceed the true NTL "unbleachable" component due to this early growth by retrapping, and so lead to an underestimate of the readily bleachable component. The significance of this effect would vary with sample, dosage and illumination conditions, but is probably minor.

An unexpected feature is the relative bleaching rate of the 160°C and 220°C peaks. During the initial five minutes, bleaching proceeds more rapidly at 160°C than at 220°C, an expected finding given the relative trap depths. However, for longer exposure times, the 220°C peak undergoes the greater reduction. This anomaly has several possible explanations, among which are (a) the peak at 160°C has an unusually strong resistance to bleaching, (b) the 220°C peak is readily bleachable by all wavelengths (similar in behaviour to the 325°C peak), (c) the 220°C peak is preferentially bleached by certain wavelengths present in the simulated sunlight spectrum.

The latter explanation is favoured, and bleach data from narrow waveband illumination experiments are given in section 5.2 which support a hypothesis that preferential bleaching of the 220°C peak trap sites occurs at wavelengths $\approx$ 500nm.

Other than the initial retrapping effects, the bleaching behaviour at temperatures $>$ 250°C for the additive dose case is similar to that where only NTL is bleached. Fig. 4.4.3 compares the bleach curves at

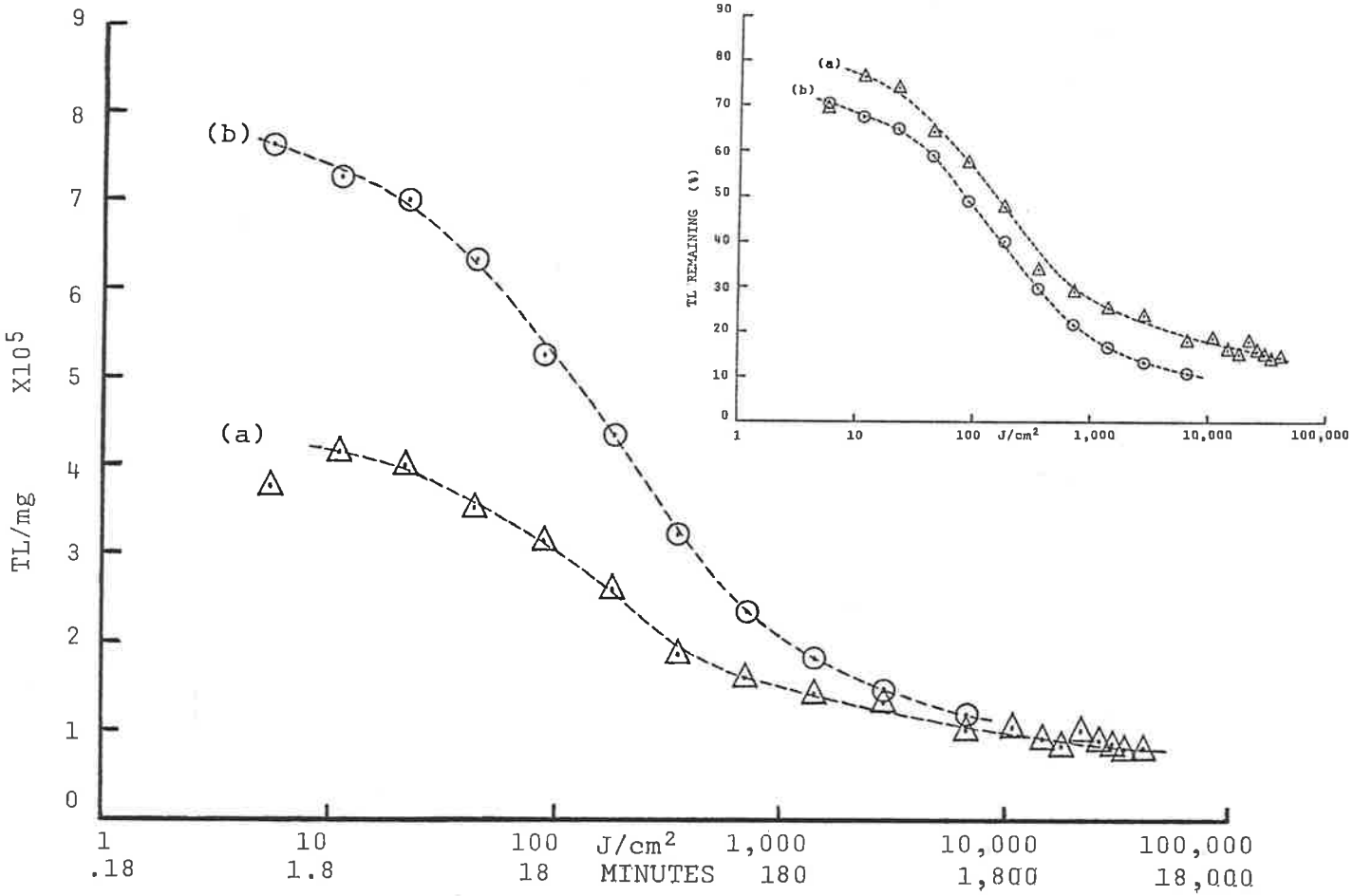

FIG. 4.4.3 Shows the bleaching of Lake Woods (S3,TD,1m) Quartz by simulated sunlight for (a) NTL only and (b) NTL + 48 Gy ^{90}Sr-^{90}Y β. The maximum exposures correspond to 124 hours and 20 hours of natural sunlight respectively. Simulated sunlight flux 5.5 J/cm²/minute.
TL integration range 44°C centred on 370°C.
The insert displays the same data but as a percentage of the initial TL.

370°C for these cases, both in "absolute" units (TL counts/mg, with no correction for detection efficiency) and as a proportion (percentage) of the initial TL content.

It is seen that as bleach times exceed ~20 hours, the absolute TL content (TL/mg) in both cases tends towards a similar value, an expected finding given the conclusion in section 4.3 that the residual is independent of the initial TL level and instead relates to the untrapping-retrapping balance of a crystal specific concentration of charge.

The insert to Fig. 4.4.3 presents the same data as a percentage of the initial TL. It is apparent that the assumption of equal fractions bleaching in equal times appears to be valid. However, as the residual region is approached, the false dependence of the residual on the initial TL level introduced by this form of data presentation becomes quite misleading. A conclusion is that TL data, particularly bleach data, is correctly expressed in terms of absolute units, such as TL/mg, rather than as percentages of the initial TL.

Two further studies on the bleaching of additive dose samples were conducted, and confirmed the earlier finding that the residual reached after long bleach times is independent of initial TL content, within the constraints of experimental error.

The first used 90-125μm, HF etched quartz separated from the Roonka near-surface sample EB 1/S/0.10. Two sets of eight discs each received ^{60}Co γ doses of 0, 34, 67 and 118 Gy (giving TL contents varying by up to an order of magnitude), followed by a two day delay after which one set received a 20 hour natural sunlight bleach. A least squares fit to this bleach data (integration range 44°C centred on 370°C) gave a straight line ~parallel to the dose axis, from which the above conclusion was drawn.

The second investigation involved administering additive ^{90}Sr-^{90}Y β doses of 0, 7.65, 15.3 and 23.0 Gy to pairs of LW (S3,TD,1m) quartz sample discs, followed by two days delay before exposure to simulated sunlight for periods of 0, 1, 2, 4, 8, 16, 32, 64, 128, 256, 512 and 1024 minutes. The residual reached after 1024 minutes was effectively independent of dose (~9×10^4 counts/mg, for a 44°C summation centred on 370°C) and closely approaches the residual value attainable for this material after long bleaches under similar conditions (see Fig. 4.3.4 - the data are directly comparable as both cases used similarly treated samples of the same sediment, and the same TL measurement apparatus).

A significant finding is that the partial bleach method seems inapplicable at these temperatures (~370°C) due to the absence of a suitable readily bleached component. From the data shown in section 4.3, and unpresented supplementary work, the mean life of an electron trapped at a 325°C peak trap under the standard illumination conditions was estimated to be ≈ tens of seconds at most, (cf 50±5 minutes for the 370°C peak), thus giving the 325°C peak an extraordinary susceptibility to optical bleaching. It is concluded that the 325°C peak constitutes the readily bleachable component utilized by the partial bleach method when applied to quartz possessing glow curves and bleaching behaviour comparable to these Australian quartz samples, while the 370°C peak plays the role of "unbleachable" component, for short bleach times. Application of the partial bleach method to such quartz therefore requires the selection of a temperature range for TL integration centred at ≈ 350°C, which provides sufficient representation of the 325°C peak to give a usable TL reduction, as well as the 370°C peak component to effectively resist bleaching for the short bleach times (<2 minutes) necessary to erase the 325°C peak component. Such a specific combination of integration range and bleach time offers the possibility of valid ED estimates for these quartz samples using the partial bleach method.

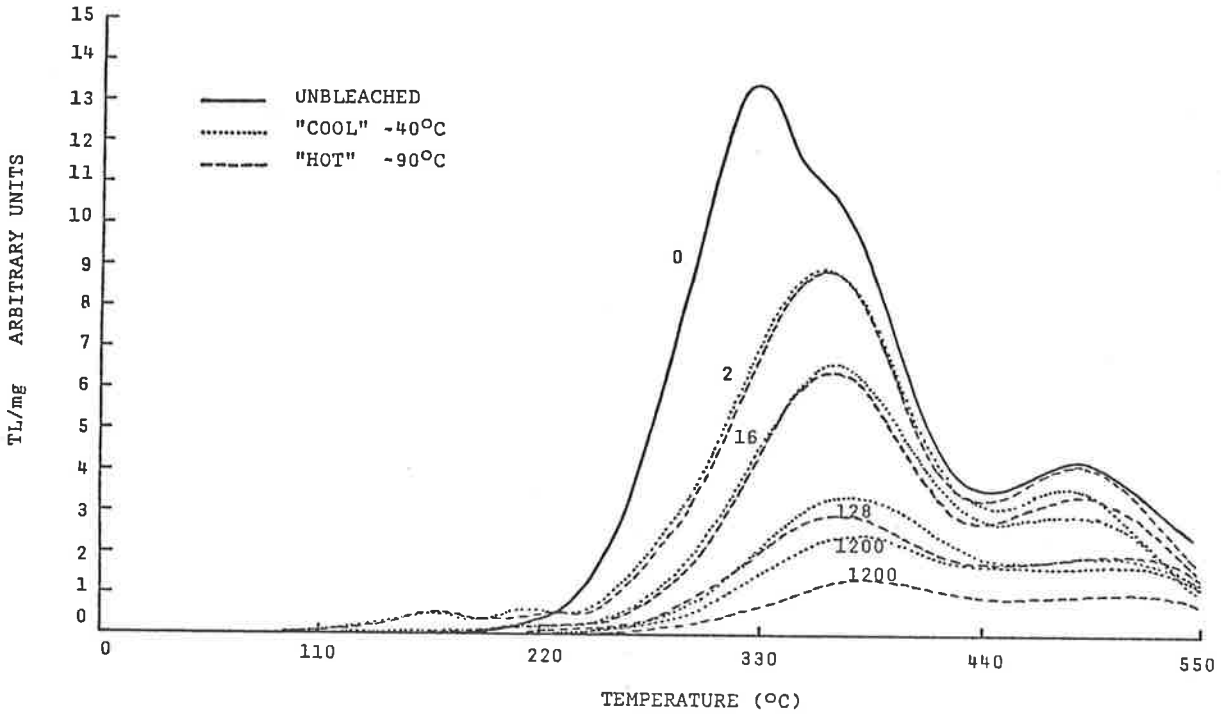

FIG. 4 .5.1. Shows the effect of crystal temperature on the bleaching of LW (S3,TD,1m) quartz NTL by simulated sunlight (5.5 J/cm^2/minute). Two similar sets of samples were used, one being held at -40°C ("COOL"), the other at -90°C ("HOT"). Exposure times as shown (minutes).

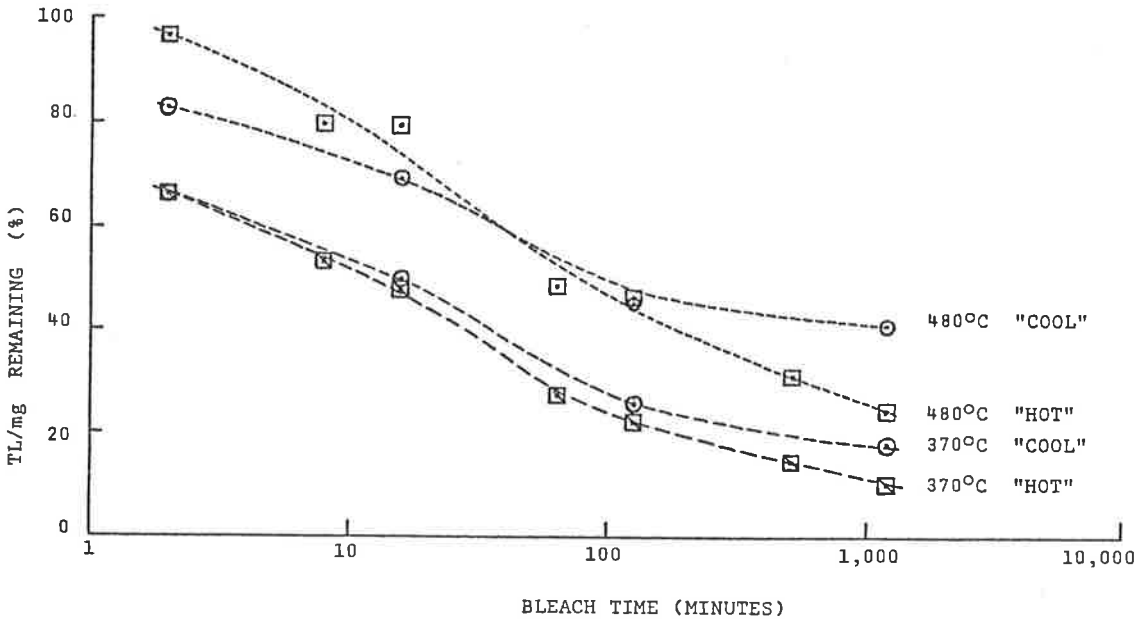

FIG. 4 .5.2. Shows the reduction of LW (S3,TD,1m) quartz NTL by various exposures to simulated sunlight (5.5 J/cm^2/minute), at crystal temperatures of -40°C ("COOL") and -90°C ("HOT"). Shown above are Σ44°C centred at 370°C and 480°C. (From Fig 4 .5.1.).

4.5 Some effects of site conditions

Much TL laboratory work is performed on quartz grains separated from the parent sediment by procedures similar to those outlined in section 2.2, and bleached by unfiltered natural or simulated sunlight under controlled conditions. Though these conditions may vary considerably from those experienced by the quartz grains during depositional exposure, the assumption is that the TL behaviour of separated, HF etched grains is unchanged by such separation treatments. A brief investigation was conducted to assess the significance of some of the on-site physical conditions that may affect bleaching rate or extent, specifically: (a) grain temperature during exposure and (b) the presence of a natural coating (usually oxides) on grains.

Considering each: (a) Fig. 4.5.1 shows a family of LW (S3,TD,1m) quartz glow curves generated by exposing two similar sets of sample discs simultaneously, with the only difference in exposure conditions being the temperature at which the grains were held. One set, "cool", was positioned on a cooled Al plate which maintained a sample disc surface temperature of ~40°C, while the second set, "hot", rested on a slab of uncooled black rubber at the same distance from the illumination source, and rapidly reached an equilibrium temperature of ~90°C. Temperatures were measured at the grain surface of the sample discs by means of a thermocouple probe.

The TL reduction at the 370°C and 480°C peaks is shown in Fig. 4.5.2.

While the early bleaching behaviours at 370°C appear similar, after bleach times exceed ~100 minutes the rate of bleaching of the "hot" samples declines more slowly than that of the "cool", permitting bleaching to proceed to a lower TL level in the former case, for a given long exposure. The greater "hot" TL content at 480°C during the first 20

minutes is attributable to enhanced retrapping probabilities for these traps due to the effective prevention of competition from 110°C peak traps by the relatively high crystal temperature.

In conclusion, the ambient temperature during depositional exposure becomes important with respect to the residual reached after long exposures, and so is of direct relevance to total bleach-based methods.

(b). One consequence of the separation procedure, particularly HF etching, is the removal of the grain's natural coatings. The possibility that these coatings may bias or attenuate the incident natural sunlight, and so alter or slow the bleaching pattern, was investigated by comparing the effect of natural sunlight on two sets of samples. These sets, prepared from LW (S3,TD,1m) sediment, differed only in that following HCl digestion, sieving and magnetic separation, one set received a 40 minute HF etch while the other remained unetched.

Three unbleached sample discs from each set provided a normalization factor to account for signal attenuation, transparency changes on heating and α contribution differences between the sets, resulting from the presence of the outer grain layers in the unetched case (see caption for Fig. 4.5.3). Any disparities between the bleached glow curves were then considered to be consequences of attenuation of the incident sunlight by the grain coatings. Fig. 4.5.3 shows the families of bleached glow curves, and as no differences are seen after normalization it is concluded that the natural oxide coatings have no significant effect on bleaching behaviour, at least for the monolayer configurations in which the grains were exposed.

This raises a supplementary question: to what depth must a grain be covered for bleaching to cease? For example; given a low opacity sediment, bleaching may continue, albeit at a reduced rate, for grains several mm below the surface layer, resulting in the most-bleached layer

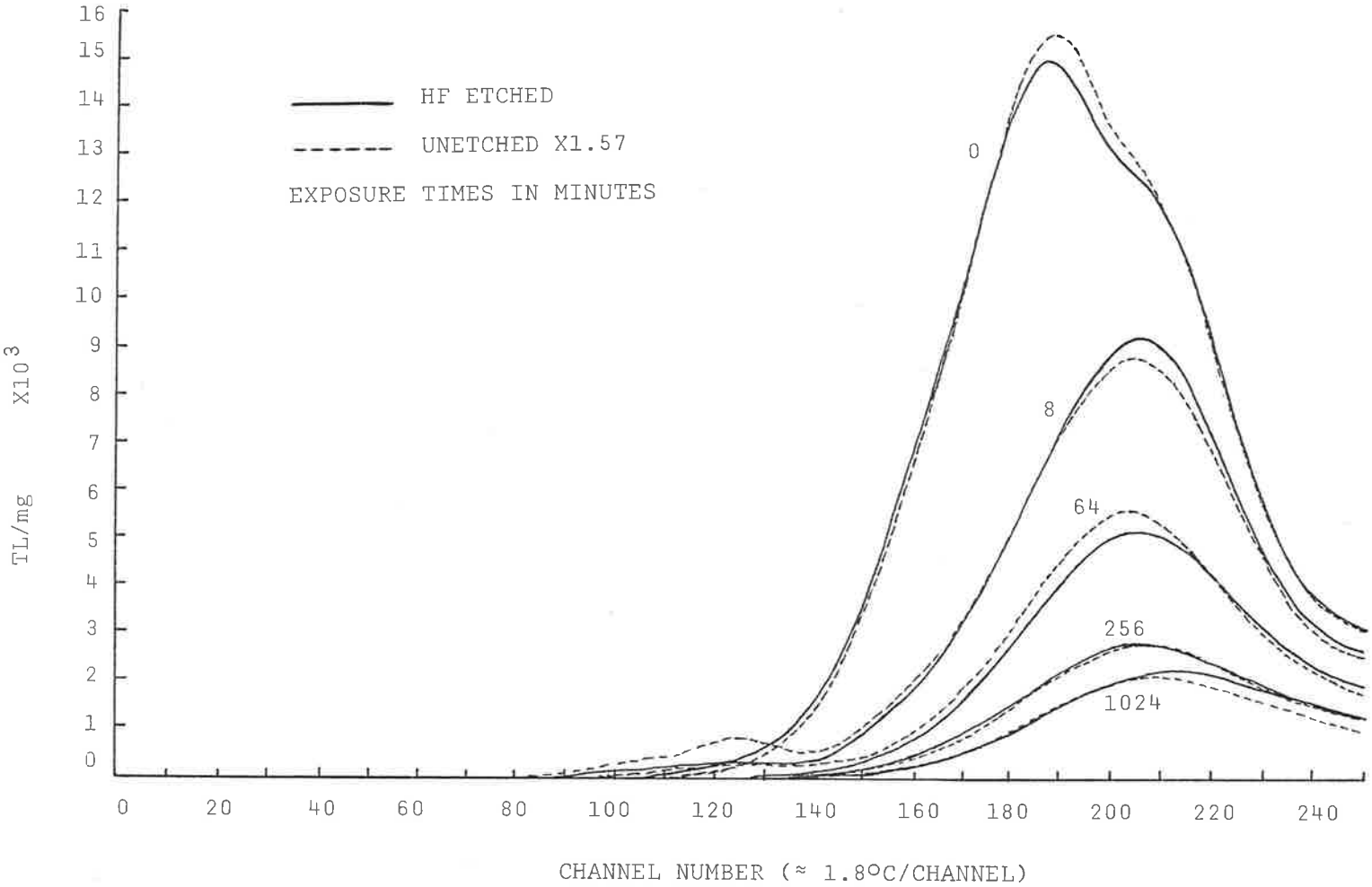

FIG. 4 .5.3. Shows the effect of HF etching on the natural sunlight bleaching of LW (S3,TD,1m) quartz NTL.
Procedural: The 90-125μm, magnetically separated fraction was divided into two portions: the first received 40 minutes etching in 50% HF acid, the second remained unetched. The TL of three unbleached samples prepared from each portion was measured, and the ratio of the total glowcurve areas was taken as the normalization factor to account for influences such as signal attenuation by any oxide coating, transparency changes on heating and α contribution. Found Σ(etched)/Σ(unetched) = 1.57. Heating rate was $10 K sec^{-1}$ to 470°C maximum.

being sub-surface and so causing surface layer sampling to give an erroneously high residual compared to that finally reached.

An experiment to determine the minimum thickness of sediment required to prevent bleaching was conducted by positioning known thickness layers of untreated Roonka sediment between the simulated sunlight source and samples prepared from EB 1/S/1.9 quartz. Exposure times were 1 hour only. It was found that 1mm of sediment was sufficient to prevent detectable TL reduction at 370°C, indicating strong absorption of the active bleaching wavelengths. However, >6mm of sediment were necessary before bleaching of the 325°C peak ceased, leading to the conclusion that bleaching of susceptible glow peaks can continue in the near-surface layers under suitable conditions, and so produce longer effective bleach times in these cases, (it must be noted that the Roonka sediment is of low opacity, lacking in both organic content and significant oxide discolouration).

CHAPTER 5 THE EFFECT OF WAVELENGTH ON THE BLEACHING OF QUARTZ TL

5.1 Introduction

Preceding work considered the bleaching of quartz TL by a simulated sunlight beam closely approximating clear-day natural sunlight in both intensity and spectrum.

However, little is currently known concerning the dependence of bleaching on the wavelengths present in the incident beam (see section 1.10), though such information is useful in predicting how bleaching proceeds in various environments, particularly those which selectively attenuate the incident sunlight (eg, fluvial and marine sedimentation), and for tailoring the spectrum of laboratory light sources to match.

Furthermore, the behaviour of the NTL glow peaks under illumination by specific wavelengths assumes some practical importance with the introduction of optical stimulation of an NTL component as the essential feature of a promising new technique of TL measurement (Huntley et al, 1985).

This chapter reports a study on the relative efficiencies of fourteen "natural" wavebands for the bleaching of Lake Woods (S3,TD,1m) quartz NTL. The effect of three of these selected wavebands on the TL of Lake Woods (S3,TD,1m) quartz was also examined for the additive dose case, and a further study compared the bleaching of Roonka (EB 1/S/1.9) and Woakwine (WK 1S/4) quartz NTL by the same three wavebands.

In all the above experiments the illuminating beam was separated from the output of the Oriel solar simulator by interference filters (see Appendix 2). Finally, the bleaching of quartz NTL by ultra-violet free "white" light was briefly investigated.

5.2 The effect of illumination wavelength

The relative efficiency with which the NTL of quartz is bleached by the various wavelengths present in natural sunlight is of significance for reliably predicting the bleaching behaviours encountered in a range of environments where attenuation of the incident sunlight introduces a wavelength bias. Furthermore, such information may help elucidate the nature of the traps probed. Consequently this study was undertaken to examine the dependence of bleaching behaviour on illumination wavelength.

Experimental: bleaching illumination was provided by means of the selected interference filters (see Appendix 2) used to separate fourteen wavebands from the output of the Oriel solar simulator. As some of these wavebands contained longer wavelengths than those passed by the plastic colour filters used to provide laboratory safelight illumination, a precautionary experiment was conducted to determine what effect, if any, prolonged exposure to the ambient safelight illumination had on the quartz TL. The findings are given in Appendix 4, and it was concluded that significant disruption to the quartz TL is induced by $\gtrsim$ 4 hours exposure. As a result, "Chris James" 179 (orange) plastic colour filters were substituted for the yellow "Cinemoid" No.1 filters previously in use, and a new batch of Lake Woods (S3,TD,1m) quartz was prepared as per section 2.2, but under only the low intensity red light emitted by a 15W fluorescent tube wrapped in three layers of "Chris James" 164 (red).

Sets of twenty-four similar samples prepared from this quartz (Lake Woods (S3,TD,1m); 90-125μm fraction, magnetically separated and HF etched, NTL only) were exposed to illumination from each of the chosen wavebands for periods of 0,1,2,4,8,16,32,64,128,256,512 and 1200 minutes (two sample discs per exposure time). Heating conditions for TL measurement were $5Ks^{-1}$ to 550°C maximum, with reheats subtracted.

Figs. 5.2.1(a)-(n) show the mass normalized, averaged glow curves from the pairs of sample discs exposed to 0,1,4,16,64,256 and 1200 minutes illumination by each waveband.

From inspection, a number of broad conclusions can be drawn. In general, the IR wavelengths appear incapable of untrapping from any of the NTL traps, visible light untraps from 325°C peak traps only, with increasing efficiency as wavelength decreases, and UV untraps from all traps, also with increasing efficiency as wavelength decreases.

While this progression of increasing bleaching efficiency with decreasing wavelength was expected, it was not expected that any of the NTL peaks would be significantly affected by visible wavelengths. Other occurrences, as the 325°C peak is removed, are some growth by retrapping at the remaining higher temperature peaks and the generation and subsequent bleaching of the 160°C and 220°C peaks.

Also noteworthy is the apparent absence of any bleaching resonances at any wavelength.

Fig. 5.2.2. shows a representation of the energy required at given wavelengths to reduce the NTL glow peaks to specified levels - 80% of initial TL for the 370° and 480°C peaks, and complete removal for the 325°C peak. "Complete removal" refers to reduction below the level at which a 325°C peak component can be resolved from the glow curve (this requires ~ 4 times the energy needed for a 20% reduction of the peak). The rule that similar fractions of TL are removed by similar exposures (see insert to Fig. 4.4.3) indicates that the energies necessary for these reductions will remove the corresponding fractions for any initial TL level, excepting the near-residual case. The fractions chosen were determined by several considerations. For the 325°C peak: the rapid bleaching of this peak under "normal" daylight conditions ensures its rapid and complete removal in the great majority of environments, and so

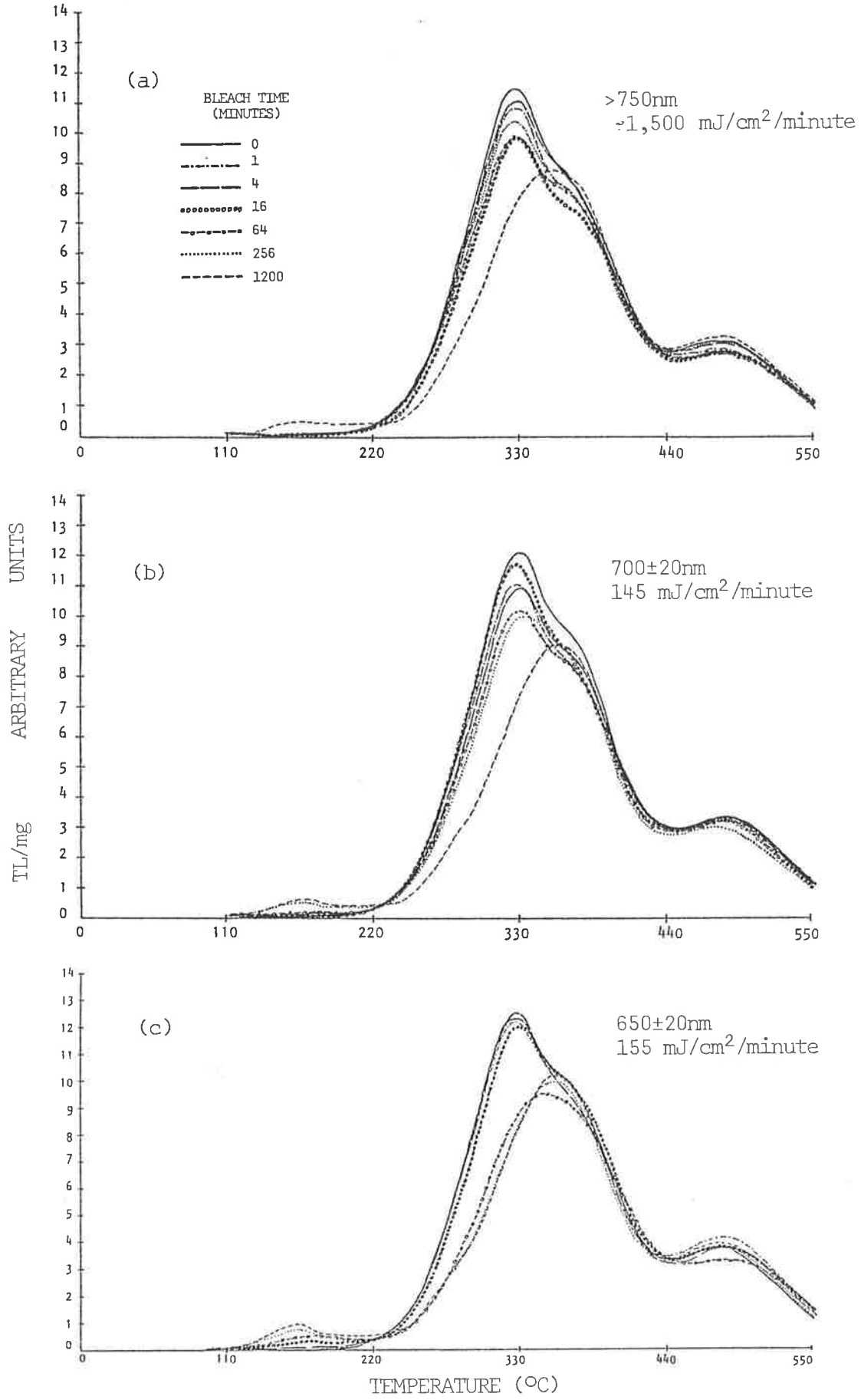

Fig 5.2.1. Shows the bleaching of LW (S3,TD,1m) quartz by various exposures to selected wavebands.
Illumination beams: simulated sunlight transmitted through the respective interference filters (see App.2). Preparation: 90-125μ, HF etched fraction, NTL only. Two sample discs per exposure time.

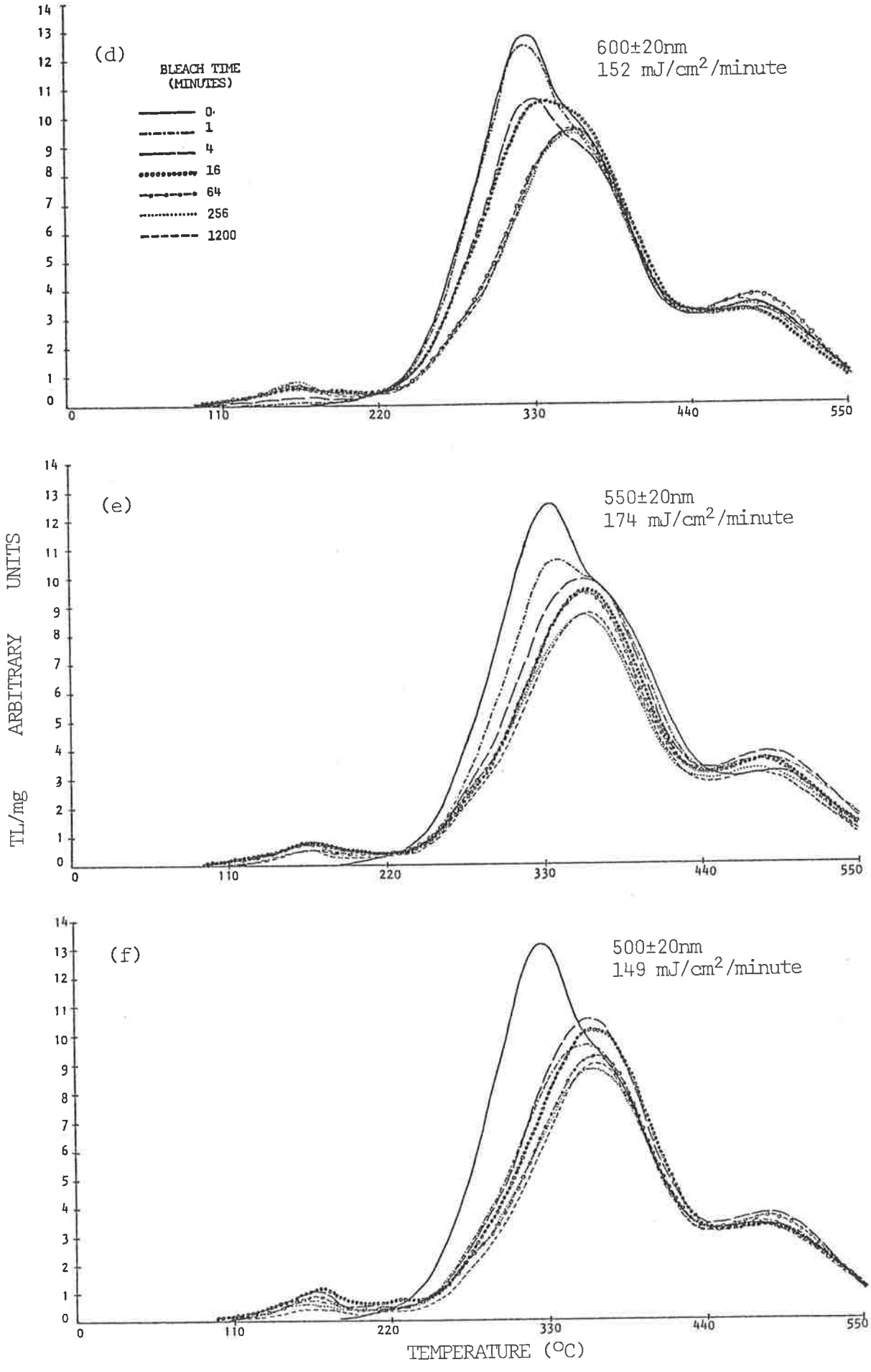
(d)
BLEACH TIME (MINUTES)
0
1
4
16
64
256
1200
600±20nm
152 mJ/cm²/minute
(e)
550±20nm
174 mJ/cm²/minute
(f)
500±20nm
149 mJ/cm²/minute
TL/mg ARBITRARY UNITS
TEMPERATURE (°C)
0
110
220
330
440
550

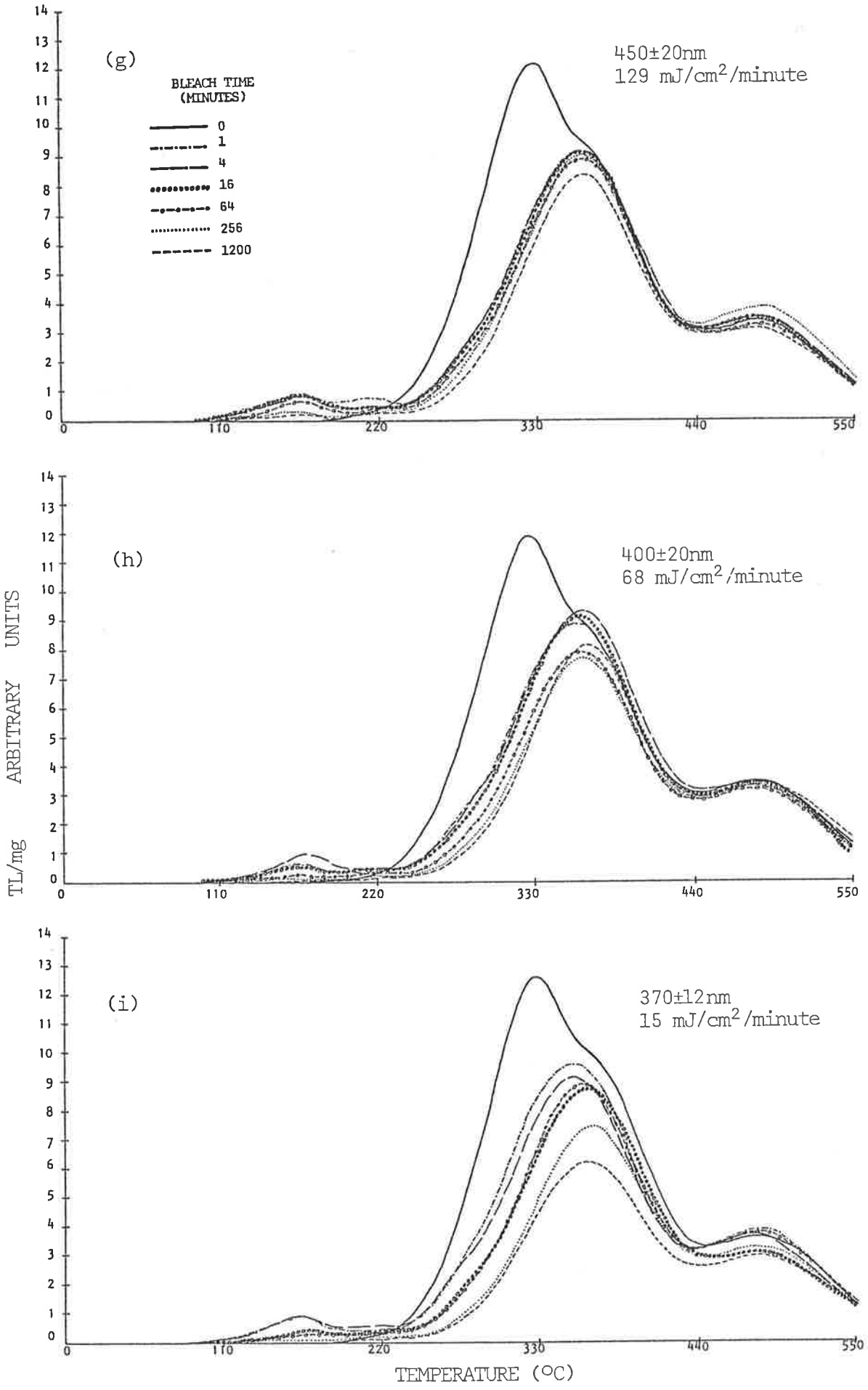
(g)
BLEACH TIME (MINUTES)
0
1
4
16
64
256
1200
450±20nm
129 mJ/cm²/minute
(h)
400±20nm
68 mJ/cm²/minute
(i)
370±12nm
15 mJ/cm²/minute
TL/mg ARBITRARY UNITS
TEMPERATURE (°C)
0
110
220
330
440
550

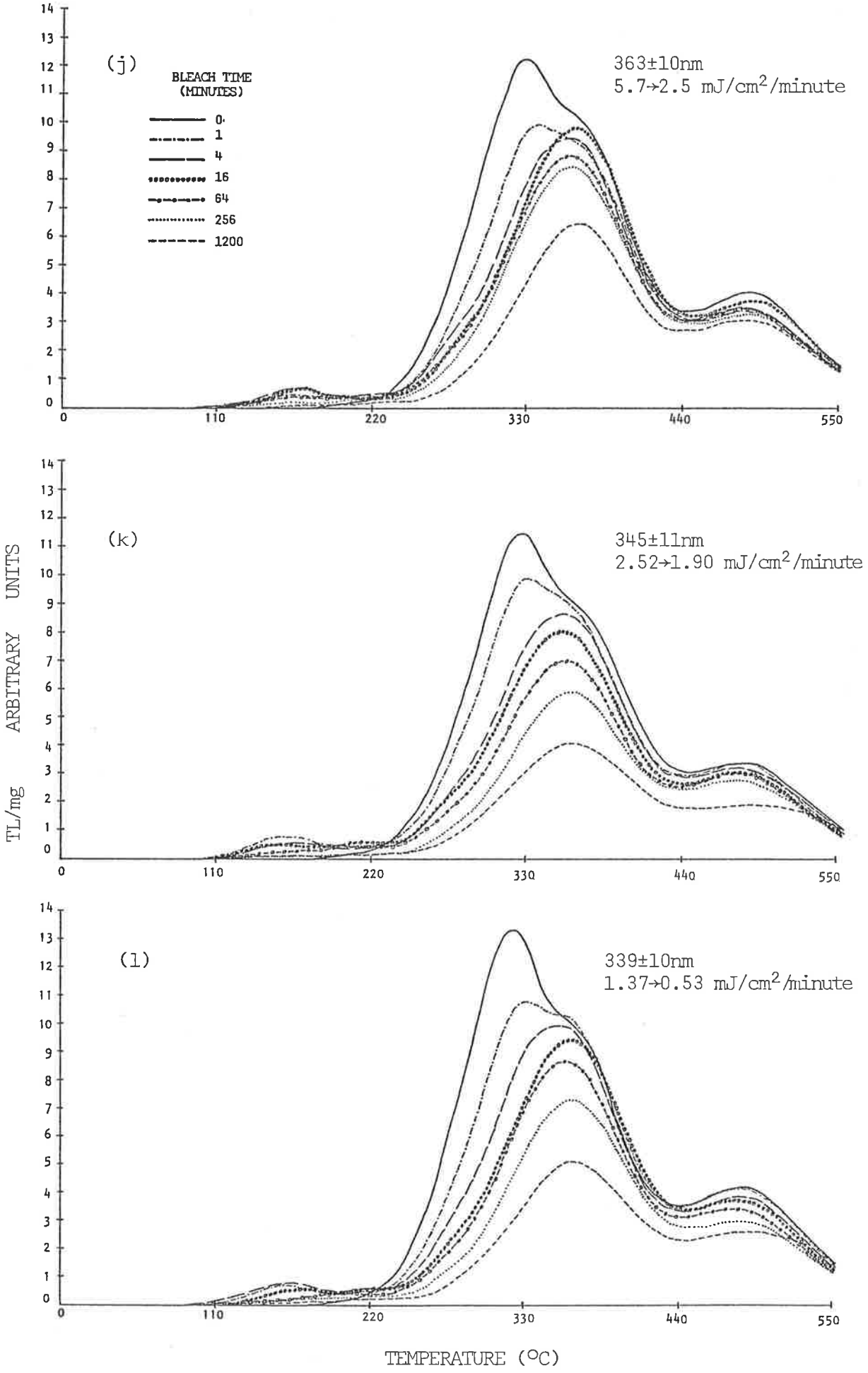
(j)
BLEACH TIME (MINUTES)
0
1
4
16
64
256
1200
363±10nm
5.7→2.5 mJ/cm²/minute
(k)
345±11nm
2.52→1.90 mJ/cm²/minute
(l)
339±10nm
1.37→0.53 mJ/cm²/minute
TL/mg ARBITRARY UNITS
TEMPERATURE (°C)
0
110
220
330
440
550

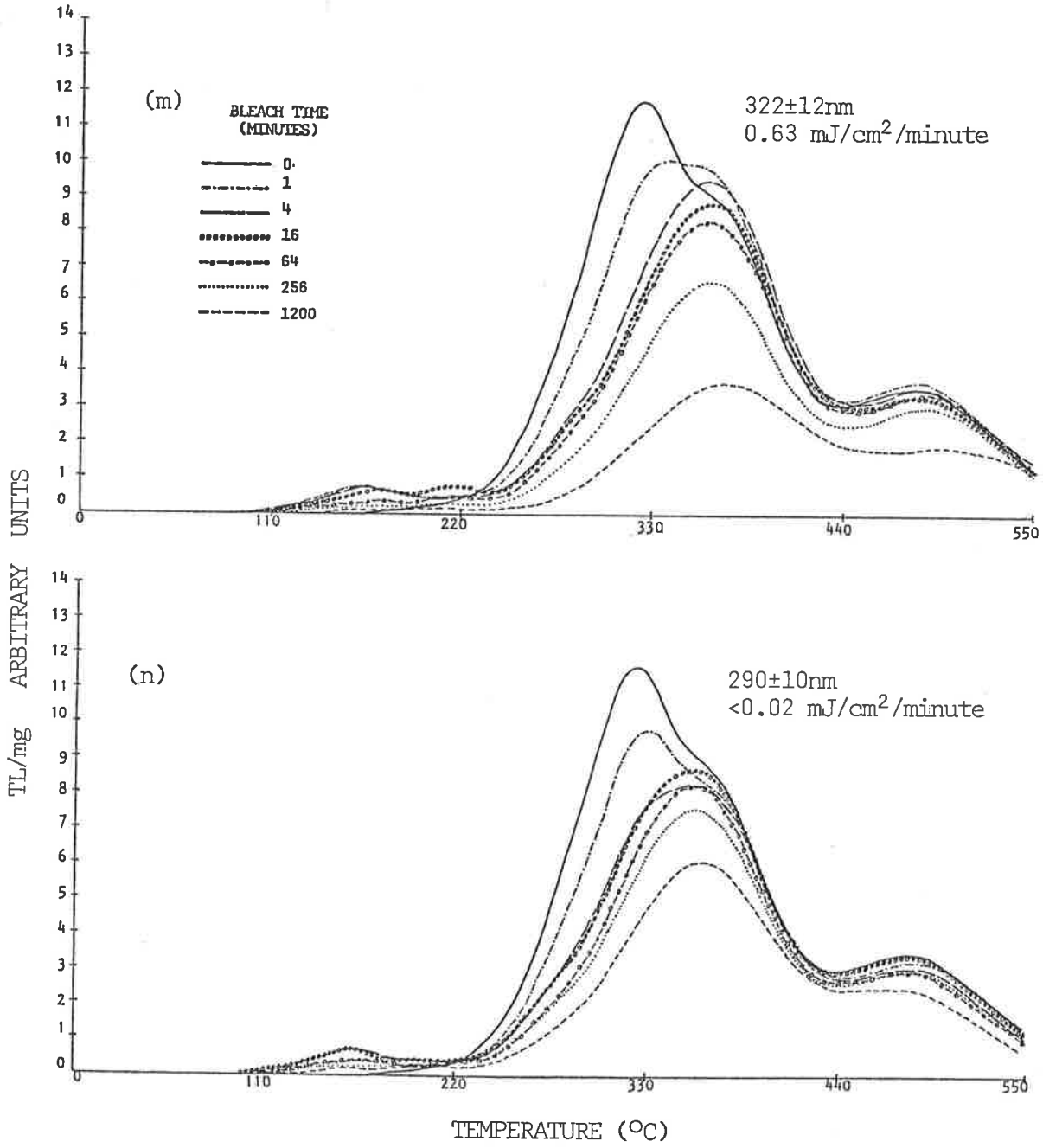
(m)
BLEACH TIME (MINUTES)
0
1
4
16
64
256
1200
322±12nm
0.63 mJ/cm²/minute
(n)
290±10nm
<0.02 mJ/cm²/minute
TL/mg ARBITRARY UNITS
TEMPERATURE (°C)
0
110
220
330
440
550

in the archaeometrical context the energies required for complete removal are of particular interest (examples: predicting the applicability of partial bleaching, or design of optical stimulation experiments). For the 370°C and 480°C peaks: the slow rate of bleaching by wavelengths > 350 nm, and the apparent resistance to any bleaching by wavelengths > 400 nm, prevented collection of data on reductions exceeding 20% in the exposure times available. Conversely, at the 325°C peak, complete bleaching occurred within 4 minutes for all wavelengths < 600 nm, and in most cases less than 2 minutes, so limiting the data available for all but the complete removal case.

It is notable that the 325°C peak bleaches without leaving a detectable residual - a finding not unexpected from a consideration of e^- trap and L centre populations. Simply, given there exists an activated L centre corresponding to each of the e^-'s trapped at all classes of trap, when untrapping occurs only from 325°C peak traps, the population of L centres exceeds the number of these e^-'s available for recombination. Assuming the known high bleaching susceptibility ensures rapid re-eviction of any e^-'s retrapped at 325°C peak traps, and the apparently favourable probability of recombination rather than retrapping, these conditions permit the effective removal of this trapped e^- population without retrapping dominating at any stage, even at the lowest concentrations of trapped e^-'s.

Inspection of Fig. 5.2.2. shows a similarity in response to light by the 370°C and 480°C peaks in the early stages of bleaching. It is only as bleaching proceeds further that the 480°C peak traps display the greater resistance to bleaching expected from their greater resistance to thermal untrapping. The absence of knowledge concerning these e^- traps prevents confident interpretation of this observation, although the similarity in bleaching response does tend to support the earlier

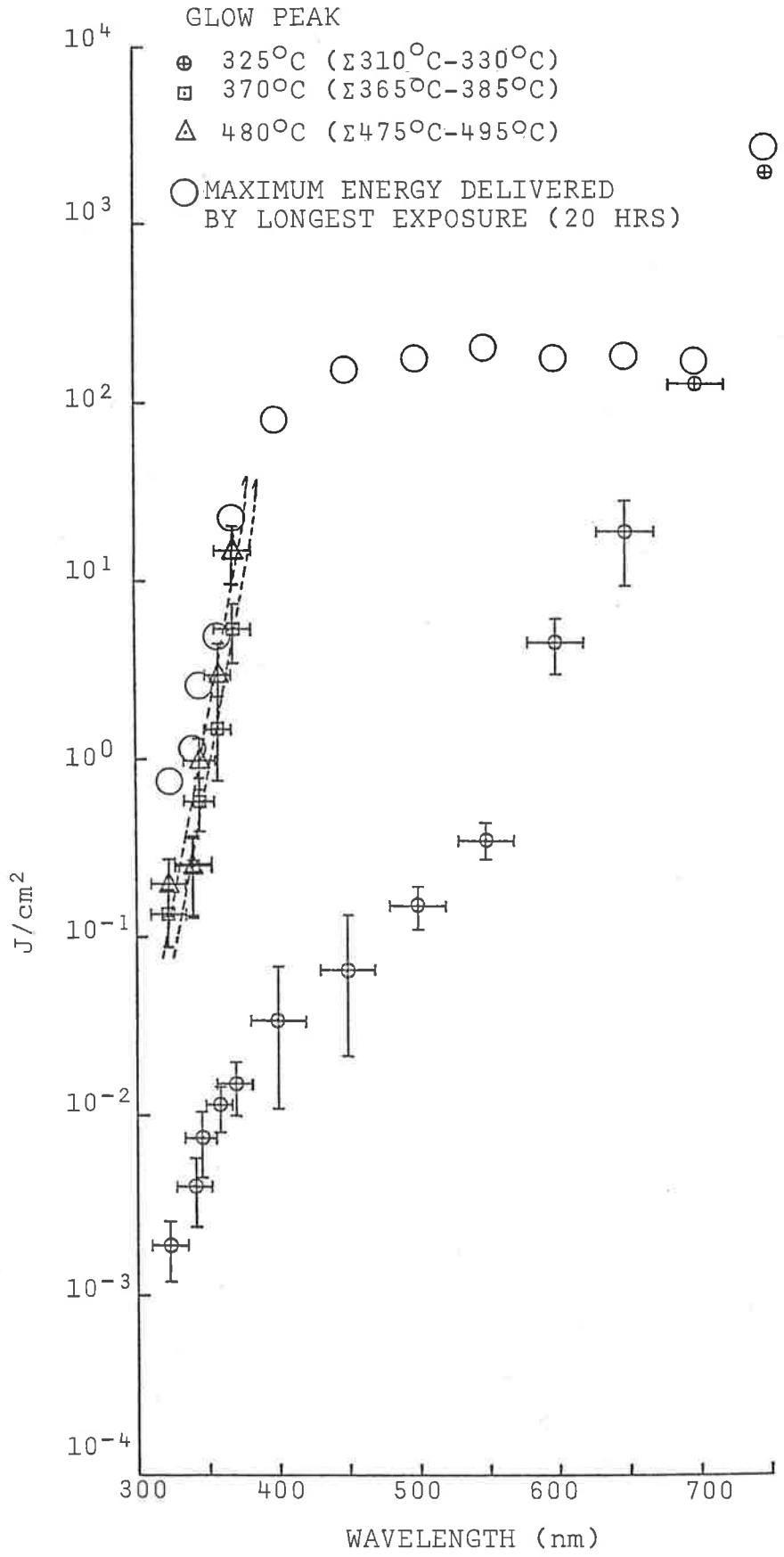

FIG. 5.2.2 Shows the energy required at selected wavelengths to reduce the NTL glow peaks of LW (S3,TD,1m) quartz to given specific levels. The 370°C and 480°C peak data is shown for a reduction to 80% of the initial TL level; however for the 325°C peak, due to its great susceptibility to bleaching, the energies shown at each wavelength are those required for complete removal of this peak.

suggestion, arising from the behaviour of annealed quartz (see section 3.4), that these traps have a similar physical nature.

An unexpected finding is that thermally determined trap depths are not necessarily good indicators of the sensitivity of the traps to optical bleaching. For example, the 325°C and 370°C peak traps have similar trap depths as determined by kinetic studies, but when probed optically the 325°C peak traps appear two orders more sensitive at the shorter "natural" wavelengths, with the disparity increasing with increasing wavelength.

The kinetically determined trap depth may represent the limiting photon energy capable of untrapping. For instance, at wavelengths $\geq$ 700 nm, the exposure times required to remove the 325°C peak are long enough for "leakage" of unwanted wavelengths through the filters to become significant, and the bleaching seen for wavelengths $\geq$ 750nm is consistent with "leaked" light being the dominant, if not only, bleaching agent. This implies IR wavelengths do not bleach at all, and so indicates the existence of a threshold wavelength beyond which the photon energies are insufficient for untrapping. Considering the 325°C peak: if it is assumed that leaked light accounts for the apparent bleaching by IR, then the longest active bleaching wavelengths are ~ 700 nm, and so have a photon energy (~ 1.8 eV) close to the kinetically determined trap depth of 1.69 eV (Wintle, 1977).

The case for the 370°C (and 480°C) peak does not appear so straight forward - the apparent threshold wavelength, ~ 400 nm, has a photon energy (~ 3.1 eV) significantly exceeding trap depth. The mechanism requiring this discrepancy in threshold energy remains unknown.

Leaving aside the physical nature of the e^- traps and their interactions with photons for a more phenomenological description of the dependence of bleaching on wavelength, a reasonable fit to the wavelength response curves (Fig. 5.2.2) is obtained by a simple exponential of the form:

$$\text{energy for specified reduction } (J/cm^2) = A.e^{\lambda/k}$$

The equations fitted for each glow peak are:

$$E_{325^oC,\ \text{removal}} = (1.9 \times 10^{-7}).\ e^{\lambda/35} \quad (J/cm^2)$$

$$E_{370^oC,\ 20\%\ \text{reduction}} = (4.7 \times 10^{-16}).\ e^{\lambda/10} \quad (J/cm^2)$$

$$E_{480^oC,\ 20\%\ \text{reduction}} = (1.0 \times 10^{-15}).\ e^{\lambda/10} \quad (J/cm^2)$$

The constants "k" indicate that bleaching efficiency changes by a factor of "e" every 35 nm for the 325°C peak, and every 10 nm for the 370°C and 480°C peaks.

Errors on k are: $k_{325^oC} = 35 \pm 5$; $k_{370^oC} = 10 \pm 2$; $k_{480^oC} = 10 \pm 3$

For practical applications, it is instructive to represent the reduction induced by specific wavelengths against equivalent minutes of natural sunlight - this is shown in Figs. 5.2.3 (a), (b) and (c) for each NTL peak. "Equivalent minutes of natural sunlight" refers to the duration of exposure to natural sunlight required to deliver the same total energy in the given waveband. The conversion equation from real-time filtered simulated sunlight exposures (minutes) to equivalent minutes of natural sunlight is:

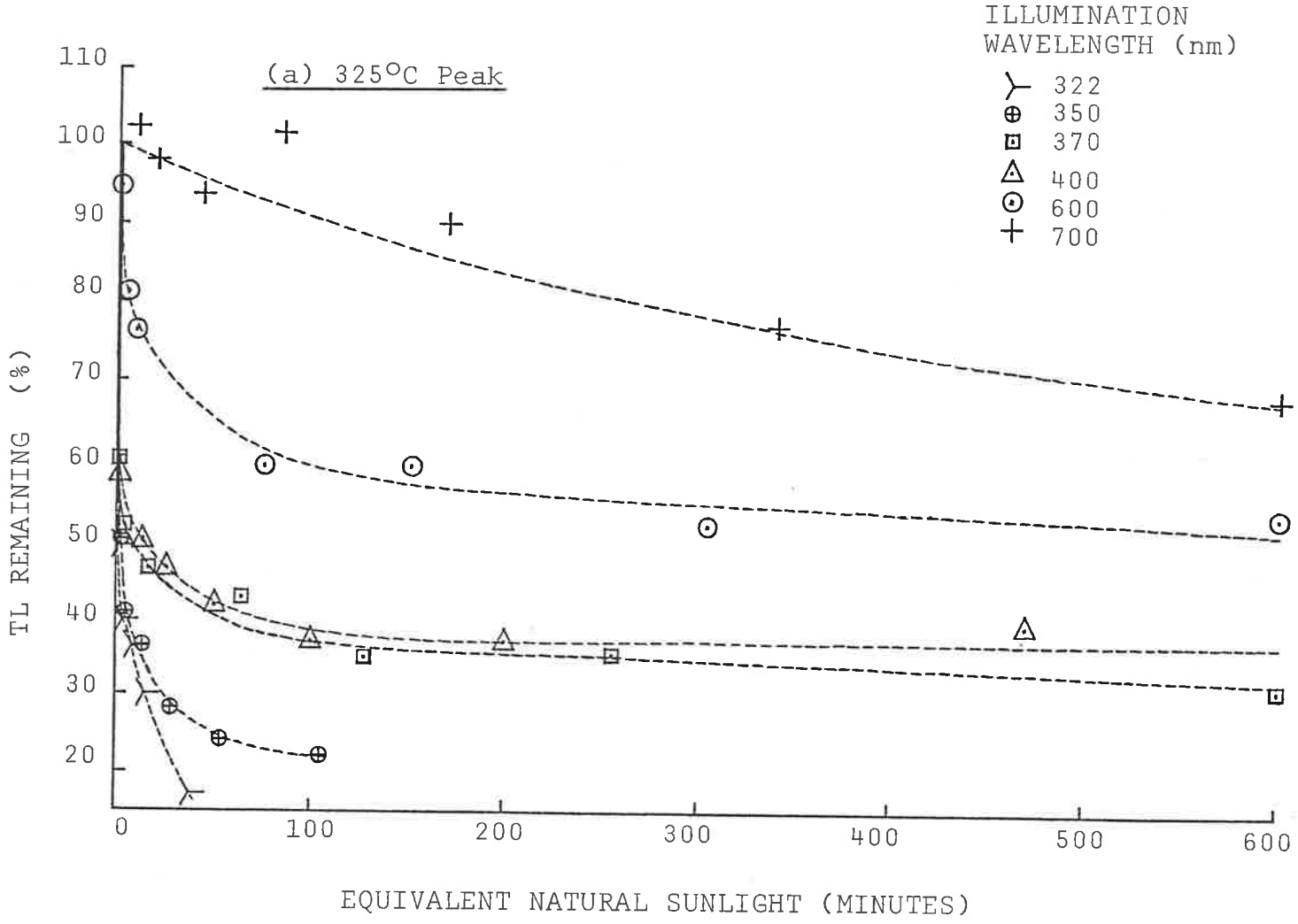

FIG. 5.2.3. (a),(b),(c) Show the reduction of the prominent NTL peaks of LW (S3,TD,1m) quartz by exposures to various wavebands. "Equivalent Natural Sunlight" refers to the duration of exposure to natural clear-day sunlight (Solar zenith angle ~48°) required to deliver the same total energy in a given waveband.

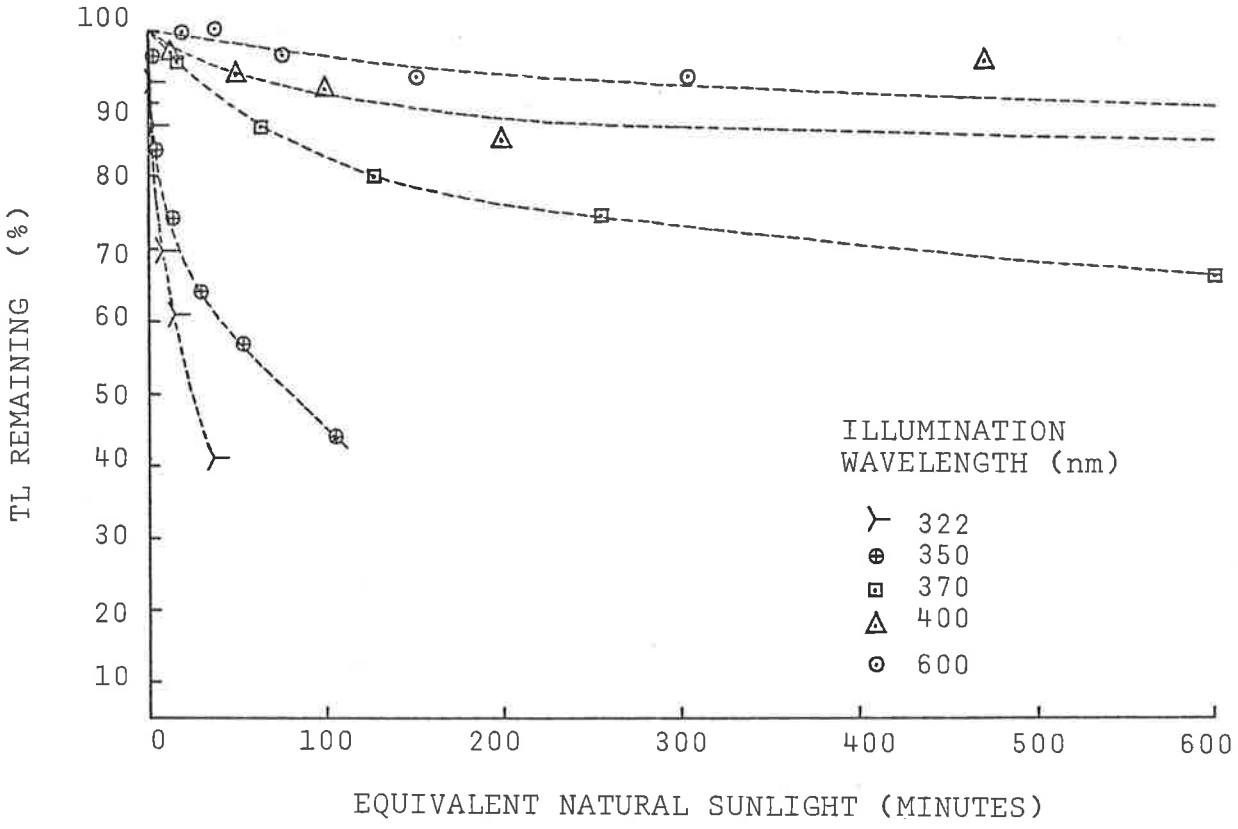

(b) 370°C Peak

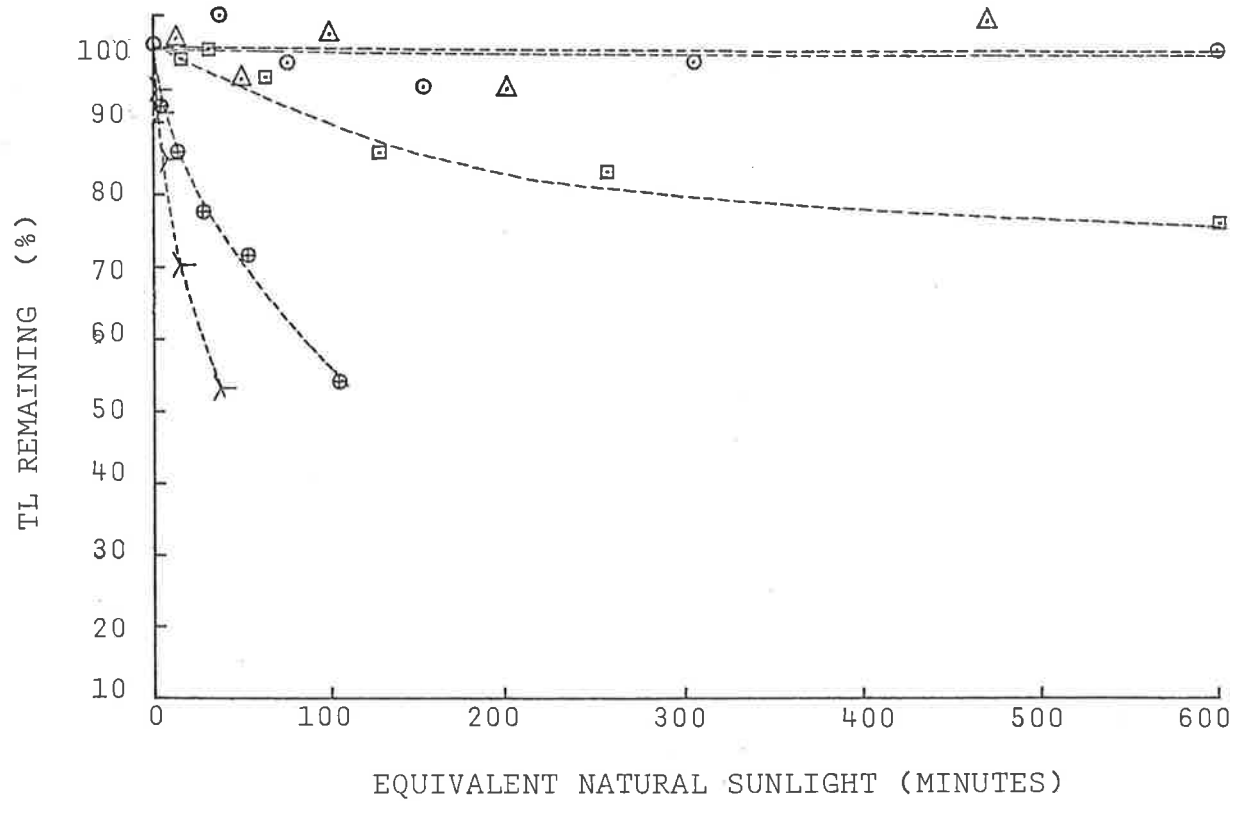

(c) 480°C Peak

$$\text{Equiv. Sunlight (mins)} = \text{Exposure Time} \times \frac{\text{Filter}}{\text{Transmittance}} \times \frac{\text{Simulator Power}}{\text{Sunlight Power}}$$

Comparison between Figs. 5.2.3 (a), (b) and (c) shows the ability of visible wavelengths to bleach only the 325°C peak, and highlights the efficiency of UV as the dominant bleaching wavelengths. Also shown is that bleaching is most efficient by the shortest UV wavelengths.

Consider the bleaching of each NTL glow peak in turn: (a) the 325°C peak temperature range integrated (310°C - 330°C) contains principally TL from this peak, but also contributions from the adjacent 280°C and 370°C peaks amounting to ~ 40% of the initial NTL. Visible wavelengths remove the 325°C peak component with increasing rapidity as wavelength decreases, but do not affect the other components. UV reduces the 325°C peak TL more rapidly still, but also removes the previously resistant "overlap" TL component (the 370 ± 12 nm waveband appears to contain the longest wavelengths capable of bleaching the more stable 370°C (and 280°C) peak TL). (b) The 370°C peak (TL integration 365°C - 385°C): the unbleached NTL in this temperature range consists of ~ 90% 370°C peak TL and ~ 10% 325°C peak TL. Exposure to visible light reduces the total TL to ~ 90% by removing only the 325°C peak contribution. The remaining TL is bleachable only by UV light, with bleaching efficiency increasing as wavelength decreases. (c) 480°C peak (TL integration 475°C - 495°C). This glow peak lacks any readily bleachable component, being reduced only by UV light, and also shows an increasing susceptibility to bleaching as UV wavelength decreases, similar to the 370°C peak.

The above investigation examines the wavelength dependence of the bleaching of quartz NTL; a supplementary study was conducted to indicate how, if at all, the presence of lower temperature (ATL) peaks affects the response of the NTL peaks.

For the ATL peaks themselves, in general, greater bleaching efficiency was expected from shorter wavelengths, and greater bleaching susceptibility to be exhibited at lower glow curve temperatures.

Three wavebands only were selected for this trial:-
500 ± 20 nm, 370 ± 12 nm and 322 ± 12 nm - representing the most abundant visible natural sunlight wavelengths and the longer and shorter naturally occurring UV wavelengths respectively. Exposure, TL measurement and analysis conditions are as described above, and the material (LW (S3,TD,1m) quartz) was from the same prepared batch, differing only in that each sample now received a 47 Gy ^{90}Sr - ^{90}Y β-irradiation, followed by a two day delay prior to exposure. Fig. 5.2.4 shows the families of bleached glow curves for each wavelength - these are directly comparable to Figs. 5.2.1. (f), (i) and (m).

Consider first the 370°C and 480°C glow peaks. As expected, neither is affected by 500 nm illumination (the slight reduction seen after 20 hours is consistent with bleaching by the UV leakage through the filter). Similarly, the 370 nm and 322 nm illuminations both induce TL reductions comparable to those expected, though a slightly greater proportion of TL (~ 8%) is removed in a given exposure time than for the NTL case. This discrepancy is attributed to the greater ratio of empty/occupied traps in the latter case, so giving a greater probability of retrapping, and a consequent decline in the rate of nett TL reduction. Otherwise, there are no detectable alterations to the bleaching behaviour of either the 370°C or 480°C peaks.

The 325°C peak appeared unaffected by the presence of lower temperature peaks, both in rate of reduction and response to given wavelengths. The 160°C and 220°C ATL peaks generally behaved as expected in that progressively shorter wavelengths bleached more efficiently. However, although both peaks are readily bleachable by 322nm and 370nm

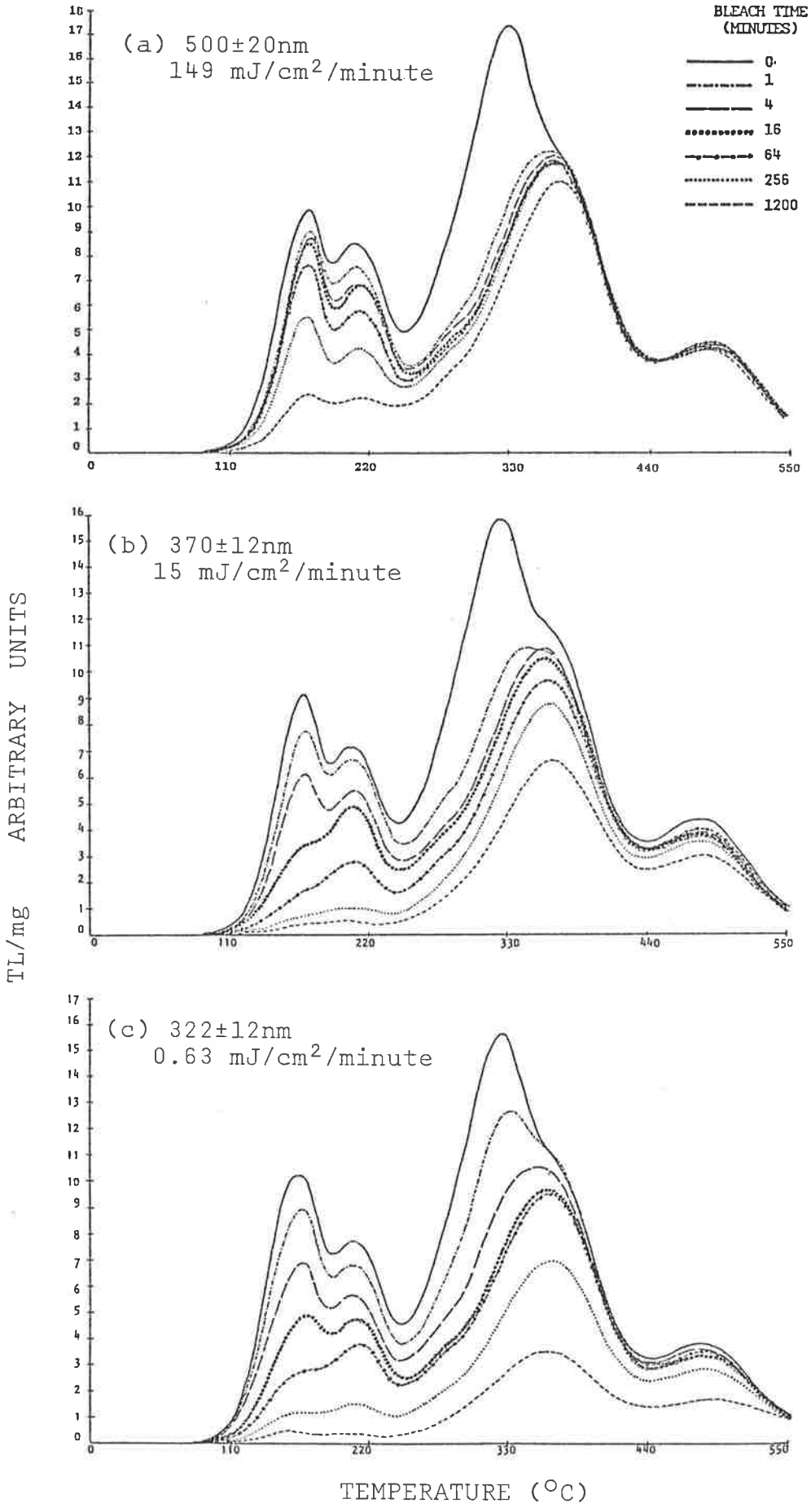

FIG 5.2.4 Shows the bleaching of irradiated LW (S3,TD,1m) quartz by exposure to three selected wavebands.
Irradiation: 47 Gy ^{90}Sr-^{90}Y, followed by two day delay before bleaching.
Other conditions as shown in Fig. 5.2.1.

light, it appears the 220°C peak is the more susceptible to 500 nm light, and so provides evidence of a preferential bleaching response. Further work is required to accurately determine the most efficient wavelengths. (Although there is also a suggestion of similar behaviour by 325°C peak traps at similar wavelengths, experimental uncertainty prevents firm conclusions being drawn from the available data (see Fig. 5.2.2)).

5.3 A comparison between dissimilar quartz

This section describes an investigation in which the generality of the previous findings (section 5.2) was empirically examined by comparing the bleaching behaviour of a further two dissimilar quartz samples. These were separated from sediment collected at the Roonka (EB 1/S/1.9) and Woakwine (WK 1S/4) sites. All details of sample preparation and experimental design are as for the preceding study, this comparative study differing only in that fewer wavebands were utilized - those selected were 322 ± 12nm, 370 ± 12nm and 500 ± 20nm. The 322nm waveband was chosen as representative of the shortest solar UV commonly reaching sea level (Diffey, 1977), 370nm as approximating the UV/visible boundary, and containing the longest wavelengths apparently capable of significantly bleaching all the quartz NTL peaks, and 500nm was chosen as the most abundant region of the solar spectrum and representative of visible light, (additionally, the existence or otherwise of an NTL component readily bleachable by these wavelengths is of interest given this waveband contains the 514.5nm Argon-ion line used in reading TL by the optical stimulation technique of Huntley et al (1985)).

Figs. 5.3.1 and 5.3.2 show the families of glow curves for each waveband from the Roonka and Woakwine quartz respectively. The reproducibility of these glow curves is not accurately known, but from the higher proportions of contaminant grains found in each, compared to Lake Woods (S3,TD,1m) quartz, (see chapter 6), and some unpresented work, ±8% is probably a reasonable estimate. Figs. 5.3.1 and 5.3.2 are directly comparable to each other and to the similarly bleached Lake Woods (S3,TD,1m) quartz glow curves shown in Fig. 5.2.1 (f), (i) and (m).

On comparison, the most noticeable feature is the close similarity in the behaviour of all three samples at each bleaching wavelength - corresponding peaks are bleached at similar rates by a given waveband, appearing to have similar proportions removed by given exposures. Also, in each case the 500nm illumination removes the 325°C peak within the first minute of exposure, but thereafter has no significant effect, showing the 325°C peak effectively constitutes a thermally stable component of NTL readily bleachable by visible light, and so suggests the applicability of the optical stimulation technique to these sediments.

In conclusion, for the Australian quartz samples on which this work was performed, the NTL changes induced by a given exposure duration and wavelength are remarkably similar.

In extension, if some assumptions are made concerning the trap types and populations, the earlier findings on the susceptibility of each glow peak to various illuminating wavelengths have universal applicability. Consider a glow curve as the sum of its component glow peaks, each of which corresponds to a specific type of e^- trap; then by inference the different glow curve shapes from quartz with different origins and histories are attributable to varied proportions of the same, relatively few, classes of e^- trap. The physical nature of each of these e^- trap classes gives them a characteristic response to any given wavelength and so makes the bleaching of each individual peak, and hence the complete

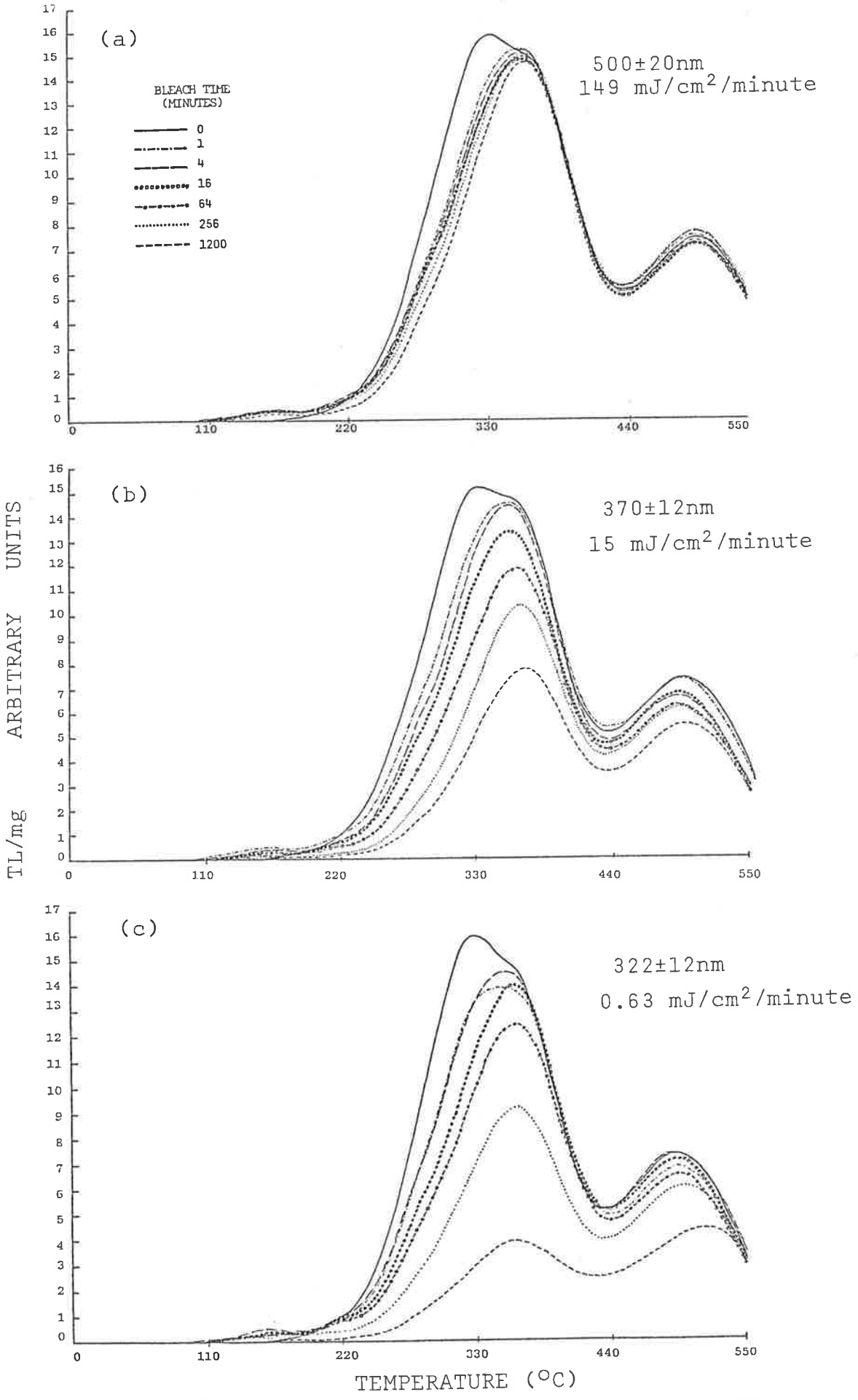

FIG. 5.3.1 Shows the bleaching of Roonka (EB 1/S/1.9) quartz NTL by three selected wavebands filtered from simulated sunlight. Conditions: HF etched, 90-125μm fraction; two sample discs per exposure time.

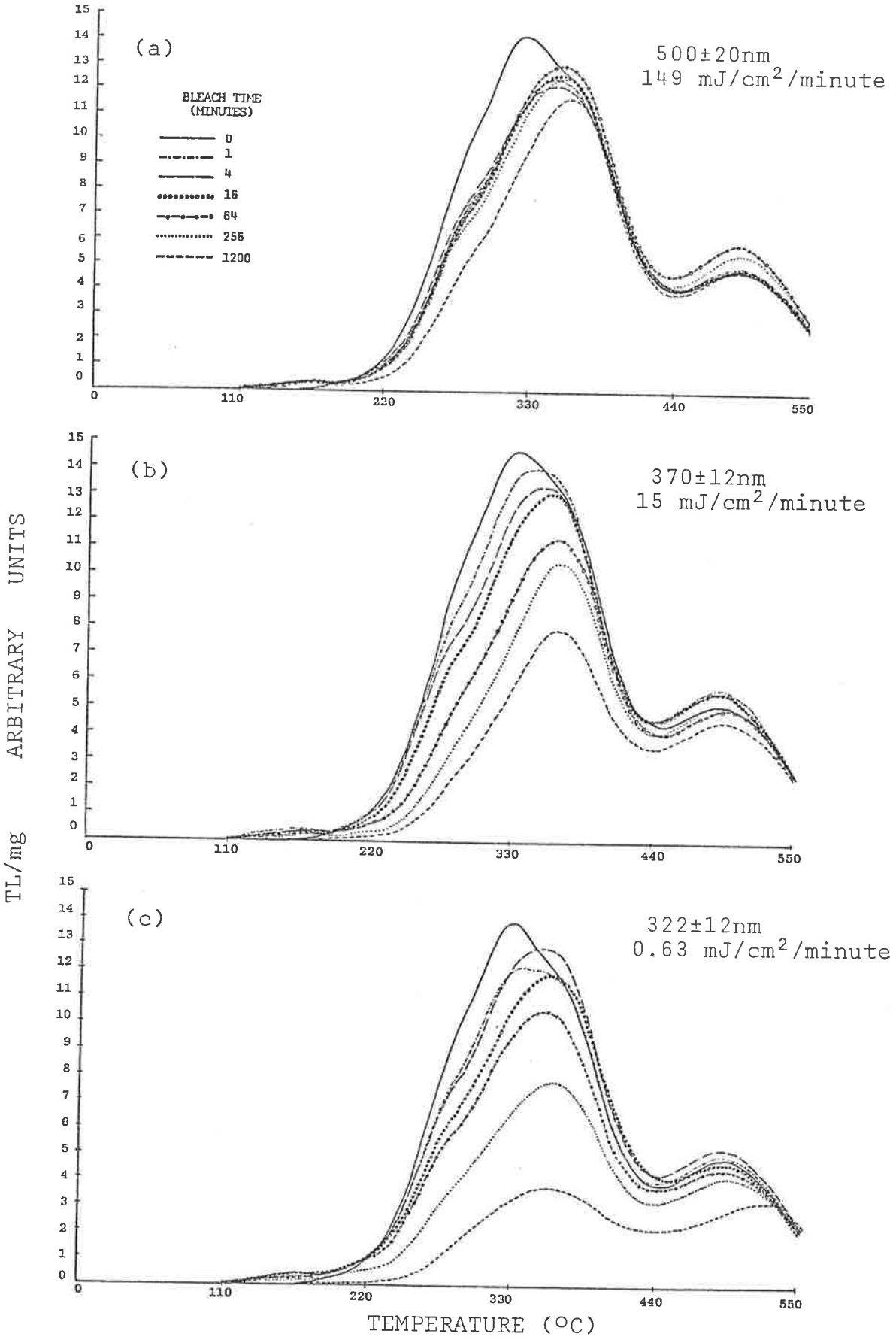

FIG. 5.3.2 Shows the bleaching of Woakwine (WK 1S/4) quartz NTL by three selected wavebands.
Conditions: HF etched, 90-125μmfraction; two sample discs per exposure time.

glow curve, predictable. An example: the similar relative peak heights, and hence relative trap populations of the three quartz samples compared here makes the observed similarity of bleaching behaviour the expected result.

The above argument and empirical support suggest the possibility of reliably predicting the bleaching behaviour of any given quartz under any specified illumination conditions.

5.4 Bleaching by UV-free "white" light

A final investigation into the dependence of bleaching on illumination wavelength examined the bleaching by a simulated sunlight beam from which the UV component was removed. This filtering was done by stacking three 400nm long wave pass plastic filters, giving a transmitted "white" light beam of approximately natural clear-day intensity (Fig. 5.4.2 shows total transmittance of the three stacked filters).

Experimental design - material (Lake Woods (S3,TD,1m) quartz), bleaching conditions, TL measurement and analysis - was as described in section 5.2, differing only in that the 400 nm long wave pass filter was substituted for the interference filters. Fig. 5.4.1 shows the resulting family of bleached glow curves.

Notable features include the removal of the 325°C peak within the first minute of exposure, and the simultaneous growth by retrapping of peaks at 160°C and 220°C and their subsequent reduction with increasing bleach times.

Given the absence of UV from the illuminating beam, no significant changes were expected at either the 370°C or 480°C peaks. However, 20 hours of "white" light exposure, totalling approximately 4.8 kJ/cm^2 (energy flux ≈ 4 J/cm^2/minute), induced a TL reduction of about 15% at

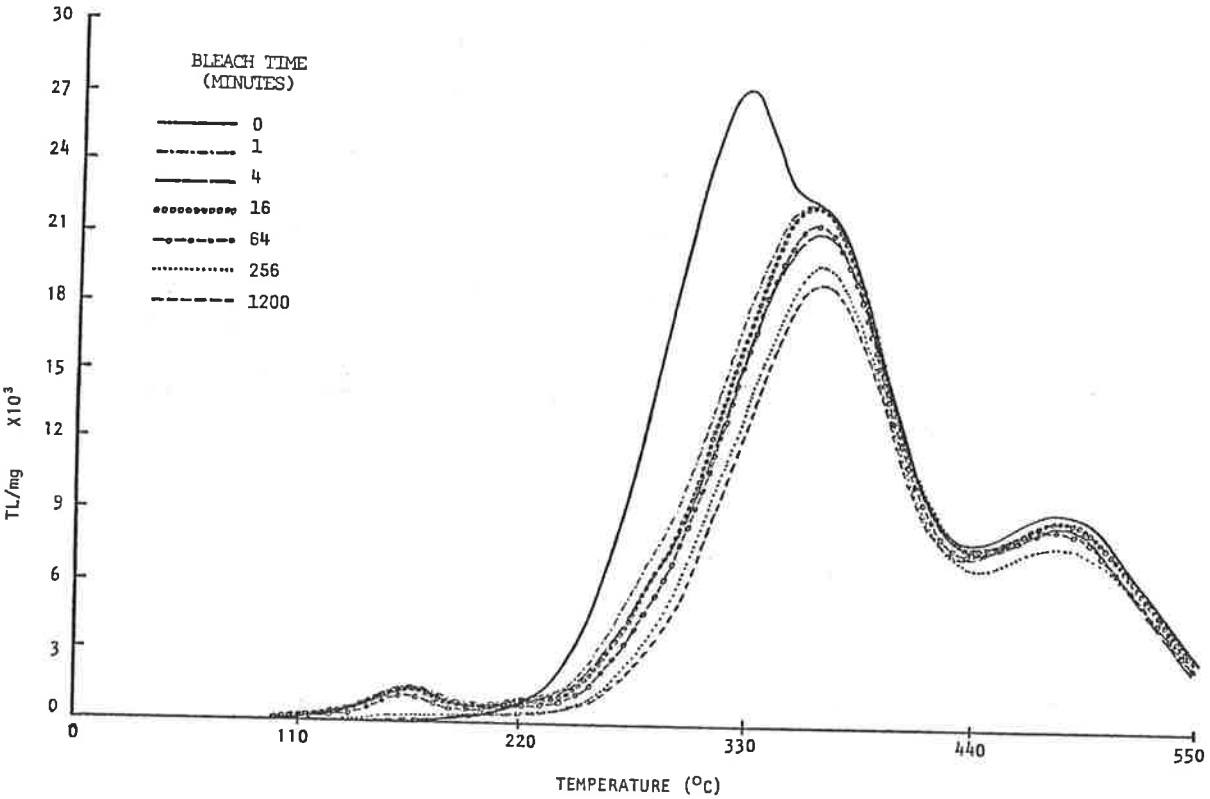

FIG 5.4.1. Shows the bleaching of LW (S3,TD,1m) quartz by various exposures to simulated sunlight from which wavelengths <400nm have been removed by three stacked long wave pass filters (see fig. 5.4.2).
Preparation: 90-125μ, HF etched fraction, NTL only. Two sample discs per bleach time.

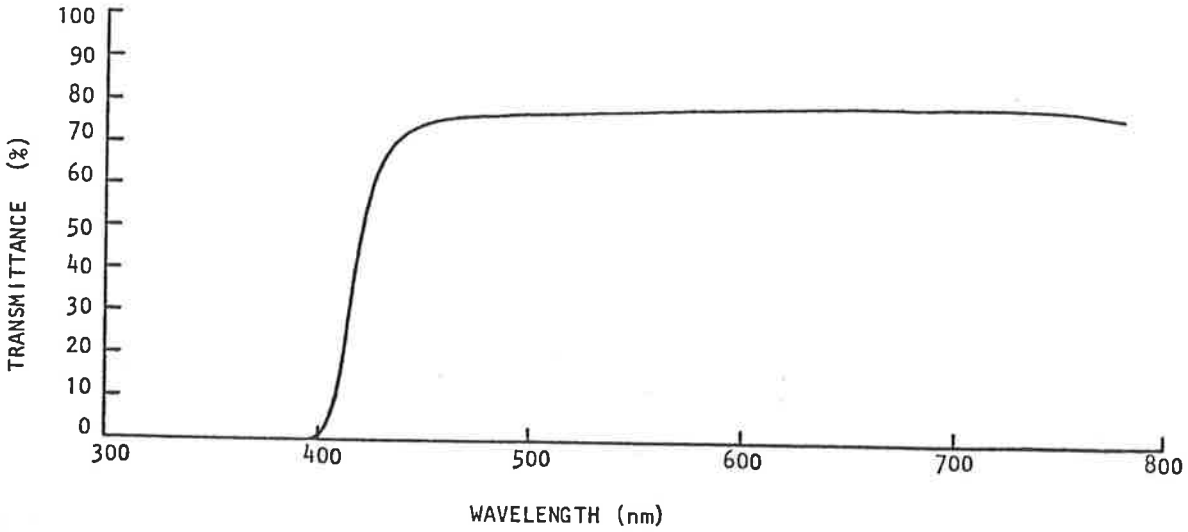

FIG. 5.4.2. Shows transmittance Vs wavelength for the three stacked sheets of "Sola Optical" UV blockout material used as a 400nm long wave pass filter (see fig.5.4.1.).

both peaks. Several possible explanations for the observed reduction exist: (a) sufficient UV "leaks" through the plastic filters (b) coincidental statistical fluctuations (unlikely), (c) sufficient energy of visible wavelengths is delivered by the longer exposures to account for some of the reduction (see Fig. 5.2.2).

The data does not permit a conclusion as to which of the above is dominant - it is possible that all three factors contribute.

Irrespective of the precise cause, the total TL decrease at the 370°C and 480°C peaks is small considering the total illumination energy delivered (4.8 kJ/cm^2), and supports the findings given in section 5.2. that UV is the sole active bleaching component of the solar spectrum for quartz NTL at all glow curve temperatures (the 325°C peak excepted).

A corollary: the spectrum of the illumination used above is an approximate analogue to that of the UV-depleted natural sunlight encountered when sedimentation occurs underwater, and the bleaching behaviour seen is consistent with the conclusions of Mejdahl (1985) and Berger (1985a) that waterlaid quartz is poorly bleached. However, neither author noted the susceptibility of the 325°C peak to bleaching by wavelengths > 400 nm, and the consequent role it gives this peak as an NTL component bleachable by UV-depleted illumination. Such selective removal of the 325°C peak can introduce peculiarities as the natural regeneration of the bleached glow curve proceeds. For example, Smith (1983) found a double plateau in some Spencer Gulf quartz samples, and attributed this to preferential attenuation by gulf waters of the shorter wavelengths required to bleach higher temperature NTL, so permitting bleaching only of the lower temperature NTL. This interpretation appears essentially correct, and it is now apparent that removal of the lower temperature NTL - the 325°C peak - does not require <u>any</u> UV, and can be expected in all situations where reasonable exposure to visible light occurs.

The relevance of this to dating waterlaid sediments is self-evident - only techniques reading the readily bleached 325°C NTL component, such as partial bleaching or optical stimulation, are applicable to these deposits, and only then if there has been sufficient pre-depositional exposure to light to remove the 325°C peak (equivalent to $<$ 1 minute unattenuated sunlight).

Additionally, this further emphasises the need to protect the sample from inadvertent bleaching during sample collection and preparation (see Appendix 4).

CHAPTER 6 REPRODUCIBILITY OF QUARTZ TL - SOME INVESTIGATIONS

6.1 Introduction

Occasional references exist in the literature to the poor reproducibility of coarse grain quartz TL, with disc-to-disc variations commonly 10% or more.

In agreement with these, previous work at Adelaide by Smith (1983) has shown a typical scatter of ± 10% S.D., or greater, for 3mg aliquots of South Australian quartz. Smith also noted that dose normalization usually gave a much closer grouping of values than weight normalization.

The principal cause of this variability is now widely accepted to be the presence of some "bright" grains in a sample.

The existence of similar disc-to-disc scatter in the Lake Woods quartz became apparent with personal experience, and gave motivation for a series of tests aimed at determining the extent of this scatter, then locating and characterizing the bright grains presumed responsible.

6.2 Variations in the high temperature NTL of Lake Woods quartz

As only high temperature TL was used throughout this study, and is of interest in sediment dating, comparison of TL variations was restricted to the high temperature glow curve peaks. These occur at 325°C, 370°C and 480°C in Lake Woods quartz.

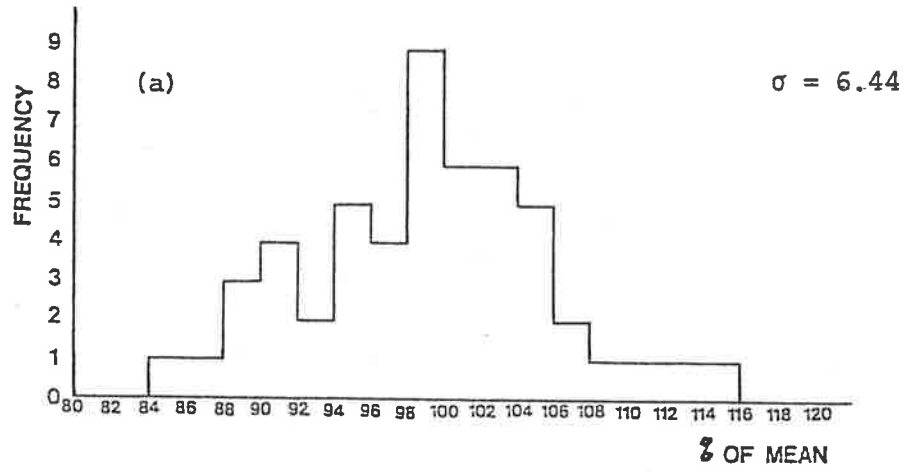

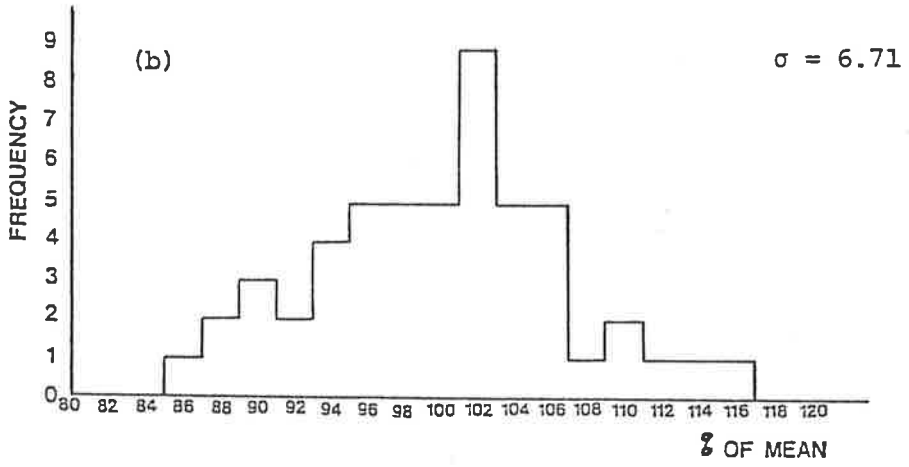

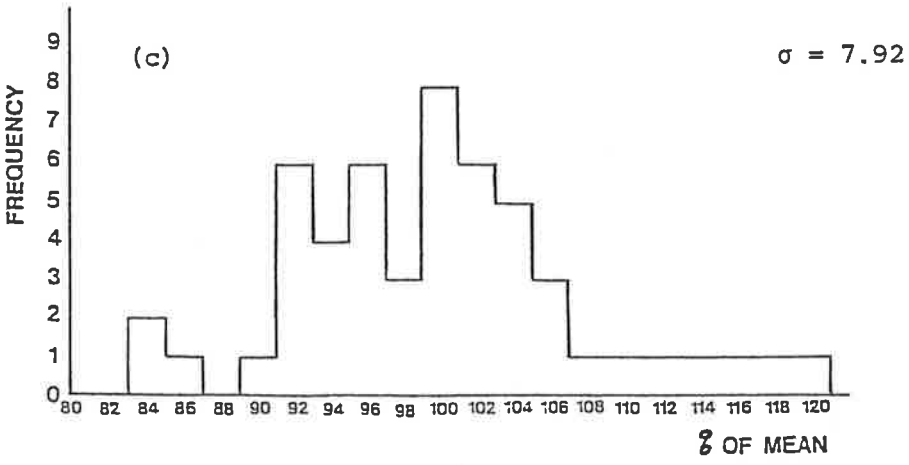

Fig 6.2. Distribution of high temperature NTL for 52 sample discs at (a) 325°C peak (b) 370°C peak (c) 480°C peak.

The distribution of the disc-to-disc scatter was found by comparing the NTL of 52 similar discs of LW (S3,TD,1m) quartz. These discs comprised two sets - 28 being "zero bleach" discs from previous work, and the remaining 24 prepared specifically for this comparison. The quartz was from the same separated, etched batch, ensuring an identical preparation history and so allowing combination of all the data. The batch preparation was as described in section 2.2. All discs were heated at $5Ks^{-1}$ to 550°C maximum, with reheats subtracted.

Figs 6.2 (a), (b) and (c) show the NTL at the 325°C, 370°C and 480°C peaks respectively. The TL for each peak is expressed as a percentage of the mean. Summations for the 325°C and 480°C peaks were over the peak 44°C. For the 370°C peak, which appeared as a "shoulder" on the 325°C peak, optical stripping of the latter revealed the 370°C peak to lie between channels 156 and 176, (343°C to 387°C), this was the temperature region summed over.

The 1 σ values of 6-8% of all three high temperature NTL peaks confirm the existence of disc-to-disc scatter of a magnitude great enough to be troublesome in dating applications.

6.3 Variations in high temperature second glow TL

The reproducibility of high temperature artificially induced TL (ATL) was examined and compared to the NTL reproducibility of the same set of discs.

After first glow, each of a set of 24 discs received a 21.7 Gy ^{90}Sr-^{90}Y β dose, followed by immediate heating at $5Ks^{-1}$ to 550°C maximum, with reheats subtracted. Both the NTL and second glow data are shown in Figs. 6.3 (a), (b) and (c).

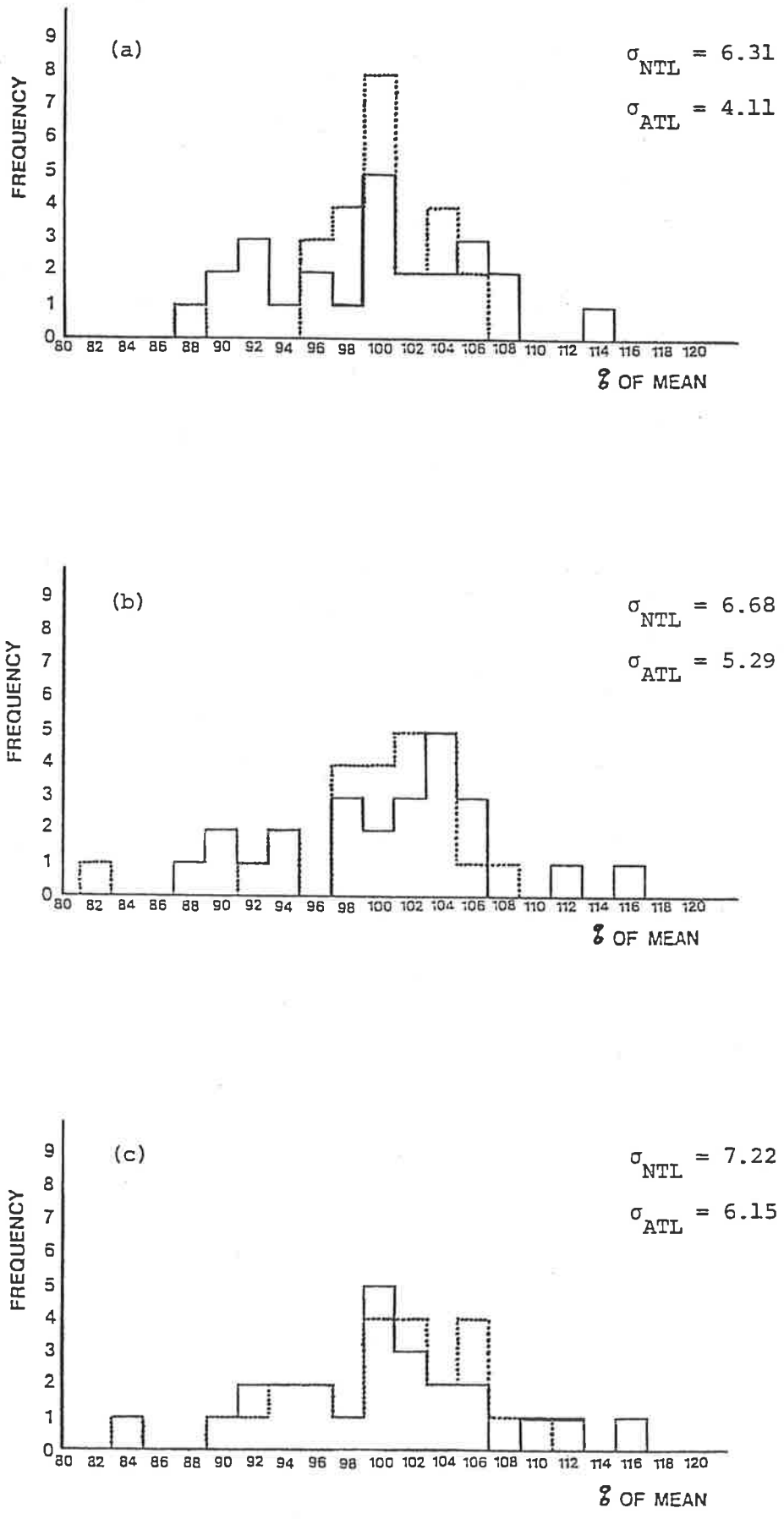

Fig 6.3. Distributions of high temperature NTL and ATL for 24 discs at (a) 325° C peak (b) 370° C peak (c) 480° C peak. —— NTL ------ ATL

Inspection shows an apparent narrowing of the distributions after irradiation, in agreement with the previously mentioned findings of Smith (1983). The significance of the narrowing was assessed by "F" testing the variances.

At 5% significance level, for (23,23) degrees of freedom, the cut-off for significance is 2.02.

$325^{o}C$ peak

$$\frac{(S.D._{NTL})^2}{(S.D._{ATL})^2} = \frac{(6.31)^2}{(4.11)^2} = 2.36$$

$2.36 > 2.02$ => difference is significant.

$370^{o}C$ peak

$$\frac{(S.D._{NTL})^2}{(S.D._{ATL})^2} = \frac{(6.68)^2}{(5.29)^2} = 1.59$$

$1.59 < 2.02$ => no significant difference.

However, each distribution contained an extreme value, at 2.4 σ NTL and 3.4 σ ATL, in populations of 24. Neglecting both extreme values gives a cut-off of 2.05 for (22,22) degrees of freedom at 5% significance level, and a ratio of the variances of 3.09.

$3.09 > 2.05$ => difference is significant.

$480^{o}C$ peak

$$\frac{(S.D._{NTL})^2}{(S.D._{ATL})^2} = \frac{(7.12)^2}{(6.15)^2} = 1.34$$

$1.34 < 2.02$ => no significant difference.

(Neglecting the 2 extreme values from each distribution raised the ratio of the variances to 1.41; still no significant difference).

It is concluded that the 325°C and 370°C second glow peaks have greater reproducibility than the corresponding NTL peaks.

The 480°C peak reproducibility is unaffected, for reasons which remain unclear. A possibility is that the poor signal/noise ratio at these elevated temperatures, compounded by subtraction of the reheat data, introduces an additional variability to the data during TL measurement which obscures the true ATL:NTL differences.

6.4 Possible causes of disc-to-disc variation

The possible sources of the observed scatter fall into the categories of sample preparation, disc loading technique and intrinsic sample variability.
Considering each:

1. Sample Preparation

   (a) Insufficient magnetic separation or inadequate HF etching could permit the survival of contaminant grains, such as feldspars or zircons, into the final "pure" quartz sample.
   No assessment of such contamination could be made at this stage (see section 6.5).

   (b) The HF etching is inadequate to fully remove the oxide coatings of the quartz grains, resulting in variable attenuation of the TL.
   This possibility was investigated and dismissed by Smith (1983).

2. Disc Loading Technique

The large aliquot masses (7.60±0.35mg) may cause deviation from the assumed monolayer, and consequent variation of both emitted TL signal and effective dose rate upon irradiation.

SEM and binocular microscope inspection of typical discs showed < 1% of grains obscured by others (see Plates 2.3.1 - 2.3.4), so these multilayer effects could be neglected. Furthermore, the homogeneous coverage of the entire disc surface also eliminates periphery-centre effects (Plates 2.3.1 and 2.3.2).

3. Intrinsic Sample Variability - the existence of "bright" grains

Quartz grains may be "bright" - producing a significant excess of NTL relative to "normal" grains - for several reasons:

a) High concentrations of elemental impurities enhancing the sensitivity, eg, Al and the alkali metals.

b) Mineral inclusions within quartz grains - either sensitive TL minerals such as feldspars, or minerals rich in U and Th such as zircon and monazite.

c) Enhanced sensitivity as a consequence of thermal history.

d) The existence of large regions of high radioactivity, as reported by Sutton and Zimmerman (1978), delivering internal α dose rates greatly exceeding the environmental dose rate. (However, they found these regions to correlate with regions of low luminous efficiency - if this correlation holds generally, this category may be neglected).

6.5 SEM testing of sample purity

The efficiency of sample separation and the possible existence of bright grains could not be tested using the available TL apparatus, hence electron-optical techniques were applied to this end.

Sample purity could be tested by SEM inspection of aliquots of quartz that had undergone the standard separation procedure but received various HF etch times. If the procedure was adequate, the standard etch-time aliquot should be free of contaminant grains.

Also, as SEM techniques penetrate only a thin surface layer of a few microns, various etch times ideally permit different depths within grains to be searched for mineral inclusions and impurity concentrations.

For the first trial, a quantity of LW (S3,TD,1m) sediment was cleaned with HCl/NaOH, sieved for the 90-125µm fraction, magnetically separated, divided into 100mg batches, then HF etched for times ranging from 0-200 minutes. Sample discs were loaded from each of the 0, 20, 40, 60 and 200 minute batches, and given a 20 nm carbon coating prior to SEM examination.

The instrument was a Philips SEM 505 with an on-line Tracor-Northern TN5500 X-ray spectrum analyser. An X-ray mode available on the SEM allowed CRT display of the abundance and spatial distribution of an

element of interest. Low magnification viewing in this mode permitted rapid inspection of many grains for the element of interest, and selection of anomalous features for full compositional analysis with the Tracor-Northern system. The unetched material contained a small but significant proportion of impurity grains - feldspars from their X-ray emission spectra - as well as chemically complex surface contaminants of the quartz grains - probably iron oxides and clays. The 20, 40, 60 and 200 minute etch samples revealed none of these, indicating the 40 minute etch time of the standard separation procedure is adequate, and so ruling out inefficiency of the etching step as a source of scatter.

No conclusions could be drawn regarding the existence of high impurity levels, as surface irregularities prevented the microprobe analyses required to detect these. Also inconclusive was the absence of any mineral inclusions, as it was possible the etching process destroyed or dislodged them from the quartz matrix.

As the preceding work ruled out probable causes of scatter except for bright grains, an electron microprobe search for anomalies in quartz grains was commenced. From a consideration of electron microprobe techniques (Long; in "Physical Methods in Determinative Mineralogy", Ed. J. Zussman) grains could be most usefully prepared for examination by making thin sections of the sediment samples. Grains sectioned and polished in this process could be searched for mineral inclusions, and, if detection limits permitted, varied levels of impurities. The impurities sought were those enhancing TL sensitivity, particularly Al and the alkali metals, and those delivering a significant internal α dose rate - U and Th. See Appendix 5 for details of thin section preparation.

6.6 Electron microprobe examination of thin sections

Areas of the thin sections of 90-125µm, HF-etched Roonka quartz (EB 1/S/2.1), Lake Woods quartz (S3,TD,1m) and Woakwine quartz (WK 1S/4) were inspected by electron microprobe for the compositional anomalies that may produce bright grains. All investigations were performed using a JEOL 733 Superprobe model electron microprobe analyser, with an attached KEVEX 7000 Series energy dispersive system. Calibration was first on a pure Cu standard, then on a silicate standard, Kaersutite.

Analysis conditions were: accelerating voltage 15 kV, electron beam current 5nA. The X-ray spectra were acquired on the KEVEX system with a take-off angle = 40°, a "live" counting time of 60 seconds and detection limits of ~ 0.1 wt%. Data were corrected using standard ZAF procedures ("Z" - backscatter effect, dependent on atomic number; "A" - absorption of radiation in sample; "F" - fluorescence). The thin sections were rinsed with freon prior to evaporative coating with 20 nm carbon using a Denton Vacuum DV-502 unit.

The inspection of the Lake Woods and Woakwine samples was qualitative in nature, with instrument familiarisation also a goal. Both samples contained numerous small inclusions within quartz grains, few being greater than 10µm in maximum dimension. Analysis revealed most to be K-feldspars and ilmenite, with an occasional plagioclase feldspar and biotite. It was noted that certain grains were found to contain many very small inclusions, <3-5µm, although the matrix was pure quartz to the detection limits.

The JEOL 733 gives a choice of detection modes, of which the most suitable to locate inclusions is the backscattered electron imaging mode, "compositional". This mode utilizes the higher probability of backscattering electrons from higher atomic number elements, hence a higher mean atomic number mineral phase produces a greater backscattered electron signal which the system then represents as a brighter image. Also available was a "topographic" mode, in which a stereoscopic detector arrangement enables the display of sample relief. This was useful for discriminating true inclusions from fragments embedded into the surface during grinding or polishing. A typical K-feldspar inclusion, viewed in both modes, is shown in Plate 6.6.1.

Having established the presence of inclusions, an area of the Roonka thin section was studied to estimate the (a) mineral species present, (b) size of typical inclusions, (c) abundance of various species.

The procedure was to inspect the section at X300 in compositional mode - at this magnification about two sectioned grains were displayed - if apparent inclusions were present, they were classified by topographic mode as "inclusions" or "remnants", then identified by microprobe analysis. A new field was then brought into view and the procedure repeated.

The total number of fields viewed was 120, containing about 250 sectioned grains. The results are shown in Table 6.6.1. Some examples of spot analyses from the X-ray emission spectra are shown in Table 6.6.2.

PLATE 6.6.1. A typical K-feldspar inclusion in Roonka (EB 1/S/2.1) quartz shows as the bright central patch in the lower image, taken in compositional mode. An ilmenite fragment is also apparent to the right of the grain.
The upper image, in topographic mode, shows the K-feldspar to be an integral part of the grain, whereas the ilmenite is unconnected to it, and so classed as a preparation remnant.

Analysis of the matrix showed pure quartz to the detection limits.

Scale is given by the 10μm bar, lower right.

Table 6.6.1. Results of electron microprobe search of 250 sectioned grains of Roonka quartz.

Mineral	Number	Typical Size	Typical U, Th concentrations (PPM)*		Th/U Ratio
			U	Th	
K-feldspar	7	up to ~10μm	0.2-3	3-7	2-6
plagioclase	2	<8μm	0.2-5	0.5-3	1-5
biotite	7	<5μm	1-40	0.5-50	0.5-3
amphibole	2	3-5μm	-	-	-
ilmenite	6 others	one ~10μm; <3μm	1-50	-	-
sphene	1	rodlike ~5x1μm	100-700	100-600	1-2
apatite	2	<5μm	5-150	20-150	1
monazite	1	~5μm	500-3,000	25,000-200,000	25-50
zircon	2	<5μm	300-3,000	100-2,500	0.2-1

(* After Adams et al, 1959).

Only the concentrations of α emitters are given above. β and γ contributions are neglected as the much greater track lengths deposit the majority of the energy outside the grains containing source inclusions.

Other species detected, but classed as remnants, were $BaSO_4$ (two fragments), iron oxide (two), and rutile (two). Fragments of K-feldspar, plagioclase, zircon, apatite and ilmenite were also identified.

The total volume probed was $\approx 4.8 \times 10^6$ μm^3. (The mean diameter of a sectioned grain was estimated at ~90μm, giving a mean area of $\approx 6.3 \times 10^3$ μm^2, the effective probe penetration depth was 3μm and 250 grains were probed). This corresponds to complete volume examination of ~12-13 equivalent spherical 90μm grains, or ~7 equivalent spherical 110μm grains.

K-FELDSPAR	
SIO2	67.86
TIO2	0.26
AL2O3	19.49
K2O	12.31
NA2O	1.60
SUMME	101.52

FELDSPAR	
SIO2	76.50
AL2O3	12.10
K2O	10.59
NA2O	0.46
SUMME	99.65

PLAGIOCLASE	
SIO2	53.09
AL2O3	30.67
MGO	0.19
CAO	13.99
K2O	0.06
NA2O	3.00
SUMME	101.01

BIOTITE	
SIO2	45.16
TIO2	1.47
AL2O3	17.86
FEO	16.07
MGO	9.65
K2O	8.39
SUMME	98.59

AMPHIBOLE	
SIO2	65.71
AL2O3	11.75
FEO	11.54
MGO	9.21
K2O	0.40
SUMME	98.62

SPHENE	
SIO2	69.26
TIO2	16.64
AL2O3	1.11
FEO	0.49
MGO	0.23
CAO	13.89
SUMME	103.63

APATITE	
P2O5	36.51
SIO2	14.49
CAO	49.18
SUMME	100.18

ILMENITE	
SIO2	0.67
TIO2	51.51
CR2O3	0.14
FEO	45.06
MGO	0.29
SUMME	97.67

ZIRCON(1)	
P2O5	45.14
SIO2	48.05
TIO2	0.16
AL2O3	0.36
V2O3	0.20
CR2O3	0.25
FEO	0.43
NIO	0.33
MGO	0.21
CAO	0.10
K2O	0.14
SO3	3.60
SUMME	99.19

MONAZITE(2)	
P2O5	24.24
TIO2	0.50
V2O3	9.53
CR2O3	4.95
FEO	0.61
MNO	1.58
SUMME	41.40

RUTILE OR ANATASE	
P2O5	0.24
SIO2	1.88
TIO2	95.63
AL2O3	0.43
FEO	1.21
MGO	0.43
CAO	0.09
NA2O	0.35
SUMME	100.26

QUARTZ	
SIO2	98.77
AL2O3	0.16(3)
MGO	0.12
K2O	0.09
SUMME	99.15

QUARTZ	
SIO2	99.68
AL2O3	0.18
MGO	0.12
SUMME	99.98

TABLE 6.6.2 Typical Spot Analyses of Inclusions in Roonka Quartz, from the X-ray Emission Spectra.

(1) $P_{K\alpha}, K_{\beta 1}, S_{K\alpha}$ Lines interpreted as Zr $L_{\alpha 1}, L_{\beta 1}, L_{\gamma 1}$

(2) $Cr_{K\alpha}, V_{K\alpha}$ Lines interpreted as $Ce_{L\beta}, Ce_{L\alpha}$

Low Summe due to rough inclusion surface.

(3) Al, Mg probably from line overlap and so not real.

The abundance of small inclusions suggests they are not responsible for all the observed disc-to-disc variations, but would contribute or induce a component of NTL lacking in subsequent glows.

However, the limited volume searched suggests larger inclusions are present, and it must be noted that a typical 20μm monazite would deliver an internal dose-rate to a 100μm grain of about 100mGy/a. This could induce in the host grain a relative TL overabundance of up to 100 times, given typical young sediment conditions of linear TL growth and 1mGy/a dose-rate. Such larger high radioactivity inclusions would adequately account for the scatter component removed on first glow.

6.7 Cathodoluminescence investigations

There remained the problem of scatter for second and subsequent glows. As this was regenerated by irradiation, the cause was assumed to be the enhanced TL sensitivity of some grains. Further, as the grains sought were bright in TL, it seemed reasonable to assume they were also prominent in cathodoluminescence (CL).

A CL detection system was available on the Philips SEM 505. It consisted of two fish-eye collecting lenses attached by optical fibres to a Philips Type PW 6765/00 photomultiplier tube. Samples were given the standard 20nm carbon coating.

Inspection of the Lake Woods, Roonka and Woakwine thin sections revealed a wide range of grain luminosities in all three, with a few especially bright grains in each. A field of the LW quartz is shown in Plate 6.7.1. These grains were obviously not accessible for TL examination, so a procedure for the detection and separation of CL bright grains was designed: an array of grains laid onto double sided tape on a

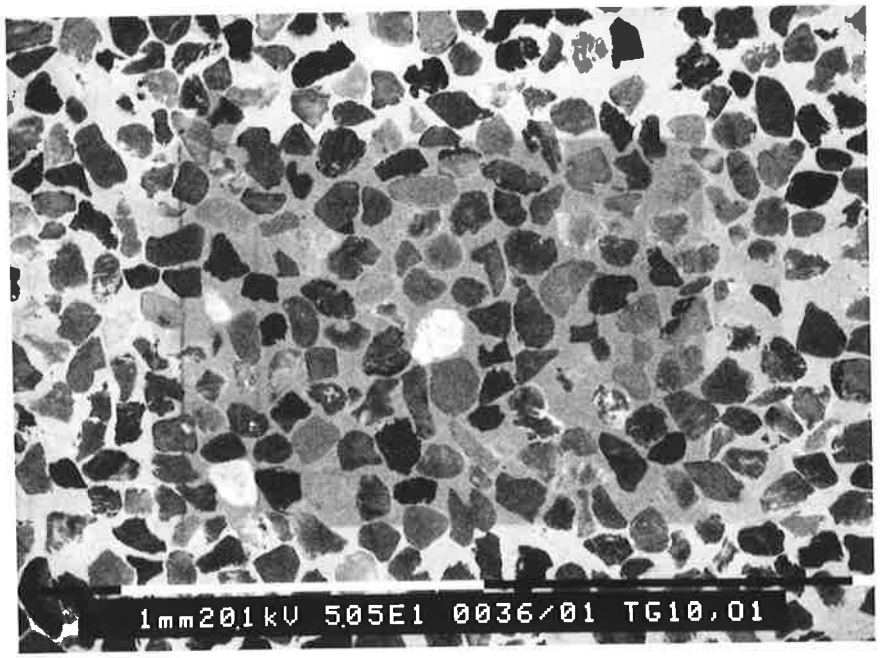

PLATE 6.7.1. A CL inspection shows four very bright grains in a selected field of the LW (S3,TD,1m) quartz thin section. The abundance of these grains was about 1 in 200. Analysis found them to be pure SiO_2 to detection limits (~0.1 wt%). The remaining grains exhibit a range of luminosities.

Magnification is 50X.

glass substrate is carbon coated, then photographed in CL mode. This permits grains of interest to be later identified under a binocular microscope and removed with fine tweezers to a TL sample disc. Initially a 200μm mesh was used to produce the array, but this proved unsatisfactory. Following a suggestion by B. Griffin of the Electron Optical Centre, TEM biological sample mounting grids were successfully tried. These grids were attached to the double sided tape/glass substrate, and grains positioned by tweezers in each aperture, under the binocular microscope. A typical prepared array is shown in Plate 6.7.2.

Huntley and Kirkey (1985) reported the detection of bright grains in sedimentary quartz from the South East of South Australia (SESA). Their apparatus was a glow oven monitored by an image intensifier/camera combination, hence the grains detected were TL bright, and so should be CL bright. Consequently, the first sample searched for bright CL grains was from the SESA region - WK 1S/4,(90-125μm fraction, magnetically separated and HF etched).

Plate 6.7.2 shows a typical array of Woakwine quartz in CL mode. The grains classified CL "bright" or "dark" are keyed in Fig. 6.7.1. Seven arrays were laid, totalling 380 quartz grains. The broad classes of "bright" and "dark" contained about 19% and 26% respectively, the remainder were of various intermediate luminosities. No grains bright and rare (≪ few percent) enough to account for the scatter were seen, contrary to the CL survey of the thin sections. This was considered a consequence of small sample population.

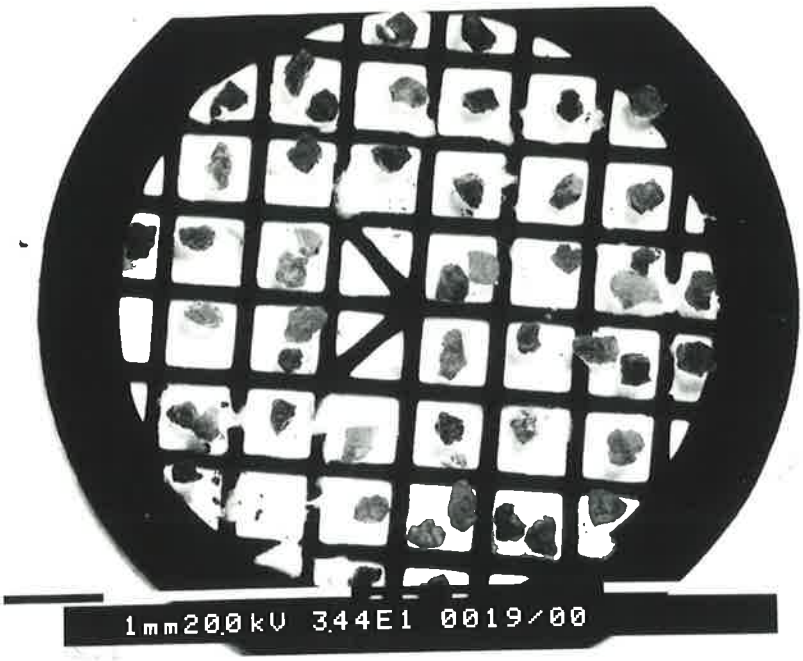

PLATE 6.7.2 A typical array of WK 1S/4 quartz grains seen in CL showing a range of grain luminosities. Magnification is 34.4X.

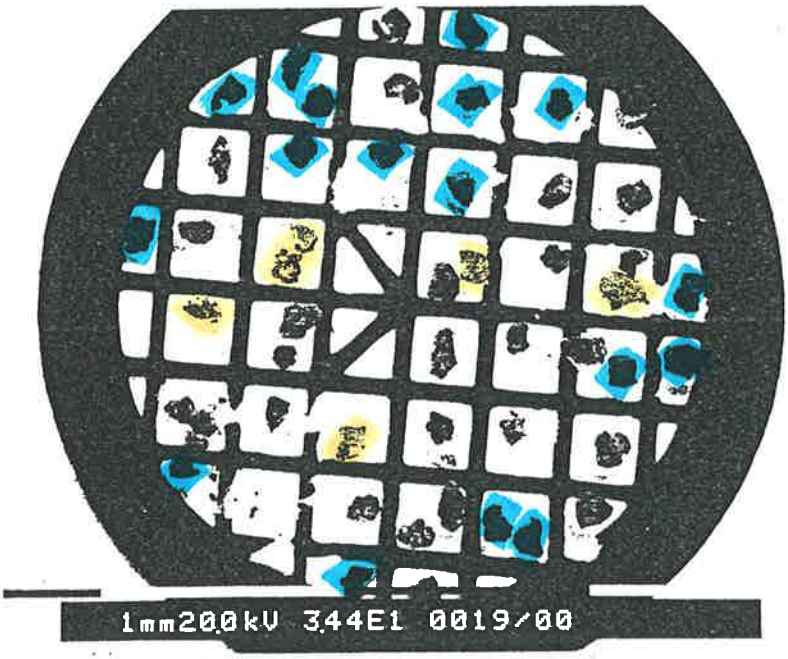

FIG 6.7.1 shows the broad classification of grains from the above array as "bright" and "dark".
bright, dark.

To determine the TL characteristics of each class, two TL sample discs were prepared: one loaded with 35 bright grains, the other with 35 dark. Both were heated at $5Ks^{-1}$ to 550°C maximum, and background subtracted. The first glow data were discarded due to a dominant chemiluminescence peak from glue and coating residues at ~ 200°C.

To record ATL, each disc was given a 174 Gy ^{90}Sr-^{90}Y β dose, allowed two days "settling", then heated as for the first glow. A second 174 Gy ^{90}Sr-^{90}Y β dose/two day settling was followed by a one hour bleach by simulated sunlight (~330 J/cm^2) to indicate the components of the bulk sample residual TL contributed by each class of grains.
Fig. 6.7.2 shows the ATL and ATL + 1 hr bleach for the bright grains and Fig. 6.7.3 for the dark.

Further doses of 29 Gy ^{90}Sr-^{90}Y β followed by immediate heating gave the near-saturation TL levels of the 110°C peaks. The bright:dark ratio for a TL summation over 40°C centred on the 110°C peak T_{max} is 2.4. This suggests the prominent 110°C peak is possibly the principal source of the bright grain's extra luminosity in CL.

Notably, the ATL differences are pronounced over the entire temperature range, yet the sum of the ATL curves yields a close approximation to the bulk sample glow curve, as shown in Fig. 6.7.4. Deviations can be attributed to the omission of grains of intermediate luminosities , which comprise about 55% of the bulk material.

Few studies have been directed towards measuring the TL yield of individual grains. Benkö (1983), in a study principally concerned with grain transparency effects, found grain-to-grain intensity variations of up to an order of magnitude which seemed independent of grain size and optical appearance. However, no major differences in glow curve form were reported.

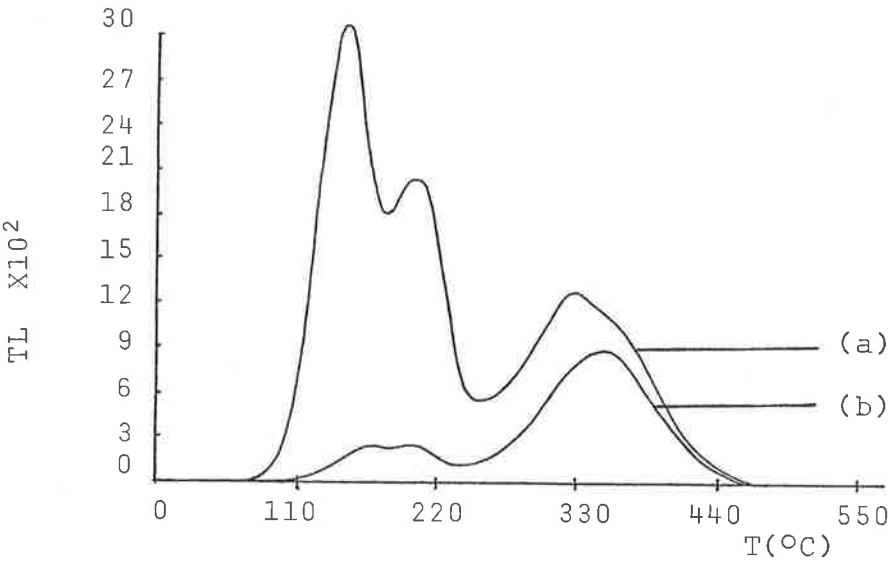

FIG. 6.7.2 WK 1S/4 quartz selected by CL as "bright", (a) 174 Gy β, 2 days settling, (b) as for (a) + 1 hr simulated sunlight.

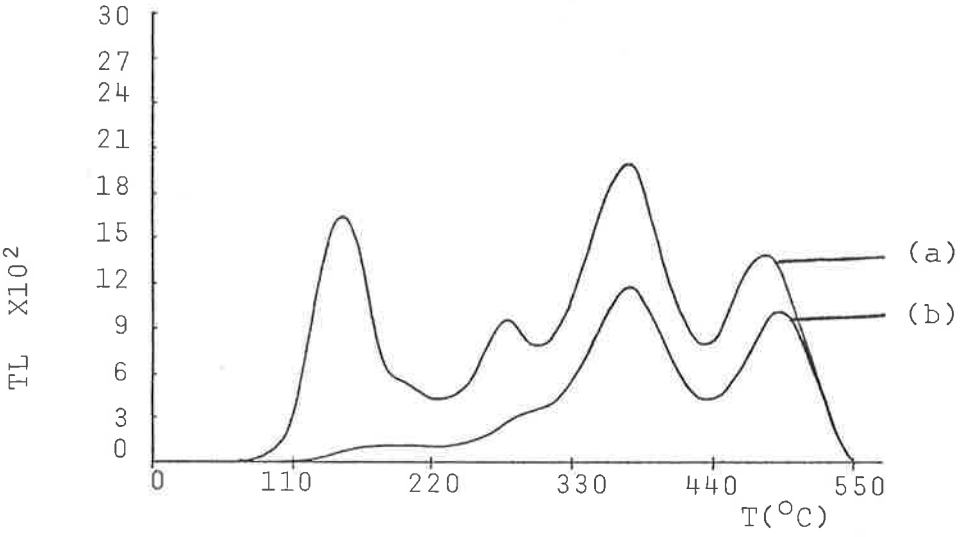

FIG. 6.7.3 As above for "dark" grains.

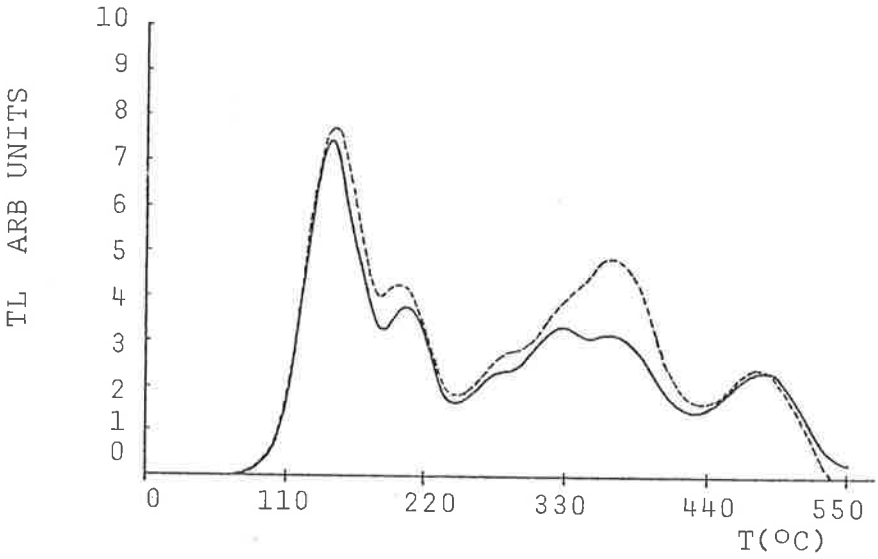

FIG 6.7.4 Comparison of (a)——— Wk 1S/4 bulk sample ATL (49 Gy) with (b)----- summed glowcurves of bright and dark grains, from Fig 6.7.2 (a) and Fig 6.7.3 (a).

Huntley and Kirkey (1985), working with a SESA sample similar to WK 1S/4, found grains bright in various temperature ranges. Specifically, they noted a grain bright between 250°C and 400°C, but barely visible between 400°C and 450°C - possibly a grain similar to the above "bright" class.

The variations between the quartz glow curves of samples from widely different geographical locations is well known (e.g., Singhvi and Zimmerman (1978), for identified samples from Iran, England, Sicily and Thailand), and may also occur in samples of greater proximity. However, the preceding CL study is taken to show the existence of at least two varieties of quartz at the same site having distinctly different glow curve characteristics. Further examination of the unsampled 55% of the material may reveal additional glow curve forms in the WK 1S/4 quartz.

The superficial resemblance of the bright grain's glow curve to that of annealed quartz, and the unexpected occurrence of various glow curve forms, led to a repeat of the experiment using annealed quartz. It was hoped that high temperature annealing would erase any varied thermal histories of the grains, and so simplify interpretation of the results.

The material chosen was EB 1/S/2.1 quartz, 90-125μm, magnetically separated and HF etched. Annealing was at 800°C for 24 hrs in air. Plate 6.7.3 and Fig. 6.7.7 show the classes identified and separated. Twelve arrays were laid, totalling 600 grains, from which 5 "very bright", 28 "intermediate brightness", 50 "bright" and 59 "dark" grains were separated. The very bright grains comprised 0.8% of the grains examined, the other classes were about 5%, ~40% and ~40% respectively.

The ATL and ATL + 1 hr simulated sun were measured as for the WK 1S/4 grains. Additionally, weight normalization was carried out. The masses were too small for available balances, so the TL from each class was normalized for 5 grain units - the normalization factors being 1,

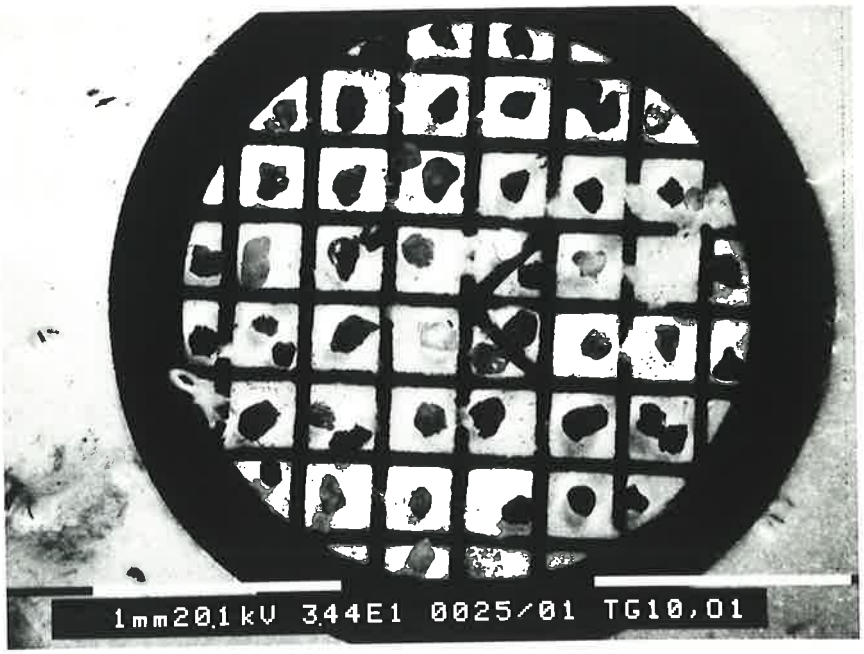

PLATE 6.7.3 An array of annealed Roonka quartz (EB 1/S/2.1) seen in CL.

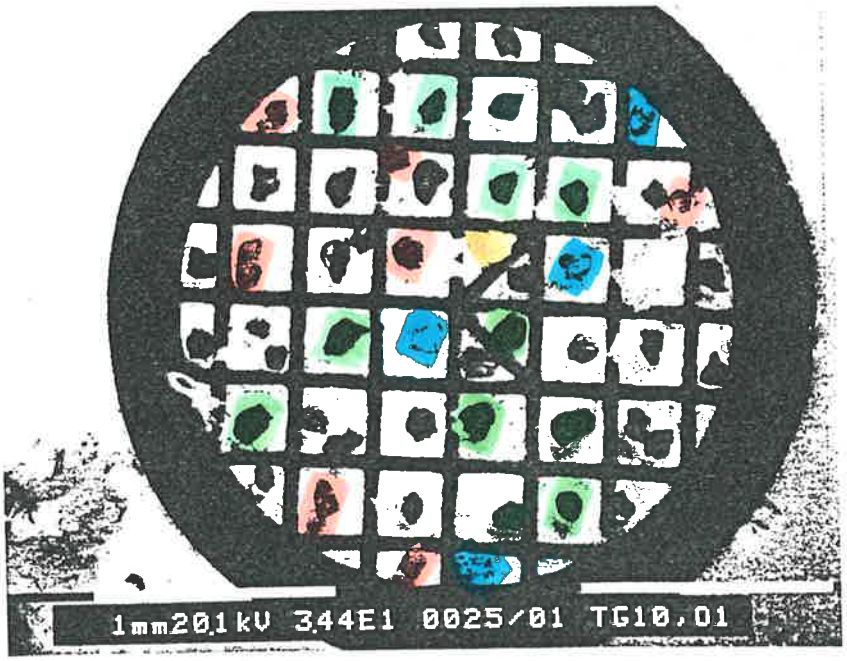

FIG. 6.7.7 Classifications of the above grains are
(a) very bright, (b) intermediate brightness
(c) bright, (d) dark.

1/5.6, 1/10, 1/11.8 respectively. The results are shown in Fig. 6.7.5 and Fig. 6.7.6. The almost tenfold TL reduction with 1 hr bleaching is characteristic of annealed quartz.

As was shown in section 3.4, the thermal treatment received by the EB 1/S/2.1 sample produces a sensitivity enhancement at 325°C of about six times. This opens the possibility that similar heating, eg, by bushfire, vulcanism or man's campfires, could produce similarly bright grains. However, no difference was seen in total CL luminosity between annealed and natural EB 1/S/2.1 - enhancement thus appears to be specific to certain glow curve peaks. Furthermore, no evidence was found in this study of naturally occurring thermal enhancement of sensitivity (the similarities between the WK 1S/4 "bright" and annealed quartz glow curves are superficial only).

It is concluded that the range of TL outputs shown in Fig. 6.7.5 and Fig. 6.7.6 is due to varied levels of elemental impurities - an expected result, as parts per million of foreign atoms can make a marked difference to the luminescence behaviour (Townsend and Kelly, 1973). The wide range of CL behaviour supports this, and is illustrated by Plate 6.7.4. This shows a field of annealed EB 1/S/2.1 sprinkled onto double sided tape. At centre are 3 grains classed as very bright, bright and dark, while at lower left and lower centre are grains exhibiting veins of very bright material in a dark matrix. Also seen are four grains that appear to have no CL output (two left of centre, two at right hand edge) interpreted as indicating an absence of luminescence centres. Throughout this study, no correlation was observed between luminescence properties and the optical appearance of grains ("frosty" and "shiny"). Plate 6.7.5, showing the same field as Plate 6.7.4 but in "normal" mode, illustrates this.

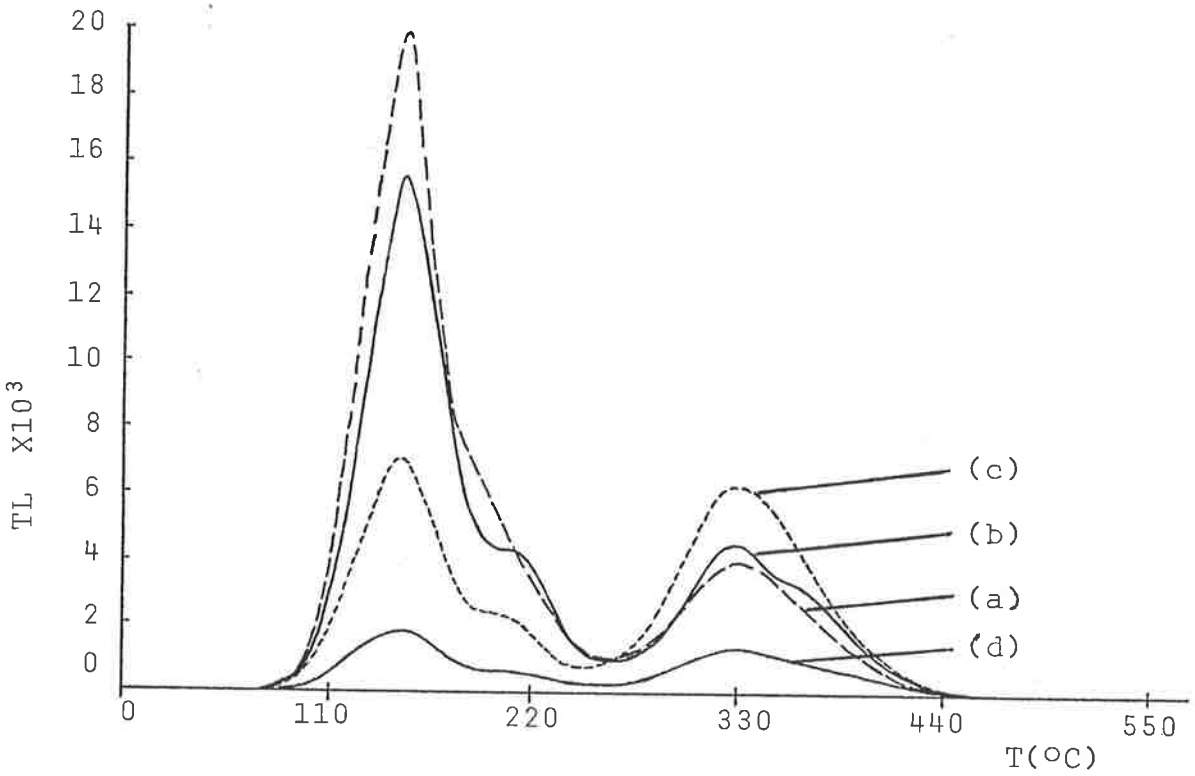

FIG. 6.7.5 EB 1/S/2.1 quartz, annealed at 800°C for 24 hours, selected by CL as (a)— — very bright, (b)——— intermediate brightness, (c)------ bright (d)——— dark. All classes received 174 Gy β; weight normalized.

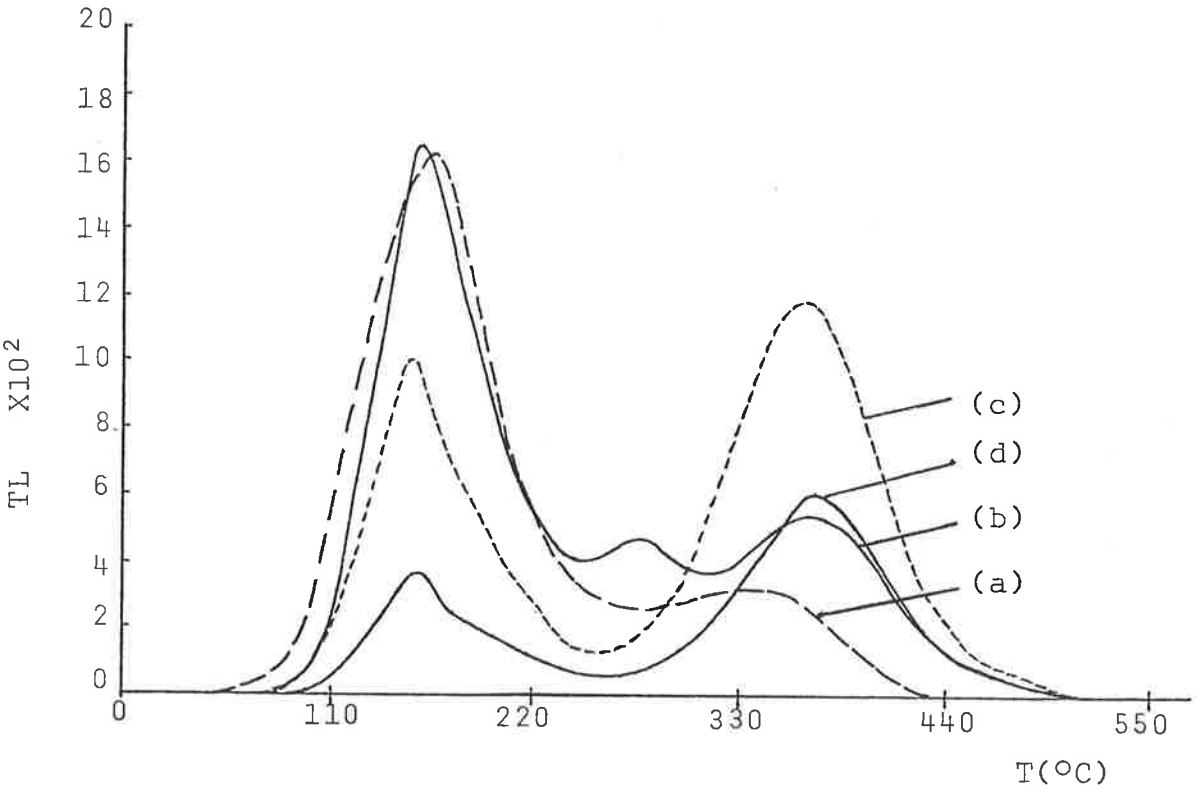

FIG. 6.7.6 As above + 1 hr simulated sunlight.

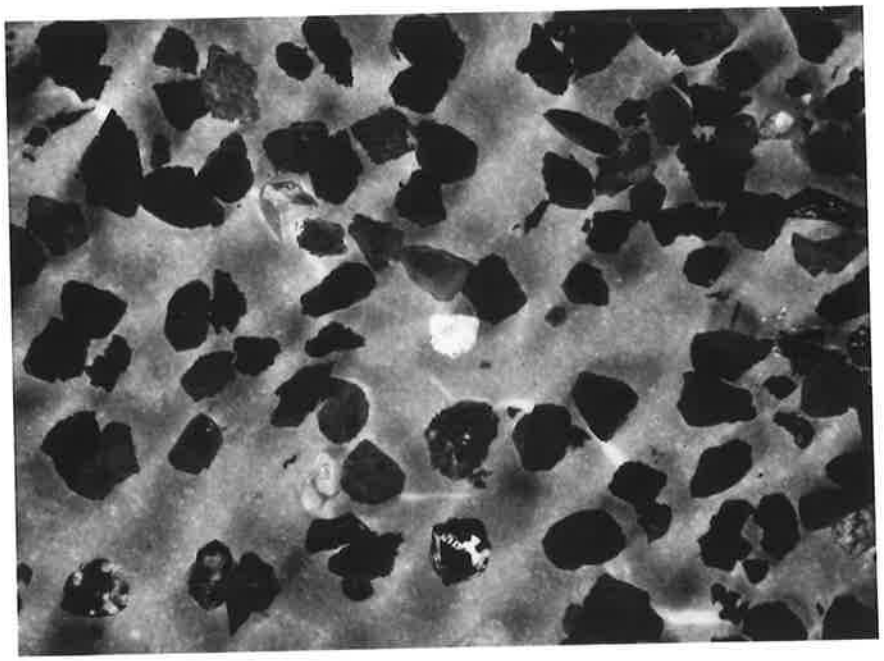

PLATE 6.7.4 Annealed EB 1/S/2.1 in CL, X81.5. Luminosities range from very bright to no apparent output. The latter (4) being arrowed as "transparent".

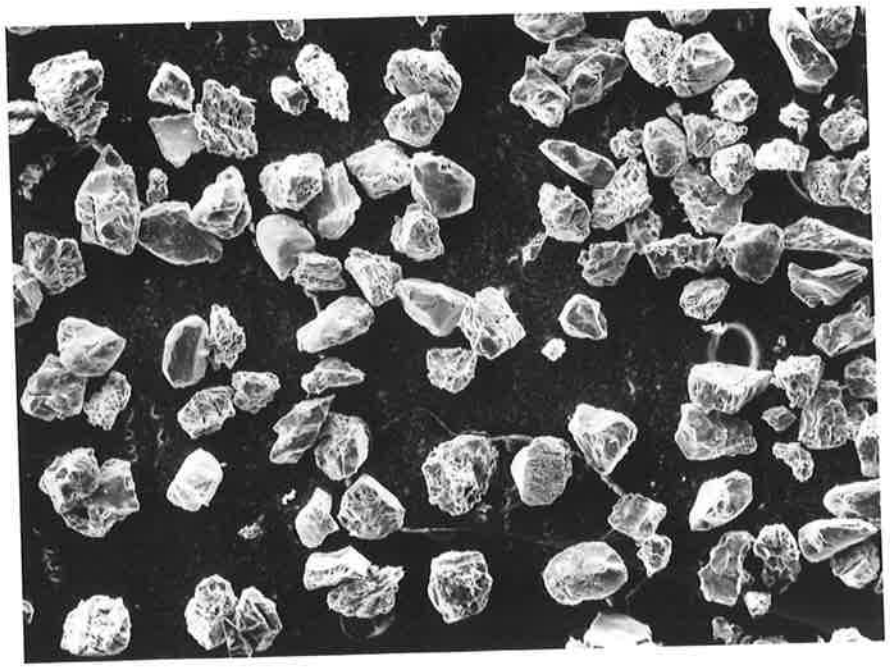

PLATE 6.7.5 The same field as above in "normal" mode. The absence of any relation between CL characteristics and optical appearance is marked.

Magnification is X81.5.

It must be noted that no very bright unheated CL grains (as seen in Plate 6.7.1) were separated for TL examination, hence the question of their being very bright in high temperature TL remains unanswered.

This highlights a limitation of CL searches - grains bright in CL are not necessarily TL bright in the temperature range of interest.

A preferred method for detecting and separating unusual TL grains would combine the previously mentioned image intensifier - camera rig of Huntley and Kirkey (1985) with the technique used here for isolating CL bright grains, based on prepared arrays of grains.

6.8 Conclusions

It is concluded that intrinsic sample variability is the principal cause of disc-to-disc scatter.

Of the possible sources outlined in section 6.4, the presence of mineral inclusions is confirmed, and the existence of varied levels of elemental impurities is deduced - an expected result given the samples are reworked dune sands. These sources alone can account for the observed variability.

The remaining sources may contribute significantly in special cases.

It is apparent that the nature of the bright grains precludes their removal by feasible physical or chemical techniques. A heavy liquid separation step, routinely used in some TL laboratories, may remove most grains hosting relatively large mineral inclusions, but cannot distinguish those grains owing their excess TL sensitivity to favourable

elemental impurity levels. Minimizing the scatter thus becomes minimizing the influence of bright grains.

A possible solution is the use of larger sample aliquots to reduce fluctuations in the disc-to-disc bright grain population. The monolayer constraint restricts practical aliquot masses to below ~10mg for a 1cm diameter disc, so consideration may need to be given to either increasing the size of the sample discs or increasing the number of 1cm sample discs used.

CHAPTER 7 FUTURE DIRECTIONS

7.1 Introduction

The principal topics considered in the thesis are the factors affecting the residual TL level remaining in natural quartz after exposure to sunlight, and the relative efficiencies with which the component wavelengths of sunlight bleach. This work is presented in Chapters 4 and 5 and will not be reiterated here, though the conclusions are drawn upon.

This chapter first suggests some investigations further to define the response of natural quartz to sunlight (largely based on the questions given in section 1.11), then proposes, from the observed bleaching behaviour of sedimentary quartz, that effort be directed into the development of techniques for TL measurement by "optical stimulation", similar to that described by Huntley et al (1985), and with the specific intent of "reading" the 325°C glow peak of quartz.

7.2 Suggestions for further bleaching studies

Earlier work (Chapter 4) examined properties of the residual TL level, but the question of there being a "recovery" of TL following a long bleach has not been resolved. Though the existence of such an effect is problematical, and the very absence of convincing reports of detection indicate a minor significance at most for TL sediment dating, the importance to an understanding of the e^- traps is much greater,

implying as it does the possibility of a "link", such as quantum mechanical tunnelling, between some classes of traps. A study aimed at detecting this effect would therefore be worthwhile.

Crystal temperature during exposure was found to affect the residual level reached - the significance of this to total-bleach based methods suggests further work is needed. A possible method of accurately maintaining a known crystal temperature during exposure is shallow immersion in a thermostat water bath.

Natural coatings on grains were found to have no detectable effect on bleaching. Though this conclusion seems generally valid, it requires confirmation, particularly for grains possessing severe discolouration or carbonate jackets.

As a more detailed follow-up study to the work on the wavelength dependence of bleaching described in Chapter 5, it is proposed that the work be repeated for the UV waveband ~ 200-400 nm, but using instead a monochromator/calibrated UV photodetector combination to construct higher resolution power vs wavelength curves for each NTL glow peak. Emphasis would be on determining threshold wavelengths beyond which bleaching ceases, and detecting bleaching resonances, if present. It is also noted that the bleaching responses of the 110°C, 160°C and 220°C ATL peaks remain little known - a similar study of their bleaching at UV and visible wavelengths would be worthwhile.

The bleaching of waterlaid sediments can effectively be considered a special-case illustration of the sensitive dependence of bleaching on illumination spectrum, and given that the depositional illumination spectrum is determined by the ambient environmental conditions, further general studies are not recommended. A conclusion is that dating of waterlaid sedimentary quartz should only be attempted using a technique exploiting the readily bleachable NTL component, identified as the 325°C

glow peak and only if a minimum depositional exposure of ~ 1 minute of sunlight can be assumed. Such techniques are partial bleaching with a suitably filtered light source, and optical stimulation. Samples receiving briefer depositional exposures must be considered undatable by current techniques.

An aspect of bleaching not considered here is that of sensitivity changes induced by optical bleaching. A study to detect such changes and determine the wavelength dependence (assuming photo-activated mechanisms) would be of value, particularly for applications of the total bleach-regeneration method, (speculating that independence of the untrapping and sensitization mechanisms may allow the existence of a "window" of wavelengths capable of bleaching but not of inducing sensitivity changes).

Finally, a whole range of further studies on the bleaching of feldspars would be very valuable.

7.3 The optical stimulation technique

The optical stimulation technique, proposed by Huntley et al (1985), represents an extension of the approach to ED estimation that gave rise to the partial bleaching method (Wintle and Huntley, 1980). Both are based on the principle that only the readily bleachable NTL component can be assumed removed at deposition, and so should be the NTL component measured by a TL dating technique in cases where long depositional exposures are unlikely.

From a consideration of the observed bleaching responses of the quartz NTL glow peaks it was concluded that quartz is ideally suited for application of the optical stimulation method. If visible stimulating wavelengths are used, the only NTL glow peak probed is that at 325°C, so removing problems of isolating the signal component of interest.

Additionally, the high susceptibility to bleaching exhibited by this peak ensures it fulfills the essential requirement for TL dating in that not only does a TL reduction take place, but that under most depositional conditions it can also be assumed that effectively complete zeroing occurs, so eliminating the need to assess a residual TL level.

In partial justification of this conclusion it is useful to summarize some of the bleaching characteristics of the prominent quartz NTL glow peaks.

(a) Long wavelength limits for bleaching:

≈ 700 nm for 325°C peak, ≈ 400 nm for 370°C and 480°C peaks.

(b) Mean life when exposed to natural sunlight:

~ tens of seconds for 325°C peak, ~ 50 minutes for 370°C peak,

~ 4 hour for 480°C peak.

(c) Residuals: effectively no residual from 325°C peak (1 minute sunlight),

~ 8-15% of saturation TL level for 370°C peak (20 hours sunlight),

~ 30% of saturation TL level for 480°C peak (20 hours sunlight).

(d) Energy required for similar specified reductions of peaks is over two orders of magnitude greater for the 370°C and 480°C peaks than for the 325°C peak (see section 5.2.).

(e) Energies required for specified peak reductions are approximately exponentially dependent on wavelength, changing by "e" every 35 ± 5 nm for 325°C peak, 10 ± 2 nm for 370°C peak and 10 ± 3 nm for 480°C peak.

Clearly the only NTL glow peak bleachable by visible light is that at 325°C, suggesting that only the traps corresponding to this peak are probed by the stimulation wavelengths currently used for optical reading (514.5 nm).

Support for this interpretation is indirectly given from the report by Huntley et al (1985) that the optically stimulated signal emitted by a SESA quartz sample exposed to 514.5 nm illumination of intensity ~ 50 mW/cm^2 declines after ~ 20 seconds to a ~ few percent of the initial value. This corresponds to ~1J total energy, in agreement with the value found (by interpolation on Fig. 5.2.2) for complete removal of the 325°C peak by this wavelength. Further indirect support is given by the deduction that no significant glow curve structure exists at higher temperatures than ~ 550°C (see section 4.3), so limiting the probable sources of the optically induced emission to the observed NTL glow peaks. Finally, this proposition can be simply verified by the pre-illumination annealing of NTL to remove only the 325°C peak component, and comparison of the resultant optically stimulated signal with that from a similar but unannealed sample.

Assuming that the NTL component measured by the optical stimulation technique is the 325°C peak, some comments regarding choice of stimulating wavelengths are given below, and some questions posed concerning the nature of this glow peak.

All wavelengths $\lesssim$ 700 nm may, in principle, be used for optical stimulation, but the desirability of not reading signal originating from 370°C and 480°C peak traps precludes use of the UV wavelengths, and the superposition of scattered illumination with the quartz TL emission rules out wavelengths of ~ 400-500 nm.

The rapid increase with wavelength of total energy required to remove a given proportion of the peak weighs against the practical use of wavelengths much exceeding ~ 600 nm (for example; the total energy required from a He-Ne laser (632.8 nm) to induce a given reduction is ~ 30 times that from an Ar-ion laser (514.5 nm) for a similar reduction). It is concluded that the optimum wavelengths are those of ~ 500-600 nm.

Regarding the optically stimulated signal: inspection of Fig. 5.2.1.(f) indicates that the retrapping at ATL peak trap sites of e^-'s released from 325°C peak traps will compete with luminescent recombination and so reduce the magnitude of the initial signal. However, the response of these ATL peaks (see Fig. 5.2.4 (a)) to 500 nm light indicates they too will be bleached by the stimulating wavelengths, but at a lesser rate than the 325°C peak, and so will contribute a "tail-off" signal. Presumably the 110°C peak is similarly bleached and so will exacerbate the significance of the "tail-off". An additional problem may be posed by post-illumination thermal decay of the ATL peaks inducing some regrowth of the 325°C peak by retrapping.

The above effects may be circumvented by maintaining the sample at an elevated temperature (say ~ 100-200^{0}C) during illumination, the purpose being to thermally prevent retrapping at ATL peak trap sites.

However, regarding the above, cautions are raised by the apparent full reliance of the optical stimulation technique on the behaviour of the enigmatic 325°C peak. Much work remains before an understanding of

the nature and properties of this peak is achieved. Not the least significant questions raised are:

(a) what is the "pre-dose" mechanism operating?

(b) can optical wavelengths induce sensitivity changes in this peak, and if so, which wavelengths, and to what extent?

(c) Is 325°C peak regrowth in nature affected by the presence of unbleached 370°C and 480°C NTL peaks (e.g., enhanced by reduced e^- trapping competition)?

(d) What traps are responsible for the 325°C peak, and what mechanism gives them the observed susceptibility to light?

(e) Emission spectra indicate all NTL peaks share common L-centres, though "thermal quenching" is seen only at the 325°C peak, implying that the observed "thermal quenching" is a property of one class of e^- trap, and <u>not</u> the L centres. If so, what process is occurring and what is its significance?

(f) Following point "(e)" above, is the 325°C peak stable over time-spans exceeding 10^5 a?

APPENDIX 1

Laboratory irradiation sources

1. β Sources.

The laboratory β sources were Amersham SIP ^{90}Sr-^{90}Y plaques. Those available were nominally 20μCi, 500μCi, 5mCi, 21mCi, a "housed" 40mCi and the 40mCi incorporated within the automated TL reader system. The latter was used for the majority of irradiations.

The 5mCi source is the local standard, having been calibrated against a known ^{60}Co γ source for three different sample materials (Smith, 1983). Consequently, the other sources were calibrated against the 5mCi source. When mounted in the "HI" configuration, this source was found by Prescott and Smith to deliver a dose rate to coarse grain quartz on stainless steel of 0.216 ± 0.003 Gy/minute, as at Feb. 1980. Correction for the 28.0 year half-life of ^{90}Sr gave the dose rate as at Feb. 1985 to be 0.191 ± 0.003 Gy/minute.

Calibrations for $CaSO_4$ are given below (annealed at 500°C in N_2; stainless steel discs; lead shielding used).

Source Configuration	Ratio	Group values*
$\frac{\text{HI } 500\mu\text{Ci}}{\text{HI } 20\mu\text{Ci}}$	25.83 ± 0.02	26.1 ± 0.4 (JRP)
$\frac{\text{HI } 5\text{mCi}}{\text{HI } 20\mu\text{Ci}}$ **	294.7 ± 2.8	299.6 ± 6.6 (JRP) 296.8 ± 8.8 (GBR)
$\frac{\text{HI } 5\text{mCi}}{\text{HI } 500\mu\text{Ci}}$	11.41 ± 0.10	11.48 ± 0.18 (JRP) 11.37 ± 0.29 (GBR)
$\frac{\text{HI } 5\text{mCi}}{\text{HI } 21\text{mCi}}$	0.233 ± 0.001	-
$\frac{\text{HI } 5\text{mCi}}{\text{Housed } 40\text{mCi (on-plate)}}$	0.139 ± 0.001	-
$\frac{\text{HI } 5\text{mCi}}{\text{Housed } 40\text{mCi (AU)}}$	0.151 ± 0.001	-
$\frac{\text{Housed } 40\text{mCi (AU)}}{\text{Housed } 40\text{mCi (HI)}}$	0.920 ± 0.01	0.917 ± 0.01 (JRP)

AU - Automatic irradiation unit

HI - "High" mount on Littlemore unit heater plate

Errors are $\sigma/\sqrt{n}$.

*Determined by other group members, initials given.

**Calculated from the 500μCi/20μCi and 5mCi/500μCi values.

The automated TL reader β source was calibrated against the housed 40mCi source, for the HF etched, 90-125μm fraction of Lake Woods (S3,TD,1m) quartz on stainless steel. Pretreatment to erase NTL consisted of twice heating to 550°C maximum at $5Ks^{-1}$. Relative dose-rates were assessed by matching the 325°C and 480°C peaks from timed standard irradiations with those from test irradiations. Found

$$\frac{\text{Housed 40mCi (AU)}}{\text{Automated TL } \beta \text{ source}} = 0.8798 \pm 0.0014 \quad (\sigma/\sqrt{n}).$$

Giving a dose-rate = 84.80 ± 0.13 Gy/hour, as at Nov. 1985.

"Leakage" through the closed shutter was ~8mGy/hour onto the position directly beneath the source, ~1mGy/hour onto the two adjacent sites, and negligible at the other 21 positions.

"Spillover", during irradiation, onto the two adjacent positions was ~50mGy/hour; the next two positions received ~4mGy/hour, with negligible dose at the remaining 19 sites.

2. Gamma Sources

The Department of Geology kindly permitted use of their nominally 600Ci ^{60}Co γ source. This was calibrated against the housed 40mCi (AU) source for Lake Woods (S3,TD,1m) quartz, (90-125μm, HF etched, on stainless steel). Irradiations were 2 minutes ^{60}Co γ, matched at the 325°C peak by 1 hour housed 40mCi (AU). Samples for irradiation by this source are held in 16 position plastic sample holders. The dose-rates given below are for all positions of the "green" sample holder as at November 1984. (kGy/hour; errors $\sigma/\sqrt{n}$).

Upper 8 positions.

1 3.97 ± 0.21	2 4.47 ± 0.20	3 4.50 ± 0.15	4 3.97 ± 0.13
5 3.87 ± 0.15	6 4.56 ± 0.18	7 4.57 ± 0.17	8 4.03 ± 0.13

Lower 8 positions.

9 3.59 ± 0.18	10 4.11 ± 0.18	11 4.12 ± 0.14	12 3.60 ± 0.09
13 3.59 ± 0.20	14 4.07 ± 0.19	15 4.15 ± 0.10	16 3.67 ± 0.14

3. The use of α sources was not required in this study.

APPENDIX 2

Interference filters

Central to this study was an investigation of the dependence of bleaching on the illumination spectrum (see Chapter 5), specifically, on the relative bleaching efficiencies of various wavelengths. This was done by selecting representative wavebands from the simulated sunlight spectrum by means of high quality interference filters, chosen to sample almost all wavelengths present in the natural solar spectrum incident at sea level (see Figs. 4.2.1, App. 2.1, App. 2.2). The filters are 50x50mm square, (permitting the simultaneous exposure of several sample discs) and give $\gtrsim 3$ optical density blocking of unwanted wavelengths (manufacturer's specifications). Consequently, the "leakage" of unwanted wavelengths during a 1000 minute exposure should be equivalent to ≤ 1 minute of unfiltered illumination. In practice, leakage was found to be negligible, equivalent to several seconds exposure at most.

Some specifications for the interference filters, and data on the illumination delivered when used with the Oriel Solar simulator, are shown below.

(1) FILTER $\lambda_o \pm \Delta\lambda$ nm.	(2) EFFECTIVE PEAK TRANSMITTANCE %	(3) POWER IN BANDWIDTH mW/cm^2	(4) POWER DELIVERED TO WORKPLANE mW/cm^2	ENERGY DELIVERED TO WORKPLANE mJ/cm^2/minute	MEAN PHOTON ENERGY (λ_o) eV	PHOTON FLUX PHOTONS/ nm^2/minute
290±10	18.3	<0.002	<0.0004	<0.02	4.28	<0.3
322±12	15.2	0.072	0.011	0.63	3.85	10
339±10(5)	28.3→10.9	0.084	.023→.009	1.37→0.53	3.66	23→9
345±11(5)	23.0→17.4	0.187	.042→.032	2.52→1.90	3.59	44→33
363±10(5)	32.2→14.3	0.31	.095→.042	5.7→2.5	3.41	104→46
370±12	47.4	0.54	0.25	15	3.35	280
400±20	32.4	3.60	1.14	68	3.10	1,400
450±20	48.5	4.60	2.15	129	2.76	2,900
500±20	53.7	4.80	2.48	149	2.48	3,700
550±20	62.5	4.88	2.91	174	2.25	4,800
600±20	51.8	5.08	2.53	152	2.07	4,600
650±20	58.5	4.60	2.69	155	1.91	5,100
700±20	63.3	4.02	2.41	145	1.77	5,100
>750	~80	~32	~25	~1,500	<1.65	>60,000

(1). 290, 322nm filters from Acton Research Corp., (Acton, Mass., U.S.A., 01720), remainder from Corion Corp., (Holliston, MA., U.S.A., 01746).

(2). Transmittance for equivalent filter having bandwidth $2\Delta\lambda$.

(3). Power from Oriel Solar Simulator (see Fig. 4.2.1) summed over bandwidth $2\Delta\lambda$.

(4). Power in bandwidth X effective peak transmittance X Solar Simulator calibration factor.

(5). The value of the parameter is shown both before use and after 20 hours exposure of the filter to simulated sunlight, for these defective filters.

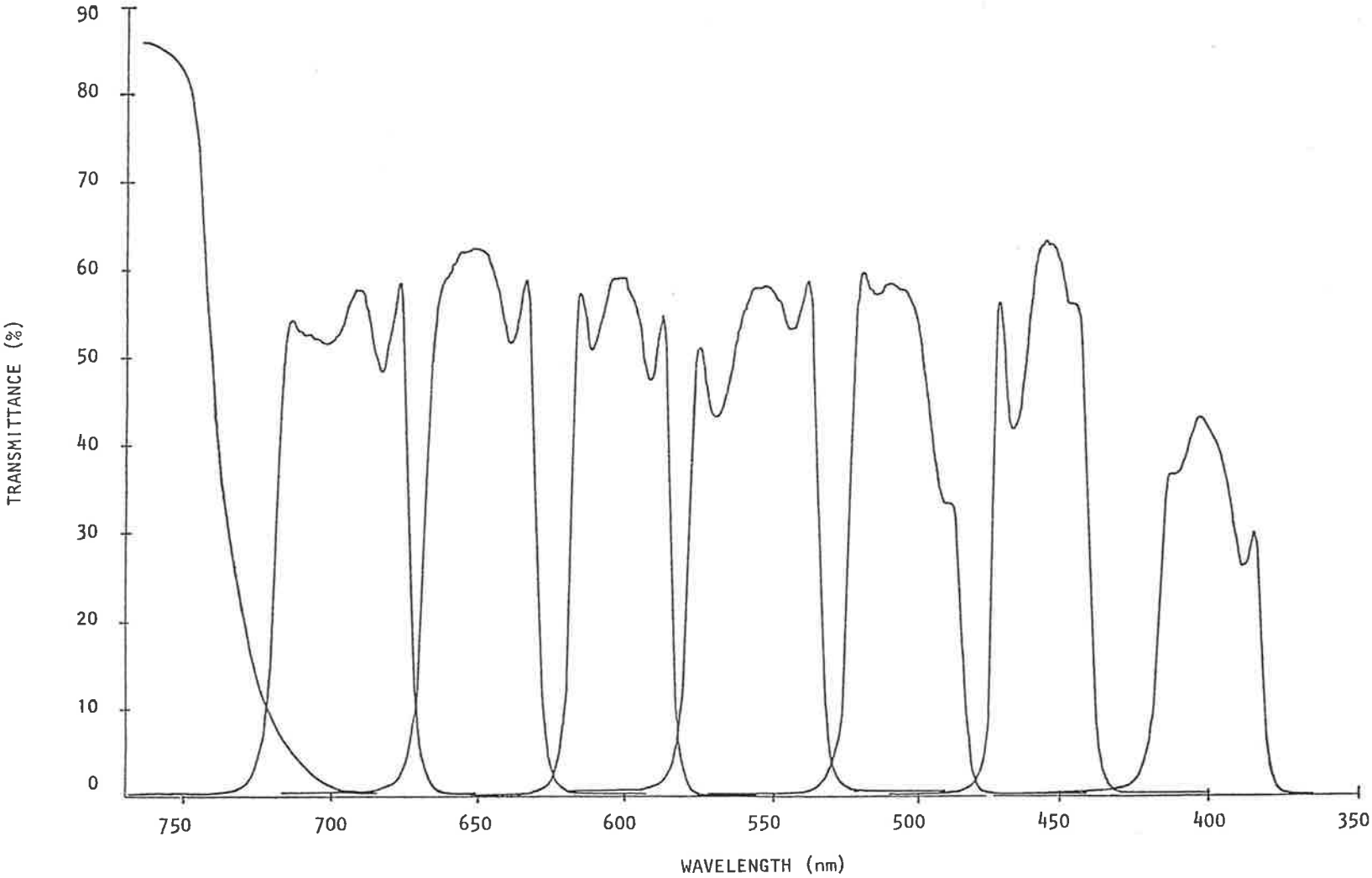

FIG. APP. 2.1. Shows transmittance vs wavelength for the Corion 40nm visible band pass filters and 750nm long wave pass filter.

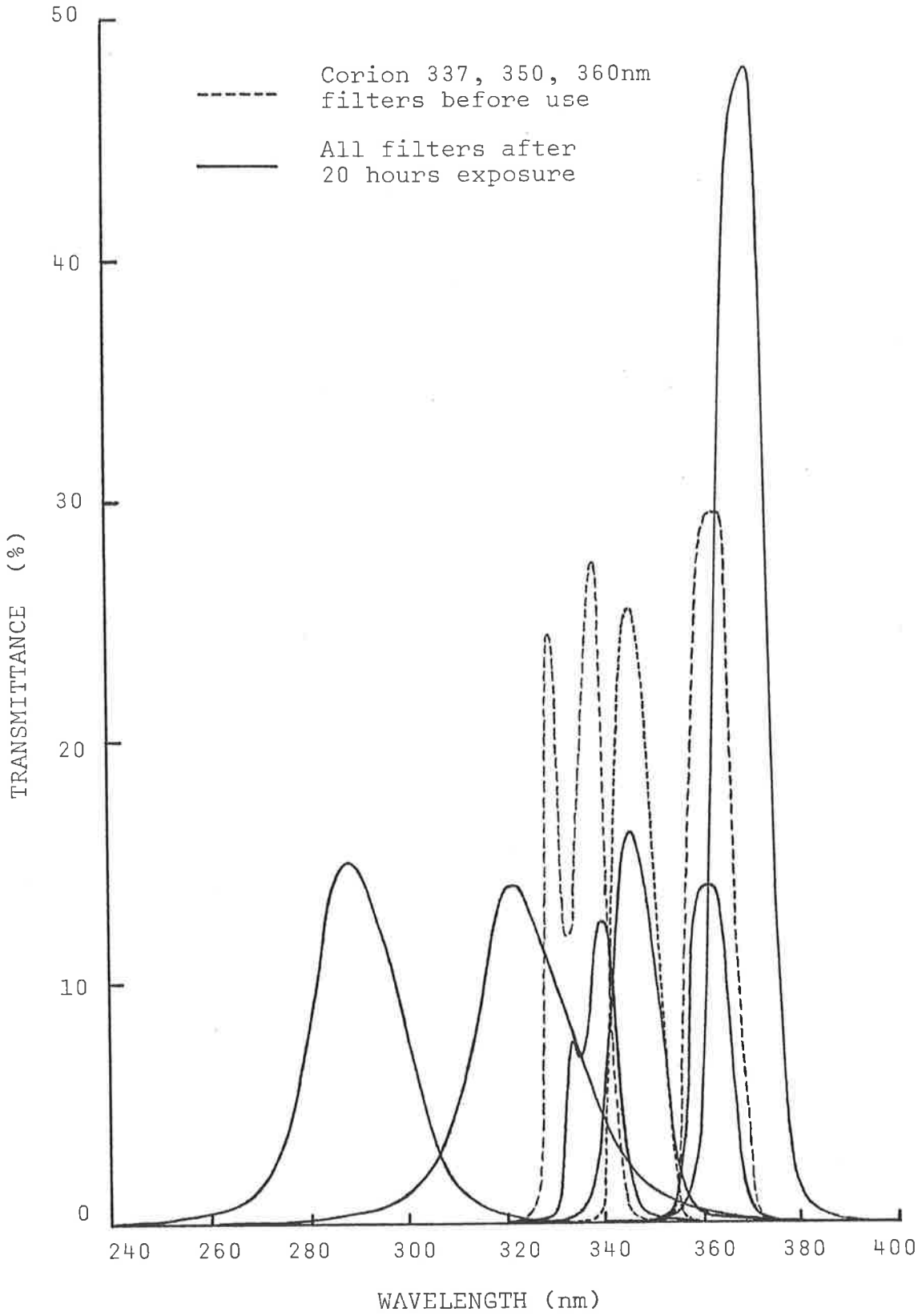

FIG. APP. 2.2. Shows transmittance vs wavelength for Corion 337, 350, 360, 370nm and Acton 290, 322nm narrow band pass interference filters. Changes induced in the defective filters (Corion 337, 350, 360nm) by 20 hours exposure to simulated sunlight are shown. All other filters, for both UV and visible wavelengths, were unaffected by use.

The three defective Corion UV filters (λ_o values nominally 337, 350, and 360nm) posed problems in that the transmittance changes were not found until the bleaching work had been completed. However, as the same wavebands were sampled throughout (λ_o remained ~unchanged in each case), allowance need only be made for the altered transmittance. This was done by assuming a linear change with time in the absence of any data on the true rate of change. The unknown validity of this assumption is accounted for in greater uncertainties assigned to the total irradiance delivered in these wavebands.

APPENDIX 3

Automated TL reader software

The software package (written in HP-basic at the Risφ National Laboratory, Denmark) supplied with the automated-TL reader system consisted of three control programs and a primary analysis program.

The control programs were adequate for the needs of this study, and required only superficial changes. A brief description of their functions follows:

"LEDTEST" : for system self-calibration, using an inbuilt LED.

"ENTSEQ" : Permits the operator to enter a set of instructions for irradiating and/or ramping selected groups of sample discs. This "sequence" can be stored for repeated use.

"RUNSEQ" : The hardware control program - runs the system using instructions ("sequence") written and stored by program "ENTSEQ".

The analysis program "RECALL" was structured around an "ON-KEY" routines menu. Available hardcopy outputs were counts from each of the 250 channels into which the temperature range is divided, and a graphical representation of the same. An additional feature was a peak summation

routine which integrated over a nominated temperature "width" in a user specified "area of interest" temperature range.

The program structure permitted user authored routines to be added to the "ON-KEY" menu - this was done for weight normalization, 5 channel summations, 10 channel summations and a curve averaging routine (produces the mean of two glow curves). The summation subroutine algorithms are based on those in the program "MCS19" written by B. Smith.

The considerable "hands-on" time required to output analysed data led to the creation of two automatic output programs, based on "RECALL". These give graphical and 5 channel sum hardcopy of the weight normalized data, along with run details. Program "AWN5CS" does this for each of up to 250 records, whereas "AVCURV" produces the same output format for averaged pairs of records (up to 125 pairs). Listings of "RECALL" "AWN5CS", and "AVCURV" follow.

RECALL

```
10 ! PROGRAM RECALLING MEASUREMENTS MADE BY OTHER TL-MEASUREMENT PROGRAMS
20 ON ERROR GOTO 40
30 LOADBIN "GDUMP.PROG"
40 OFF ERROR
50 !
60 ! ********** DIMENSION AND INITIALIZE STRING VARIABLES,ARRAYS. **********
70 !
80 DIM D$[1041],F$[36],NAME$$[75],ID$[75]
90 REAL A(260),B(260)
100 FOR Y=1 TO 260
110 A(Y)=0
120 B(Y)=0
130 NEXT Y
140 PRINTER IS 701
150 AVCURVE=0
160 CLEAR
170 !
180 ! ********** CATALOGUE DATA DISC,SELECT FILE OF INTEREST. **********
190 !
200 CAT ".DATA"
210 DISP "ENTER FILENAME";
220 INPUT A$
230 ASSIGN# 1 TO  A$&".DATA"
240 !
250 ! ********** OPTION TO BYPASS DISPLAY OF FILE DIRECTORY. **********
260 !
270 CLEAR @ DISP "DO YOU KNOW THE NUMBER OF THE RECORD YOU WANT TO SEE   (Y/N)";
280 INPUT RECNO$
290 RECNO$=UPC$ (RECNO$)
300 IF RECNO$="N" THEN 370
310 IF RECNO$="Y" THEN DISP "ENTER RECORD NO. YOU WANT TO SEE";
320 INPUT X
330 GOTO 690
340 !
350 ! ********** DISPLAY OF FILE DIRECTORY. **********
360 !
370 READ# 1,1 ; D$
380 CLEAR
390 DISP USING "K,K,K,ZZ,ZZ,ZZ" ; "FILE "&A$&" CONTAINING ",NUM (D$[1]),"  RECORD
S MEASURED : ",NUM (D$[15]),NUM (D$[16]),NUM (D$[17])
400 DISP "FILE WRITTEN BY TL-MEASUREMENT PROGRAM ";D$[2,4]
410 DISP
420 DISP "REC SAMPLE  RUN NO.  SECOND NAME  MAX-TEMP  RAMP TIME  TEST-DOSE STATI
ON"
430 FOR A=1 TO NUM (D$[1])
440 READ# 1,A ; D$
450 IF NUM (D$[20,20])<20 THEN D$[20,20]=CHR$ (NUM (D$[20,20])*10) @ PRINT# 1,A
; D$
460 S=NUM (D$[18])
470 R=NUM (D$[19])
480 T=INT (FNR(21)*10/NUM (D$[20])*10)/10
490 B=NUM (D$[33])*FNR(21)*.000128*20/19.6608
500 D=NUM (D$[38])
510 C=INT ((FNR(40)*.008*20/19.6608+NUM (D$[39])*65535*20/19.6608*.008)*100)/100
520 IF D THEN DISP USING 530 ; A,S,R,D$[5,14],T,B,C,D ELSE DISP USING 540 ; A,S,
R,D$[5,14],T,B
530 IMAGE DDZ,2X,DZ,7X,DZ,6X,10A,3X,3DZ.D,5X,2DZ.2D,5X,6DZ.D,3X,Z
540 IMAGE DDZ,2X,DZ,7X,DZ,6X,10A,3X,3DZ.D,5X,2DZ.2D,6X,"NO RADIATION"
550 NEXT A
560 DISP
570 !
580 ! ********** ENTER RECORD NO. OF GLOWCURVE TO BE ANALYSED. **********
590 !
600 DISP "ENTER RECORD No. YOU WANT TO SEE";
610 INPUT X
620 IF X<A THEN 650
630 DISP "RECORD NOT PRESENT IN FILE"
640 GOTO 380
650 CLEAR
660 !
670 ! ********** RECORD DATA READ FROM STORAGE DISC. **********
680 !
690 READ# 1,X ; D$
700 !
710 ! ********** CRT DISPLAY OF DETAILS OF RECORD UNDER ANALYSIS. **********
720 !
730 DISP "FILE : ";A$
740 DISP "MEASURED BY TL-MEASUREMENT PROGRAM ";D$[2,4]
750 DISP "RECORD NO.:";X
760 DISP "SECOND NAME : ";D$[5,14]
770 DISP USING "K,ZZ,ZZ,ZZ" ; "DATE : ";NUM (D$[15]),NUM (D$[16]),NUM (D$[17])
780 DISP "SAMPLE No. :";NUM (D$[18])
790 DISP "RUN No. :";NUM (D$[19])
800 DISP "MAX. TEMPERATURE :";INT (FNR(21)*10/NUM (D$[20])*10)/10;"DEGREES"
```

```
810 DISP "RAMP TIME :";INT (FNR(21)*NUM (D$[23])*.000128*20/19.6608*100)/100;"SE
CONDS"
820 FOR A=0 TO 2
830 IF NOT FNR(24+4*A) THEN 870
840 DISP "PAUSE TEMPERATURE :";INT (FNR(24+4*A)*10/NUM (D$[20]));"DEGREES"
850 DISP "PAUSE TIME :";INT (FNR(26+4*A)*.008*20/19.6608);"SECONDS"
860 NEXT A
870 DISP "INTEGRATION AREA :";NUM (D$[37])-NUM (D$[36])+1;"CHANNELS"
880 DISP "LOW TEMPERATURE :";INT (NUM (D$[36])*FNR(21)*10/250/NUM (D$[20]));"DE
GREES"
890 DISP "HIGH TEMPERATURE :";INT (NUM (D$[37])*FNR(21)*10/250/NUM (D$[20]));"DE
GREES"
900 IF D$[38,38]=CHR$ (0) THEN DISP "NO RADIATION" @ GOTO 930
910 DISP "TEST-DOSE TIME :";INT ((FNR(40)*.008*20/19.6608+NUM (D$[39])*65535*20/
19.6608*.008)*100)/100;"SECONDS"
920 DISP "TEST DOSE STATION No.";NUM (D$[38,38])
930 DISP @ DISP TAB (12);"**********    PLEASE WAIT FOR KEY LABELS.    ********
*"
940 !
950 ! ************************** FOR ALL CHANNELS - COUNTS DATA RECOVERED FROM
STRING STORAGE THEN CORRECTED FOR NEGATIVE NUMBERS. ************************
960 !
970 FOR Y=1 TO 250
980 A(Y)=1048576*NUM (D$[38+4*Y])+4096*NUM (D$[39+4*Y])+16*NUM (D$[40+4*Y])+NUM
(D$[41+4*Y])
990 IF A(Y)>268000000 THEN A(Y)=A(Y)-268435696
1000 NEXT Y
1010 !
1020 ! ******* ASSIGN,INITIALIZE VARIABLES.NO HARDCOPY OR DATA STORAGE. ******
1030 !
1040 B=NUM (D$[20])/10
1050 D4,D5=0
1060 D6=NUM (D$[36])
1070 D7=NUM (D$[37])
1080 F=D7-D6+1
1090 B$="N" ! HARDCOPY NOT REQUIRED.
1100 C$="N" ! DO NOT STORE DATA
1110 B3=FNR(21)/250
1120 WEIGHT=0
1130 NAMES$=""
1140 ID$=""
1150 E=0 ! INITIALIZE,SET Y-SCALE ON AUTOMATIC.
1160 E$="    RECALL"
1170 A2=NUM (D$[18])
1180 IF AVCURVE=10 THEN 4640 ! REDIRECT PROGRAM FLOW FOR AV.CURVES SUBROUTINE
1190 !
1200 ! ********* ASSIGN'FUNCTIONS AND BRANCHING INSTRUCTIONS TO KEYS  *******
1210 !
1220 ON KEY# 1,"Y-SCALE" GOSUB 3140
1230 ON KEY# 2,"LOW" GOSUB 3220
1240 ON KEY# 3,"HIGH" GOSUB 3400
1250 ON KEY# 4,"WIDTH" GOSUB 3580
1260 ON KEY# 5,"HARDCOPY" GOSUB 3030
1270 ON KEY# 6,"CURVE" GOSUB 1400
1280 ON KEY# 7,"COUNTS" GOSUB 2620
1290 ON KEY# 8,"NEW REC" GOSUB 270
1300 ON KEY# 9,"NEW FILE" GOSUB 160
1310 ON KEY# 10,"WGHT. NORM." GOSUB 3760
1320 ON KEY# 11,"5 CHN. SUM" GOSUB 3890
1330 ON KEY# 12,"SUM 10CHN" GOSUB 4200
1340 ON KEY# 13,"AV.CURVES" GOSUB 4390
1350 ON KEY# 14,"EXIT PROG" GOTO 1380
1360 KEY LABEL
1370 GOTO 1370 ! IDLE LOOP FOR KEY LABELS.
1380 CLEAR @ DISP TAB (25);"****** Program ENDED ******" @ BEEP @ END
1390 !
1400 ! ************************
1410 ! DISPLAY SUB ROUTINE
1420 ! A()=COUNTS FROM THE 250
1430 ! CHANNELS
1440 ! B=NUMBER OF TEMPERATURE
1450 ! STEPS PER DEGREE
1460 ! D4=LOW TEMPERATURE OF
1470 ! AREA OF INTEREST
1480 ! D5=HIGH TEMPERATURE
1490 ! F=NUMBER OF CHANNELS TO
1500 ! INTEGRATE
1510 ! B$="Y" IF HARDCOPY
1520 ! B3=NUMBER OF TEMPERATURE
1530 ! STEPS PER CHANNEL
1540 ! E=Y-SCALE (0=AUTOMATIC)
1550 ! E$=NAME OF CURVE (I.E.
1560 ! "PRE" OR "POST")
1570 ! A2=SAMPLE NUMBER TO BE
1580 ! DISPLAYED
1590 ! ************************
1600 !
```

```
1610 IF NOT D4 THEN 1640 ! TEMPERATURE OR CHANNELS
1620 D6=INT (D4*B/B3) ! CONVERT TEMPERATURE TO CHANNEL NUMBERS
1630 D7=INT (D5*B/B3)
1640 IF D6>0 AND D6<251 AND D7>= D6 AND D7<251 THEN 1680
1650 DISP "Integration area out of range" @ DISP "Caused by a PROGRAMMING ERROR"

1660 BEEP
1670 STOP
1680 D2=0 @ D9=D6
1690 FOR A9=D6 TO D7 ! SEARCH PEAK
1700 IF A(A9)>D2 THEN D2=A(A9) @ D9=A9 ! LOCATE,STORE PEAK COUNT AND CHANNEL.
1710 NEXT A9
1720 IF F>0 THEN D8=F ELSE D8=INT (-(F*B/(2*B3)))*2+1 ! FIND NUMBER OF CHAN IF I
NT AREA IN TEMP
1730 D0=D9-(D8-1)/2 ! LOWEST INTEGRATION CHANNEL
1740 D1=D9+(D8-1)/2 ! HIGHEST
1750 IF D0>0 AND D1<251 THEN 1790 ! WIDTH OK ?
1760 D8=-(MIN (250-D9,D9-1)*2+1) ! CALCULATE NEW WIDTH
1770 D0=D9-((-D8-1)/2)
1780 D1=D9+((-D8-1)/2)
1790 D$[36,36]=CHR$ (D0) ! STORE INTEGRATION AREA
1800 D$[37,37]=CHR$ (D1)
1810 D3=0
1820 FOR A9=D0 TO D1
1830 D3=D3+A(A9) ! INTEGRATE OVER AREA OF INTEREST.
1840 NEXT A9
1850 !
1860 ! ************************** SET Y-SCALE. **************************
1870 !
1880 D=E ! SET SCALE
1890 IF NOT D THEN D=MAX (1,D2) ! AUTOMATIC Y-SCALE (MIN 1)
1900 E4=LEN (VAL$ (INT (D))) ! NUMBER OF FIGURES IN Y-SCALE
1910 D=(INT ((D-1)/10^(E4-1))+1)*10^(E4-1) ! SCALE ?*10^?
1920 E4=LEN (VAL$ (D)) ! CORRECT
1930 !
1940 ! ************************ DRAW GRAPH ON CRT. ************************
1950 !
1960 GRAPH ! GRAPHICS MODE
1970 GCLEAR
1980 SCALE 0,260,-(.1*D),1.05*D
1990 XAXIS 0,50 ! DRAW AXIS
2000 YAXIS 0,.1*D,0,D
2010 FOR A9=0 TO 4 ! PRINT UNITS
2020 PEN UP
2030 MOVE 40+50*A9,-(.1*D)
2040 LABEL VAL$ (INT (50*(A9+1)*B3/B)) ! TEMPERATURE ON X AXIS
2050 NEXT A9
2060 FOR A9=.1*D TO D STEP .1*D
2070 PEN UP
2080 MOVE 10,A9
2090 LABEL VAL$ (A9/10^(E4-2)) ! COUNTS ON Y AXIS
2100 NEXT A9
2110 PEN UP
2120 MOVE 30,.9*D
2130 LABEL "X10" ! PRINT MULTIPLICATOR
2140 MOVE 45,.94*D
2150 LABEL VAL$ (F4-2)
2160 PEN UP
2170 MOVE 0,0
2180 FOR A9=1 TO 250
2190 PLOT A9,A(A9) ! PLOT CURVE
2200 PEN UP
2210 NEXT A9
2220 PEN UP
2230 MOVE D0,0 ! DRAW INTEGRATION AREA
2240 DRAW D0,A(D0)
2250 PEN UP
2260 MOVE D1,0
2270 DRAW D1,A(D1)
2280 PEN UP
2290 !
2300 ! *************** LABEL GRAPH,DISPLAY INTEGRATION VALUE. ***************
2310 !
2320 F$=E$&"#"&VAL$ (A2)&" T="&VAL$ (INT (D9*B3/B))&" I="
2330 IF D8>0 THEN F$=F$&VAL$ (INT (D3)) ELSE F$=F$&"["&VAL$ (INT (D3-D8/1000))&"
]"
2340 MOVE 130-4*LEN (F$),D
2350 LABEL F$
2360 PEN UP
2370 !
2380 ! ***** PRINT DETAILS OF GLOWCURVE IF GRAPHICAL HARDCOPY IS REQUIRED. ****
2390 !
2400 IF B$="Y" THEN 2410 ELSE 2570
```

```
2410 IF NAMES$="0" THEN GOTO 2430
2420 PRINT ;ID$
2430 PRINT @ PRINT "FILE        : ";A$&"              MEASURED BY TL-MEASUREMENT
PROGRAM : ";D$[2,4]
2440 PRINT "SAMPLE NO.  :";NUM (D$[18]),"              RUN NO. :";NUM (D$[19])
2450 PRINT "RECORD NO.  :";X,"              SECOND NAME : ";D$[5,14]
2460 MAXTEMP=FNR(21)*10/NUM (D$[20])
2470 HEATRATE=MAXTEMP/(FNR(21)*NUM (D$[23])*.000128*20/19.6608)
2480 PRINT "HEATING RATE:";INT (HEATRATE*100)/100;"DEG/SEC.,TO A MAXIMUM TEMPERA
TURE OF ";INT (MAXTEMP*10)/10;"DEG. CELSIUS."
2490 LET DDD=NUM (D$[15]) @ MMM=NUM (D$[16]) @ YYY=NUM (D$[17])
2500 PRINT "DATE OF RUN : ";DDD;"/";MMM;"/";YYY
2510 PRINT "IRRADIATION TIME :";INT ((FNR(40)*.008*20/19.6608+NUM (D$[39])*65535
*20/19.6608*.008)*100)/100;"SECONDS"
2520 IF WEIGHT>0 THEN PRINT "DATA WEIGHT NORMALISED FOR SAMPLE MASS :";WEIGHT;"m
g."
2530 !
2540 ! ************** IF HARDCOPY REQUIRED,ADVANCE PRINTER 9 LINES FROM DETAILS,
PRINT GRAPH,ADVANCE TO TOP OF NEXT FORM.STORE DATA IF REQUIRED. **************
2550 !
2560 PRINT @ PRINT @ PRINT @ PRINT @ PRINT @ PRINT @ PRINT @ PRINT @ PRINT
2570 IF B$="Y" THEN DUMP GRAPHICS 0.0,1 @ PRINT @ PRINT @ PRINT @ PRINT
2580 IF B$="Y" THEN PRINT CHR$ (12) ELSE 2590
2590 IF C$="Y" THEN PRINT# 1 ; D$
2600 RETURN
2610 !
2620 ! ************************
2630 ! PRINT COUNTS ROUTINE
2640 ! ************************
2650 !
2660 !
2670 ! ************ IF HARDCOPY COUNTS REQUIRED,PRINT DETAILS. ************
2680 !
2690 IF B$="Y" THEN 2700 ELSE 2860
2700 IF NAMES$="0" THEN GOTO 2720
2710 PRINT ;ID$
2720 PRINT @ PRINT "FILE        : ";A$&"              MEASURED BY TL-MEASUREMENT
PROGRAM : ";D$[2,4]
2730 PRINT "SAMPLE NO.  :";NUM (D$[18]),"              RUN NO. :";NUM (D$[19])
2740 PRINT "RECORD NO.  :";X,"              SECOND NAME : ";D$[5,14]
2750 MAXTEMP=FNR(21)*10/NUM (D$[20])
2760 HEATRATE=MAXTEMP/(FNR(21)*NUM (D$[23])*.000128*20/19.6608)
2770 PRINT "HEATING RATE:";INT (HEATRATE*100)/100;"DEG/SEC.,TO A MAXIMUM TEMPERA
TURE OF ";INT (MAXTEMP*10)/10;"DEG. CELSIUS."
2780 LET DDD=NUM (D$[15]) @ MMM=NUM (D$[16]) @ YYY=NUM (D$[17])
2790 PRINT "DATE OF RUN : ";DDD;"/";MMM;"/";YYY
2800 PRINT "IRRADIATION TIME :";INT ((FNR(40)*.008*20/19.6608+NUM (D$[39])*65535
*20/19.6608*.008)*100)/100;"SECONDS"
2810 IF WEIGHT>0 THEN PRINT "DATA WEIGHT NORMALISED FOR SAMPLE MASS :";WEIGHT;"m
g."
2820 PRINT @ PRINT
2830 !
2840 ! ******** DISPLAY COUNTS ON CRT,AND PRINT HARDCOPY IF REQUIRED. *******
2850 !
2860 IF B$="Y" THEN PRINT ALL
2870 FOR Y=1 TO 251 STEP 5
2880 DISP USING 2940 ; Y,A(Y),A(Y+1),A(Y+2),A(Y+3),A(Y+4)
2890 NEXT Y
2900 DISP USING 2940 ; Y,A(Y),A(Y+1),A(Y+2),A(Y+3)
2910 NORMAL
2920 IF B$="Y" THEN PRINT CHR$ (12) ! ADVANCE PRINTER TO TOP OF FORM.
2930 KEY LABEL @ RETURN
2940 IMAGE 3Z,6X,8DZ,6X,8DZ,6X,8DZ,6X,8DZ,6X,8DZ
2950 !
2960 ! ******************** DEFINE USER-DEFINED FUNCTIONS. ******************
2970 !
2980 DEF FNR(X) = 256*NUM (D$[X])+NUM (D$[X+1])
2990 DEF FND$(X) = VAL$ (INT (NUM (D$[X,X])/10))&VAL$ (RMD (NUM (D$[X,X]),10))
3000 !
3010 ! ****************** ON/OFF SWITCH FOR HARDCOPY MODE. ******************
3020 !
3030 CLEAR
3040 IF B$="Y" THEN B$="N" @ DISP "HARDCOPY OFF" ELSE B$="Y" @ DISP "HARDCOPY ON
"
3050 IF B$="Y" THEN GOTO 3060 ELSE CLEAR @ GOTO 3090
3060 DISP "ENTER TITLE (UP TO 75 CHARACTERS)   - 0 IF TITLE NOT REQUIRED.
                    (BUT DO NOT USE COMMAS)  - P IF PREVIOUSLY ENTERED.";
3070 INPUT NAMES$
3080 IF NAMES$#"0" AND NAMES$#"P" THEN ID$=NAMES$
3090 KEY LABEL
3100 RETURN
3110 !
3120 ! ************************ ENTER NEW Y-SCALE. ************************
3130 !
```

```
3140 CLEAR @ DISP "Enter new y-scale  (0=Automatic)";
3150 INPUT E
3160 IF E>= 0 THEN KEY LABEL @ RETURN
3170 BEEP
3180 GOTO 3140
3190 !
3200 ! ************** SET LOWER BOUNDARY OF AREA OF INTEREST. **************
3210 !
3220 CLEAR
3230 DISP "Enter low temp. or channel "
3240 DISP "(1 to";INT (FNR(21)/NUM (D$[20])*10);"or C1 to C250)";
3250 INPUT A1$
3260 A1$=UPC$ (A1$)
3270 IF A1$="" THEN BEEP @ GOTO 3230
3280 IF A1$[1,1]="C" THEN D4=0 @ D6=VAL (A1$[2]) @ GOTO 3330
3290 D4=INT (VAL (A1$))
3300 D6=INT (D4/(FNR(21)/NUM (D$[20])*10)*250+.5)
3310 DISP D4;"= CHANNEL";D6
3320 D4=0
3330 IF D6>0 AND D6<250 THEN 3350
3340 DISP "Low channel out of range" @ BEEP @ GOTO 3230
3350 IF D6<D7 THEN KEY LABEL @ RETURN
3360 GOTO 3410
3370 !
3380 ! ************** SET UPPER BOUNDARY OF AREA OF INTEREST. **************
3390 !
3400 CLEAR
3410 DISP "Enter high temp. or channel "
3420 DISP "(1 to";INT (FNR(21)/NUM (D$[20])*10);"or C1 to C250)";
3430 INPUT A1$
3440 A1$=UPC$ (A1$)
3450 IF A1$="" THEN BEEP @ GOTO 3410
3460 IF A1$[1,1]="C" THEN D4=0 @ D7=VAL (A1$[2]) @ GOTO 3510
3470 D5=INT (VAL (A1$))
3480 D7=INT (D5/(FNR(21)/NUM (D$[20])*10)*250+.5)
3490 DISP D5;"= CHANNEL";D7
3500 D5=0
3510 IF D6>0 AND D6<250 THEN 3530
3520 DISP "High channel out of range" @ BEEP @ GOTO 3410
3530 IF D6<D7 THEN KEY LABEL @ RETURN
3540 GOTO 3230
3550 !
3560 ! ******************** SET WIDTH OF AREA TO INTEGRATE. ********************
3570 !
3580 CLEAR
3590 DISP "Enter width of area to integrate";
3600 DISP "(In temperature 1 to";INT (FNR(21)/NUM (D$[20])*10)
3610 DISP "degrees or in channels C1 to" @ DISP "C249(If channels an odd number
)";
3620 INPUT A1$
3630 IF A1$="" THEN 3690
3640 IF A1$[1,1]#"C" THEN F=-VAL (A1$) @ GOTO 3710
3650 F=VAL (A1$[2])
3660 IF RMD (F,2) AND F>0 AND F<250 THEN KEY LABEL @ RETURN
3670 DISP "Number of channels to integrate"
3680 DISP "out of range"
3690 BEEP
3700 GOTO 3590
3710 IF -F>0 AND -F<FNR(21)/NUM (D$[20])*10 THEN KEY LABEL @ RETURN
3720 DISP "Width of integration area out of";@ DISP "range"
3730 BEEP
3740 GOTO 3590
3750 !
3760 ! ******************* WEIGHT NORMALISATION SUBROUTINE. *******************
3770 !
3780 CLEAR @ DISP TAB (30);"WEIGHT NORMALISATION."
3790 DISP @ DISP "(TO WEIGHT NORMALISE AN AVERAGED CURVE,USE (MASS SAMPLE 1 +MA
SS SAMPLE 2)/2 AS "&CHR$ (34)&"SAMPLE MASS."&CHR$ (34)&")" @ DISP @ DISP
3800 DISP "ENTER MASS OF SAMPLE,IN mg,(ie: 5.3)";
3810 INPUT WEIGHT
3820 FOR Y=1 TO 255 STEP 1
3830 A(Y)=A(Y)*1/WEIGHT
3840 NEXT Y
3850 CLEAR @ DISP "WEIGHT NORMALISATION COMPLETED." @ KEY LABEL @ RETURN
3860 !
3870 ! ******************* 5 CHANNEL SUMMATION SUBROUTINE. *******************
3880 !
3890 IF B$="Y" THEN PRINT ALL ! PRINT HARDCOPY IF REQUIRED.
3900 IF B$="Y" THEN 3910 ELSE 4030 ! IF HARDCOPY REQUIRED,PRINT DETAILS.
3910 IF NAMES$="0" THEN GOTO 3930
3920 PRINT ;ID$
3930 PRINT @ PRINT "FILE         : ";A$&"              MEASURED BY TL-MEASUREMENT
PROGRAM : ";D$[2,4]
3940 PRINT "SAMPLE NO.  :";NUM (D$[18]),"              RUN NO. :";NUM (D$[19])
3950 PRINT "RECORD NO.  :";X,"              SECOND NAME : ";D$[5,14]
3960 MAXTEMP=FNR(21)*10/NUM (D$[20])
3970 HEATRATE=MAXTEMP/(FNR(21)*NUM (D$[23])*.000128*20/19.6608)
```

```
3980 PRINT "HEATING RATE:";INT (HEATRATE*100)/100;"DEG/SEC.,TO A MAXIMUM TEMPERA
TURE OF ";INT (MAXTEMP*10)/10;"DEG. CELSIUS."
3990 LET DDD=NUM (D$[15]) @ MMM=NUM (D$[16]) @ YYY=NUM (D$[17])
4000 PRINT "DATE OF RUN : ";DDD;"/";MMM;"/";YYY
4010 PRINT "IRRADIATION TIME :";INT ((FNR(40)*.008*20/19.6608+NUM (D$[39])*65535
*20/19.6608*.008)*100)/100;"SECONDS"
4020 IF WEIGHT>0 THEN PRINT "DATA WEIGHT NORMALISED FOR SAMPLE MASS :";WEIGHT;"m
g."
4030 CLEAR @ DISP @ DISP TAB (30);"5 CHANNEL SUMMATIONS."
4040 IF WEIGHT>0 THEN DISP TAB (20);"WEIGHT NORMALISED FOR SAMPLE MASS";WEIGHT;"
mg."
4050 DISP "                CHANNELS       SUM                  CHANNELS       SUM"
4060 FOR K9=0 TO 25
4070 V2=0 @ V3=0
4080 FOR K8=0 TO 4
4090 V2=V2+A(K8+K9*10+1)
4100 NEXT K8
4110 FOR K8=5 TO 9
4120 V3=V3+A(K8+K9*10+1)
4130 NEXT K8
4140 DISP USING 4150 ; 10*K9+1;10*K9+5;V2;10*K9+6;10*K9+10;V3
4150 IMAGE 14X,3D,"-",3D,3X,10D,12X,3D,"-",3D,3X,10D
4160 NEXT K9
4170 IF B$="Y" THEN PRINT CHR$ (12)
4180 NORMAL @ KEY LABEL @ RETURN
4190 !
4200 ! ******************** 10 CHANNEL SUMMATION SUBROUTINE. ******************
4210 !
4220 IF B$="Y" THEN PRINT ALL ! PRINT SUMS IF HARDCOPY REQUIRED.
4230 DISP @ DISP TAB (30);"10 CHANNEL SUMMATIONS."
4240 IF WEIGHT>0 THEN DISP TAB (20);"WEIGHT NORMALISED FOR SAMPLE MASS";WEIGHT;"
mg."
4250 DISP "                CHANNELS       SUM                  CHANNELS       SUM"
4260 FOR K9=0 TO 12
4270 V2=0 @ V3=0
4280 FOR K8=1 TO 10
4290 V2=V2+A(K8+K9*20)
4300 NEXT K8
4310 FOR K8=11 TO 20
4320 V3=V3+A(K8+K9*20)
4330 NEXT K8
4340 DISP USING 4350 ; 20*K9+1;20*K9+10;V2;20*K9+11;20*K9+20;V3
4350 IMAGE 14X,3D,"-",3D,3X,10D,12X,3D,"-",3D,3X,10D
4360 NEXT K9
4370 NORMAL @ DISP @ DISP @ KEY LABEL @ RETURN
4380 !
4390 ! ********************* GLOWCURVE AVERAGING SUBROUTINE. *********************
4400 !
4410 CLEAR
4420 DISP "THIS SUBROUTINE RETURNS THE AVERAGE OF TWO GLOWCURVES."
4430 DISP "THE FIRST CURVE IS THAT CURRENTLY HELD IN MEMORY,THE SECOND IS READ I
N BY THIS  SUBROUTINE."
4440 DISP @ DISP "BOTH GLOWCURVES MUST BE ENTERED AS RAW COUNTS-IF THE COUNTS HE
LD IN MEMORY HAVE BEEN WEIGHT NORMALISED,THEY MUST BE CONVERTED BACK TO RAW "
4450 DISP "COUNTS BY MULTIPLYING BY THE SAMPLE MASS."
4460 DISP "THE SECOND GLOWCURVE CAN THEN BE READ IN."
4470 DISP @ DISP "NO CORRECTION IS MADE FOR CHANNEL SHIFTING."
4480 DISP @ DISP "HAVE THE COUNTS CURRENTLY IN MEMORY BEEN WEIGHT NORMALISED (Y
/N)";
4490 ! ***** IF FIRST RECORD WGHT. NORM.,THEN CONVERT TO RAW DATA VALUES. ****
4500 INPUT WN$
4510 IF WN$="Y" THEN 4520 ELSE 4570
4520 DISP "ENTER SAMPLE MASS (mg.)";
4530 INPUT WEIGHT
4540 FOR Y=1 TO 260
4550 A(Y)=A(Y)*WEIGHT
4555 NEXT Y
4560 ! ************** STORE FIRST RECORD DATA IN B(). **************
4570 FOR Y=1 TO 260
4580 B(Y)=A(Y)
4590 NEXT Y
4600 AVCURVE=10
4610 ! ************** READ IN THE SECOND GLOWCURVE. *************
4620 GOTO 160
4630 ! ************** AVERAGE FIRST AND SECOND RECORDS. *************
4640 FOR Y=1 TO 260
4650 A(Y)=A(Y)/2+B(Y)/2
4660 NEXT Y
4670 AVCURVE=0
4680 CLEAR @ DISP "AVERAGING COMPLETED-THE DATA MAY NOW BE OUTPUT IN ANY "&CHR$
(34)&"ON-KEY"&CHR$ (34)&" FORM." @ KEY LABEL @ RETURN
```

AWN5CS

```
10 ! "AWN5CS" - AUTO WEIGHT NORMALIZED 5 CHANNEL SUMS
20 CLEAR @ DISP "THIS PROGRAM AUTOMATICALLY OUTPUTS WEIGHT NORMALIZED 5 CHANNEL
SUMS FOR EACH OF UP TO 250 RECORDS."
30 DISP @ DISP "THE OPERATOR MUST ENTER THE RECORD NUMBERS AND CORRESPONDING Sam
PLE WEIGHTS,AND HAS THE OPTION TO ENTER SAMPLE NAMES."
40 ON ERROR GOTO 60
50 LOADBIN "GDUMP.PROG"
60 OFF ERROR
70 !
80 ! ********** DIMENSION AND INITIALIZE STRING VARIABLES,ARRAYS. **********
90 !
100 OPTION BASE 1
110 DIM D$[1041],F$[36],N$(250)[75]
120 REAL A(260),RECORDS(250),WEIGHTS(250)
130 FOR Y=1 TO 260
140 A(Y)=0
150 NEXT Y
160 FOR I=1 TO 250
170 RECORDS(I)=0
180 WEIGHTS(I)=0
190 N$(I)=""
200 NEXT I
210 PRINTER IS 701
220 CLEAR
230 !
240 ! ********** CATALOGUE DATA DISC,SELECT FILE OF INTEREST. **********
250 !
260 CAT ".DATA"
270 DISP "ENTER FILENAME";
280 INPUT A$
290 ASSIGN# 1 TO  A$&".DATA"
300 !
310 ! ********** OPTION TO BYPASS DISPLAY OF FILE DIRECTORY. **********
320 !
330 CLEAR @ DISP "DO YOU KNOW THE RECORD NUMBERS OF THE RECORDS YOU WANT TO ANAL
YSE   (Y/N)";
340 INPUT RECNO$
350 RECNO$=UPC$ (RECNO$)
360 IF RECNO$="N" THEN 410
370 IF RECNO$="Y" THEN GOTO 600
380 !
390 ! ********** DISPLAY OF FILE DIRECTORY. **********
400 !
410 READ# 1,1 ; D$
420 CLEAR
430 DISP USING "K,K,K,ZZ.ZZ.ZZ" ; "FILE "&A$&" CONTAINING ",NUM (D$[1]),," RECORD
S MEASURED : ",NUM (D$[15]),NUM (D$[16]),NUM (D$[17])
440 DISP "FILE WRITTEN BY TL-MEASUREMENT PROGRAM ";D$[2,4]
450 DISP
460 DISP "REC SAMPLE  RUN NO.  SECOND NAME  MAX TEMP  RAMP TIME  TEST-DOSE STATI
ON"
470 FOR A=1 TO NUM (D$[1])
480 READ# 1,A ; D$
490 IF NUM (D$[20,20])<20 THEN D$[20,20]=CHR$ (NUM (D$[20,20])*10) @ PRINT# 1,A
; D$
500 S=NUM (D$[18])
510 R=NUM (D$[19])
520 T=INT (FNR(21)*10/NUM (D$[20])*10)/10
530 B=NUM (D$[23])*FNR(21)*.000128*20/19.6608
540 D=NUM (D$[38])
550 C=INT ((FNR(40)*.008*20/19.6608+NUM (D$[39])*65535*20/19.6608*.008)*100)/100
560 IF D THEN DISP USING 570 ; A,S,R,D$[5,14],T,B,C,D ELSE DISP USING 580 ; A,S,
R,D$[5,14],T,B
570 IMAGE DDZ,2X,DZ,7X,DZ,6X,10A,3X,3DZ.D,4X,2DZ.2D,5X,6DZ.D,3X,Z
580 IMAGE DDZ,2X,DZ,7X,DZ,6X,10A,3X,3DZ.D,4X,2DZ.2D,6X,"NO RADIATION"
590 NEXT A
600 WAIT 2000 @ CLEAR
610 !
620 ! ********** INPUT QUEUE LOOP TO REQUEST AND STORE RECORD NUMBERS,SAMPLE
WEIGHTS AND SAMPLE NAMES   (NAMES MAY BE UP TO 75 CHARACTERS LONG).**********
630 !
640 DISP "THE RECORD NUMBERS,CORRESPONDING SAMPLE WEIGHTS (mg) AND SAMPLE NAMES
FOR EACH  RECORD MUST BE ENTERED TOGETHER.   (IF NO SAMPLE NAME,ENTER 0)"
650 DISP @ DISP "         SEPARATE EACH ITEM BY COMMAS.(ie:   27,5.3,LW#2 N+6MIN5
B40)"
660 DISP "                  COMMAS MUST NOT BE USED IN THE SAMPLE NAME."
670 DISP @ DISP "ENTER THE FIRST RECORD NO.,SAMPLE WEIGHT,SAMPLE NAME.";
680 INPUT RECORDS(1),WEIGHTS(1),N$(1)
690 FOR I=2 TO 250
700 DISP "NEXT RECORD NO.,SAMPLE WEIGHT,SAMPLE NAME     (0,0,0 IF NO MORE.)";
710 INPUT RECORDS(I),WEIGHTS(I),N$(I)
720 IF RECORDS(I)=0 AND WEIGHTS(I)=0 THEN GOTO 740
730 NEXT I
740 TOTRECS=I
750 CLEAR
760 !
```

```
770 ! ****************** SELECT Y-SCALE FOR ALL RECORDS. ******************
780 !
790 DISP "ENTER Y-SCALE FOR ALL RECORDS.  (0=AUTOMATIC)";
800 INPUT YSCALE
810 !
820 ! ****************** OUTPUT LOOP - PRINTS WEIGHT NORMALIZED GRAPHICAL AND TA
BULAR HARDCOPY FOR EACH RECORD ENTERED ON THE INPUT QUEUE. ******************
830 !
840 FOR I=1 TO TOTRECS-1
850 X=RECORDS(I)
860 NORMAL
870 CLEAR
880 ! ******** DATA READ FROM STORAGE DISC. ********
890 READ# 1,X ; D$
900 ! ******** CRT DISPLAY OF DETAILS OF RECORD UNDER ANALYSIS. ********
910 DISP "FILE : ";A$
920 DISP "MEASURED BY TL-MEASUREMENT PROGRAM ";D$[2,4]
930 DISP "RECORD NO.:";X
940 DISP "SECOND NAME : ";D$[5,14]
950 DISP USING "K,ZZ,ZZ,ZZ" ; "DATE : ";NUM (D$[15]),NUM (D$[16]),NUM (D$[17])
960 DISP "SAMPLE No. :";NUM (D$[18])
970 DISP "RUN No. :";NUM (D$[19])
980 DISP "MAX. TEMPERATURE :";INT (FNR(21)*10/NUM (D$[20])*100)/100;"DEGREES"
990 DISP "RAMP TIME :";INT (FNR(21)*NUM (D$[23])*.000128*20/19.6608*100)/100;"SE
CONDS"
1000 FOR A=0 TO 2
1010 IF NOT FNR(24+4*A) THEN 1050
1020 DISP "PAUSE TEMPERATURE :";INT (FNR(24+4*A)*10/NUM (D$[20]));"DEGREES"
1030 DISP "PAUSE TIME :";INT (FNR(26+4*A)*.008*20/19.6608);"SECONDS"
1040 NEXT A
1050 DISP "INTEGRATION AREA :";NUM (D$[37])-NUM (D$[36])+1;"CHANNELS"
1060 DISP "LOW TEMPERATURE :";INT (NUM (D$[36])*FNR(21)*10/250/NUM (D$[20]));"DE
GREES"
1070 DISP "HIGH TEMPERATURE :";INT (NUM (D$[37])*FNR(21)*10/250/NUM (D$[20]));"D
EGREES"
1080 IF D$[38,38]=CHR$ (0) THEN DISP "NO RADIATION" @ GOTO 1120
1090 DISP "TEST-DOSE TIME :";INT ((FNR(40)*.008*20/19.6608+NUM (D$[39])*65535*20
/19.6608*.008)*100)/100;"SECONDS"
1100 DISP "TEST DOSE STATION No.";NUM (D$[38,38])
1110 ! *************** LOOP TO RECOVER COUNTS DATA FROM STRING STORAGE THEN CORR
ECT FOR NEGATIVE NUMBERS ON SUBTRACTION THEN WEIGHT NORMALIZE. ***************
1120 FOR Y=1 TO 250
1130 A(Y)=1048576*NUM (D$[38+4*Y])+4096*NUM (D$[39+4*Y])+16*NUM (D$[40+4*Y])+NUM
 (D$[41+4*Y])
1140 IF A(Y)>268000000 THEN A(Y)=A(Y)-268435696
1150 A(Y)=A(Y)/WEIGHTS(I)
1160 NEXT Y
1170 ! ***** CALCULATION OF AREA OF INTEREST,INTEGRAL PARAMETERS - USES THE VALU
ES FROM STRING STORAGE INPUT BY OPERATOR USING ENTSEQ/RUNSEQ PROGRAMS. *****
1180 B=NUM (D$[20])/10
1190 D4,D5=0
1200 D6=NUM (D$[36])
1210 D7=NUM (D$[37])
1220 F=D7-D6+1
1230 B3=FNR(21)/250
1240 E$="    RECALL"
1250 A2=NUM (D$[18])
1260 !
1270 ! ************************
1280 ! DISPLAY SUB ROUTINE
1290 ! A()=COUNTS FROM THE 250
1300 ! CHANNELS
1310 ! B=NUMBER OF TEMPERATURE
1320 ! STEPS PER DEGREE
1330 ! D4=LOW TEMPERATURE OF
1340 ! AREA OF INTEREST
1350 ! D5=HIGH TEMPERATURE
1360 ! F=NUMBER OF CHANNELS TO
1370 ! INTEGRATE
1380 ! B$="Y" IF HARDCOPY
1390 ! B3=NUMBER OF TEMPERATURE
1400 ! STEPS PER CHANNEL
1410 ! E=Y-SCALE (0=AUTOMATIC)
1420 ! E$=NAME OF CURVE (I.E.
1430 ! "PRE" OR "POST")
1440 ! A2=SAMPLE NUMBER TO BE
1450 ! DISPLAYED
1460 ! ************************
1470 !
1480 IF NOT D4 THEN 1510 ! TEMPERATURE OR CHANNELS
1490 D6=INT (D4*B/B3) ! CONVERT TEMPERATURE TO CHANNEL NUMBERS
1500 D7=INT (D5*B/B3)
1510 IF D6>0 AND D6<251 AND D7>= D6 AND D7<251 THEN 1550
1520 DISP "Integration area out of range" @ DISP "Caused by a PROGRAMMING ERROR
```

```
1530 BEEP
1540 STOP
1550 D2=0 @ D9=D6
1560 FOR A9=D6 TO D7 ! SEARCH PEAK
1570 IF A(A9)>D2 THEN D2=A(A9) @ D9=A9
1580 NEXT A9
1590 IF F>0 THEN D8=F ELSE D8=INT (-(F*B/(2*B3)))*2+1 ! FIND NUMBER OF CHAN IFI
NT AREA IN TEMP
1600 D0=D9-(D8-1)/2 ! LOWEST INTEGRATION CHANNEL
1610 D1=D9+(D8-1)/2 ! HIGHEST
1620 IF D0>0 AND D1<251 THEN 1660 ! WIDTH OK ?
1630 D8=-(MIN (250-D9,D9-1)*2+1) ! CALCULATE NEW WIDTH
1640 D0=D9-((-D8-1)/2)
1650 D1=D9+((-D8-1)/2)
1660 D$[36,36]=CHR$ (D0) ! STORE INTEGRATION AREA
1670 D$[37,37]=CHR$ (D1)
1680 D3=0
1690 FOR A9=D0 TO D1
1700 D3=D3+A(A9) ! INTEGRATE
1710 NEXT A9
1720 ! ************************** Y SCALE SET. **************************
1730 D=YSCALE ! SET SCALE
1740 IF NOT D THEN D=MAX (1,D2) ! AUTOMATIC Y-SCALE (MIN 1)
1750 E4=LEN (VAL$ (INT (D))) ! NUMBER OF FIGURES IN Y-SCALE
1760 D=(INT ((D-1)/10^(E4-1))+1)*10^(E4-1) ! SCALE ?*10^?
1770 E4=LEN (VAL$ (D)) ! CORRECT
1780 ! ************************ DRAW GRAPH ON CRT ************************
1790 GRAPH ! GRAPHICS MODE
1800 GCLEAR
1810 SCALE 0,260,-(.1*D),1.05*D
1820 XAXIS 0,50 ! DRAW AXIS
1830 YAXIS 0,.1*D,0,D
1840 FOR A9=0 TO 4 ! PRINT UNITS
1850 PEN UP
1860 MOVE 40+50*A9,-(.1*D)
1870 LABEL VAL$ (INT (50*(A9+1)*B3/B)) ! TEMPERATURE ON X AXIS
1880 NEXT A9
1890 FOR A9=.1*D TO D STEP .1*D
1900 PEN UP
1910 MOVE 10,A9
1920 LABEL VAL$ (A9/10^(E4-2)) ! COUNTS ON Y AXIS
1930 NEXT A9
1940 PEN UP
1950 MOVE 30,.9*D
1960 LABEL "X10" ! PRINT MULTIPLICATOR
1970 MOVE 45,.94*D
1980 LABEL VAL$ (E4-2)
1990 PEN UP
2000 MOVE 0,0
2010 FOR A9=1 TO 250
2020 PLOT A9,A(A9) ! PLOT CURVE
2030 PEN UP
2040 NEXT A9
2050 PEN UP
2060 MOVE D0,0 ! DRAW INTEGRATION AREA
2070 DRAW D0,A(D0)
2080 PEN UP
2090 MOVE D1,0
2100 DRAW D1,A(D1)
2110 PEN UP
2120 ! *************** LABEL GRAPH,DISPLAY INTEGRATION VALUE. ***************
2130 F$=E$&"#"&VAL$ (A2)&" T="&VAL$ (INT (D9*B3/B))&" I="
2140 IF D8>0 THEN F$=F$&VAL$ (INT (D3)) ELSE F$=F$&"["&VAL$ (INT (D3-D8/1000))&"
]"
2150 MOVE 130-4*LEN (F$),D
2160 LABEL F$
2170 PEN UP
2180 ! ********* PRINT DETAILS PRECEDING HARDCOPY GRAPHICAL OUTPUT. *********
2190 IF N$(I)="0" THEN GOTO 2220
2200 PRINT ;N$(I)
2210 PRINT
2220 PRINT "FILE        : ";A$&"              MEASURED BY TL-MEASUREMENT PROGRAM
: ";D$[2,4]
2230 PRINT "SAMPLE NO.  :";NUM (D$[18]),"                RUN NO. :";NUM (D$[19])
2240 PRINT "RECORD NO.  :";X,"               SECOND NAME : ";D$[5,14]
2250 MAXTEMP=FNR(21)*10/NUM (D$[20])
2260 HEATRATE=MAXTEMP/(FNR(21)*NUM (D$[23])*.000128*20/19.6608)
2270 PRINT "HEATING RATE:";INT (HEATRATE*100)/100;"DEG/SEC.,TO A MAXIMUM TEMPERA
TURE OF ";INT (MAXTEMP*10)/10;"DEG. CELSIUS."
2280 LET DDD=NUM (D$[15]) @ MMM=NUM (D$[16]) @ YYY=NUM (D$[17])
2290 PRINT "DATE OF RUN : ";DDD;"/";MMM;"/";YYY
2300 PRINT "IRRADIATION TIME :";INT ((FNR(40)*.008*20/19.6608+NUM (D$[39])*65535
*20/19.6608*.008)*100)/100;"SECONDS"
2310 PRINT "DATA WEIGHT NORMALISED FOR SAMPLE MASS :";WEIGHTS(I);"mg."
```

```
2320 ! ********************** ADVANCE PRINTER 9 LINES FROM PRINTED DETAILS,
PRINT GRAPH,THEN ADVANCE PRINTER TO TOP OF NEXT FORM. ************************
2330 PRINT @ PRINT @ PRINT @ PRINT @ PRINT @ PRINT @ PRINT @ PRINT @ PRINT
2340 DUMP GRAPHICS 0,0,1 @ PRINT @ PRINT @ PRINT @ PRINT
2350 PRINT CHR$ (12)
2360 ! ******************* DEFINE USER-DEFINED FUNCTIONS. ******************
2370 DEF FNR(X) = 256*NUM (D$[X])+NUM (D$[X+1])
2380 DEF FND$(X) = VAL$ (INT (NUM (D$[X,X])/10))&VAL$ (RMD (NUM (D$[X,X]),10))
2390 ! ******** PRINT DETAILS PRECEDING HARDCOPY 5 CHANNEL SUM OUTPUT. ********
2400 IF N$(I)="0" THEN GOTO 2430
2410 PRINT ;N$(I)
2420 PRINT
2430 PRINT "FILE        : ";A$&"              MEASURED BY TL-MEASUREMENT PROGRAM
: ";D$[2,4]
2440 PRINT "SAMPLE NO.  :";NUM (D$[18]),"              RUN NO. :";NUM (D$[19])
2450 PRINT "RECORD NO.  :";X,"              SECOND NAME : ";D$[5,14]
2460 MAXTEMP=FNR(21)*10/NUM (D$[20])
2470 HEATRATE=MAXTEMP/(FNR(21)*NUM (D$[33])*.000128*20/19.6608)
2480 PRINT "HEATING RATE:";INT (HEATRATE*100)/100;"DEG/SEC.,TO A MAXIMUM TEMPERA
TURE OF ";INT (MAXTEMP*10)/10;"DEG. CELSIUS."
2490 LET DDD=NUM (D$[15]) @ MMM=NUM (D$[16]) @ YYY=NUM (D$[17])
2500 PRINT "DATE OF RUN : ";DDD;"/";MMM;"/";YYY
2510 PRINT "IRRADIATION TIME :";INT ((FNR(40)*.008*20/19.6608+NUM (D$[39])*65535
*20/19.6608*.008)*100)/100;"SECONDS"
2520 ! ************** PRINT COLUMN HEADINGS FOR DATA TABLE. **************
2530 PRINT @ PRINT TAB (30);"5 CHANNEL SUMMATIONS."
2540 PRINT TAB (20);"WEIGHT NORMALISED FOR SAMPLE MASS";WEIGHTS(I);"mg."
2550 PRINT "              CHANNELS      SUM              CHANNELS      SUM"
2560 ! ************** LOOP TO PRINT 5 CHANNEL SUM DATA TABLE. **************
2570 FOR K9=0 TO 25
2580 V2=0 @ V3=0
2590 FOR K8=0 TO 4
2600 V2=V2+A(K8+K9*10+1)
2610 NEXT K8
2620 FOR K8=5 TO 9
2630 V3=V3+A(K8+K9*10+1)
2640 NEXT K8
2650 PRINT USING 2660 ; 10*K9+1;10*K9+5;V2;10*K9+6;10*K9+10;V3
2660 IMAGE 14X,3D,"-",3D,3X,10D,12X,3D,"-",3D,3X,10D
2670 NEXT K9
2680 ! ***************************** ADVANCE PRINTER TO TOP OF NEXT FORM,RETURN
 TO START OF OUTPUT LOOP FOR NEXT RECORD. *****************************
2690 PRINT CHR$ (12)
2700 NEXT I
2710 CLEAR @ DISP @ DISP @ DISP @ DISP @ DISP TAB (25);"*****   PROGRAM ENDED
*****" @ END
```

AVCURV

```
10 ! "AVCURV" - AVERAGE OF TWO RECORDS AUTOMATICALLY OUTPUT AS WEIGHT NORMALIZED
 FIVE CHANNEL SUMS.
20 CLEAR @ DISP "THIS PROGRAM AUTOMATICALLY OUTPUTS WEIGHT NORMALIZED 5 CHANNEL
SUMS FOR PAIRS OF RECORDS,WITH A MAXIMUM OF 125 PAIRS."
30 DISP @ DISP "THE OPERATOR MUST ENTER THE RECORD NUMBERS AND CORRESPONDING SAM
PLE WEIGHTS;    CONSECUTIVE PAIRS OF RECORDS ARE AVERAGED."
40 ON ERROR GOTO 60
50 LOADBIN "GDUMP.PROG"
60 OFF ERROR
70 !
80 ! ********** DIMENSION AND INITIALIZE STRING VARIABLES,ARRAYS. **********
90 !
100 DIM D$[1041],F$[36]
110 REAL A(260),B(260),RECORDS(250),WEIGHTS(250)
120 FOR Y=1 TO 260
130 A(Y)=0
140 B(Y)=0
150 NEXT Y
160 FOR I=1 TO 250
170 RECORDS(I)=0
180 WEIGHTS(I)=0
190 NEXT I
200 AVCURVE=0
210 PRINTER IS 701
220 CLEAR
230 !
240 ! ********** CATALOGUE DATA DISC,SELECT FILE OF INTEREST. **********
250 !
260 CAT ".DATA"
270 DISP "ENTER FILENAME";
280 INPUT A$
290 ASSIGN# 1 TO  A$&".DATA"
300 !
310 ! ********** OPTION TO BYPASS DISPLAY OF FILE DIRECTORY. **********
320 !
330 CLEAR @ DISP "DO YOU KNOW THE NUMBERS OF THE RECORDS YOU WANT TO ANALYSE  (
Y/N)";
340 INPUT RECNO$
350 RECNO$=UPC$ (RECNO$)
360 IF RECNO$="N" THEN 410
370 IF RECNO$="Y" THEN GOTO 600
380 !
390 ! ******************** DISPLAY OF FILE DIRECTORY. ********************
400 !
410 READ# 1,1 ; D$
420 CLEAR
430 DISP USING "K,K,K,2Z,2Z,2Z" ; "FILE "&A$&" CONTAINING ",NUM (D$[1]),"  RECORD
S MEASURED : ",NUM (D$[15]),NUM (D$[16]),NUM (D$[17])
440 DISP "FILE WRITTEN BY TL-MEASUREMENT PROGRAM ";D$[2,4]
450 DISP
460 DISP "REC SAMPLE  RUN NO.  SECOND NAME  MAX TEMP  RAMP TIME  TEST-DOSE STATI
ON"
470 FOR A=1 TO NUM (D$[1])
480 READ# 1,A ; D$
490 IF NUM (D$[20,20])<20 THEN D$[20,20]=CHR$ (NUM (D$[20,20])*10) @ PRINT# 1,A
; D$
500 S=NUM (D$[18])
510 R=NUM (D$[19])
520 T=INT (FNR(21)*10/NUM (D$[20])*10)/10
530 B=NUM (D$[23])*FNR(21:*.000128*20/19.6608
540 D=NUM (D$[38])
550 C=INT ((FNR(40)*.008*20/19.6608+NUM (D$[39])*65535*20/19.6608*.008)*100)/100

560 IF D THEN DISP USING 570 ; A,S,R,D$[5,14],T,B,C,D ELSE DISP USING 580 ; A,S,
R,D$[5,14],T,B
570 IMAGE DDZ,2X,DZ,7X,DZ,6X,10A,3X,3DZ.D,4X,2DZ.2D,5X,6DZ.D,3X,Z
580 IMAGE DDZ,2X,DZ,7X,DZ,6X,10A,3X,3DZ.D,4X,2DZ.2D,6X,"NO RADIATION"
590 NEXT A
600 WAIT 2000 @ CLEAR
610 !
620 ! ** INPUT QUEUE LOOP TO REQUEST AND STORE RECORD NUMBERS,SAMPLE WEIGHTS. **
630 !
640 DISP "THE RECORD NUMBERS AND CORRESPONDING SAMPLE WEIGHTS (mg) MUST BE ENTER
ED IN     PAIRS     (ie: 27,5.3)"
650 DISP @ DISP "ENTER THE FIRST PAIR.";
660 INPUT RECORDS(1),WEIGHTS(1)
670 FOR I=2 TO 250
680 DISP "NEXT PAIR (0,0 IF NO MORE.)";
690 INPUT RECORDS(I),WEIGHTS(I)
700 IF RECORDS(I)=0 AND WEIGHTS(I)=0 THEN GOTO 720
710 NEXT I
720 TOTRECS=I
730 CLEAR
740 !
750 ! ******************** SELECT Y-SCALE FOR ALL RECORDS. ********************
760 !
770 DISP "ENTER Y-SCALE FOR ALL RECORDS.    (0=AUTOMATIC)";
780 INPUT YSCALE
```

```
790 !
800 ! ****************** OUTPUT LOOP - PRINTS WEIGHT NORMALIZED GRAPHICAL AND
TABULAR HARDCOPY FOR EACH RECORD ENTERED ON THE INPUT QUEUE. ****************
810 !
820 FOR I=1 TO TOTRECS-1
830 X=RECORDS(I)
840 NORMAL
850 CLEAR
860 ! ***************** DATA READ FROM STORAGE DISC. ***************
870 READ# 1,X ; D$
880 ! ********** CRT DISPLAY OF DETAILS OF RECORD UNDER ANALYSIS. **********
890 DISP "FILE : ";A$
900 DISP "MEASURED BY TL-MEASUREMENT PROGRAM ";D$[2,4]
910 DISP "RECORD NO.:";X
920 DISP "SECOND NAME : ";D$[5,14]
930 DISP USING "K,ZZ,ZZ,ZZ" ; "DATE : ";NUM (D$[15]),NUM (D$[16]),NUM (D$[17])
940 DISP "SAMPLE No. :";NUM (D$[18])
950 DISP "RUN No. :";NUM (D$[19])
960 DISP "MAX. TEMPERATURE :";INT (FNR(21)*10/NUM (D$[20])*100)/100;"DEGREES"
970 DISP "RAMP TIME :";INT (FNR(21)*NUM (D$[23])*.000128*20/19.6608*100)/100;"SE
CONDS"
980 FOR A=0 TO 2
990 IF NOT FNR(24+4*A) THEN 1030
1000 DISP "PAUSE TEMPERATURE :";INT (FNR(24+4*A)*10/NUM (D$[20]));"DEGREES"
1010 DISP "PAUSE TIME :";INT (FNR(26+4*A)*.008*20/19.6608);"SECONDS"
1020 NEXT A
1030 DISP "INTEGRATION AREA :";NUM (D$[37])-NUM (D$[36])+1;"CHANNELS"
1040 DISP "LOW TEMPERATURE :";INT (NUM (D$[36])*FNR(21)*10/250/NUM (D$[20]));"DE
GREES"
1050 DISP "HIGH TEMPERATURE :";INT (NUM (D$[37])*FNR(21)*10/250/NUM (D$[20]));"D
EGREES"
1060 IF D$[38,38]=CHR$ (0) THEN DISP "NO RADIATION" @ GOTO 1100
1070 DISP "TEST-DOSE TIME :";INT ((FNR(40)*.008*20/19.6608+NUM (D$[39])*65535*20
/19.6608*.008)*100)/100;"SECONDS"
1080 DISP "TEST DOSE STATION No.";NUM (D$[38,38])
1090 ! ************ LOOP TO RECOVER COUNTS DATA FROM STRING STORAGE THEN CORRECT
 FOR NEGATIVE NUMBERS ON SUBTRACTION THEN WEIGHT NORMALIZE. ***************
1100 FOR Y=1 TO 250
1110 A(Y)=1048576*NUM (D$[39+4*Y])+4096*NUM (D$[39+4*Y])+16*NUM (D$[40+4*Y])+NUM
 (D$[41+4*Y])
1120 IF A(Y)>268000000 THEN A(Y)=A(Y)-268435696
1130 A(Y)=A(Y)/WEIGHTS(I)
1140 NEXT Y
1150 IF AVCURVE=10 THEN GOTO 1260 ! IF BOTH RECS. PRESENT,AVERAGE THEN PRINT.
1160 ! ***** FOR FIRST RECORD - STORE SAMPLE NO.,RECORD NO.,WEIGHT,COUNTS.****
1170 WGHT1=WEIGHTS(I)
1180 SAM1=NUM (D$[18])
1190 REC1=X
1200 FOR Y=1 TO 260
1210 B(Y)=A(Y)
1220 NEXT Y
1230 AVCURVE=10 ! INDICATES FIRST REC. COUNTS AND PARAMETERS STORED IN MEMORY.
1240 NEXT I
1250 ! ********** AVERAGE THE RECORDS,STORE AVERAGED DATA IN A(). **********
1260 FOR Y=1 TO 260
1270 A(Y)=A(Y)/2+B(Y)/2
1280 NEXT Y
1290 AVCURVE=0 ! RESET FOR NEXT PAIR.
1300 ! ******** CALCULATE AREA OF INTEREST AND INTEGRAL USING THE VALUES FROM
   STRING STORAGE (INPUT BY OPERATOR USING ENTSEQ/RUNSEQ PROGRAMS.) ********
1310 B=NUM (D$[20])/10
1320 D4,D5=0
1330 D6=NUM (D$[36])
1340 D7=NUM (D$[37])
1350 F=D7-D6+1
1360 B3=FNR(21)/250
1370 E$="    RECALL"
1380 A2=NUM (D$[18])
1390 !
1400 ! ************************
1410 ! OUTPUT SUB ROUTINE
1420 ! A()=COUNTS FROM THE 250
1430 ! CHANNELS
1440 ! B=NUMBER OF TEMPERATURE
1450 ! STEPS PER DEGREE
1460 ! D4=LOW TEMPERATURE OF
1470 ! AREA OF INTEREST
1480 ! D5=HIGH TEMPERATURE
1490 ! F=NUMBER OF CHANNELS TO
1500 ! INTEGRATE
1510 ! B3=NUMBER OF TEMPERATURE
1520 ! STEPS PER CHANNEL
1530 ! E=Y-SCALE (0=AUTOMATIC)
1540 ! E$=NAME OF CURVE (I.E.
1550 ! "PRE" OR "POST")
1560 ! A2=SAMPLE NUMBER TO BE
```

```
1570 ! DISPLAYED
1580 ! **********************
1590 !
1600 IF NOT D4 THEN 1630 ! TEMPERATURE OR CHANNELS
1610 D6=INT (D4*B/B3) ! CONVERT TEMPERATURE TO CHANNEL NUMBERS
1620 D7=INT (D5*B/B3)
1630 IF D6>0 AND D6<251 AND D7>= D6 AND D7<251 THEN 1670
1640 DISP "Integration area out of range" @ DISP "Caused by a PROGRAMMING ERROR

1650 BEEP
1660 STOP
1670 D2=0 @ D9=D6
1680 FOR A9=D6 TO D7 ! SEARCH PEAK
1690 IF A(A9)>D2 THEN D2=A(A9) @ D9=A9
1700 NEXT A9
1710 IF F>0 THEN D8=F ELSE D8=INT (-(F*B/(2*B3)))*2+1 ! FIND NUMBER OF CHAN IF I
NT AREA IN TEMP
1720 D0=D9-(D8-1)/2 ! LOWEST INTEGRATION CHANNEL
1730 D1=D9+(D8-1)/2 ! HIGHEST
1740 IF D0>0 AND D1<251 THEN 1780 ! WIDTH OK ?
1750 D8=-(MIN (250-D9,D9-1)*2+1) ! CALCULATE NEW WIDTH
1760 D0=D9-((-D8-1)/2)
1770 D1=D9+((-D8-1)/2)
1780 D$[36,36]=CHR$ (D0) ! STORE INTEGRATION AREA
1790 D$[37,37]=CHR$ (D1)
1800 D3=0
1810 FOR A9=D0 TO D1
1820 D3=D3+A(A9) ! INTEGRATE
1830 NEXT A9
1840 ! ************************** Y SCALE SET. **************************
1850 D=YSCALE ! SET SCALE
1860 IF NOT D THEN D=MAX (1,D2) ! AUTOMATIC Y-SCALE (MIN 1)
1870 E4=LEN (VAL$ (INT (D))) ! NUMBER OF FIGURES IN Y-SCALE
1880 D=(INT ((D-1)/10^(E4-1))+1)*10^(E4-1) ! SCALE ?*10^?
1890 E4=LEN (VAL$ (D)) ! CORRECT
1900 ! ************************ DRAW GRAPH ON CRT. ************************
1910 GRAPH ! GRAPHICS MODE
1920 GCLEAR
1930 SCALE 0,260,-(.1*D),1.05*D
1940 XAXIS 0,50 ! DRAW AXIS
1950 YAXIS 0,.1*D,0.D
1960 FOR A9=0 TO 4 ! PRINT UNITS
1970 PEN UP
1980 MOVE 40+50*A9,-(.1*D)
1990 LABEL VAL$ (INT (50*(A9+1)*B3/B)) ! TEMPERATURE ON X AXIS
2000 NEXT A9
2010 FOR A9=.1*D TO D STEP .1*D
2020 PEN UP
2030 MOVE 10,A9
2040 LABEL VAL$ (A9/10^(E4-2)) ! COUNTS ON Y AXIS
2050 NEXT A9
2060 PEN UP
2070 MOVE 30,.9*D
2080 LABEL "X10" ! PRINT MULTIPLICATOR
2090 MOVE 45,.94*D
2100 LABEL VAL$ (E4-2)
2110 PEN UP
2120 MOVE 0,0
2130 FOR A9=1 TO 250
2140 PLOT A9,A(A9) ! PLOT CURVE
2150 PEN UP
2160 NEXT A9
2170 PEN UP
2180 MOVE D0,0 ! DRAW INTEGRATION AREA
2190 DRAW D0,A(D0)
2200 PEN UP
2210 MOVE D1,0
2220 DRAW D1,A(D1)
2230 PEN UP
2240 ! *************** LABEL GRAPH,DISPLAY INTEGRATION VALUE.***************
2250 F$=E$&"#"&VAL$ (A2)&" T="&VAL$ (INT (D9*B3/B))&" I="
2260 IF D8>0 THEN F$=F$&VAL$ (INT (D3)) ELSE F$=F$&"["&VAL$ (INT (D3-D8/1000))&"
]"
2270 MOVE 130-4*LEN (F$),D
2280 LABEL F$
2290 PEN UP
```

```
2300 ! ********* PRINT DETAILS PRECEDING HARDCOPY GRAPHICAL OUTPUT. *********
2310 WEIGHTS(I)=(WEIGHTS(I)+WGHT1)/2
2320 PRINT "FILE         : ";A$&"                MEASURED BY TL-MEASUREMENT PROGRAM
: ";D$[2,4]
2330 PRINT "SAMPLE NOS.  :";SAM1;"AND";NUM (D$[18]),"          RUN NO. :";NUM (D
$[19])
2340 PRINT "RECORD NOS.  :";REC1;"AND";X,"          SECOND NAME : ";D$[5,14]
2350 MAXTEMP=FNR(21)*10/NUM (D$[20])
2360 HEATRATE=MAXTEMP/(FNR(21)*NUM (D$[23])*.000128*20/19.6608)
2370 PRINT "HEATING RATE:";INT (HEATRATE*100)/100;"DEG/SEC.,TO A MAXIMUM TEMPERA
TURE OF ";INT (MAXTEMP*10)/10;"DEG. CELSIUS."
2380 LET DDD=NUM (D$[15]) @ MMM=NUM (D$[16]) @ YYY=NUM (D$[17])
2390 PRINT "DATE OF RUN : ";DDD;"/";MMM;"/";YYY
2400 PRINT "IRRADIATION TIME :";INT ((FNR(40)*.008*20/19.6608+NUM (D$[39])*65535
*20/19.6608*.008)*100)/100;"SECONDS"
2410 PRINT "DATA WEIGHT NORMALISED FOR SAMPLE MASS :";WEIGHTS(I);"mg."
2420 ! ********************** ADVANCE PRINTER 9 LINES FROM PRINTED DETAILS,
PRINT GRAPH,THEN ADVANCE PRINTER TO TOP OF NEXT FORM. **********************
2430 PRINT @ PRINT @ PRINT @ PRINT @ PRINT @ PRINT @ PRINT @ PRINT @ PRINT
2440 DUMP GRAPHICS 0,0,1 @ PRINT @ PRINT @ PRINT @ PRINT
2450 PRINT CHR$ (12)
2460 ! ****************** DEFINE USER-DEFINED FUNCTIONS. ******************
2470 DEF FNR(X) = 256*NUM (D$[X])+NUM (D$[X+1])
2480 DEF FND$(X) = VAL$ (INT (NUM (D$[X,X])/10))&VAL$ (RMD (NUM (D$[X,X]),10))
2490 ! ******** PRINT DETAILS PRECEDING HARDCOPY 5 CHANNEL SUM OUTPUT. ********
2500 PRINT "FILE         : ";A$&"                MEASURED BY TL-MEASUREMENT PROGRAM
: ";D$[2,4]
2510 PRINT "SAMPLE NOS.  :";SAM1;"AND";NUM (D$[18]),"          RUN NO. :";NUM (D
$[19])
2520 PRINT "RECORD NOS.  :";REC1;"AND";X,"          SECOND NAME : ";D$[5,14]
2530 MAXTEMP=FNR(21)*10/NUM (D$[20])
2540 HEATRATE=MAXTEMP/(FNR(21)*NUM (D$[23])*.000128*20/19.6608)
2550 PRINT "HEATING RATE:";INT (HEATRATE*100)/100;"DEG/SEC.,TO A MAXIMUM TEMPERA
TURE OF ";INT (MAXTEMP*10)/10;"DEG. CELSIUS."
2560 LET DDD=NUM (D$[15]) @ MMM=NUM (D$[16]) @ YYY=NUM (D$[17])
2570 PRINT "DATE OF RUN : ";DDD;"/";MMM;"/";YYY
2580 PRINT "IRRADIATION TIME :";INT ((FNR(40)*.008*20/19.6608+NUM (D$[39])*65535
*20/19.6608*.008)*100)/100;"SECONDS"
2590 ! ***************** PRINT COLUMN HEADINGS FOR DATA TABLE. *****************
2600 PRINT @ PRINT TAB (30);"5 CHANNEL SUMMATIONS."
2610 PRINT TAB (20);"WEIGHT NORMALISED FOR SAMPLE MASS";WEIGHTS(I);"mg."
2620 PRINT "              CHANNELS      SUM                CHANNELS      SUM"
2630 ! ***************** LOOP TO PRINT 5 CHANNEL SUM DATA TABLE. ***************
2640 FOR K9=0 TO 25
2650 V2=0 @ V3=0
2660 FOR K8=0 TO 4
2670 V2=V2+A(K8+K9*10+1)
2680 NEXT K8
2690 FOR K8=5 TO 9
2700 V3=V3+A(K8+K9*10+1)
2710 NEXT K8
2720 PRINT USING 2730 ; 10*K9+1;10*K9+5;V2;10*K9+6;10*K9+10;V3
2730 IMAGE 14X,3D,"-",3D,3X,10D,12X,3D,"-",3D,3X,10D
2740 NEXT K9
2750 ! ********************************** ADVANCE TO TOP OF NEXT FORM,RETURN TO
 START OF OUTPUT LOOP FOR NEXT RECORD. ***************************************
2760 PRINT CHR$ (12)
2770 NEXT I
2780 CLEAR @ DISP @ DISP @ DISP @ DISP @ DISP TAB (25);"*****   PROGRAM ENDED
*****" @ END
```

APPENDIX 4

Laboratory Illumination

As it was proposed to examine the relative bleaching efficiencies of various wavelengths (see Chapter 5), preliminaries involved identifying any sources of bias in the experimental design. One possible source considered was the laboratory darkroom illumination.

Lighting at the Adelaide laboratory is provided by white fluorescent tubes converted to safelights. This is cheaply and conveniently done by jacketing the tubes with plastic theatrical colour filters possessing suitable spectral transmission characteristics (Sutton and Zimmerman (1978), Jensen and Barbetti (1979)).

Given the apparent innocuous nature of yellow light, and the greatly increased operator comfort compared to red light, the Rank Strand Electric filter "Cinemoid" No.1 (yellow) has been used for a number of years, with the standard safelight being one 40W fluorescent tube wrapped in at least two layers of this material.

To ascertain whether this illumination had any effect on quartz TL, two sets of quartz samples were exposed to a safelight for times of up to 72 hours. Both sets were positioned about 1.6m from the centre of the fluorescent tube.

The results are shown in Fig. App. 4.1 (a),(b). Clearly there is considerable disruption of the initial signal. Most notable are the apparent removal of the 325°C peak in (a) and the 25% reduction in peak height at ~330^{0}C in (b). Although in case (a) the bleaching appears only at the 325°C peak, the remaining peaks grow, presumably by retrapping, whereas in case (b) the reduction is general, though to differing

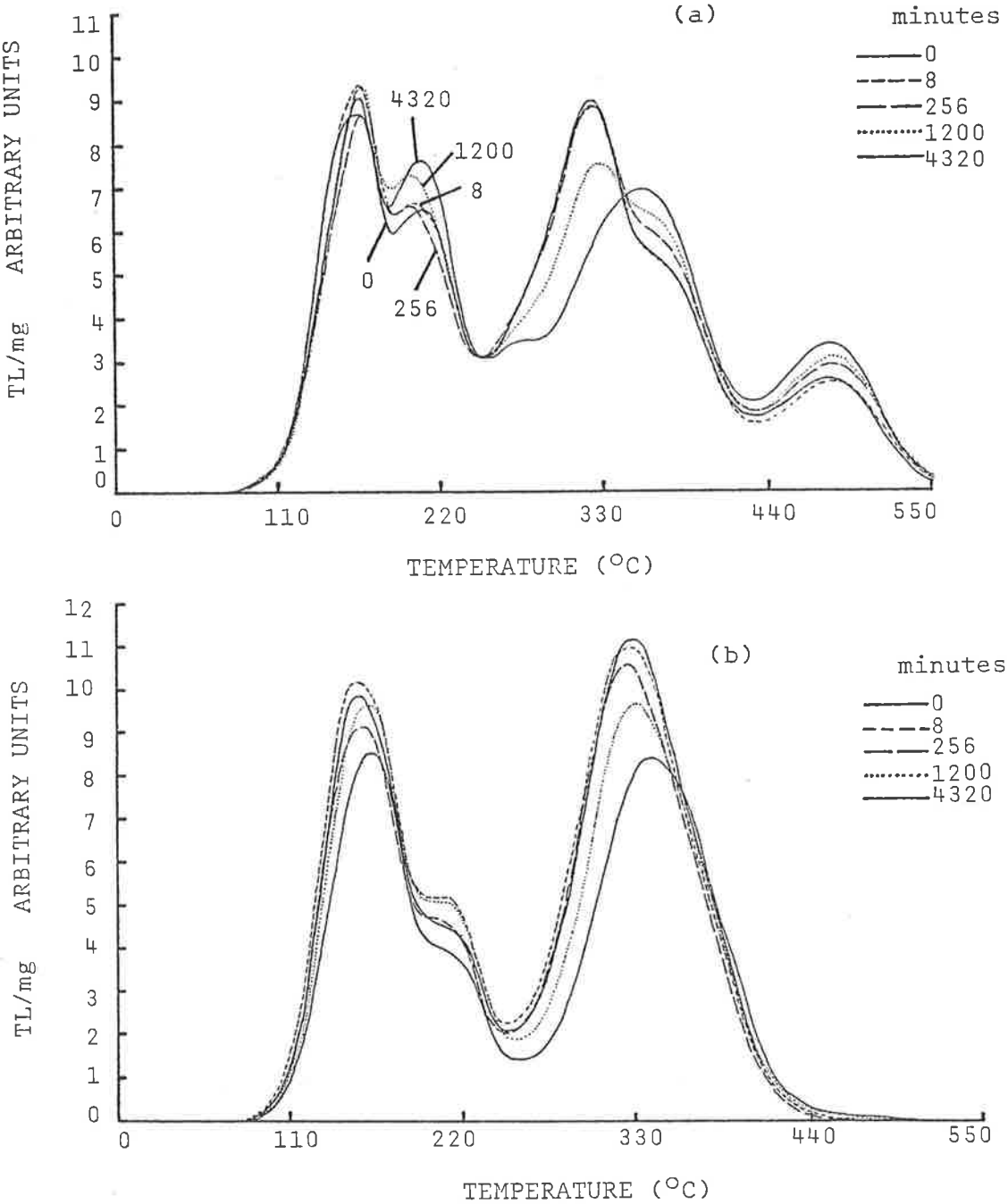

FIG. APP. 4.1.(a),(b) Shows the bleaching of Lake Woods Quartz from a 40W fluorescent tube wrapped in two layers of "Cinemoid" No.1 (yellow) filter. The samples were positioned ~1.6m from the tube; exposure times as shown.

Treatments: (a) Lake Woods (S3,TD,1m) Quartz; pre-heated to 550°C at 5K/second to erase NTL; 74.5 Gy ^{90}Sr-^{90}Y β irradiation; two days delay before bleaching.

(b) Lake Woods (S3,TD,1m) Quartz; annealed at 800°C for 24 hours in air, slow cooled; 96 Gy ^{90}Sr-^{90}Y β irradiation; two days delay before bleaching.

extents, across the entire glow curve. Both cases illustrate changes of an extent unacceptable in TL work. Mejdahl (Pers. Comm., 1984) also reports disruption to both quartz and feldspar glow curves by exposure to a 40 W incandescent bulb (30 cms distant from samples) through two layers of "Cinemoid" No.1 filter.

Fortunately, the time required for these effects to become prominent is long (>4 hours) compared to normal laboratory operations. Nevertheless, this unexpected susceptibility of quartz TL to bleaching indicated that the safelight spectrum required further restriction, with the transmission cut-off at longer wavelengths.

The "Cinemoid" line was no longer readily available, hence a number of possible substitutes were vetted using a Perkin-Elmer Model 137 UV spectrophotometer, Physics Department.

A range of "Rosco" filters were found to have excellent cut-off properties, but were marred for TL purposes by narrow "windows" of 5-20% transmission in the near UV/blue region.

Further searching revealed an ideal range of filters for safelight use, manufactured by "Chris James and Co.," of 19 New Wharf Road, London, N1 9RT, and available through local agents. The transmission curves of the more suitable filters are shown in Fig. App. 4.2, with a "Cinemoid" No.1 curve for comparison. As a consequence of the above, new fluorescent tubes were wrapped in two layers of "Chris James" No. 179 (chrome orange). This provides adequate lighting for normal darkroom operations, combined with significant reduction of <550 nm light relative to "Cinemoid" No.1, and better than 99.99% blockout of the blue/UV wavelengths. Further restriction of "yellow" wavelengths is possible using "Chris James" No. 105 (orange) or No. 158 (deep orange), but is probably unnecessary. The red filters No. 164 (flame red) or No. 106 (primary red) reduce the intensity to a level uncomfortable after protracted sessions.

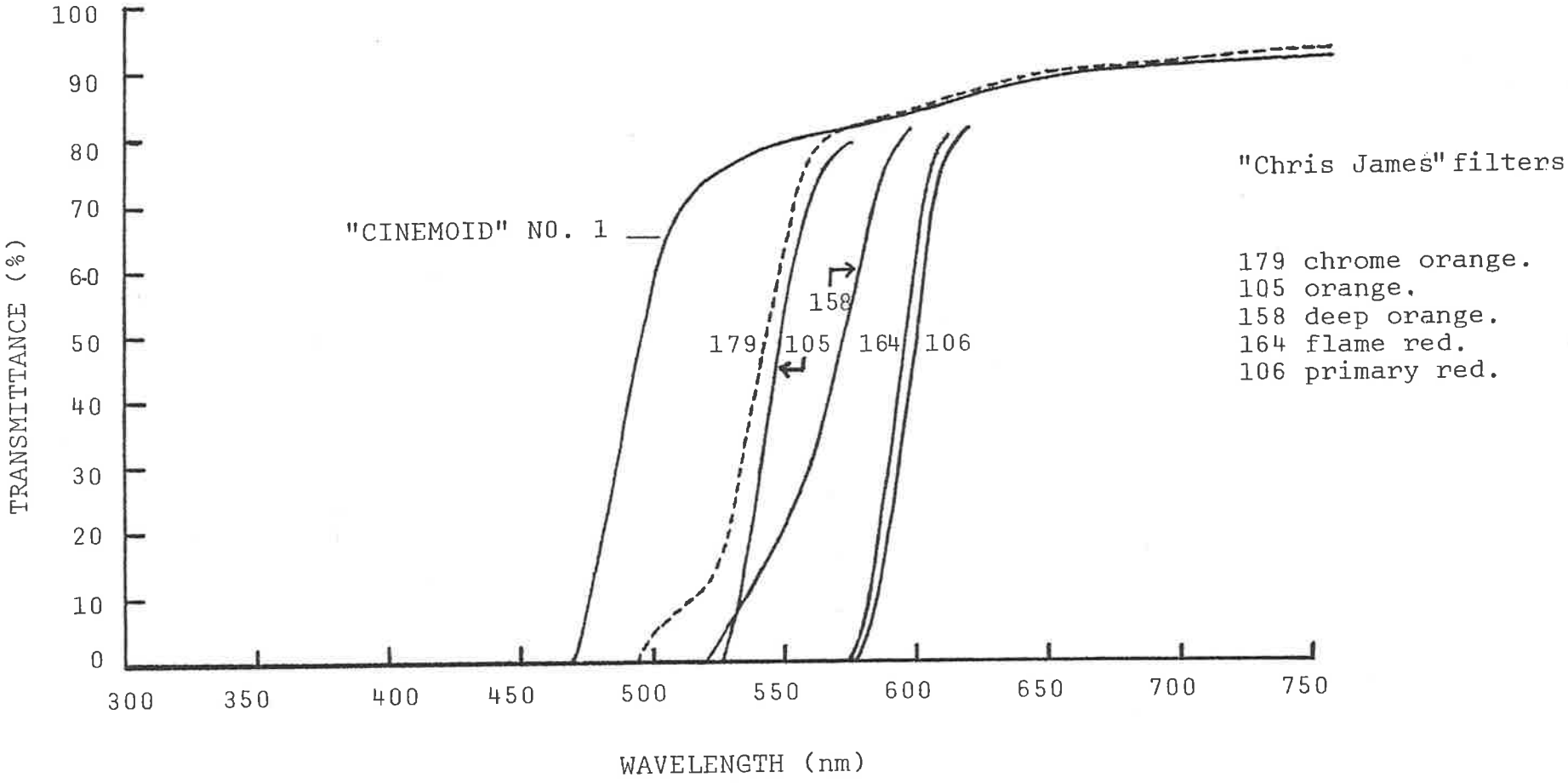

FIG.APP. 4.2 Shows transmittance Vs wavelength for a selection of "Chris James" colour filters. "Cinemoid" No.1. (yellow) is shown for comparison.

APPENDIX 5

Preparation of thin sections

The thin sections were prepared at the Mineralogy Section of the CSIRO Division of Soils, Glen Osmond, Adelaide, under the guidance of Mr H. Konczalla and with the kind permission of the Chief of the Division.

Among the samples selected were WK 1S/4, EB 1/S/2.1 and LW (S3,TD,1m). All were the 90-125μm fraction, magnetically separated and HF etched for 40 minutes.

The procedure in summary is:

1. Approximately 100mg of sample placed in 2cm diameter plastic mold.

2. Embedding araldite selected and mixed. The proportions were 2 parts LC191 (resin) and 1 part LC177 (hardener). This gives a slow curing type mix, with S.G. ≈ 1.08.

3. Mix carefully dripped onto sample until araldite layer is ≈ 5mm thick.

4. Cured in oven overnight at 50°C. (Recommended time for curing at 50°C is 10 hrs).

5. Glass mounting substrate prepared and labelled - standard 75 x 25mm microscope slides are ground and figured to 28 x 25 mm, to fit electron microprobe sample holder.

6. Araldite disc removed from mold, labelled, and grain face ground flat with successively finer grades of emery paper (grades 400, 500, 600).

7. Top surface of araldite disc ground flat with grade 400 emery paper (Figs. APP.5.1, APP.5.2).

8. Ground araldite disc glued to substrate with "grain face" adjacent to glass substrate. Tight clamping ensures an extremely thin glue layer (Fig. APP.5.2).

9. After two days curing at ambient temperatures, excess araldite is cut from the disc by diamond saw, leaving a ~0.5 mm layer of araldite and grains attached to the substrate.

10. "Rough" grinding by a purpose - built grinding wheel reduces the araldite/grain layer to ~100μm. (Figs. APP.5.1, APP.5.3).

11. "Fine" grinding by hand with progressively finer emery papers (grades 400, 500 and 600) removes grooves left by the grinding wheel.

12. Continued hand grinding with grade 600 emery paper reduces the layer to desired thickness of 30μm, monitored by polarizing microscope throughout the fine grinding stages.

13. Polishing used successively finer grades of diamond grit (6μm, 3μm, 1μm) on three separate laps for about twenty minutes/grade.

Each finished thin section is about 30μm thick, 2cm in diameter, and displays polished sections for ~12,000 - 14,000 90-125μm grains.

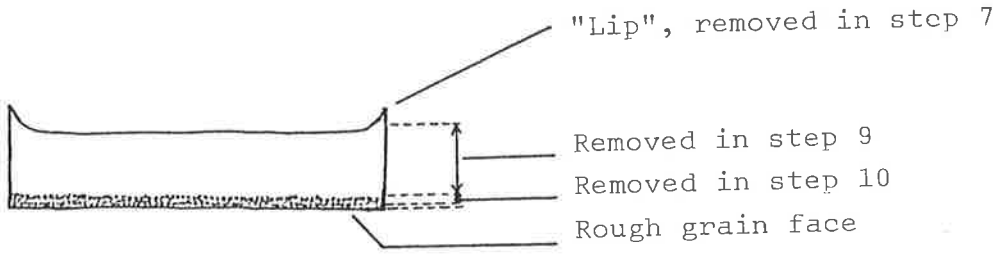

FIG. APP.5.1 Araldite disc with embedded grains as removed from mold.

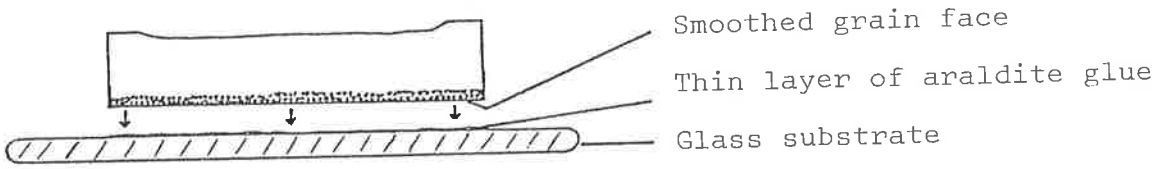

FIG. APP.5.2 Arrangement of disc and substrate at gluing and clamping (step 8).

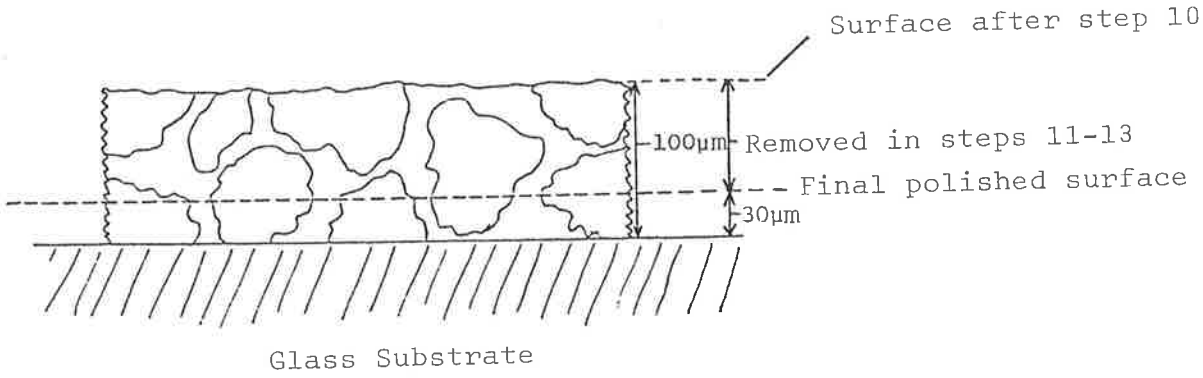

FIG. APP.5.3 Final grinding and polishing to produce 30µm thin section.

BIBLIOGRAPHY

Adams, J.A.S., Osmond, J.K., Rogers, J.J.W., (1959).
"The geochemistry of Thorium and Uranium".
Phys. Chem. Earth 3, 298-348.

Aitken, M.J., Tite, M.S., Reid, J., (1964).
"TL dating of ancient ceramics".
Nature, 202, 1032-1033.

Aitken, M.J., Zimmerman, D.W., Fleming, S.J., (1968b).
"TL dating of ancient pottery".
Nature, 219, 442-444.

Aitken, M.J., Bussell, G.D., (1982).
"TL dating of fallen stalactites".
PACT, 6, 550-554.

Bailiff, I.K., Bowman, S.G.E., Mobbs, S.F., Aitken, M.J., (1977).
"The phototransfer technique and its use in thermoluminescence dating".
Journal of Electrostatics, 3, 269-280.

Balescu, S., Dupuis, C., Quinif, Y., (1986).
"Paleographical and stratigraphical inferences from TL properties of Saalian and Weichselian loess of N.W. Europe".
Ancient TL, 4, (1), 16-23.

Bell, W.T., Mejdahl, V., Winther-Nielsen, M., (1980).
"The refinement of the automated TL dating procedure and perspectives for the archaeological application of the method as demonstrated by the results from sites of known age".
Revue d'Archéométrie, no.4, 127-137.

Belperio, A.P., Smith, B.W., Polach, H.A., Nittrouer, C.A., DeMaster, D.J., Prescott, J.R., Hails, J.R., Gostin, V.A., (1984).
"Chronological studies of the Quaternary marine sediments of Northern Spencer Gulf, South Australia".
Marine Geol., 61, 265-296.

Benkö, L., (1983).
"TL properties of individual quartz grains".
PACT 9, 175-181.

Berger, G.W., (1984).
"Thermoluminescence dating studies of glacial silts from Ontario".
Can. J. Earth Sci., 21, 1393-1399.

Berger, G.W., (1985a).
"Thermoluminescence dating studies of rapidly deposited silts from south-central British Columbia".
Can. J. Earth Sci., 22, 704-710.

Berger, G.W., (1985b).
"Thermoluminescence dating applied to a thin winter varve of the late glacial South Thompson silt, south-central British Columbia".
Can. J. Earth Sci., 22, 1736-1739.

Berger, G.W., Huntley, D.J., (1982).
"TL dating of terrigenous sediments".
PACT 6, 495-504.

Berger, G.W., Huntley, D.J., (1983).
"Dating volcanic ash by thermoluminescence".
PACT 9, 581-592.

Berger, G.W., Huntley, D.J., Stipp, J.J., (1984).
"Thermoluminescence studies on a ^{14}C -dated marine core".
Can. J. Earth Sci., 21, 1145-1150.

Bhandari,N.,SenGupta,D.,Singhvi,A.K.,Nijampurkar,V.N.,Vohra, C.P.,(1983).
"Thermoluminescence dating of glaciers".
PACT 9, 513-521.

Bluszcz, A., Pazdur, M.F., (1985).
"Comparison of TL and ^{14}C dates of young aeolian sediments - a check of the zeroing assumption".
Nucl. Tracks, 10, 703-710.

Boden, G., Sahre, P., Ebert, I., Hennig, H.P., Jedamzik, J., Prösch, U., (1985).
"Investigations of the TL and EPR of mechanically activated and irradiated quartz".
Cryst. Res. Technol., 20, 1101-1107.

Bøtter-Jensen, L., Bundgaard, J., (1978).
"An automated reader for TL dating".
PACT 2, 48-56.

Bøtter-Jensen, L., Mejdahl, V., (1980).
"Determination of archaeological doses for TL dating using an automated TL apparatus".
Nuc. Instr. and Methods, 175, 213-215.

Bøtter-Jensen, L., Bundgaard, J., Mejdahl, V., (1983).
"An HP-85 microcomputer-controlled automated reader system for TL dating".
PACT 9, 343-349.

Borsy, Z., Félszerfalvi, J., Szabó, P.P., (1979).
"TL dating of several layers of the loess sequence at Paks and Mende (Hungary)".
Acta Geologica of the Academy of Science, Hungary, 22, 451-459.

Bothner, M.H., Johnson, N.M., (1969).
"Natural thermoluminescence dosimetry in late Pleistocene pelagic sediments".
Journal of Geophysical Research, 74, 5331-5338.

Boyle, R., (1664).
"Experiments and considerations upon colours with observations on a diamond that shines in the dark".
Henry Herringham, London.

Castagnoli, G.C., Bonino, C., Miono, S., (1982).
"Thermoluminescence in sediments and historical supernovae explosions".
Il Nuovo Cimento, 5C, 488-492.

Daniels, F., Boyd, C.A. and Saunders, D.F., (1953).
"TL as a research tool".
Science, 117, 343-349.

David, M., Sunta, C.M., Ganguly, A.K., (1977).
"TL of quartz: Part 1 - glow curve and spectral characteristics".
Ind. J. Pure and Appl. Phys., 15,, (3), 201-204.

David, M., Sunta, C.M., (1981).
"Thermoluminescence of Quartz - Part VI: Effect of Ultraviolet Rays".
Ind. J. Pure and App. Phys., 19, 1041-1047.

Debenham, N.C., (1985).
"TL dating of loess deposition in Normandy".
Ancient TL, 3, (1), 9-10.

Debenham, N.C., (1985).
"Use of U.V. emissions in TL dating of sediments".
Nucl. Tracks. 10, 717-724.

Debenham, N.C., and Walton, A.J., (1983).
"TL properties of some wind-blown sediments".
PACT 9, 531-538.

Diffey, B.L., (1977).
"The calculation of the spectral distribution of natural ultraviolet radiation under clear day conditions".
Phys. Med. Biol., 22, (2), 309-316.

Dreimanis, A., Hütt, G., Raukas, A., Whippey, P.W., (1978).
"Dating methods of Pleistocene deposits and their problems:
1. Thermoluminescence Dating".
Geoscience Canada, 5, 55-60.

Fleming, S.J., (1966).
"Study of TL of crystalline extracts from pottery".
Archaeometry, 9, 170-173.

Fleming, S.J., (1973).
"The pre-dose technique: a new thermoluminescence dating method".
Archaeometry, 15, 13-30.

Fleming, S.J., (1979).
"Thermoluminescence techniques in Archaeology".
Clarendon Press, Oxford.

Fleming, S.J., Stoneham, D., (1973).
"The subtraction technique of thermoluminescence dating".
Archaeometry, 15, 229-238.

Fremlin, J.H., Srirath, S., (1964).
"Thermoluminescent dating: examples of non-uniformity of luminescence".
Archaeometry, 7, 58-62.

Gemmell, A.M.D., (1985).
"Zeroing of the TL signal of sediment undergoing fluvial transportation: a laboratory experiment".
Nucl. Tracks, 10, 695-702.

Göksu, H.Y., Fremlin, J.H., Irwin, H.T., Fryxell, R., (1974).
"Age determination of burnt flint by a thermoluminescent method".
Science, 183, 651-654.

Göksu Ögelman, Y., Kapur, S., (1982).
"Thermoluminescence reveals weathering stages in basaltic rocks".
Nature, 296, 231.

Grögler, N., Houtermans, F.G., Stauffer, H., (1960).
"Ueber die Datierung von Keramik und Ziegel durch Thermolumineszenz".
Helvetica Physica Acta 33, 595-596.

Huntley, D.J., (1985).
"On the zeroing of the thermoluminescence of sediments".
Phys. Chem. Minerals, 12, 122-127.

Huntley, D.J., Johnson, H.P., (1976).
"Thermoluminescence as a potential means of dating siliceous ocean sediments".
Can. J. Earth Sci., 13, 593-596.

Huntley, D.J., Godfrey-Smith, D.I., Thewalt, M.L.W., (1985).
"Optical dating of sediments".
Nature, 313, 105-107.

Huntley, D.J., Hutton, J.T., Prescott, J.R., (1985).
"South Australian sand dunes: a TL sediment test sequence: preliminary results".
Nucl. Tracks, 10, 757-758.

Huntley, D.J., Kirkey, J.J., (1985).
"The use of an image intensifier to study the TL intensity variability of individual grains".
Ancient TL, 3, (2), 1-4.

Hütt, G., Smirnov, A., (1982).
"Thermoluminescence dating in the Soviet Union".
PACT 7, 97-103.

Hütt, G., Smirnov, A., (1982).
"Detailed thermoluminescence dating studies of samples from geological reference profiles in Central Russia".
PACT 6, 505-513.

Hütt, G., Punning, J.M., Smirnov, A., (1982).
"The potential use of the TL dating method in chronological studies of the late Pleistocene".
PACT 7, 105-114.

Hutton, J.T., Prescott, J.R., Twidale, C.R., (1984).
"TL dating of coastal dune sand related to a higher stand of Lake Woods, Northern Territory, Australia".
Aust. J. Soil Res., 22, 15-21.

Huxtable, J., Aitken, M.J., Weber, J.C., (1972).
"Thermoluminescent dating of baked clay balls of the Poverty Point Culture".
Archaeometry, 14, 269-275.

Huxtable, J., Aitken, M.J., Bonhommet, N., (1978).
"Thermoluminescence dating of sediment baked by lava flows of the Chaine des Puys".
Nature, 275, 207-209.

Jensen, H., Barbetti, M., (1979).
"More on filters for laboratory illumination".
Ancient TL, 7, 10.

Jerlov, N.G., (1976).
Marine Optics, 2nd ed., 231p.
Elsevier Scientific Publishing Company, New York.

Jungner, H., (1983).
"Preliminary investigations on TL dating of geological sediments from Finland".
PACT 9, 565-572.

Jungner, H., (1985).
"Some experiences from an attempt to date post-glacial dunes from Finland by TL".
Nucl. Tracks, 10, 749-756.

Kennedy, G.C., Knopff, L., (1960).
"Dating by Thermoluminescence".
Archaeology, 13, 147-148.

Kronborg, C., (1983).
"Preliminary results of age determination by TL of interglacial and interstadial sediments".
PACT 9, 595-605.

Lamothe, M., (1984).
"Apparent TL ages of St-Pierre sediments at Pierreville, Quebec, and the problem of anomalous fading".
Can. J. Earth Sci., 21, 1406-1409.

Levy, P.W., (1979).
"Thermoluminescence studies having applications to geology and archaeometry".
PACT 3, 466-480.

Levy, P.W., (1982).
"Thermoluminescence and optical bleaching in minerals exhibiting second order kinetics and other charge retrapping characteristics".
PACT 6, 224-242.

Long, J.V.P., "Electron Probe Microanalysis",
in "Physical Methods in Determinative Mineralogy",
Ed. J. Zussman. pg. 216-254, Acad. Press, London, (1977).

McDougall, D.J., (Ed), (1968).
"Thermoluminescence of geological materials".
Acad. Press, London.

McKeever, S.W.S., (1984).
"Thermoluminescence in quartz and silica".
Radiation Protection Dosimetry, 8, 81-98.

McKeever, S.W.S., (1985).
"Thermoluminescence of Solids".
Cambridge University Press.

McKeever, S.W.S., Sears, D.W., (1979).
"Meteorites and thermoluminescence".
Meteorites, 14, 29.

Medlin, W.L., (1968).
"The nature of traps and emission centres in thermoluminescent rock materials" In "Thermoluminescence of Geological Materials".
Ed. McDougall D.J., Acad. Press, London. pg. 193.

Mejdahl, V., (1983).
"Feldspar inclusion dating of ceramics and burnt stones".
PACT 9, 351-354.

Mejdahl, V., (1985).
"Thermoluminescence dating of partially bleached sediments".
Nucl. Tracks, 10, 711-715.

Mobbs, S.F., (1979).
"Phototransfer at low temperatures".
PACT 3, 407-413.

Murray , A.S., Gemmell, A.M.D., Kennedy, S., Lamb, M., (1983).
"The dating of inwashed material derived from glacial deposits: preliminary results".
PACT 9, 573-579.

Nambi, K.S.V., (1981).
"Thermoluminescence - a versatile new tool".
Science Today, Dec. 1981, 12.

Nambi, K.S.V., Bapat, V.N., David, M., (1978).
"Geochronology and prospecting of radioactive ores by their thermoluminescence".
Ind. J. Earth Sci., 5, 154.

O'Brien, M.C.M., (1955).
"The structure of the colour centres in smoky quartz".
Proc. Roy. Soc. Lond., A231, 404-414.

Prescott, J.R., (1983).
"Thermoluminescence dating of sand dunes at Roonka, South Australia".
PACT 9, 505-512.

Prescott, J.R., Polach, H.A., Pretty, G.L., Smith, B.W. (1982).
"Comparison of ^{14}C and TL dates from Roonka, South Australia".
PACT 8, 205-211.

Prószyńska, H., (1983).
"TL dating of some subaerial sediments from Poland".
PACT 9, 539-546.

Prószyńska-Bordas, H., (1985).
"TL dating of loess and fossil soils from the last interglacial - glacial cycle".
Nucl. Tracks, 10, 737-742.

Readhead, M.L., (1982).
"Extending TL dating to geological sediments", In "Archaeometry: an Australian perspective".
Eds. Ambrose, W., Duerden, P., 276-281, ANU Press, Canberra.

Rendell, H.M., (1985).
"The precision of water content estimates in the thermoluminescence dating of loess from Northern Pakistan".
Nucl. Tracks., 10, 763-768.

Rendell, H.M., Gamble, I.J.A., Townsend, P.D., (1983).
"TL dating of loess from the Potwar Plateau, Northern Pakistan".
PACT 9, 555-562.

Shelkoplyas, V.N., Morozov, G.V., (1966).
"Application of the Thermoluminescence Method in Geology".
"Scientific thought" publishing house, Kiev.

Singhvi, A.K., Zimmerman, D.W., (1978).
"The luminescent minerals in fine-grain samples from archaeological ceramics".
PACT 2, 12-17.

Singhvi, A.K., Sharma, Y.P., Agrawal, D.P., (1982).
"Thermoluminescence dating of sand dunes in Rajasthan, India".
Nature, 295, 313-315.

Singhvi, A.K., Sauer, W., Wagner, G.A., (1986).
"Thermoluminescence dating of loess deposits at Plaidter Hummerich and its implications for the chronology of Neanderthal Man".
To appear in Naturwissenschaften.

Smith, B.W., (1983).
"New applications of thermoluminescence dating".
Unpublished Ph.D. thesis, University of Adelaide.

Smith, B.W., Prescott, J.R., Polach, H.A., (1982).
"TL dating of marine sediments from Spencer Gulf", In
"Archaeometry; an Australian perspective".
Eds., Ambrose, W., Duerden, P., pg. 282-289, ANU Press, Canberra.

Stoffler, D., (1974).
Fortschr, Miner., 51, 256.

Sutton, S.R., Zimmerman, D.W., (1978).
"A blue-UV absorbing filter for laboratory illumination".
Ancient TL, 5, 5.

Sutton, S.R., Zimmerman, D.W., (1978).
"Thermoluminescence dating: radioactivity in quartz".
Archaeometry, 20, 67-69.

Townsend, P.D., Kelly, J.C., (1973).
"Colour centres and imperfections in insulators and semiconductors".
Sussex University Press.

Wintle, A.G., (1973).
"Anomalous fading of thermoluminescence in mineral samples".
Nature, 245, 143-144.

Wintle, A.G., (1977).
"Thermoluminescence dating of minerals - traps for the unwary".
Journal of Electrostatics, 3, 281-288.

Wintle, A.G., (1981).
"TL dating of late Devensian loesses in Southern England".
Nature, 289, 479-480.

Wintle, A.G., (1985).
"Thermoluminescence dating of loess deposition in Normandy".
Ancient TL, 3, (1), 11-15.

Wintle, A.G., (1985).
"Sensitization of TL signal by exposure to light".
Ancient TL, 3, (3), 16-21.

Wintle, A.G., (1985).
"Stability of TL signal in fine grains from loess".
Nucl. Tracks, 10, 725-730.

Wintle, A.G., Brunnacker, K., (1982).
"Ages of volcanic tuff in Rheinhessen obtained by TL dating of loess".
Naturwissenschaften, 69, 181-183.

Wintle, A.G., Huntley, D.J., (1979a).
"Thermoluminescence dating of a deep sea sediment core".
Nature, 279, 710-712.

Wintle, A.G., Huntley, D.J., (1979b).
"Thermoluminescence dating of sediments".
PACT 3, 374-380.

Wintle, A.G., Huntley, D.J., (1980).
"Thermoluminescence dating of ocean sediments".
Can. J. Earth Sci., 17, 348-360.

Wintle, A.G., Huntley, D.J., (1982).
"Thermoluminescence dating of sediments".
Quaternary Science Reviews, 1, 31-53.

Wintle, A.G., Murray, A.S., (1977).
"Thermoluminescence dating: reassessment of the fine grain dose-rate".
Archaeometry, 19, 95-98.

Wintle, A.G., Prószyńska, H., (1983).
"TL dating of loess in Germany and Poland".
PACT 9, 547-554.

Zimmerman, D.W., (1967).
"Thermoluminescence from fine grains from ancient pottery".
Archaeometry, 10, 26-28.

Zimmerman, D.W., (1970).
"The dependence of thermoluminescence on energy and type of ionizing radiation and its significance for archaeologic age determination".
Unpublished Ph.D. thesis, Oxford University.

Zimmerman, J., (1971).
"The radiation-induced increase of the 100°C thermoluminescence sensitivity of fired quartz".
J. Phys. C: Solid St. Phys., 4, 3265-3276.